Design and Verification of Delfi-PQ Satellite Propulsion Subsystem

Experimental Analysis and Design Improvements of the Technology Demonsration Payload for Micro-Thrusters

A. Melaika

Technische Universiteit Delft

TU Delft

Design and Verification of Delfi-PQ Satellite Propulsion Sub-system

Experimental Analysis and Design Improvements of the Technology Demonsration Payload for Micro-Thrusters

by

A. Melaika

in partial fulfillment of the requirements for the degree of

Master of Science

in Space Engineering

at the Delft University of Technology,

to be defended publicly on Tuesday July 02, 2019 at 10:00 AM.

Student number:	4048210	
Project duration:	September 13, 2018 – July 02, 2019	
Thesis committee:	dr. A. Cervone,	TU Delft, supervisor
	ir. B.T.C. Zandbergen,	TU Delft, chairperson
	dr. ir. D. Dirkx,	TU Delft, examiner

This thesis is confidential and cannot be made public until July 02, 2019.

TU Delft

Preface

I present you my Master thesis on *Design and Verification of Delfi-PQ Satellite Propulsion Sub-system*. This was one of the biggest challenges I have experienced in my life. It not only tested my intelligence level, but also the emotional intelligence. I have really enjoyed writing my thesis and have learned a lot in the process. By choosing a very practical thesis, I could apply a lot of my previous practical skills and creativity. Therefore, nothing brings more joy than when you can see the actual design of the technology being implemented in real life.

I would like to thank Vidhya for supporting me in ordering the parts and providing information throughout my thesis, Sevket for helping to prepare sensors and other testing hardware for the clean-room, and good-deep conversations about life and jobs, Barry for having a critical and analytical view on the tests and providing insightful ideas on the tests, and most importantly Angelo, my thesis supervisor, who has always helped me, given good advice, always been positive and supportive during the whole time of thesis.

But, of course, the biggest gratitude and love I want to express to my parents and my brother. Without their support my work would have been many times more harder and challenging. My parents told me to never give up and keep strong at the worst, which is the best perseverance advice I could get. Thanks to my brother, the best friend, who was the only person to understand what it is to be a technical university student and what it takes to write Masters thesis.

A. Melaika
Delft, June 2019

Abstract

Ever since the increase to have a short temporal resolution for a global coverage, one of the best solutions is to have a constellation (swarm) of satellites. Furthermore, these days a lot of space missions require to achieve a very specific mission goal, which requires only a single instrument on-board of the satellite. To overcome such challenges, one of the best solutions is to use nano- or picosatellites. Nanosatellites, such as the CubeSat platform, are very well established in the market for such purposes. But now a new standard, which is spinned-off from the CubeSat, is being brought to the space industry. And that is a picosatellite type of spacecraft called *PocketQube*.

Aerospace Engineering faculty at University of Technology Delft (TU Delft) is currently developing a *PocketQube* satellite under the name of *Delfi-PQ*. It is a 3P unit spacecraft, which purpose is to show its capabilities and demonstrate on-board technologies. Following the previous study performed on a high level systems engineering on Propulsion Payload Demonstrator (PPD), there is a need to verify the demonstrator's design, final operational envelope values, and propulsion sub-system's requirements by using TEST and ANALYSIS methods. The tests are split into: *Component*, *Integration*, *Prototype*, and *Flight Model* tests. 4 out of 11 total tests have been conducted. Each test requires a description of an experimental setup, which includes a methodology, test set-up, parameters, success criteria, and test procedure. *TEST-INT-01: Leak Test* required to test the whole propulsion system for any possible leaks and determine an acceptable leak rate. Apparently, the current components and the set-up of the propulsion system has a leak, which is almost undetectable with any existing leak detection methods. A possible supersonic leak of a size of 0.0015 - 0.0026 [mm] is expected. At the end, a suggested acceptable leak rate is determined, which is 0.2 - 3 [mbar] per 24 [h]. However, various size tubes affect the leak rate and integration of the components. *TEST-INT-02: Volume and Mass Test* required to test if the first concept of the detailed design fulfills the volume and mass requirements and their budgets. The biggest issue observed so far is the appearing kinks in the tubes at the bending locations. Furthermore, the valves fit marginally in the required 42x42x30 [mm] volume. An updated propulsion system's cage improves the placement of the components and reduces the risks of contaminating other satellite sub-systems. *TEST-COM-01: Solenoid Valve Pulse-Width Modulated (PWM) Test* shows that in order to achieve Low Pressure Micro-Resistojet (LPM) thruster's plenum target pressures of 50 -300 [Pa], the required tank pressure is 1 [bar] instead of Final Operational Envelope (FOE) value of 0.2 [bar]. The optimal pulse width modulated frequency is 250 [Hz]. *TEST-COM-04: Heater Efficiency Test* provided preliminary information on the required power-pressure inputs to have a minimum vaporization temperature in the chamber. The trend lines, which followed from the data processing results, can be used to predict various power levels at the required mass flows and chamber pressure levels. The mas flow values of 0.5 to 2 [mL/h] provide power levels within the 4 [W] power budget.

The verification tests of the PPD design provided a lot of valuable information. Not only some of the propulsion sub-system requirements have been verified, but also the underlying design issues have been observed, registered, and described for the future researchers who are going to test PPD and optimize its design.

Contents

List of Acronyms

a.k.a. also known as viii, 2, 7, 31

AE Aerospace Engineering viii, 31

CAD Computer-Aided Design viii, xvii, 4, 10, 21, 23, 37, 47, 59, 120, 121, 122, 129, 182

COTS Commercial Off-The-Shelf viii, 1, 11, 19, 21

DAQ Digital Acquisition viii, 21, 23, 24, 33, 34, 42, 66, 69, 82, 87, 88, 90, 96, 105, 106, 134

DASML Delft Aerospace Structures Materials Laboratory viii, 37, 39, 64

DOT Design Option Tree viii, 58

ECSS European Cooperation for Space Standardization viii, 12

FFKM Perfluoroelastomer viii, 120

FOE Final Operational Envelope v, viii, xv, 11, 62, 63, 72, 80, 85, 98, 99, 104, 110, 115, 116, 119, 130, 150, 152, 176, 181, 182, 183, 216, 218, 238

FTP File Transfer Protocol viii, 157

GPFS General Purpose Feed System viii, 21, 23, 24, 34, 42, 49, 53, 65, 73, 81, 95, 99, 101, 105, 106, 130, 142, 143, 150

He Helium viii, 31, 33

HW Hardware viii, 12, 21, 23, 24

I.D. Inner Diameter viii, 65, 127

LIDAR LIght Detection And Ranging viii

LPM Low Pressure Micro-Resistojet v, viii, xv, xvii, xviii, 2, 3, 5, 7, 8, 9, 10, 11, 21, 24, 26, 29, 30, 34, 42, 45, 46, 49, 55, 57, 59, 60, 61, 62, 63, 64, 65, 66, 69, 70, 93, 97, 98, 101, 103, 104, 106, 121, 122, 124, 125, 127, 129, 133, 134, 153, 181, 182, 183

MEMS Micro Electro Mechanical System viii, 1

N.A. Not Applicable viii, 40, 48, 52, 60, 70, 85, 98, 104, 126

NASA National Aeuronautics and Space Administration viii, 31

NI National Instruments viii, 34, 66, 69, 82

NTC Negative Temperature Coefficient viii, 66

OD Outer Diameter viii, 34

PC Personal Computer viii, 21, 23, 24, 34, 42, 82, 87

PCB Printed Circuit Board viii, xvii, 23, 38, 55, 58, 59, 60, 61, 65, 82, 122, 123, 124, 126, 127

PCTFE Polychlorotrifluoroethylene viii, 120, 121

PEEK Polyetheretherketone viii, 120

PoI Point of Interest viii, xvii, 33, 35, 36, 37, 46, 51, 94, 101, 105, 106

PPD Propulsion Payload Demonstrator v, viii, xv, 3, 4, 5, 7, 8, 9, 10, 11, 12, 14, 18, 20, 21, 23, 24, 26, 29, 31, 33, 38, 55, 57, 60, 62, 63, 65, 93, 105, 106, 121, 122, 125, 127, 128, 142, 143, 150, 152, 153, 181, 183, 195

PQ PocketQube viii, 55

PS Propulsion System viii, xvii, 3, 10, 20, 23, 40, 42, 49, 52, 53, 55, 59, 67, 70, 73, 74, 75, 96, 97, 98, 101, 107, 108, 109, 110, 117, 118, 121, 122, 123, 124, 126, 129, 183

PSU Power Supply Unit viii, 42, 66, 73, 74, 75, 82, 85, 87, 88, 90, 157

PTFE Polytetrafluoroethylene viii, 34, 39

PWM Pulse-Width Modulated v, vii, viii, 19, 20, 21, 26, 62, 63, 64, 65, 69, 70, 72, 77, 78, 129, 130, 131, 133, 134, 135, 137, 138, 139, 141, 142, 143, 145, 146, 147, 149, 150, 151, 152, 182

RoD Review of Design viii, 12, 18

ROI Region of Interest viii, xvi, xviii, xix, 131, 132, 139, 140, 141

SE Systems Engineering viii, 55

SMD Surface-Mount Device viii, 38, 127

SSE Space Systems Engineering viii, 3, 33, 126

SW Software viii, 12, 21, 23, 24, 87

TBC To Be Corrected viii, 7, 119, 153

TBD To Be Determined viii, 15, 152

TU Delft University of Technology Delft v, viii, 1, 2, 3, 5, 31, 33, 108, 157, 181

USB Universal Serial Bus viii, 34, 42, 87

VLM Vaporizing Liquid Micro-Resistojet viii, xv, xvi, xvii, 2, 3, 5, 7, 8, 9, 10, 11, 21, 24, 26, 29, 30, 34, 47, 49, 51, 53, 55, 57, 59, 60, 61, 62, 63, 80, 81, 82, 85, 87, 90, 93, 97, 98, 101, 104, 111, 121, 122, 124, 125, 127, 153, 156, 178, 181, 183, 184, 197, 198, 200, 202, 204, 206, 208

w.r.t. with respect to viii, xviii, 63, 70, 134, 135, 151

List of Symbols

A Cross-sectional area [m^2] viii, 114

A^* Throat area [m^2] viii, 155

A_l Cross-sectional area of the contracted control volume [m^2] viii, 112

A_l Cross-sectional area of the leak orifice [m^2] viii, 112, 114

A_s Cross-sectional area of the control volume [m^2] viii, 112

A_t Cross-sectional area of the inner diameter tube [m^2] viii, 112

C_d Discharge coefficient [-] viii, 112

C_P Molar specific heat at constant pressure [J/mol K] viii, 115

c_{pg} Specific heat of the gaseous phase at constant pressure [J/K/kg] viii, 154, 155

c_{pl} Specific heat of the liquid phase at constant pressure [J/K/kg] viii, 154, 155

C_V Molar specific heat at constant volume [J/mol K] viii, 115

CO_2 Carbon Dioxide [-] viii, 33, 107, 108, 109

c^* Characteristic velocity [m/s] viii, 112

Δ_{displ} Displacement by the pendulum [μm] viii, 85, 177

d_{leak} diameter of the leak orifice [m] viii, 118

DC Duty Cycle [-] viii, 64, 70, 130, 138, 139, 182

ΔM Pressurant gas change in mass [kg] viii, 103, 104, 110

ΔP_{avg} Average of the pressure difference [bar] viii, 96, 98, 99, 101

Δp Pressure difference [Pa] viii, 114, 119

ΔP Pressure difference between two data points [bar] viii, 96, 98, 99, 101

$\Delta P_{avg}(t)$ Average pressure change over time difference [bar/s] viii

ΔQ_M Mass leak rate difference [kg/s] viii

Δt time step of the iterations [s] viii, 113

d_l Diameter of the leak orifice [m] viii, 112

D_{st} Inner diameter of the propellant storage tube [m] viii, 103, 104, 112

f_{PWM} Pulse Width Modulation frequency [Hz] viii, 70

f_s Sampling frequency [Hz] viii, 96, 98, 99, 101

F_t Thrust [N] viii, 85

g_0 Gravitational acceleration 9.81 [m/s^2] viii, 155

γ Specific heat ratio [-] viii, 112, 115, 155

Γ Specific heat ratio [-] viii

H_2O Dihydrogen Monoxide (Water) [-] viii, 15, 40, 52, 53, 107

h_{vap} Latent heat of vaporization [kJ/kg] viii, 154, 155

I_{sp} Specific impulse [s] viii, 155

I_i Input current [A] viii, 85, 159, 160, 163, 164, 166, 167, 169, 170, 173, 174, 177

Kn Knudsen number [-] viii, 118

L characteristic channel length [m] viii, 118

$l_{st,total}$ total storage length [m] viii, 103, 104

λ mean free path of a molecule [m] viii, 118

m Initial mass [kg] viii

M Molecular weight [g/mol] viii, 104, 109

$\dot{m}$ mass flow [kg/s] viii, 85, 154, 160, 164, 168, 171, 174

$M_{PPD,dry}$ Dry mass of the Propulsion Payload Demonstrator [kg] viii, 60

$M_{PPD,wet}$ Wet mass of the Propulsion Payload Demonstrator [kg] viii, 60

$M_{PS,0}$ Total initial mass of the propulsion system [kg] viii, 40, 52

$M_{PS,dry}$ Dry mass of the propulsion system [kg] viii, 40

$M_{PS,F}$ Total final mass of the propulsion system [kg] viii, 40, 48, 52

M_{PS,H_2O} mass of the water in the propulsion system [kg] viii, 40, 52

M_{PS,N_2} mass of the nitrogen in the propulsion system [kg] viii, 48

M_W Molecular mass of water vapour [g/mol] viii, 155

$\dot{m}_{H_2O}$ water mass flow [mL/h] viii, 85

$\dot{m}_{N_2}$ Mass flow of nitrogen gas [kg/s] viii, 70

N_2 Nitrogen [-] viii, 11, 15, 21, 23, 24, 36, 38, 40, 42, 48, 49, 52, 53, 55, 63, 65, 70, 73, 93, 94, 99, 104, 111, 213

P Pressure [Pa] viii, 111

P_0 Initial pressure [mbar] viii, 93

P_1 Water pressure at the boiling point [atm] [bar] [Pa] viii, 155

$P_{avg}(t)$ Average pressure change over time [bar/s] viii, 96, 98, 99, 101

P_c Pressure in the chamber [Pa] [bar] viii, 85, 155, 160, 164, 168, 171, 174

P_{hl} Hold Power [W] viii, 151

P_{outlet} Outlet (tank) pressure [Pa] viii, 143

P_{pl} Pressure at the plenum inlet [bar] viii, 70, 159, 160, 163, 164, 166, 167, 168, 169, 170, 171, 173, 174, 177

P_{sp} Spike Power [W] viii, 151

$P_{st,0}$ Initial propellant storage pressure [bar] viii, 40, 48, 52, 70, 96, 98, 99, 101, 104, 110

$P_{st,F}$ Final propellant storage pressure [bar] viii, 40, 96, 98, 99, 101, 104

$P_{st,t}$ Propellant storage pressure over time [bar] viii, 40

P_{target} Target (plenum) pressure [Pa] viii, 143

P_a Ambient pressure [Pa] viii, 114

P_i Input power [W] viii, 85, 159, 160, 163, 164, 166, 167, 168, 169, 170, 171, 173, 174, 177

$\dot{Q}$ Power required to receive [W] viii, 85, 154, 160, 164, 168, 171, 174

Q_m Molar leak rate [mol/s] viii, 102, 110

Q_M Mass leak rate [kg/s] viii, 102, 104, 110, 181

Q_V Volume leak rate [m^3/s] viii, 102, 110

Q_{Vc} Corrected volumetric leak rate [m^3/s] viii, 110

R_{N_2} Nitrogen gas constant [J/kg K] viii, 104, 111, 112

R_A Universal gas constant 8.314 [J/K/mol] viii, 155

$\bar{R}$ Universal gas constant 8.314 [kJ/mol K] viii, 104

R_{coil} Coil resistance [Ω] viii, 70, 151

R_{ini} Initial resistance [Ω] viii, 153

R Molar gas constant 8.314 4598 [J/(mol · K)] viii, 111, 112, 115

R_h Thruster heater resistance [Ω] viii, 85

R_{He} Helium gas constant [J/(kg · K)] viii, 109, 110

T Temperature [°C] [K] viii, 111, 113, 114

T_0 Temperature of the propellant [°C] [K] viii, 85, 154, 159, 160, 163, 164, 166, 167, 168, 169, 170, 171, 173, 174, 177

T_1 Water boiling temperature at 1 atmosphere [°C] [K] viii, 155

T_c Temperature in the nozzle [°C] [K] viii, 85, 155, 179

t_L Leak time [s] viii, 40, 42, 49, 53, 103, 104

t_{pd} Pulse duration [ms] viii

T_{pl} Temperature at the plenum inlet [K] viii, 70

t_s Sampling time [s] viii, 70, 85, 96, 98, 99, 101

$T_{st,0}$ Initial propellant storage temperature [°C] [K] viii, 70, 104, 110

$T_{st,F}$ Final propellant storage temperature [°C] [K] viii, 104, 110

T_{sv} Temperature of the solenoid valve [K], [°C] viii, 70, 151

T_{vap} Temperature of vaporization [°C] [K] viii, 154, 155, 160, 164, 168, 171, 174, 179

T_{amb} Ambient temperature [°C] [K] viii, 70, 110

T_c Chamber temperature [°C] [K] viii, 112, 154

V Volume [m^3] viii, 111

$V_{H_2O,0}$ Initial volume of water in the propulsion system [m^3] viii, 40, 52

$V_{H_2O,F}$ Final volume of the water in the propulsion system [m^3] viii, 40, 52

V_{hl} Hold voltage [V] viii, 151

$V_{N_2,0}$ Initial volume of nitrogen in the propulsion system [m^3] viii, 48

$V_{N_2,F}$ Final volume of the nitrogen in the propulsion system [m^3] viii, 48

V_{pl} Volume of the plenum [m^3] viii

V_{PPD} Volume of the Propulsion Payload Demonstrator [m^3] viii, 60

V_{sp} Spike voltage [V] viii, 151

V_{st,N_2} Volume of the propellant storage [m^3] viii, 103, 104, 110, 111

V_{tube} Inner volume of the tube [m^3] viii, 11, 40

v_i Injection velocity [m/s] viii, 113

V_i Input voltage [V] viii, 85, 159, 160, 163, 164, 166, 167, 169, 170, 173, 174, 177

Z Compressibility factor [-] viii, 104, 109, 110

ζ total loss factor [-] viii, 112

ζ_c Loss factor due to a sudden contraction in the flow [-] viii, 112

ζ_e Loss factor due to a sudden expansion in the flow [-] viii, 112

List of Tables

List of Figures

1 Introduction

In this chapter a general information is presented about the developments in the satellite and micro-propulsion industry as well as at TU Delft. After that, the motivation about why this thesis needs to be conducted is discussed. Then, the research objectives and questions are formulated after which the thesis outline is presented.

1.1. General Information and Motivation

A rapid increase of need in almost instantaneous global solutions nowadays requires a technology, which can be accessed any time and has a global coverage. In a very fast evolving and technology oriented world, space industry has become one of the main markets, which provides such a range of technologies, services, and solutions. This is where a satellite is being used as an instrument to solve these challenges. In the past 2 decades spacecraft size has decreased, but their number in space has become higher. It has to do with the mentioned reasons above. In order to have a global coverage and frequent revisit times, one solution is to have a constellation of spacecraft [7]. However, to have a constellation of spacecraft can be costly and the build-up to a full spacecraft constellation can be time consuming. One of the methods to decrease cost and the development time is to reduce the size of the spacecraft [8] [9]. Therefore, nano-satellite class spacecraft are becoming popular ever since their introduction. The best known nano-satellite class spacecraft is CubeSat.

Ever since the CubeSat concept was introduced in 1999, its popularity has grown between the academia, start-ups, space market leaders, and space amateurs. Its success factor is the miniaturization of the technology, reduction in the development and launch costs, availability of Commercial Off-The-Shelf (COTS) products, and innovative technology demonstrations [10] [11] [12].

Back in 2009 after 10 years when a CubeSat concept was first introduced, an even smaller version of a satellite was conceptualized, which is called *Pocketqube*. It is 1/8 of 1 unit CubeSat size, which is around 5x5x5 [cm] and does not weigh more than 250 [g] [13]. 5x5x5 [cm] is considered as a 1 unit and called 1P. Two units would be called 2P and so on. Its purpose is to reduce the development and launch costs even further, as well as to create opportunities to develop new Micro Electro Mechanical System (MEMS) technologies. Only 4 *PocketQube* satellites have been launched since 2009: *T-LogoQube*, *$50Sat*, *QubeScout-S1*, and *WREN* [14], [15], [16], [17], [18]. The trend of developing *PocketQube* satellites has been picked up

recently. There are around 27 new missions being developed around the world, where some of them are intended to be launched in 2019 [19].

At Aerospace Engineering faculty of TU Delft the first *PocketQube* mission concept, called *Delfi-PQ*, was introduced in 2016 and is being developed ever since then [20]. It is a 3P unit satellite, where one of the units is going to accommodate a novel propulsion sub-system. Figure 1.1 shows a render of *Delfi-PQ* satellite and the propulsion sub-system inside:

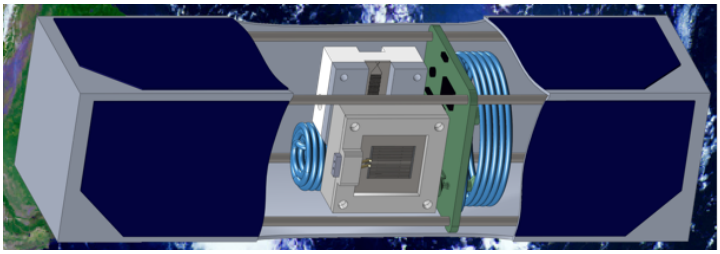

Figure 1.1: *Delfi-PQ* satellite render with the propulsion sub-system inside it. (Picture credit: [4])

During the development of *Delfi-PQ*, two innovative micro-propulsion thrusters were being researched in parallel. This presented a good opportunity to showcase the capabilities of the new micro-thrusters and *PocketQube* technology together in a single system. The two thrusters which need to be demonstrated are: Low Pressure Micro-Resistojet (LPM) and Vaporizing Liquid Micro-Resistojet (VLM).

One of the initiators of LPM (also known as (a.k.a.) Free Molecule Micro-Resistojet) thruster research is*Ketsdever et al.* [21]. The thruster uses various gases as a propellant: helium, nitrogen, argon, or carbon dioxide. Such a thruster is aimed for nano-satellites with less than 10 [kg] mass. The obtained thrust is 1.7 [mN]. The required steady-state power for the heaters is 3.2 [W]. The plenum pressure ranges from 0 to 110 [Pa].

A further study was performed on LPM capabilities by *Palmer et al.* [22]. The concept uses either gases or water as the propellant and can be stored in a liquid or solid phase. The thrust levels achieved at vacuum conditions are in the range of micro-newtons. The measured plenum pressure range from 300 to 900 [Pa]. The required power is up to 1.6 [W]. A similar concept to LPM has been researched by *Blanco et al.* [23]. The design uses xenon gas as the propellant. The required plenum pressure is 100 [Pa] and the required power is below 5 [W]. Around 2.2 [mN] thrust can be obtained. The micro-propulsion research group at TU Delft has introduced its own LPM thruster concept. Originally, the design was intended to work on a sublimating water molecules at a low plenum pressure, which escape through the heated chip slots [24]. The plenum pressure ranges from 50 to 300 [Pa]. The thrust can be obtained up to 2.7 [mN], where the power required ranges 1.46 - 9.68 [W]. A detailed overview of the current LPM design at TU Delft is presented in Chapter 2.

VLM is the second micro-thruster which is considered to be used in *Delfi-PQ*. One of its first concepts was presented in 2000 by *Mukerjee et al.* [25]. It requires 5 [W] for the heaters. The thrust is between 0.15 - 0.46 [mN]. The propellant is a liquid water. Another concept of VLM was researched by [26]. It uses relatively low vaporization temperatures in a range of 125 - 150 [^{o}C] for power levels of 7 - 9 [W]. Source [27] presents results of a design and fabrication method of VLM using layering of wafers to integrate the components of the thruster. Another research done on VLM is presented by *Giorgi et al.* [28]. The thruster uses a linear configuration of the heaters. TU Delft has designed its own unique VLM thruster by implementing

serpentine and diamond shape configurations of the heaters. A full overview of its design is presented in Chapter 2.

Although, both of the thrusters, which are being researched at TU Delft, are still in a prototype phase. Therefore, as it was mentioned before, both, the research of VLM and LPM, and introduction of the *Delfi-PQ* mission, presented and opportunity to create a Propulsion Payload Demonstrator (PPD). The purpose of PPD is to combine two different thrusters in a single propulsion sub-system and demonstrate their capabilities in space, while at the same time introducing the opportunity to use a propulsion sub-system on-board the *PocketQube* satellite. Such an innovation presents new challenges on how to design, test, and integrate both VLM and LPM concepts in only 1P unit of the *PocketQube*. Therefore, a high-level systems engineering approach has been used to create the first concept of PPD by *Turmaine* [3]. The overview of the design and the expected performance parameters are provided in Chapter 2.

In order to achieve a flight model of *Delfi-PQ* propulsion sub-system, a verification of its design is necessary. The purpose of this thesis is to verify the design of the PPD, according to the propulsion requirements, through TEST and ANALYSIS methods, and suggest its further design improvements and performance optimization.

1.2. Research Objective

The intention of this thesis is to further develop and improve *Delfi-PQ* satellite propulsion system demonstrator, investigate its underlying issues and create additional knowledge on the micro-propulsion systems based on the research outcome. The detailed design of the PPD established on the high level systems engineering approach has been created by *Turmaine* [3]. However, the verification of this detailed design is required in order to have a flight model design. In general, the PPD uses a novel set-up of the propulsion components and has not been tested fully as a whole system at Space Systems Engineering (SSE) department, yet. There can be many unforeseen performance and technical issues with such a Propulsion System (PS). At the moment, the LPM and VLM thrusters were only researched separately by *Guerrieri* [1] and *Silva* [2]. They have never been integrated and tested in the PPD to work as a single propulsion system. Similarly, the same applies to the solenoid valve. It has been extensively researched by *Silvestrini* [29], but only as a separate component and only at ambient conditions. For example, a tubular tank, which accommodates two propellants (water and nitrogen) in a single tube, has not been tested or used previously for such a propulsion system set-up. As the verification is one of the most crucial parts in the systems engineering and product development, the testing and analysis as the verification methods of the propulsion system are required to have a flight prototype version in the end.

To successfully conduct such a thesis, a research objective has to be defined. From the introduced purpose in Section 1.1 and presented information in this section, the following research objective is determined:

To improve the detailed design and verify the propulsion sub-system requirements of the LPM and VLM Propulsion Payload Demonstrator for the Delfi-PQ satellite mission using testing and analysis as the verification methods

The research objective is broken down into smaller sub-objectives (sub-goals). They give a detailed overview of what is being tried to achieve with the main research goal. Additionally, for each of the sub-goals a condition of an achievement is created. In such a case the researcher knows if the sub-objective is fulfilled. A list of these sub-goals are:

1. **Perform component tests and analysis of the PPD.**
   - *Condition of achievement*: when the defined component tests are performed according to the test method and procedure, and the success criteria is achieved.
2. **Perform assembly and integration tests and analysis of the PPD.**
   - *Condition of achievement*: when the defined assembly and integration tests are performed according to the test method and procedure, and the success criteria is achieved.
3. **Perform prototype tests and inspections of the PPD.**
   - *Condition of achievement*: when the defined prototype tests are performed according to the test method and procedure, and the success criteria is achieved.
4. **Obtain, analyze, and document the data from all the test phases.**
   - *Condition of achievement*: when the obtained test data is saved on the computer, then processed with *Matlab* to show graphs or provide calculation results, and, lastly, backed-up on the server or external disk.
5. **Analyze and, if necessary, optimize the detailed design of PPD.**
   - *Condition of achievement*: when the inspections and analysis is documented, recommendations are provided, and the optimizations are created using CAD models, 3D printing or described in text.
6. **Document all the test plans, set-ups, and procedures for other researchers to be able to reproduce the tests.**
   - *Condition of achievement*: when all these items are documented and well described in the report.
7. **Verify and document the propulsion sub-system requirements.**
   - *Condition of achievement*: when the all of the tests and inspections are performed, their outcome analyzed, then a conclusion can be drawn whether the requirement is verifiable.
8. **Assess the tests and analysis, and provide the recommendations for further verification of the PPD design**
   - *Condition of achievement*: when all of the above sub-objectives are achieved and documented in the report.

1.3. Research Question

To help achieve the research objective and its sub-goals, the following research question is created:

What is the outcome of the Propulsion Payload Demonstrator detailed design verification by means of testing and analysis?

To help answer the main research question, smaller research questions (sub-questions) are generated:

1. **What are the possible issues of the PPD after performing the tests and inspections?**
2. **What is the success criteria of the tests?**
3. **What is the relation between the experimental data and analytical data?**
4. **How can the detailed design of the PPD be improved to meet the propulsion subsystem requirements?**

After answering the research question and reaching its objective, the thesis can be concluded and wrapped up.

1.4. Thesis Outline

The rest of the thesis is split into four chapters. Chapter 2 focuses on the background of the research done on the two microthrusters, PPD, and the verification process. A short summary is given on the latest research results of the LPM, VLM, and PPD at TU Delft. The methods of verification and its process is explained such that the reader would have a basic understanding how the verification is performed on the PPD. Furthermore, the overview of the propulsion sub-system requirements which need to be verified are given. After that, the overview of the intended tests is presented, which need to be performed to meet the propulsion sub-system requirements and research goals.

Chapter 3 contains the description of the test methodology, parameters, success criteria, and procedure of each test. The considered tests are split into 3 testing phases: *component*, *assembly and integration*, and *prototype*. The experimental set-up of each test is designed from the ground up and based on the findings of PPD described by *Turmaine* [3]. The leak test set-up is extensively described due to the fact that there was no previously leak tests performed in the clean-room at TU Delft. Similarly, the rest of the tests are explicitly described such that the reader has an in-depth understanding of the test set-ups and can be used as a guideline for the future tests.

In Chapter 4 the results of the tests, performed as described in Chapter 3, are presented and analyzed. Depending on the test outcome, some of the results analysis has been complimented by additional simulations and calculations. Actual parts have been 3D printed or manufactured to assist in the inspections. In this chapter all the information is gathered to answer the research questions and outline the conclusions.

Chapter 5 is for the performed thesis conclusions and the recommendations for the future testing and research on the PPD. It describes what has been achieved during this research, and how the research question has been answered. Furthermore, it presents the summary of the tests and simulations results, and gives the recommendations for the future investigation of *Delfi-PQ* PPD. These recommendations should be used as the basis for a more in-depth testing and understanding of the underlying issues, and for the tests which have not been performed as intended in the duration of this thesis.

2

Theoretical Background

In this chapter the theoretical background required to perform the design and verification of the Propulsion Payload Demonstrator (PPD) is discussed. In Section 2.1 an overview of the previous research done on the PPD, Vaporizing Liquid Micro-resistojet (VLM), and Low Pressure Micro-resistojet (LPM) is provided. In Section 2.2 the methods of verification and validation used in the aerospace industry are introduced. In Section 2.3 *Delfi-PQ* satellite propulsion sub-system requirements which can be verified by means of TEST and ANALYSIS are presented. Section 2.4 describes the tests, which are necessary to verify the propulsion sub-system requirements and its design. Finally, Section 2.5 presents the current detailed design of PPD.

2.1. Previous Research on PPD

After the introduction of *Delfi-PQ* as a new *PocketQube* mission, it presents an opportunity to integrate two different micro-propulsion thrusters into a single propulsion system and use them as the technology demonstrator (a.k.a. PPD) during the satellite's operation in space. The two micro-resistojet thrusters are LPM and VLM. To achieve such a combined concept, a high-level systems engineering on the PPD has been performed by *Turmaine* [3]. The in-depth research and design on LPM and VLM thrusters has been done by *Guerrieri* [1] and *Silva* [2], respectively. *Delfi-PQ* propulsion sub-system requirements are defined by *Pallichadath* [30].

First of all, a short description of each thruster in question is provided. In this way the reader gets familiarized with the micro-propulsion thrusters, which need to be demonstrated and around which design parameters the PPD concept is designed. The summary of the parameters of the latest optimal LPM thruster version is given in Table 2.1:

Table 2.1: Summary of the latest optimal LPM thruster version created by *Guerrieri* [1]

Parameter/Item	**Value/Description**
Power [W]	2 - 4
Thrust [mN]	0.5 - 1.09
Smallest heater chip area for the grid of slots [mm^2]	593.8
Smallest heater chip area for the grid of holes [mm^2]	676.6

Grid of circular channels (w/ 100 [μm] diameter hole) [-]	43x43
Grid of cuboid channels (w/ 100 [μm]x4,73 [mm] channel size) [-]	50x1
Grid of cuboid channels (w/ 100 [μm]x3.08 [mm] channel size) [-]	31x1
Minimum propellant mass [g]	11.5
Propellant tank shape	Pipe/tube
Propellant tank diameter [mm]	0.8
Plenum pressure [Pa]	50 - 300
Heater chip temperature	300 - 700
Type of propellant	Water and nitrogen
Type of interface material	Ceramic (To Be Corrected (TBC))

NOTE: Table 2.1 represents only the findings on LPM thruster for a *PocketQube* type of mission, because *Guerrieri* [1] has also performed a research on LPM design for *CubeSat* applications. Therefore, the results for a *CubeSat* mission application are not included, since this thesis focuses only on the pico-satellite class, such as *PocketQube*, applications.

The power values in Table 2.1 are needed to heat up the thruster chip and provide energy to the rarified molecules of the propellant. The thruster should achieve 0.5 - 1.09 [mN] thrust at vacuum conditions. There are currently two options of the heater configuration: circular (holes), and slots (cuboid channels). The minimum heater chip area and the configuration of the slots is presented in Table 2.1. The graphical representation of the heaters and their configuration is provided in Figure 2.1:

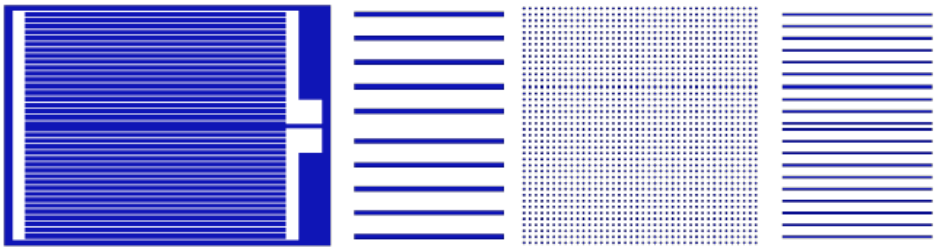

Figure 2.1: LPM heaters (white area) and slots (blue lines or dots) configurations (Picture credit: [1])

LPM is designed to be used with water and nitrogen as the propellants. An innovative propellant tank concept is introduced. Instead of using a conventional tank design, for example, a rectangular box or a spheroid, a pipe or a tube with a very small inner diameter of 0.8 [mm] can be used. 11.5 [g] of a propellant is necessary to achieve the required performance. The required pressure inside the plenum of the thruster is sub-atmospheric and is in the range of 50 - 300 [Pa]. The design parameters introduced in Table 2.1 create a solid design basis to create a PPD concept.

Next, the description of the second micro-resistojet design, VLM, is presented. The following summary of the parameters of the latest optimal VLM thruster version is given in Table 2.2:

Table 2.2: Summary of the latest optimal VLM thruster version created by *Silva* [2]

Parameter/Item	**Value/Description**
Plenum pressure [bar]	4.8 - 5.15 (measured at steady state)
Chip temperature [K]	423.03 - 425.65
Mass flow rate [mg/s]	0.55 - 0.83
Measured power [W]	7.29 - 8.76
Efficiency [%]	20.2 - 27
Nozzle throat area [m^2]	1- $5 \cdot 10^{-9}$
Nozzle exit area [m^2]	$5 \cdot 10^{-8}$
Area ratio [-]	10 - 50
Shape of heater channels	Diamond or Serpentine
Shape of the nozzle	Long (L), Wide (W), Bell (B)
Calculated thrust [mN]	0.67 - 0.98
Calculated specific impulse [s]	119.8 - 124.02
Type of propellant	Water
Validated thrusters	01-LS1-01 01-BS2-01 01-Ld1-01 01-WD2-01

The acquired values in Table 2.2 are determined either from testing or calculations. All of them are under the assumptions of ambient conditions. The ranges of the parameters in the table represent the four validated thruster chips. These chips are considered operational and can be investigated further. VLM uses only water as the propellant in this case. By looking at the required higher end of plenum pressure, chip temperature, and power ranges, they can be considered as the upper design limit for the future PPD concept. All the chips use two distinct shapes of the heaters: *diamond* and *serpentine*, which are shown in Figure 2.2:

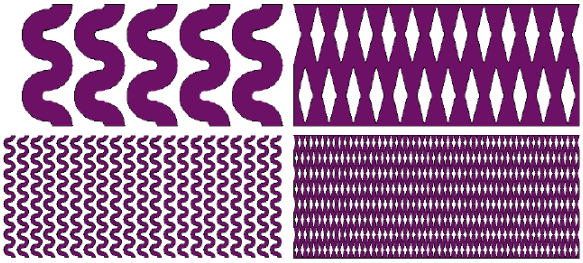

Figure 2.2: VLM heater channel configurations: big serpentine (Top Left), small serpentine (Bottom Left), big diamond (Top Right), and small diamond (Bottom Right) (Picture credit: [2]

Currently, LPM and VLM micro-thrusters use the following housing interfaces, which are purposely made for the testing in the laboratory:

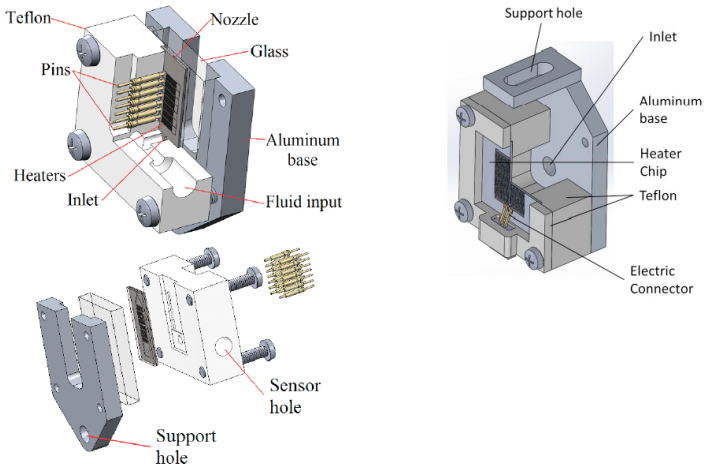

Figure 2.3: Breakdown of the VLM thruster interface (Left. Picture credit: [2]) and LPM thruster interface (Right. Picture credit: [1])

Each of the interfaces are produced from *Teflon* material and have special metal brackets such that both micro-resistojets can be tested on the thrust bench. More specific details about these interfaces are provided in Chapter 3. Both, VLM and LPM, are used as a basis for the design of *Delfi-PQ* PPD by *Turmaine* [3]. After using systems engineering approach, a prototype of a detailed design of PPD is created:

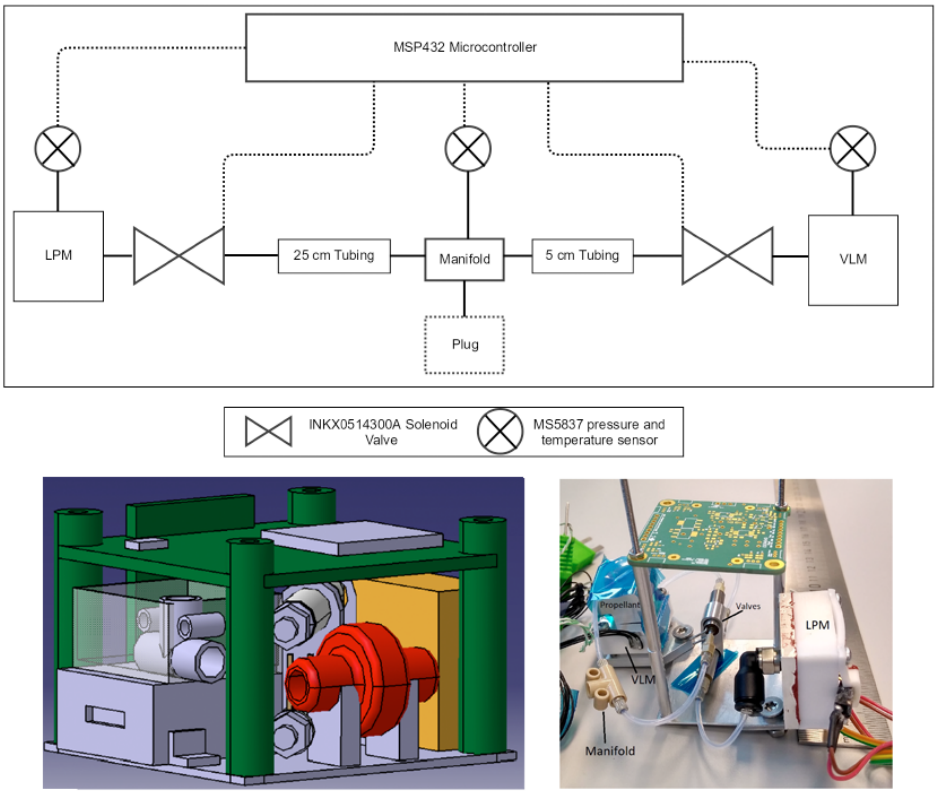

Figure 2.4: Block diagram (Top), *Catia* CAD model (Left), and part of the assembly of the PS prototype (Right) (Picture credit: [3])

The concept is unique in its ability to utilize a single propellant feed system for the two thrusters. Figure 2.5 shows a schematic principle of *Delfi-PQ* propulsion sub-system operations:

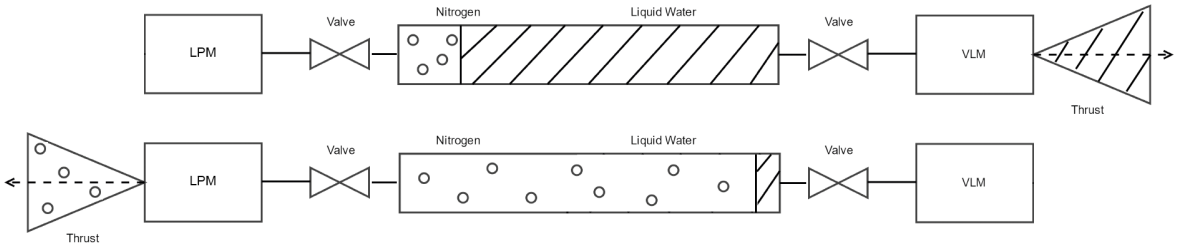

Figure 2.5: VLM thruster operational mode (Top). LPM thruster operational mode (Bottom). The sequence of the thruster demonstration is as follows: VLM is fired first, and then LPM is fired

To arrive at such a functional design, the performance parameters have to be determined. The so called *Final Operational Envelope* (FOE) was produced by *Turmaine* [3]. The values of FOE parameters are based on the minimum vaporization temperature needed to vaporize water inside the chamber of VLM. Thus, it affects the amount of water and nitrogen needed inside the tank to achieve such a goal. While the nitrogen is used as a pressurant for the water, at the end, the same nitrogen is used to operate LPM. The summary of the FOE parameters and the design details of the PPD is presented in Table 2.3:

Table 2.3: Summary of *Delfi-PQ* PPD thruster research done by [3]

Parameter/Item	**Value/Description**
Commercial Off-The-Shelf (COTS) components	*The Lee Co*
Type of component connectors	062 MINSTAC (0.138-40 UNF)
Propellant tank shape	Tube
Tank and feed tube inner diameter [mm]	1.57
Water tank tube length [cm]	25
Nitrogen tank tube length [cm]	5
Solenoid valve to thruster tube length [cm]	5
Volume of the propellant tank tube [cm^3]	0.581
Total mass of the propulsion system [g]	70
VLM heater efficiency [-]	0.6
VLM vaporization temperature [K]	600
Initial N_2 pressure in the tank [bar]	1.1
LPM propellant mass [g]	0.2
LPM thrust time [s]	200
LPM mass flow rate [mg/s]	1

VLM propellant volume fraction in tank [-]	$0.12V_{tube}$
VLM thrust time [s]	1200
LPM propellant pressure [bar]	0.201
Estimated VLM thrust [mN]	0.12 - 5.8

As the first concept of PPD is provided, it has to adhere to the given propulsion sub-system requirements. To achieve that systems engineering verification and validation approach is implemented. A detailed explanation of it is given in Section 2.2.

2.2. SE Verification & Validation Approach

According to *NASA Space Flight Program and Project Management Handbook* [31], the verification is:

- *A procedure to perform a check that the product adheres to its requirements and specifications.*

The validation, according to the same handbook [31], is:

- *A procedure to show that the product achieves the needs and expectations of the client.*

For the purpose of this thesis, the stress is only put on the verification of the PPD design. In general, there are four verification methods [5]:

- TEST
- ANALYSIS
- DEMONSTRATION
- INSPECTION

According to European Cooperation for Space Standardization (ECSS) [32], INSPECTION method falls under TEST, and DEMONSTRATION (can be also formulated as REVIEW OF DESIGN (RoD)) falls under ANALYSIS method for the propulsion system verification. Thus, only TEST and ANALYSIS is required to be used as the verification methods in this thesis. Since the proposed testing campaign by *Turmaine* [3] focuses on testing various aspects of *Delfi-PQ* propulsion sub-system aspects, TEST is the main verification method used in this thesis. For the clearness of the report, INSPECTION and Review of Design (RoD) methods are left in the overview of the requirements section (see Section 2.3), which were used by a previous student. However, in order to test something, a model has to be created. There are four types of models [5]:

- Physical
- Graphical
- Mathematical
- Statistical

For this thesis mainly a physical model is used. However, the physical model can be represented in many various forms. Those forms can be as follows:

Table 2.4: Various forms of the physical model representation used for the test method [5]

Type	Purpose	Representation	Application
Artist's impression	Visual representation	Geometrical configuration	Showcase
Mock Up (MU)	Visual representation; validation of integration process; accommodation control; architecture analysis; assessment of integration analysis	Geometrical configuration; layouts; mechanical interfaces	Showcase; aid of integration procedures
Breadboard (BB)/ Development Model (DM)	Development support, confirmation of the design feasibility	selected to-be-tested functions (e.g. mechanical, electrical, thermal or other)	development tests
Suitcase	Complete simulation of the communications system; compatibility tests with ground stations; interface tests; fault mode analyses	Full functionality of the flight model; commercial components allowed	Qualification, compatibility, component level, and system level tests
Integration Model (IM)	Functional and (electrical and software) interface tests; error mode analysis; software development; validation of procedures	Full functionality in the Hardware (HW) and Software (SW), but realization only with commercial components	Development tests; all verification levels
Structural Model (SM)	Structure qualification; FEM validation	Flight standard regarding the structural parameters	Qualification tests
Thermal Model (TM)	Qualification of the thermal design; validation of the thermal model	Flight standard regarding thermal parameters	Subsystem level (thermal control system); partial system level; qualification level
Structural Thermal Model (STM)	SM and TM objectives	Standard w.r.t. structural and thermal parameters	System level; qualification tests
Engineering Model (EM)	Functional qualification of fault tolerance	Flight representative in form, fit, function	All levels; partial functional qualification tests

Engineering Qualification Model (EQM)	Functional qualification of the design and interfaces	Full flight model	All levels; functional qualification tests
Qualification Model (QM)	Design qualification	Full flight design and flight standard	Components and subsystem level; qualification tests
Protoflight Model (PFM)	Flight application; qualification of the design	Full flight design & flight standard	All levels; prototype qualification tests

To have a fully functional and according to the propulsion requirements propulsion sub-system, the PPD has to go through all the types of the physical models, used for testing, in Table 2.4. Since it is the first iteration of *Delfi-PQ* propulsion sub-system design, MU and DM models are considered for the testing at this moment. The main reason for choosing only these two models is that the current PPD design is based on high-level systems engineering. This means that the requirements provided by *Pallichadath* [30] are only applicable for MU and DM models. After testing these two models, it is expected to gain more information and data on how the propulsion system is performing and what are the issues. This extra information and data can be used to create the other physical models. MU models are required because it is very critical to verify if the whole propulsion system fits in the required space inside the satellite and doe not exceed the maximum required mass. Furthermore, MU model helps to identify the issues of the components integration and their interaction between each other. DM model is necessary for the tests of the system performance at various conditions. These tests are mainly performed in the clean-room and require a usage of test equipment such as various sensors, measuring tools, and data processing hardware. Moreover, during DM model tests only specific parts of the propulsion system are tested alone, which require the system's set-up literally using the breadboard.

In order to verify the design of PPD through means of testing, a certain verification process has to be followed. The typical product verification process found in literature is shown in Figure 2.6:

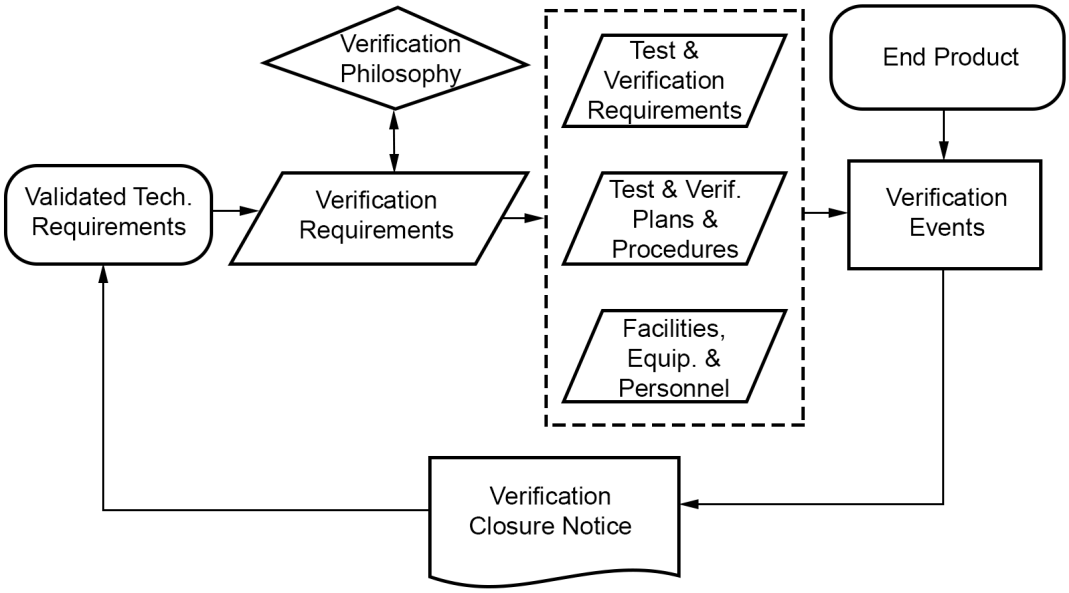

Figure 2.6: Product verification process found in literature [5] [6]

The procedure shown in Figure 2.6 can be easily applied to any technical requirement, in this case it would be propulsion sub-system requirements defined by *Pallichadath* [30].

2.3. Overview of the Requirements

After the verification method is selected, a summary of the consolidated propulsion sub-system requirements, which need to be verified by a test, is presented. This overview is based on the work by *Turmaine* [3] and cross-checked with the technical report from *Pallichadath* [30]. Table 2.5 helps to define and design the tests needed to be performed in order to verify the given requirements. Some of the requirements have undetermined values as indicated by To Be Determined (TBD). These undetermined values might be defined from the outcome of the tests or, for example, the analysis of the design.

Table 2.5: Summary of the requirements to be tested and inspected

Identifier	Requirement	Verification Method
PROP-SYST-100	The total wet mass of the propulsion system at launch shall not be higher than 75 [g].	Inspection
PROP-SYST-200	The total size of the propulsion system shall be within 42 [mm] x 42 [mm] x 30 [mm] (including thrusters, valves, electronics board, harness, connectors & propellant storage tube).	Inspection

PROP-SYST-210	The system shall adhere to the following distance specifications: Maximum component height above PCB: 4 [mm], Maximum component height below PCB: 27-28 [mm], Board spacing distance: 32-33 [mm], Pin insert depth: 4.6-5 [mm] and 3.6-5 [mm], Total stacking height: 33.6-34.6 [mm].	Inspection
PROP-SYST-300	The peak power consumption of the propulsion system during ignition or heating shall be not higher than 4 [W] and duration shall not be longer than <**TBD**> [s] per day.	Test
PROP-SYST-400	The maximum amount of propulsion system data that can be stored in the memory storage unit on board the satellite is <**TBD**> [GB].	Test
PROP-PERF-200	The thrust provided by the propulsion system shall be 3 [mN] as a maximum.	Test
PROP-PERF-210	The thrust provided by the propulsion system shall be at least 0.12 [mN].	Test
PROP-PERF-300	The maximum leak rate shall be <**TBD**> at maximum operating pressure.	Test
PROP-PERF-400	The micro-propulsion system shall operate on a single unregulated supply voltage of 3 [VDC] to 4.1 [VDC].	Review of Design, Test
PROP-FUN-100	The micro-propulsion system shall have at least two modes: idle with max. power consumption 15 [mW] and full thrust with max. power consumption 4 [W].	Review of Design, Test
PROP-FUN-200	The thruster shall be able to operate on gaseous N_2, as well as on liquid H_2O.	Review of Design, Test
PROP-FUN-300	The feed system shall operate in a normally closed configuration.	Review of Design, Test

PROP-FUN-400	The micro-propulsion payload will be turned off if the system is not undergoing any type of demonstration/operations and also when the propellant storage tank is empty.	Review of Design, Test
PROP-FUN-500	The propellant storage shall be left empty when the micro-propulsion payload demonstration is completed.	Test
PROP-INT-200	The thermal interface between the propulsion system and the satellite shall allow for the propulsion system components to stay in a temperature range between +5 ^{o}C and +85 ^{o}C during all the mission phases when propulsion system operations are required.	Inspection, Test
PROP-INT-400	The data exchange interface between the propulsion system and the satellite shall be RS-485 with a data transfer rate of <**TBD**> [bit/s].	Test
PROP-INT-500	The propellant storage system shall allow for filling and draining the propellants at any time when the fully assembled satellite is still accessible to human operators.	Test
PROP-RAMS-200	The internal pressure of all the propulsion system components shall not be higher than 10 bar	Review of the Design, Test
PROP-RAMS-400	A thermal vacuum bake-out of the propulsion system shall be carried out before launch to ensure a proper out-gassing of all the components.	Review of Design
PROP-RAMS-500	All external parts of the thruster shall be electrically grounded.	Review of Design
PROP-ERL-200	The maximum axial and lateral accelerations that the propulsion system shall withstand during the launch are as described in M. Boerci (2017) [33].	Test

PROP-ERL-300	The maximum vibration levels at the point of attachment of the satellite during the launch are as described in M. Boerci (2017) [33].	Test
PROP-ERL-400	The maximum acoustic pressures and loads that the propulsion system shall withstand during the launch are as described in M. Boerci (2017) [33].	Test
PROP-ERL-500	The maximum flight shocks that the propulsion system shall withstand during the launch are as described in M. Boerci (2017) [33].	Test
PROP-ERL-700	The maximum heating of the nose fairing during the launch is as described in M. Boerci (2017) [33].	Test
PROP-ERL-800	The maximum pressure changes inside the fairing that the propulsion system shall withstand during the launch are as described in M. Boerci (2017) [33].	Test
PROP-ERL-900	The micro-propulsion subsystem shall be compatible with the vacuum and temperature levels of the space environment in Low Earth Orbit.	Test

Some of the requirements have both REVIEW OF DESIGN RoD and TEST as the verification methods. For the RoD method part it is only needed to check if it can meet the requirements from previous tests and assumptions or calculations. To verify the detailed design of the PPD and meet the propulsion requirements, a test campaign is suggested. The proposed test campaign by *Turmaine* [3] is split into phases:

- Component Testing
- Assembly and Integration Testing
- Prototype Testing
- Flight Model Testing

The test campaign is structured to follow a chronological order, meaning the first testing phase begins with the *Component Testing* followed by the *Assembly and Integration Testing*, then the *Prototype Testing*, and, finally,the *Flight Model Testing*. For the current thesis workload *Flight Model Testing* phase is omitted.

2.4. Test Campaign

Each of the testing campaign phases mentioned in the previous section have a certain number of tests which need to be executed. A concept of this campaign has been created during the last phase of systems engineering process by *Turmaine* [3]. However, all of the tests in that campaign were designed on a basic level. It means some of the information was mainly based on the indications of how the experiments should be performed and what outcome should be expected.

2.4.1. Test Adjustments

A more detailed definition of the tests is provided in this section. To begin with, a component test called *TEST-COM-01: Valve Test* was proposed as a first test to be performed by *Turmaine* [3]. It has two purposes:

- Check the leakage and pressure specifications of the valve in the vacuum
- Check Pulse Width Modulated (PWM) signal capabilities of the valve for LPM operation in vacuum

The test focuses around the solenoid valve, but there are two completely different purposes which need to be checked. After inspecting the rest of the tests, it is noticed that there is another test concerning the check of the leakage. It is in the *Assembly and Integration Testing* phase, under the name *TEST-INT-01: Fill & Leak Test* [3]. It has four purposes:

- Find a leakage rate over time
- Define an acceptable leakage rate
- Check propellant filling method if the proposed one can be used
- Decide if a check valve is needed and if it should be tested

TEST-INT-01 requires the testing of the filling method. It suggests two filling methods: one, with a slight over-pressurization and using a plug, second, with using a check valve. Using over-pressurization and plug method would not give accurate initial pressure and volume values to perform the test. During the over-pressurization there should be a very quick method to insert the plug in order to have sufficient gas left in the tank. Furthermore, over-pressurization method is very inaccurate. Every time the tank would be filled, the overshoot of the gas could be too high. Consequently, it would require either a drain valve or a drain method to balance the pressure inside the propellant tank. At this moment, the check valve is selected as a filling method, because check valve has a uni-directional flow latch and let's the filling process to be more accurate and delicate. Furthermore, there is no need of testing the check valve separately, because it is a Commercial Off-The-Shelf (COTS) component with all the predefined technical data by the manufacturer.

A newly re-defined TEST-INT-01 test is created. It only concerns the leakage related aspects. Its purpose is:

- Detect and locate the leak at various places of the propulsion system
- Find a leakage rate over time at ambient and vacuum conditions
- Define a maximum leak rate at maximum operating pressure

Since part of TEST-COM-01 is merged with TEST-INT-01, a separate component test is created to test PWM capabilities of the solenoid valve. Its purpose is:

- Determine the power consumption during the operation of the solenoid valve
- Characterize the required frequency, duty cycle, and voltage pulse duration for PWM mode at ambient and vacuum conditions
- Determine the coil resistance of the solenoid valve at various temperatures

The newly defined tests are assigned to their names, where code names should not be confused with the old ones:

- TEST-INT-01: LeakTest
- TEST-COM-01: Solenoid Valve PWM Test

After redefining the tests, their requirements which need to be verified are also adjusted accordingly. Those assigned requirements can be found in Table 2.6 and 2.7.

By inspecting the *Assembly and Integration* testing phase further, it is noticed that there is no test devised to verify PROP-SYST-100 and PROP-SYST-200 requirements. Therefore, another assembly and integration test is created and called:

- TEST-INT-02: Volume and Mass Test

Its purpose is defined as follows:

- Determine the actual mass budget of the propulsion system
- Assemble and integrate all Propulsion System (PS) components according to the requirements and design
- Characterize the underlying volume and mass issues

After redefining the original TEST-INT-01: FIll/Drain Test, there is no test to verify PROP-INT-500 requirement. However, there is also no fill/drain valve available for the PPD, at the moment. For the testing campaign it is suggested to use the check valve as a fill valve, and the draining is performed via the solenoid valve. Although, if ,for example, a fill/drain valve is designed, it would be wise to start testing it as a stand alone component. Thus, to verify PROP-INT-500 requirement, a new *Component* testing phase test is created under the name of:

- TEST-COM-02: Fill/Drain Valve Test

Consequently, extra two requirements should be additionally verified during this test: PROP-PERF-300 and PROP-FUN-300. The purpose of the test would be:

- Determine the number of fill/drain valves needed in the PS.
- Characterize its leakage.
- Integrate it with the rest of the components.
- The valve's accessibility should comply with the open ports available on the PocketQube side panels.

The rest of the test proposed by *Turmaine* [3] remain unchanged.

2.4.2. Overview of Planned Tests

After re-purposing and redesigning the initial tests, an updated list of the intended tests to be executed during this thesis is provided in Tables 2.6, 2.7, and 2.8. Each test contains a short description of the execution (how the test is going to be performed), the expected output, purpose of the test, expected hardware and software, and the requirements which will be verified with the help of these tests. Additionally, in Section 2.4.3, a planning and time indication of the tests is provided. The purpose of each test is translated to experimental set-up and described in detail in Chapter 3. The expected output and the requirements to be verified are explained in detail as the results analysis in Chapter 4.

Table 2.6: Consolidated Component Tests

Test Name	**TEST-COM-01: Solenoid Valve PWM Test**
Reqs. to be verified	PROP-SYST-300, PROP-SYST-400, PROP-SYST-500, PROP-FUN-100, PROP-FUN-300, PROP-FUN-500, PROP-INT-200, PROP-RAMS-200
Purpose	•Determine the power consumption during the operation of the solenoid valve. •Characterize the required frequency, duty cycle, and pulse duration for PWM mode at ambient and vacuum conditions. •Determine the coil resistance of the solenoid valve at various temperatures.
Expected output	•Nitrogen pressure in the propellant tank •Pressure in the plenum of LPM •Duty cycle of the PWM signal •Frequency required to generate PWM signal •Power consumption of the valve in PWM mode •Temperature effect on the valve coil resistance •Amount of data produced for its storage on the on-board memory storage unit
Execution	LPM interface is connected to PPD. N_2 is filled to the propellant tank at various pressures. At various duty cycle settings and pulse width modulation frequencies the solenoid valve is opened and closed to achieve target pressure in the plenum. Temperature and pressure data at various locations of PPD is obtained.
Required HW and SW	Software: *LabView*, *Arduino*, and *Tera Term*. Hardware: LPM interface and chip, PPD assembly, *MEGA 2560 R3* μController, N_2 General Purpose Feed System (GPFS), K-type thermocouples, MS5837-30BA and HCLA12X5DU sensor, NI USB-9162 Digital Acquisition (DAQ), power supply unit, IECX0501350AA spike and hold electrical driver, Personal Computer (PC), multimeter, vacuum oven
Test Name	**TEST-COM-02: Fill/Drain Valve Test**
Reqs. to be verified	PROP-FUN-300, PROP-PERF-300, PROP-INT-400
Purpose	•Determine the amount fill/drain valves needed. •Characterize its leakage. •Integrate it with the rest of the components.

	•The valve's accessibility should comply with the open ports available on PocketQube side panels.
Expected output	•Verification of pressurization method •Identification of filling process problems •Leakage rate at different pressures
Execution	Custom or COTS fill/drain valve is tested as a stand alone component. Filling and draining is tested at various pressure settings of N_2. A procedure of filling water and nitrogen is created and tested. Assembly and integration with the rest of the propulsion system components and system itself is tested. Comparison between check valve and fill/drain valve is performed. If draining is unfeasible through the fill/drain valve, an alternative method should be devised, e.g. solenoid valve.
Required HW and SW	Software: *LabView*, CAD. Hardware: PPD assembly, N_2 GPFS, de-mineralized water, MS5837-30BA sensor, NI USB-8451 and NI USB-6008 DAQ, power supply unit, PC, propulsion system cage and *Delfi-PQ* mock-up, vacuum oven
Test Name	**TEST-COM-03: VLM & LPM Test**
Reqs. to be verified	PROP-PERF-100, PROP-PREF-200, PROP-PERF-210
Purpose	•Check the operation of VLM & LPM thruster chips •Check for damage and blockage
Expected output	•Constant thrust level for a range of power and pressure values •Plot of thrust versus power input
Execution	All the operational VLM and LPM chips integrated in their interfaces and tested at cold and hot cases at ambient and vacuum conditions. Various pressure and temperature settings are used according to the design parameters. The performance is registered via micro-scope and thermal imaging cameras. After every run, the chips are compared to the initial run data. In the later stage of the test, the same chips are tested on the thrust bench. The most optimal performance chips should be selected for the consideration of the flight model.
Required HW and SW	Software: *LabView*, *Research IR*,*Dino-Lite Capture*. Hardware: VLM and LPM chips and interfaces, N_2 GPFS, de-mineralized water, water tank, mass flow sensor, MS5837-30BA sensor, NI USB-8451 and NI USB-6008 DAQ, power supply unit, *AE-TB-5m* thrust bench, vacuum oven
Test Name	**TEST-COM-04: Heater Efficiency Test**
Reqs. to be verified	PROP-FUN-100, PROP-SYST-300
Purpose	•Check the power transfer to VLM thruster heater and propellant •Verify the initial nitrogen pressure of 1.1 [bar] for 4 [W]
Expected output	•Heater efficiency for a given range of input power •Heater efficiency for a given range of chamber pressure •Graph of input power vs. chamber pressure

Execution	The operational VLM chips are tested in a fixed position at ambient conditions. A range of mass flow values are used to provide the water feed to the chip heaters. A maximum initial power is set to vaporize the water. The power is reduced at increments until the overflow in the chip is reached. The overflow is observed via the micro-scope camera. After finding the overflow conditions, the same chips are tested in the thrust bench to find the power and thrust magnitude relation.
Required HW and SW	Software: *LabView*, *Research IR*,*Dino-Lite Capture*, *MS Excel*. Hardware: VLM chips and interface, de-mineralized water, syringe pump, MS5837-30BA sensor, NI USB-8451 and NI USB-6008 DAQ, power supply unit, *AE-TB-5m* thrust bench, vacuum oven, *Dino-Lite* and *FLIR* cameras

Table 2.7: Consolidated Assembly and integration Tests

Test Name	**TEST-INT-01: Leak Test**
Reqs. to be verified	PROP-PERF-300, PROP-FUN-300, PROP-FUN-500, PROP-RAMS-200, PROP-RAMS-310
Purpose	•Detect and locate leaks at various places of the propulsion components •Find a leakage rate over the time at ambient and vacuum conditions •Define a maximum leak rate at a maximum operating pressure
Expected output	•Graphs of pressure change at various nitrogen pressures in the tank •Calculations of the mass, molar, and volumetric leak rate •Leak simulation model and leak orifice size determination •Type of flow determination
Execution	The whole PPD assembly is tested at ambient and vacuum conditions. Nitrogen and water is used as the pressurant. Test duration is 24 [h]. Various pressure settings in the tan are tested. If a leak is detected, a leak detection method is used to localize the leak hole/slit and determine the rate of leak.
Required HW and SW	Software: *LabView*. Hardware: PPD assembly, N_2 GPFS, de-mineralized water, MS5837-30BA sensor, NI USB-8451 and NI USB-6008 DAQ, power supply unit, vacuum oven, various leak detection tools, PC
Test Name	**TEST-INT-02: Volume and Mass Test**
Reqs. to be verified	PROP-SYST-100, PROP-SYST-200
Purpose	•Determine the actual mass budget of the propulsion system •Assemble and integrate all PS components according to the requirements and design •Characterize the underlying mass and volume issues
Expected output	•Improved actual design of PS •Preliminary and actual mass budgets

	•Outline of a further design optimization towards a flight model
Execution	The whole propulsion system of the latest design version is assembled and a fit check is performed for the given volume requirement. If the fit check is unsuccessful, design improvements are performed. The mass of various types of propulsion segments is checked: structural, electronics, and propulsion components. An updated and actual mass budget is created.
Required HW and SW	Software: CAD. Hardware: PPD assembly, scales, *Delfi-PQ* mock-up, 3D printer, PCB, spacers, cage, PC.
Test Name	**TEST-INT-03: Electrical & Software Test**
Reqs. to be verified	PROP-SYST-300, PROP-SYST-400, PROP-PERF-400, PROP-FUN-100, PROP-INT-100, PROP-INT-400
Purpose	•Check if RS-485 interface is functioning during the operation •Check the voltage and frequency output of *MSP432* μController due to the Electric Power Supply *EPS* unregulated voltage input •Test interface between the sensors and *MS432* μController
Expected output	•Confirmation of sufficient conversion and redirection of voltage to all components from *RS485* interface and *MSP432* μController •Verification of all requirements related to this test
Execution	*MSP432* μController is connected to the power supply to perform check of various sensors outputs and its own power supply to the valves, thruster heaters, and sensors. A code is written and uploaded to the μController such that it can send commands and receive data and voltage outputs from the instruments. *MSP432* should be able to store a certain amount of data bytes received from the sensors and down-link to the ground control. *MSP432* is tested if it can work within 4 [W] power budget. Its integration should not hinder other propulsion components.
Required HW and SW	Software: *Energia*, *Arduino*, *MatLab*. Hardware: fully functional PCB board, RS485 interface, power supply, multimeter, wiring, PC.

Table 2.8: Consolidated Prototype Tests

Test Name	**TEST-PRO-01: Vaporization Test**
Reqs. to be verified	PROP-FUN-100
Purpose	•Find the exact power and pressure at which the vaporization takes place
Expected output	•Output power versus vaporization temperature correlation for the required chamber pressure

Execution	A prototype of an advanced design iteration of VLM interface is tested at vacuum conditions. The latest version of the operational VLM chips are integrated and tested in the interface. All tests should be done at vacuum conditions and operational envelope values. The nitrogen is used as the pressurant and the water is used as the propellant. Temperature senors are implemented in such a way that can measure the heaters and the nozzle temperature
Required HW and SW	Software: *LabView*. Hardware: VLM chips and interface, PC, temperature and pressure sensors, GPFS, de-mineralized water, NI USB-8451 and NI USB-6008 DAQ, NI USB-9162 DAQ
Test Name	**TEST-PRO-02: Pressure Profile Test**
Reqs. to be verified	PROP-PERF-200, PROP-PERF-210
Purpose	•Verify the pressure profile over time to confirm the choice of acceptable initial pressure and volume of nitrogen
Expected output	•Experimental graph of pressure vs. time
Execution	The latest version of PPD prototype is tested at vacuum conditions. The previous data and issues are implemented in this test to determine the required N_2 amount and pressure level in the tank. The comparison between the theoretical operational envelope, previous tests and this test data is made. The test is performed at various pressure settings to create a pressure profile
Required HW and SW	Software: *LabView*. Hardware: PPD assembly, pressure sensors, NI USB-8451 and NI USB-6008 DAQ, power supply, PC, vacuum oven, GPFS
Test Name	**TEST-PRO-03: Mass Flow Profile Test**
Reqs. to be verified	PROP-SYST-200, PROP-SYST-210
Purpose	•Verify the mass flow profile over time to confirm the choice of acceptable initial pressure and volume of nitrogen
Expected output	•Mass flow versus time plot
Execution	A mass flow sensor is attached to the propulsion system in such a way that it can measure the mass flow during the operation of VLM and LPM thrusters. The operational values of both thrusters are set according to the previous tests outcomes or the operational envelope values. The test is also performed at various nitrogen pressure settings to create a mass flow profile
Required HW and SW	Software: *LabView*. Hardware: PPD assembly, pressure sensors, NI USB-8451 and NI USB-6008 DAQ, power supply, PC, vacuum oven, *MBrooks* mass flow sensor, GPFS
Test Name	**TEST-PRO-04: Thrust Profile Test**
Reqs. to be verified	PROP-SYST-200, PROP-SYST-210
Purpose	•Propulsion system will show that it can deliver a steady 0.12 - 3 [mN] thrust

	•Obtain thrust and mass flow values in order to determine specific impulse
Expected output	•Experimental graph of thrust vs. time •Thrust values for the calculation of specific impulse
Execution	First, VLM thruster is tested on the thrust bench, then LPM. The propulsion system is in a closed system configuration and should not hinder the measurements of the thrust. The whole test is performed at vacuum conditions. The whole PPD should be handled with utmost care to avoid influencing the state of the components or initiating a leak of the propellants
Required HW and SW	Software: *LabView*. Hardware: PPD assembly, pressure/temperature sensors, NI USB-8451 and NI USB-6008 DAQ, power supply, PC, vacuum oven, *MBrooks* mass flow sensor, GPFS, *AE-TB-5m* thrust bench, de-mineralized water

2.4.3. Test Campaign Plan and Schedule

In order to successfully complete this thesis and conduct the tests, a plan and schedule should be made. However, as the PPD is relatively new system which has no extensive tests performed on, there can be a lot of unforeseen issues with the system or tests themselves. Therefore, the test plan and schedule is cautiously devised. It is already indicated that the test plan contains of four phases: *Component*, *Assembly and Integration*, and *Prototype* tests. There are in total 11 tests to be performed. Since this thesis is planned for 7 months, as a first estimation the test preparation and testing should take 4 months, data processing and results analysis, should take 2 months, and the reporting of the work should take 1 month. Although, 1 month of the contingency is added for the unforeseen delays or even personal circumstances.

To have a better overview of the test campaign planning and the order of the tests, a high level Gantt chart is generated. The preliminary test campaign Gantt chart is shown in Figure A.1 and A.2. It is based on the time indications provided above in this section. The order of the tests follows the chronological order as provided in Table 2.6, 2.7, and 2.8.

Although, during this thesis, the testing campaign and its outcome is very different than it was intended. The actual test campaign plan and schedule is shown in Figure A.3. There the Gantt chart shows the actual order and duration of the tests performed in this thesis. It can be seen that there is a difference between the preliminary schedule and the actual one. From the planned 11 tests, 4 have been conducted. The order of the performed tests is also different than in the preliminary test schedule. TEST-INT-01: Leak Test is the first test to be performed. The reason to perform this test as the very first test is that the most important *The Lee* components were available at that moment to build the propulsion system. Otherwise, the missing components, which are required for *Components* testing phase, needed to be ordered and from the ordering experience these *The Lee* components take time to be delivered. Therefore, to minimize the time management and test schedule risks, TEST-INT-01 is the first test performed. The second reason to perform this test first, is that there was nothing known on how the whole integrated propulsion system would perform as a whole, because its assembly is required for *Components* testing phase. Furthermore, the preparation for this test is very long due to the knowledge transfer from other students, PhD researchers, and testing resources management. Such a trend can be seen in other 3 remaining tests. The second test is TEST-INT-02: Volume and Mass Test. It is decided to conduct this test during

the preparation and execution of TEST-INT-01. The reasons to perform this test are given in detail in Section 3.1.4. After these two tests, the first component test TEST-COM-01 TEST: Solenoid Valve PWM Test is performed. TEST-COM-02: Fill/Drain Test is skipped, because there were no fill/drain valve options available at the time and due to the outcome of TEST-INT-02 a further design optimization is needed to implement fill/drain valve in the propulsion system. TEST-COM-03: VLM & LPM Test is also skipped, because at that time there were no unused or intact VLM chips, which otherwise would affect the test results. Therefore, the last test performed in this thesis is TEST-COM-04: Heater Efficiency Test. Its purpose is to provide the preliminary power/pressure relations of the operational VLM chips. From the existing resources at the micro-propulsion group, the test is successfully conducted with almost enough time to finish this thesis within the planned time-line.

It can be summarized that the actual time it takes to prepare, execute the test, and analyze its results is much longer than anticipated. In the preliminary schedule it can be seen that the total required time to perform all tests is split almost equally between the tests. In the actual schedule the very beginning of the testing campaign is slow and the time is reduced for the last 2 tests. By comparing the two schedules, the timing is almost 5 to 10 times longer in some cases for the actual test plan. From the testing campaign experience performed for this thesis, it can be concluded that a very good preparation of the test is almost 80% of the total work. However, testing is very adaptive job, because some of the tests can be very unpredictable and require creative solutions to successfully perform them. For example, some of the tests are very incremental, which means that the outcome of one part of the test might influence the following part of the test. Thus, it can require re-purposing or a new preparation of the test.

2.5. Overview of the Physical Architecture

During the high level systems engineering design a physical architecture of the propulsion system was created. The architecture created by *Turmaine* [3] represents only the conceptual stage of the propulsion system. After gathering the required components and information on what is exactly needed for the testing campaign, the following physical architecture is built:

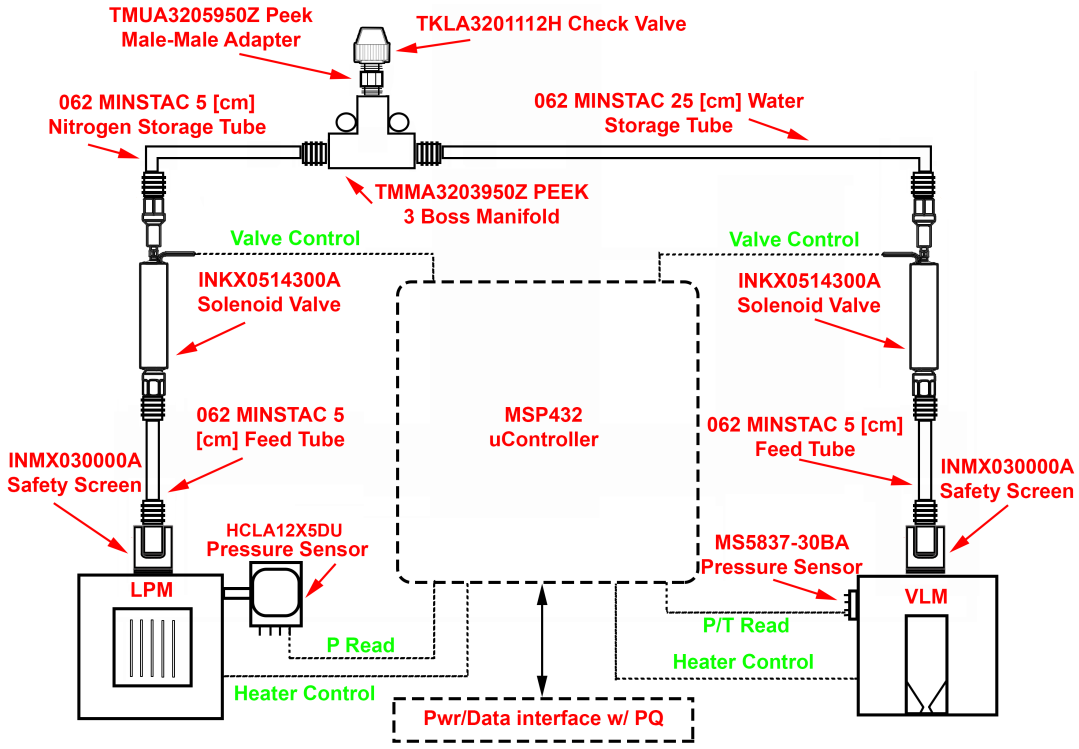

Figure 2.7: Updated physical architecture of the propulsion system for the purpose of the testing campaign

The μController is shown with the dotted lines, because it was not ready for the duration of this thesis. The physical architecture is used also as a guide to build the propulsion system for each test. All propulsion system components shown in Figure 2.7 are used during the testing campaign.

3

Experimental Set-Up

In this chapter the tests performed for each of the Component, Assembly and Integration, and Prototype testing phases of Propulsion Payload Demonstrator (PPD) are presented. Each of the tests contain a description of the methodology, test set-up, relevant parameters, success criteria, and test procedure. Such a test documentation and description structure is based on the information from [34] and [5].

3.1. Assembly and Integration Tests

In Section 2.4 it is stated that the first test to be performed for the verification of the PPD requirements is TEST-INT-01: Leak Test. This test is part of *Assembly and Integration Tests* phase. First, as a preliminary test it is decided to assemble the whole PPD system using the information according to [3]. Figure 2.7 is used as a reference graphics to help and assemble the components. Such a preliminary test gives an actual representation of the propulsion system and presents the initial assembly and integration issues.

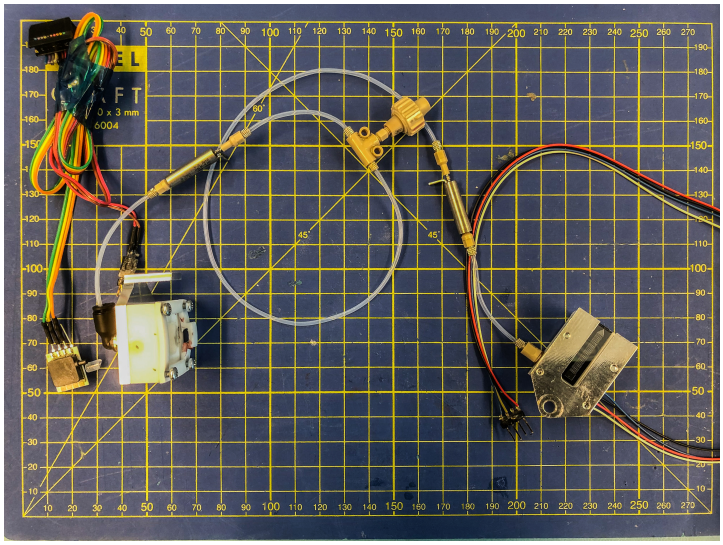

Figure 3.1: Assembled Propulsion System Demonstrator using *The Lee Company* components and clean-room version interfaces of LPM and VLM

The preliminary assembly results are shown in Figure 3.1. One of the assembly issues can be seen in Figure 3.1, where Low Pressure Micro-Resistojet (LPM) housing has a different tube interface than *The Lee* tube. Up-close view is shown in Figure 3.2:

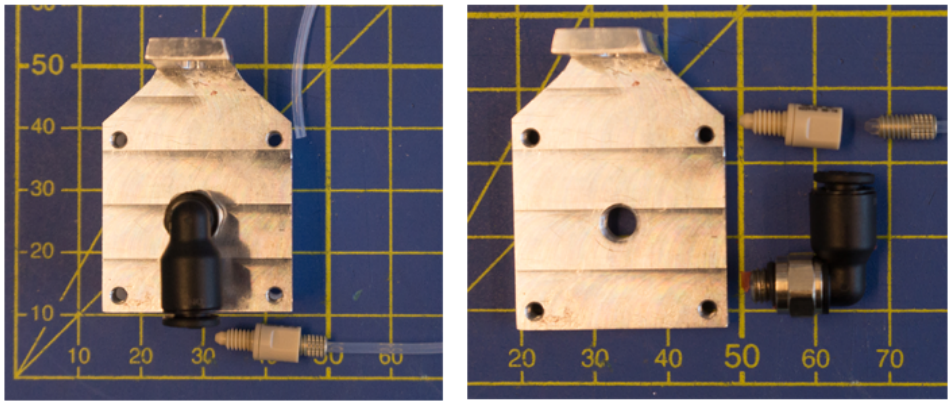

Figure 3.2: Up-close view of LPM thruster interface back plate, *Legris* elbow adapter (black part), and *The Lee* safety screen (beige part)

It uses *Legris* 4.5/32 push-in elbow fitting.and it has a 4.5/32 inches tube connection with M3 thread. For the testing purposes the M3 threaded hole in LPM interface needs to be replaced with .138-40 UNF-2B thread, which is used for all *062 MINSTAC* type *The Lee* parts. Further explanations on the LPM re-design can be found in Section 3.2.1. Moreover, an adequate tightening of *The Lee* tube spherules is required, because it is noticed while handling the rest of the propulsion system the tubes tend to unscrew easily. This issue is addressed in Section 3.1.1.

From the inspection of the propulsion system in Figure 3.1 and 2.7, it can be seen that only the propellant storage part is completely closed by the two solenoid valves and the check valve. The tubing which leads from the valves to the thrusters has open ends (it is not a closed system). As this would be a normal case in a real system in space, only the leakage at the connection points is worth checking to see if no propellant is leaking out during the thrusting mode. However, to check if the system does not leak in this case, it is decided to create a pressurized system and have no open ends. In this way a sort of ”pressurized vessel” is created. Therefore, the parts of the system where the tubes lead to the thrusters have to be somehow closed/blocked. To achieve this, it is decided to produce a special interface which replaces LPM and Vaporizing Liquid Micro-Resistojet (VLM) thrusters and is completely blocked. The blocking component in the interface would be a pressure/temperature sensor. A detailed explanation on how this is achieved is given in Section 3.1.2.

There are potentially three cases where leaks can occur from the preliminary assembly test explained above. One is between the two valves, a second one is between the LPM valve and its interface, and a third one is between the VLM valve and its interface. Therefore, it is decided to split TEST-INT-01: Leak Test into 3 parts according to each case. However, the leak tests between the thrusters and the valves are complimentary. They would give additional information on the components integration and their performance during the thrusting modes. The actual leak test and the focus of the test is put on between the two valves.

3.1.1. TEST-INT-01: Leak Test (Part 1)

As it is explained in Section 3.1, the first test of *Assembly and Integration* test phase is leak test between the two valves. In order to detect the leakage and quantify it, a leak detection and localization method must be selected first.

Methodology

A leak detection and localization is one of the most critical tasks of ensuring a successful performance of a system, which involves any liquid or gas storage, flow, and expulsion. At the micro-propulsion research group of *Space Engineering* department of Aerospace Engineering (AE) TU Delft, there has not been done any extensive in-house leak tests on any micro-propulsion system, yet. Therefore, during the design of the leak tests for *Delfi-PQ* PPD, there has not been much of a knowledge base on how to perform such kind of tests and characterize them. It is also noticed from the literature research, there is no substantial information on the satellite propulsion leak testing, but quite a few well described leak test methodologies in the chemical and food industry. Furthermore, the leak tests are even more challenging and difficult to perform on the micro-propulsion systems, because not all techniques used for the bigger systems can be applied. A short overview of the existing leak detection and localization methods is presented in this section. The overview covers mainly the space related leak testing methods.

According to [35], there are 14 leak test methods which National Aeuronautics and Space Administration (NASA) uses to verify leakage rate for spacecraft payloads. [36] presents 14 different state-of-art natural gas leak detection methods. Each of the methods is split into 3 groups: *hardware based*, *non-technical*, and *software based*. [37] presents in-depth process and results of a Helium (He) based *"sniffer"* method to detect and characterize the leak in the satellite propulsion system. [38] describes 9 leak detection and localization methods used for the satellite propulsion systems. As most of the leak detection and localization methods overlap, a summary of them is shown in a form of a list. Some of the methods can only be applied in vacuum. However, for example, not all techniques used by [36] can be applied for space related leak tests. Furthermore, not all space related leak methods can be applied for a micro-propulsion system, and are feasible or available at TU Delft. Therefore, the short-listed methods, which are space related and could possibly be applied for micro-propulsion systems, are shown. A method name, its short description, and advantages and disadvantages are provided:

1. *Mass Spectrometry* - it is based on introducing a tracing gas as a pressurant in the system. Helium gas is widely used for such a method, because it is a very small particle and is able to creep through very small spaces. Outside the pressurized system a He detector (a.k.a. a *sniffer*) is used to detect the leaking Helium gas. There are 2 mass spectrometry techniques: *vacuum* or *overpressure*. In the *vacuum* technique the air is sucked out of the system and a helium gas is sprayed around the outside of the system. The gas is being pulled-in to the system where the *sniffer* is installed inside the system [38]. *Overpressure* technique does the reverse. The system is filled with He gas and the *"sniffer"* is placed outside the system. The *overpressure* technique can be used in the vacuum chamber ([35] specifies that this method is used for total system leakage detection) or ambient conditions. **Advantages**: the leak can be detected and localized, relatively cheap, flexible and adaptable, reusable, non-hazardous. **Disadvantages**: only He gas can be used, requires equipment calibration, possible system contamination, instrument size limit, detector resolution, vacuum chamber might be required.

2. *Pressure Change* - it is based on the increase or decrease of the pressure inside the system over the time. The *pressure decrease* in the system appears when a system is filled with a gas at a higher pressure than the ambient. The gas leaks out to the ambient over the time and this pressure drop is registered by a pressure sensor inside the system. The *pressure increase* in the system appears when a system has a smaller internal pressure than the ambient. The gas/air starts flowing into the system through a leak and the pressure sensor registers a pressure change over the time in the system [35] [38]. **Advantages**: relatively cheap, theoretically any gas can be used, a single pressure sensor is required. **Disadvantages**: test can be lengthy time-wise, test data depends on the sensor accuracy, only leak detection possible (no localization), manipulation of the system or extra parts needed to integrate the pressure sensor, pressure data needs to be processed.

3. *Mass Loss* - it is based on the initial and final mass of the system. The system is weighed with the pressurant/propellant inside it. The test is initiated for a determined timespan. When the test is over, the system is weighed again. The final mass is registered. The difference between the initial and final mass indicate a possible leak. Mainly used for the battery leak. A vacuum chamber might be required to verify the total seal of the system [35]. **Advantages**: simple testing equipment required, simple data processing. **Disadvantages**: no leak localization, accurate scales required, very good scales calibration.

4. *Immersion (Bubble)* - it is based on completely submerging the pressurized system in a transparent container with a transparent liquid and observing for any visual bubbles creeping out of the system. It is a non-quantitative method to localize a leak. Most of the time a water is used as a control liquid to capture the escaping bubbles. The system can be filled with any desired gas as long as it is has a higher pressure than the ambient. For the observation purposes the container should be well lit and the opposite side of the observer should have a dark background. This helps to spot the emerging bubbles easier [35] [38]. **Advantages**: very cheap, easy to implement, leak detection. **Disadvantages**: some components need to be protected from the liquid, trapped air in the component can be mistaken for the leak, bubble propagation can be very slow and undetectable, inaccurate, not all observation angles are possible.

5. *Foam Application* - it is based on applying a special liquid, which creates foam, on the intended surface of the payload to check for the leaking gas. The payload is pressurized with, for example, nitrogen [35]. This method is also called *Bubble* method, similar to the mentioned one above in the list [38]. It is also called *Soap Bubble Screening* [36]. **Advantages**: leak localization, cheap, quick. **Disadvantages**: the foam disintegrates relatively fasts, the payload requires cleaning, non quantitative method.

6. *Hydrostatic/Visual Inspection* - it is based on filling the system with a translucent non-reactive fluid and reaching a slightly higher internal pressure than the ambient. The external surfaces of the system are cleaned and dried of any liquid or moisture. The system is placed under well lit location. The observer uses his eyes to observe of any creeping liquid from the inside of the system onto the surfaces of it [35] [38]. **Advantages**: cheap, easy implementation, leak localization. **Disadvantages**: non quantitative, requires protection of some components from the liquid contact, requires good lightning, due to liquid viscosity some leaks are not visible immediately.

7. *Optical* - there are *active* and *passive* optical methods. *Active* methods are omitted due to the fact that they are meant for industrial gas infrastructures. *Passive* methods are thermal imaging, multi-spectral imaging, and gas filter correlation radiometry [36].

Thermal imaging involves measuring the difference in temperature between the leaking gas and ambient. *Absorption* and *emission* mode are used in Multi-spectral imaging. *Absorption* mode utilizes a gas at different wavelength concentration map created by an absorption of the background radiation. *Emission* mode is similar to *Thermal* imaging method. Gas filter correlation radiometry uses a spectral filter. The radiation enters two cells in the detector through a narrow band-pass filter. One is filled with the interested gas and the other cell is empty. The spectral filter at the filled cell removes the energy at the wavelengths of the absorption lines of the gas [36]. **Advantages**: some methods have very good instrument resolutions, leak localization, quantifiable **Disadvantages**: most of the methods are really expensive, complex to implement, not applicable to all systems or gases.

8. *Conservation of mass* - is based on physics. The amount of mass inside the system at the beginning and at the end of the test is equal to the leaked amount of gas. This method is used not only to detect the leak, but also to predict the leak in the future. **Advantages**: leak detection, quantitative, estimation of the leak, fast. **Disadvantages**: no leak localization, can be expensive to implement, requires high resolution scales.

Since there is no leakage data or any leak test performed on PPD, a first step is to detect any leak in the system. If a leak is detected, a second step is to localize the leak. Therefore, for both steps an adequate method has to be chosen to successfully conduct these leakage tests:

Leak Detection Method: it is decided to use *Pressure Change* method for all 3 parts of TEST-INT-01: Leak Test. The reason behind this choice is that the current set-up of the DAQ and the equipment in the clean-room is easily adaptable to the purpose of this test. Furthermore, there is a surplus of the pressure sensors and their interfaces from the previous tests, which can be used to integrate them in the propellant storage tubes. Furthermore, such use of the existing components would reduce time and money costs for the whole PPD development project.

Leak Localization Method: It is decided to use *Immersion (Bubble)*, *Foam Application*, and *Mass Spectrometry*, *Hydrostatic/Visual Inspection*, and *Optical* methods. *Foam Application* is used first, then *Immersion Bubble* is used as a second method, *Mass Spectrometry*, *Hydrostatic/Visual Inspection*, and *Optical* methods are implemented separately, but the order of implementation depends on the availability of the tools and time management. A *Foam Application* method is used because nitrogen gas can be observed escaping the system. Any PoI (ref. Figure 3.3 orange arrows) can be sprayed with the foam forming liquid, and there is already a soap liquid *Electrolube The Solutions People* flask (ref. Appendix C) available in the clean-room. An *Immersion (Bubble)* method is chosen, because the whole propulsion system can be filled with nitrogen gas, which can be observed in the water if it is leaking to the ambient. Moreover, it is an easy to implement, and cheap method and all the necessary equipment is available in the clean-room and Space Systems Engineering (SSE) department. A *Mass Spectrometry* is chosen because helium is a very small particle which can escape through gaps easier than the nitrogen gas. Furthermore, there is Helium (He) ”sniffer” available from the *Applied Sciences* faculty, which can be borrowed free-of-charge. A *Hydrostatic/Visual Inspection* method is chosen, where a slight alteration is used. Instead of pressurizing the propulsion system with a liquid, it is decided to use a fog/smoke. This fog/smoke can be created by using CO_2 ice in the water. It is expected that by pressurizing the system with such a smoke it would leak into the ambient and the leak location can be registered. Furthermore, for no cost the dry-ice can be obtained at *Logistiek & Milieu* building at TU Delft. For the *Optical* method a thermal *FLIR* camera is used. By pressurizing the system with a lower temperature gas than the ambient temperature, it is expected to observe via the thermal camera the cold

gas escaping and disturbing the air outside the system. The observed phenomena is called *convection*.

Test Set-Up

In order to assemble the system for the intended test and for the chosen leak detection method, necessary components, tools and equipment is required. A full list of all of them is given in Table 3.1:

Table 3.1: List of components, tools and equipment needed for TEST-INT-01: Leak Test (Part 1)

Component/Tool Name	Amount	Description
TKLA3201112H check valve	1	It is used to fill the water and nitrogen into the propellant storage area, and keep the propellants in a closed system configuration
TMMA3203950Z-3-Boss manifold	1	It is used to connect the propellant tubes and the check valve adapter
IECX0501350AA spike and hold electrical driver	1	To provide power and control solenoid valve
INKX0514300A solenoid valve	2	These both valves will be used as the blocking elements to keep both of the propellants in a closed system configuration
TMUA3205959Z male-male adapter	2	One of the adapters is used in connecting the check valve to the T-shape manifold. The other adapter is used to connect to the pressure sensor's interface specially made for this test.
5 [cm] MINSTAC 0.062 Tubing w/ 0.138-40 UNF interface	1	This tube is connected from the LPM valve's inlet to the pressure sensor interface.
25 [cm] MINSTAC 0.062 Tubing w/ 0.138-40 UNF interface	1	This tube is connected from the T-shape manifold to the inlet of the VLM valve.
TTTA3201243A Torque Wrench	1	It is used to tighten all 0.138-40 UNF threaded adapters in the system
Pressure sensor wiring	-	These cables are connected from the pressure sensor to the DAQ board to acquire the pressure data.
Valve wiring	-	These cables are connected to valve control box and power supply to provide 24 [VDC] hold voltage and to open/close the valve to drain the propellant (if necessary).
MS5837-30BA sensor	1	This pressure sensor is integrated in the pressure sensor interface. It is used to measure the propellant storage pressure.

Flat bottom small pliers	1	They are used to prevent the valve from rotating when the tubes are tightened in the intlet/outlet of the valve.
De-mineralized water bottle	1	This water is used as a propellant for VLM
Nitrogen gas	-	This gas is used as the pressurant and propellant for LPM. Nitrogen gas is provided by the GPFS.
Microsyringes 2.5 [ml] H series TLL Glass Polytetrafluoroethylene (PTFE) Seal Luer Lock syringe	1	The syringe is used to fill the water to the propellant system.
General Purpose Feed System (GPFS)	-	It is used to fill nitrogen into the propellant storage system in a controlled way and provide a fixed pressure value of the gas.
PTFE or Silicon tube for the fill adapter	2	It is used to attach the fill adapter to the syringe or GPFS
1.65 [mm] Outer Diameter (OD) syringe needle with Luer lock	1	It is used to attach the syringe and the silicon tube.
Vacuum oven: *Heraeus Vacutherm*	1	This is where all the DAQ and sensor cables are connected to the PC. Air can be sucked out to create vacuum conditions. It can also measure the ambient pressure.
National Instruments (NI) *LabView* software and code	1	It is used for creating the code to obtain the data from the pressure sensor, controlling the valve, and saving data in a file.
Data Acquisition (DAQ) devices	2	These devices are used to digitize the measured data and send it to *LabView* software. The DAQ used: NI Universal Serial Bus (USB)-8451 and NI USB-6008.
Support rig or hook	1	It is used to hang the propulsion system vertically and prevent the water flowing to the nitrogen tube.
E030-10 and D030-10 Power Supply Units	2	They are used to provide spike and hold voltages for the solenoid valves.
ADAM Highland Portable Precision Balances: HCB 123	1	They are used to weigh the propulsion system at various stages of the test.

Using Figure 2.7 and Table 3.1, the following assembly for *Part 1* test is shown in Figure 3.3:

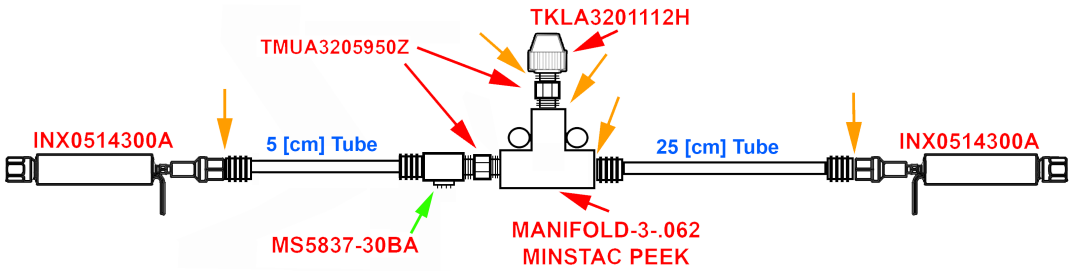

Figure 3.3: Schematic representation of the leak test set-up for TEST-INT-01: Leak Test (Part 1). Orange arrows are Point of Interest (PoI)

The orange arrows in Figure 3.3 represent the PoI between the two connecting components where a leakage might occur. The green arrow represents a location of a pressure/temperature sensor (*MS5837-30BA*) and its interface to measure the pressure of the nitrogen gas during the testing. Initially, it was proposed to manipulate *MANIFOLD-3-.062 MINSTAC PEEK* part in such a way that *MS5837-30BA* sensor fits inside the manifold. The reason behind this decision is that at this spot only N_2 gas will be present and no extra connection points are created. Furthermore, the water will be directed to the right side of the manifold and the nitrogen will occupy the left side of the manifold. A cross-sectional view of *MANIFOLD-3-.062 MINSTAC PEEK* is given:

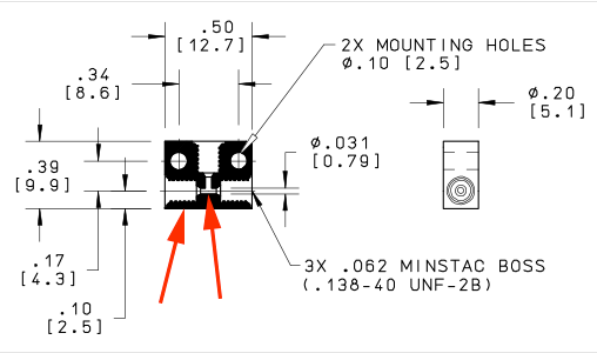

Figure 3.4: Cross-section view of MANIFOLD-3-.062 MINSTAC PEEK [39]. Possible locations of the P/T sensor are indicated by the red arrows

The red arrows in Figure 3.4 show the possible location where the pressure sensor can be incorporated. After inspecting *MANIFOLD-3-.062 MINSTAC PEEK*, it is decided to not manipulate it. If the sensor is integrated at the location shown by the left red arrow in Figure 3.4, the pressure sensor might block the flow of the nitrogen to the 5 [cm] tube due to its very small orifice diameter. Furthermore, the structural integrity of the manifold might be weakened a lot. At the second red arrow location on the right of Figure 3.4, the pressure sensor is too close to the inlet of the 25 [cm] water tube. It might be contaminated with a water during the filling. It could also block the manifold orifices or even break it. Another solution to integrate the pressure sensor is to make a dedicated interface for it.

An initial design of such an interface was done by *Turmaine* [3] and can be seen in Figure 3.5:

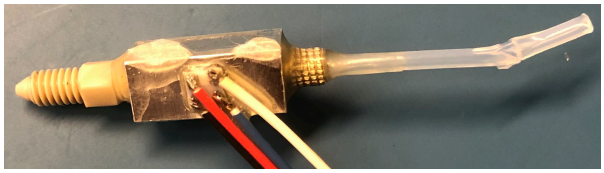

Figure 3.5: Aluminium interface of the P/T sensor. *The Lee* components are connected from both ends

It can be seen that the interface is connected to the *062 MINSTAC* tube and *TMUA3205950Z* male-male adapter. The interface is not an official *The Lee* part and is custom made at Delft Aerospace Structures Materials Laboratory (DASML) workshop. In theory, those two points would become extra two PoIs and increase a chance of a leakage. Since the interface is only used during the testing, the connections points are not considered as PoIs. The connection points on the interface are sealed hermetically at all times to avoid creating any extra leaks in the system. On the other hand, the other end of *TMUA3205950Z* adapter is tightened to the *MANIFOLD-3-.062 MINSTAC PEEK* without any glue, to able to re-use T-shape manifold if necessary. *TMUA3205950Z* adapter is also the official *The Lee Company* part so it is assumed to be leak proof by tightening it only mechanically to *MANIFOLD-3-.062 MINSTAC PEEK* according to the instructions. Furthermore, it is already known that 5 [cm] and 25 [cm] tubes have the same type of *062 MINSTAC* adapters to connect to the T-shape manifold in the actual system set-up. Therefore, for this leak test part it is assumed that the PoI on the 25 [cm] tube side will act the same as on the 5 [cm] tube side.

On the right side of Figure 3.5 can be seen that the tube is damaged and cut-off. It is decided to replace that tube with a new 5 [cm] tube. The removing of the old tube from the interface damaged the adapter and interface threads. At that moment, it was decided to make a new pressure sensor interface. Since there is no CAD drawing of the pressure sensor interface shown in Figure 3.5, a completely new one is re-drawn:

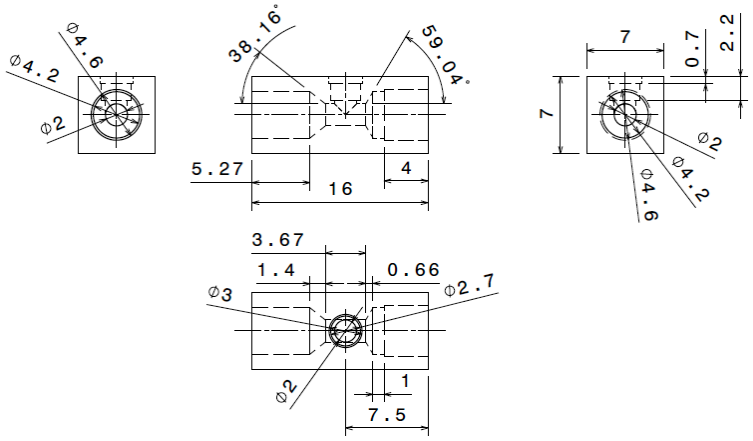

Figure 3.6: CAD drawing of the new pressure sensor interface

In this case, two different materials are used. One interface is made from teflon, and the second one is made from aluminium. Teflon is chosen, because it is more elastic than aluminium, which makes it is easer to tighten the threaded parts and seal them better.

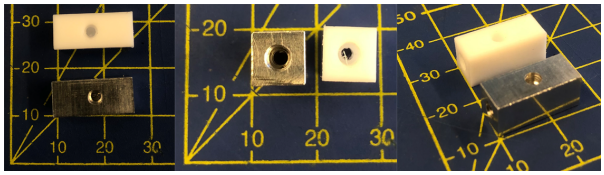

Figure 3.7: Teflon and aluminium pressure/temperature sensor interfaces

First, the pressure/temperature sensor has to be installed. The hole to put the sensor in is shown in Figure 3.7 on the left. *MS5837-30BA* sensor is a Surface-Mount Device (SMD) component, where the sensing part is enclosed in a metal case as it can be seen in Figure 3.8:

Figure 3.8: MS5837-30BA sensor without the wires showing the metal round case

At the moment of placing the sensor on the interface, there was no written procedure or manual on how to install it. Therefore, to glue and hermetically seal the sensor in the interface, the following procedure and tools are used:

1. The user should wear purple latex gloves, which are provided at the change room before entering the clean-room.
2. The teflon or aluminium interface and the metal case of the sensor has to be de-greased by using *PROSAT presatured wipes PS-911 (70% IPA 30 % DI water)*.
3. To bond the metal case with the teflon interface, *Kombi Metaal Colle Epoxy Lijm* by *Bizon* has to be prepared according to the manufacturer's instructions.
4. Using pointy tip swab found in the clean-room, a small amount of the metal epoxy is applied on the thicker metal ring (the one closer to the PCB *see Figure 3.8*) of the sensor.
5. The ring is gently inserted into the interface and pressed with the finger so that it snugs perfectly in the hole.
6. After the metal epoxy hardens, an additional layer of *Loctite EA3421* epoxy by *Henkel* is applied on top of the sensors and interface and left to harden according to the manufacturer's instructions. This way an extra layer of seal is created.

The tools and materials used in this process can be found in Appendix B. Although, all the steps were followed in the given procedure, certain issues surfaced after installing the sensor in the interface. There was a drop of the *Loctite* epoxy on the side of the teflon interface and it peeled off without applying any excessive force. It means that the epoxy did not bond with teflon. Then, a second issue was the de-lamination of the pressure sensor from the interface. It happened during a check run in the vacuum oven while pressurizing PPD with N_2 gas. The glued and de-laminated sensor is shown in Figure 3.9:

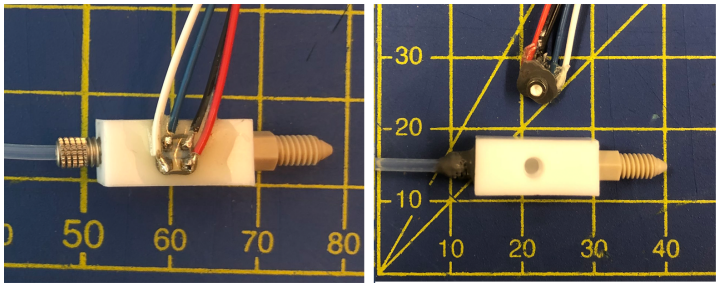

Figure 3.9: Glued (left photo) and de-laminated (right photo) MS5837-30BA sensor and the pressure teflon interface

The re-gluing of the sensor has failed 2 times following the same procedure. At this moment, it is decided to use the aluminium interface. The gluing of the tube's adapter in the aluminium interface is achieved by using only *Kombi Metaal Colle Epoxy Lijm* by *Bizon*. However, the tube itself, which is made from PTFE material, did not bond with the metal epoxy. After consulting with the employees at DASML workshop, a special glue with the primer used for PTFE products (as well as for other teflon products) was ordered. The procedure of gluing PTFE based part is as follows:

1. The surface of PTFE part and the part it needs to be glued on to has to be de-greased with an alcohol. The same *PROSAT presatured wipes PS-911 (70% IPA 30 % DI water)* are used for this step.
2. PTFE part's surface is primed 3-4 times with *MR PE/PP Primer* according to the provided instructions.
3. *MR Industriekrachtlijm* is applied on the primed surface according to the provided instructions. Additional layer of the same glue can be applied after 10 min for extra certainty. The glued parts are left to harden according to the manufacturer instructions.

The PTFE primer, glue and their respective manuals can be found in Appendix B (NOTE: *MR Industriekrachtlijm* has to be kept in the fridge at all times when not in use. It is done to prevent the glue degradation and gradual hardening over the time). The same gluing procedure as given above is used to place a new pressure sensor in the teflon interface. The glued tubes and both interfaces are shown in Figure 3.10:

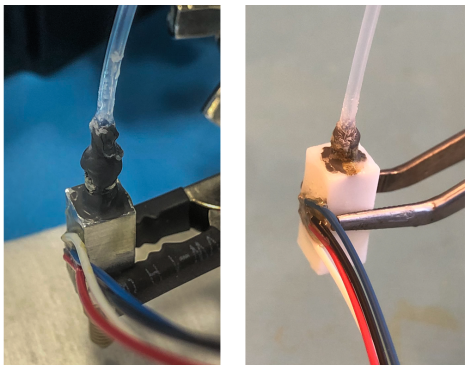

Figure 3.10: 5 [cm] tubes glued to Aluminium (left) and teflon (right) interface together with MS5837-30BA sensor

The whole assembled system ready for leak test as shown in Figure 3.3 is given below:

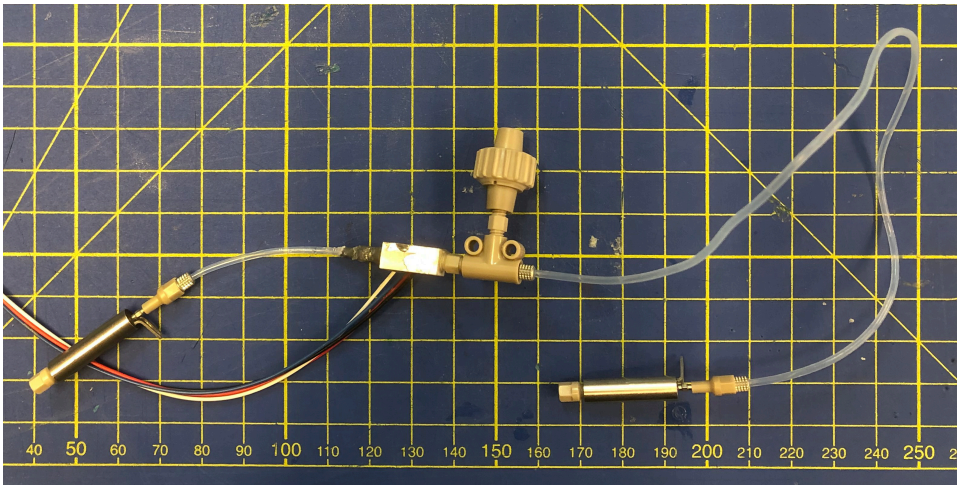

Figure 3.11: The assembled components of the system for TEST-INT-01: Leak Test (Part 1)

Parameters

In order to quantify the test results and able to process the collected data, certain parameters need to be either measured, defined by a user, or calculated. Some of them need to be noted by the user before and/or after the test. The parameters involved in this test are:

Table 3.2: Parameters involved in TEST-INT-01: Leak Test (Part 1)

Parameter	Dimension	Description	Range
$P_{st,0}$	[bar]	Initial propellant storage pressure before testing. Fully pressurized with N_2 gas and filled with H_2O.	*Controlled parameter*: 5 [bar] (just below 5.17 [bar] max. pressure of the check valve), 2.2 [bar] (max. initial pressure from the theoretical values by [3]), 1.1 [bar] (final oper. envelope value by [3]). *Accuracy*: ±0.1 [bar], however, it should preferably be on the plus side of the accuracy. This way the required values can reached and overpressure can be discarded. Except for the maximum 5.17 [bar], which should be as close as possible to 5 [bar].
$P_{st,t}$	[bar]	Propellant pressure measured during the leak test. Dependant on the testing time.	*Independent parameter*: defined by a leakage in the system. *Accuracy*: $\pm$30 [mbar] (from the technical data sheet of the sensor [40])

$P_{st,F}$	[bar]	Final pressure at the end of the measurement/testing (last data point)	*Independent parameter*. Final value, depends on the leak rate. *Accuracy: the same as* $P_{st,t}$
$M_{PS,dry}$	[kg]	Mass of the propulsion system without any propellant	*Controlled parameter*. Weighed every time before filling with the propellants. *Accuracy*: ±0.003 [g] (from the technical data sheet of the scales [41])
M_{PS,H_2O}	[kg]	Initial mass of the water in the propellant storage	*Controlled parameter*. Weighed every time after filling with water. *Accuracy: the same as* $M_{PS,dry}$
$M_{PS,0}$	[kg]	Total initial mass of the propulsion system after filling with the propellants. The mass of N_2 can be calculated from this parameter value.	*Controlled parameter*. The PS is weighed every time before testing. *Accuracy: the same as* $M_{PS,dry}$
$M_{PS,F}$	[kg]	Final mass of the propellant system after the testing. Here only the mass of the whole system is valid, because it will be hard to measure how much water was lost or N_2 gas.	*Independent parameter*. The PS is weighed right after the test. It depends on how much N_2 or H_2O has leaked. *Accuracy: the same as* $M_{PS,dry}$
t_L	[s]	Test/leak time. The time elapsed while acquiring the test data.	*Controlled parameter*. The test duration is set to at least 86 400 [s] (24 [h]). *Accuracy*: can be overshot of 24 [h] by few minutes or a couple of hours. The overtime can be discarded easily. The tester notes down every start of the test and calculates the end time of the test. *Accuracy*: Not Applicable (N.A.)
$V_{H_2O,0}$	[m^3]	Initial volume of the water in the propellant storage tube.	*Controlled parameter*. Range: 0.05 - 0.2V_{tube}. *Accuracy*: Filled with the amount of water calculated from [3], it is checked that the water is filled exactly from end to end of the tube and now air bubbles are trapped. *Accuracy*: N.A.

$V_{H_2O,F}$	$[m^3]$	Final volume of the water in the propellant storage tube.	*Independent parameter*. Depends on how much H_2O has leaked. *Accuracy*: N.A.

Success Criteria

The test success criteria is introduced in order to conclude if the test has succeeded, is completely executed, and the system itself is working. The following success criteria for this test is defined:

Table 3.3: Success criteria of TEST-INT-01: Leak Test (Part 1)

Criteria	Description
SC-TAI01-01	Parameters from Table 3.2 are obtained and documented
SC-TAI01-02	t_L is not interrupted and fully implemented
SC-TAI01-03	*.lvm* files from *LabView* are saved and backed-up
SC-TAI01-04	The components which are only part of the testing phase do not create any leakage

Test Procedure

Another important part of the experimental set-up is the test procedure. It helps the user to follow the steps in a chronological order, perform specific tasks at each step, and by noting down the execution time helps to back log if some unexpected issues arise. The TEST-INT-01: Leak Test (Part 1) procedure is as follows:

Table 3.4: TEST-INT-01: Leak Test (Part 1) procedure

Step	Sub-Step	Description	Performed (Y/N)	Time Stamp
1.		Verify that all the components are present from the Test Set-up section		
2.		Turn on the equipment to let it warm up (a certain stable temperature is required)		
	2.1	Turn on the *E030-10* and *D030-10* Power Supply Unit (PSU) and check that *E030-10* shows 24 [V] and *D030-10* shows 3 [V] (PSU warm-up time: 1 [h])		
	2.2	Turn on the computer next to the vacuum oven and log in. The current login is ".*localadmin*" and the current password is < CHECK AT THE PC IN THE CLEAN-ROOM>		
	2.3	Connect the USB hub in the vacuum chamber to PC, which connects the *NI-USB-6008* (*NI-USB-9262*) and *NI-USB-8451* DAQ		
3.		Assemble the propulsion system components:		

	3.1	Connect *INKX0514300A* (LPM) valve to the 5 [cm] *MINSTAC 0.062* tubing with *0.138-40 UNF* interface. Use *TTTA3201243A* torque wrench to tighten the tube: available torques are 0.035 [Nm] and 0.07 [Nm]. Possibly higher torques might be required. Use flat bottom pliers to hold the inlet/outlet of the valve while tightening the tube.
	3.2	Connect pressure sensor interface to *TMUA320590Z* adapter. The tightening torque is between 0.035 - 0.07 [Nm]. Most likely the *TMUA320590Z* adapter is fixed in the interface with the glue.
	3.3	Connect pressure sensor interface with the *TMUA320590Z* adapter to one of the in-line inlets of the *TMMA3203950Z* manifold. The tightening torque is between 0.035 - 0.07 [Nm]. It is possible that gluing is necessary (only for testing purpose).
	3.4	Connect the second *TMUA320590Z* adapter to the inlet perpendicular to the in-line inlets of the *TMMA3203950Z* manifold. The tightening torque is between 0.035 - 0.07 [Nm].
	3.5	Connect *TKLA3201112H* check valve to the *TMUA320590Z* adapter. The tightening torque is between 0.035 - 0.07 [Nm].
	3.6	Connect 25 [cm] *MINSTAC 0.062* tubing with *0.138-40 UNF* interface to the second horizontal inlet of the *TMMA3203950Z* manifold. The tightening torque is between 0.035 - 0.07 [Nm]. Possibly higher torques might be required. **NOTE**: if a completely new torque wrench is used, it is possible at this point it is worn off, and a manual tightening is required.
	3.7	Connect 25 [cm] *MINSTAC 0.062* tubing w/ *0.138-40 UNF* interface to the second *INKX0514300A* valve. The tightening torque is between 0.035 - 0.07 [Nm]. Possibly higher (manual) torques might be required.
4.		Perform checks:
	4.1	Check if the pressure sensor is connected to the right pins on the breadboard.
	4.2	Check if the solenoid valve is connected to the correct cables.

	4.3	Open *LabView* code called "*main\marsil\TEST\wDisplacementSensor.vi*". Choose the correct directory to save the measured data. Run the code and check if the pressure sensor data is coming in, then open and close the valve (click sound is produced). Stop the code and close *LabView*. **NOTE**: if an error is produced during this check, the user has to troubleshoot it himself
	4.4	Check if N_2 supply bottle has enough of pressurized nitrogen gas. This can be done, first, by opening the valve of N_2 bottle, then, line-in rotary valve, and reading the pressure sensor value. **NOTE**: if the pressure sensor needle shows 0 or very low values, the test should be stopped, and clean-room manager should be notified to replace the N_2 bottle with a new one.
5.		Fill the propulsion system with the propellants:
	5.1	Weigh the empty PS and write the mass value.
	5.2	Pour the de-mineralized water into a small beaker. Attach the syringe needle with the *TMDA3201950Z* adapter. Make sure there are no bubbles trapped in the syringe. Obtain X [ml] of water with the syringe. **NOTE**: there is always certain amount of water left in the needle and adapter after dispensing the water.
	5.3	Before filling the system with the water, make sure the propulsion system is placed correctly for this action. It means that the check valve should be pointing horizontally sideways, the 5 [cm] tube pointing upwards, and the beginning of the 25 [cm] tube should be pointing downwards. The rest of 25 [cm] tube at the valve location should be pointing upwards. The valve (connected to the 25 cm] tube) should be wired as in *step 4.2* and the same code used as in *step 4.3*.
	5.4	Open the valve using *step 4.3*. Attach the syringe set-up to the check valve and VERY SLOWLY dispense water. The opened valve during this process allows to escape the trapped air in the tube. Close the valve the moment the water reaches tube and valve connection point. **NOTE**: some air is allowed to be trapped in the system, at this moment. Remove syringe from the check valve and disconnect the cables from the valve.
	5.5	Weigh the PS and write down the mass value.
	5.6	Connect the pressure sensor as in *step 4.1* and connect LPM valve as in *step 4.2*. Same *LabView* code is used as in *step 4.3*. The rig and the PS should stay in the vacuum chamber.

	5.7	Attach *TMDA3201950Z* adapter with the cone adapter (it should be connected via a tube to the GPFS) to the check valve.
	5.8	Open N_2 bottle valve, then line-in rotary valve. Close N_2bottle valve. Open pressure regulator valve to obtain X [bar] pressure (the absolute pressure is X+1 [bar]). Open shut-off valve. Open the middle flow path selector. The pressure sensor should show X+1 [bar] in the *LabView* code. Close the flow path selector. Unscrew *TMDA3201950Z* adapter and release the remaining N_2 gas in the tube. If the pressure is higher than X+1 [bar], open the valve to release the pressure, let it reach X+1 [bar], and close the valve.
	5.9	Stop the code and close *LabView*.
	5.10	Weigh the PS and write down the mass value. Place PS back in the vacuum chamber.
6.		Leak testing:
	6.1	Re-open the *LabView* code immediately after *step 5.7*. Run the code and observe if the pressure changes. If the pressure is dropping at 0.005 [bar/sec] in the first minute of the test, there is an unacceptable leakage. The test should be stopped, the leakage should be localized and removed. Most likely the components need to be tightened better or sealed. If the pressure drops less than 0.005 [bar/sec] in the first few minutes, the test can proceed and be tested for t_L [s]
	6.2	If there is N_2 leakage as described in *step 6.1*, the same *steps 5.7 – 6.1* should be followed.
	6.3	If there is a water leakage as described in *step 6.1*, first, N_2 gas should be released via the *INKX0514300A* valve, then, follow *steps 5.4 – 5.10* should be followed.
7.		Stop the code and close *LabView* code. Find the stored data on PC, and make a copy of it to USB device. Always leave the original stored data file.
8.		Turn off all equipment (refer to *step 2* for all devices).
9.		Empty the vacuum oven out from all the test set-up.

3.1.2. TEST-INT-01: Leak Test (Part 2)

Part 2 of TEST-INT-01: Leak Test is detecting and localizing leaks between LPM thruster interface and its solenoid valve.

Methodology

Leak Detection Method: the same *Pressure Change* method is used as for TEST-INT-01: Leak Test (Part 1).

Leak Localization Method: the same leak localization methods are used as for TEST-INT-01: Leak Test (Part 1).

Test Set-up

Since this test set-up is very similar to TEST-INT-01: Leak Test (Part 1), only the additional components, tools or equipment are shown in the following Table 3.1. Furthermore, the components, tools or equipment which are excluded or reduced from this test are shown crossed-out in Table 3.5.

Table 3.5: List of components, tools and equipment needed for TEST-INT-01: Leak Test (Part 2)

Component/Tool Name	Amount	Description
TMUA3205959Z male-male adapter	~~2~~ 1	The adapter is used to connect the check valve to the T-shape manifold.
5 [cm] MINSTAC 0.062 Tubing w/ 0.138-40 UNF interface	~~1~~ 2	The first tube is connected between LPM valve inlet and T-shape manifold. The second tube is connected between LPM valve outlet and LPM blocked interface.
LPM blocked interface	1	It is used to connect a safety screen and insert a pressure sensor to create a closed system.
INMX0350000A 12 micron safety screen	1	Connects 5 [cm] MINSTAC 0.062 Tube to LPM blocked interface.
TechniRub O-ring	1	It is used to create seal between the safety screen and the blocked interface.

The test set-up for *Part 2* is shown in the following Figure 3.12. The orange arrows represent PoIs.

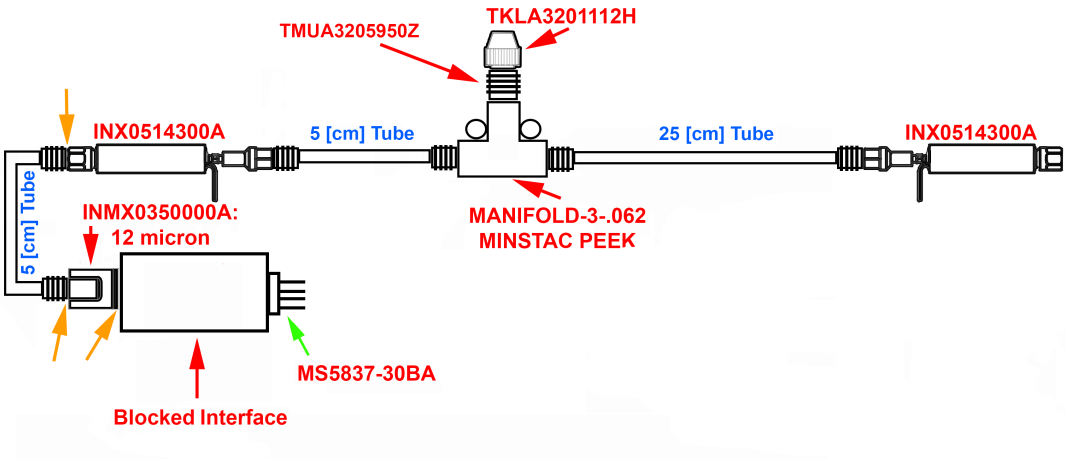

Figure 3.12: Schematic representation of the leak test set-up for TEST-INT-01: Leak Test (Part 2)

After defining all the necessary test components, the only extra part that is has to be made is the blocked interface. At the time of designing all three parts of the leakage tests, it is decided to make a single blocked interface from teflon which can be used for both *Part 2* and *Part 3* of TEST-INT-01: Leak Test. The design is based on VLM chip interface created by *Silva* [2]. The CAD drawing can be seen in Figure 3.13:

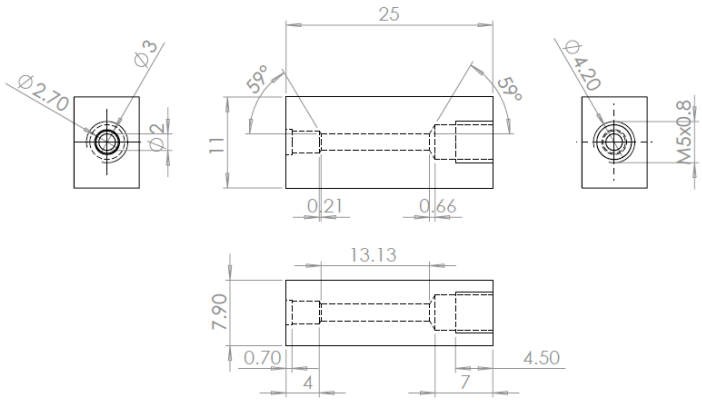

Figure 3.13: CAD drawing of the blocked interface

The same method and procedure for gluing *MS5837-30BA* sensor is used as described in Section 3.1.1 *Test Set-Up*. The final product is shown in Figure 3.14:

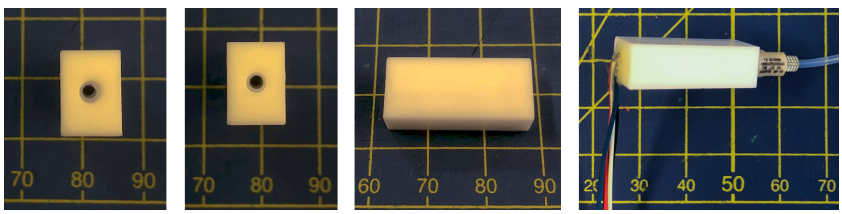

Figure 3.14: Manufactured and glued blocked interface

After completing the preparation of the components for the test, the propulsion system is as-

sembled and shown in Figure 3.15:

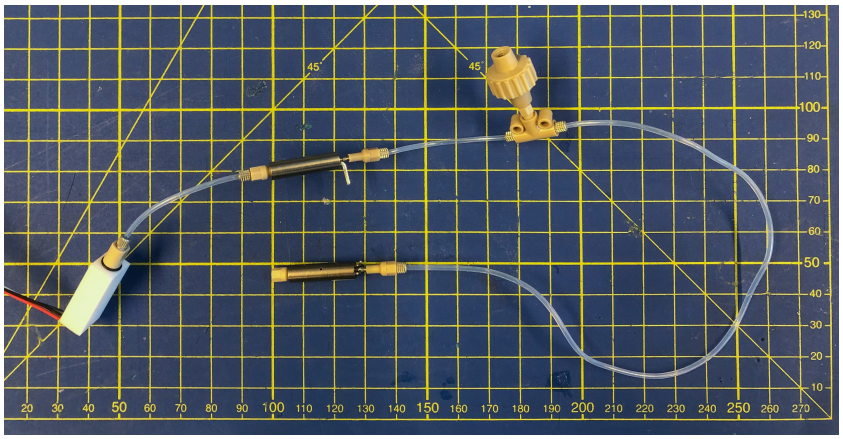

Figure 3.15: The assembled components of the system for TEST-INT-01: Leak Test (Part 2)

Using the components between the two valves are necessary for this test part, because the feed of the propellant from the tank can be represented as in the real case.

Parameters

The same parameters from Table 3.2 are used, but their values and descriptions are adjusted according to *Part 2* test requirements. The following table shows only the parameters which have been affected by this test, the rest of parameters from Table 3.2 are kept the same or are excluded in Table 3.6:

Table 3.6: Parameters involved in TEST-INT-01: Leak Test (Part 2)

Parameter	Dimension	Description	Range
$P_{st,0}$	[bar]	Initial propellant storage pressure before testing. N_2 gas is in 5 [cm] tube between the valve and interface. Possible mix of air and N_2 due to the test set-up.	*Controlled parameter*: 1.1 [bar] (Final Oper. Envelope value by [3]). *Accuracy*: $\pm$30 [mbar] (Tech. Data Sheet [40])
M_{PS,N_2}	[kg]	Initial mass of N_2 in the propellant storage	Controlled parameter. Weighed every time after filling with the nitrogen. *Accuracy*: ±0.003 [g] (Tech. Data Sheet [41])
$M_{PS,F}$	[kg]	Final mass of the propellant system after the testing.	Independent parameter. The PS is weighed right after the test. It depends on how much of N_2 has leaked. *Accuracy*: ±0.003 [g] (Tech. Data Sheet [41])

$V_{N_2,0}$	$[m^3]$	Initial volume of the nitrogen in the 5 [cm] tube and blocked interface.	*Controlled parameter*. Total volume of tube, safety screen, and interface plenum components. *Accuracy*: N.A.
$V_{N_2,F}$	$[m^3]$	Final volume of the nitrogen in the in the 5 [cm] tube and blocked interface.	*Independent parameter*. Depends on how much N_2 has leaked. *Accuracy*: N.A.

Success Criteria

The success criteria is the same as for TEST-INT-01: Leak Test (Part 1) and can be referred to Table 3.3.

Test Procedure

The test procedure is similar to TEST-INT-01: Leak Test (Part 1) procedure described in Table 3.4. As most of the steps are the same, only the adjusted procedure steps for this part are shown:

Table 3.7: TEST-INT-01: Leak Test (Part 2) procedure

Step	Sub-Step	Description	Performed (Y/N)	Time Stamp
1.		*Check Table 3.4*		
2.		*Check Table 3.4*		
3.		Assemble the propulsion system components:		
	3.1	*Check Table 3.4*		
	3.2	Connect the other half of the 5 [cm] *MINSTAC 0.062* tubing w/ *0.138-40 UNF* interface to one of the in-line inlets of the *TMMA3203950Z* manifold. The tightening torque is between 0.35 [Nm] - 0.07 [Nm]		
	3.3	Connect the second 5 [cm] *MINSTAC 0.062* tubing w/ *0.138-40 UNF* interface to the outlet *INKX0514300A* (LPM) valve and *INMX0350000A* safety screen. The tightening torque is between 0.35 [Nm] - 0.07 [Nm].		
	3.4	Connect the *TMUA320590Z* adapter to the inlet perpendicular to the in-line inlets of the *TMMA3203950Z* manifold. The tightening torque is between 0.035 - 0.07 [Nm].		
	3.5	*Check Table 3.4*		
	3.6	*Check Table 3.4*		
	3.7	*Check Table 3.4*		

	3.8	Add *TechniRub* O-ring on the *INMX0350000A* safety screen and screw it in the blocked interface inlet. The torque is adjusted accordingly. Teflon tape might be required for a better seal.
4.		*Check Table 3.4*
5.		Fill the propulsion system with the propellants:
	5.1	*Check Table 3.4*
	5.2	Connect pressure sensor cables as in *step 4.1* and connect LPM valve as in *step 4.2*. Open the same *LabView* code as in step *4.3*.
	5.3	Attach *TMDA3201950Z* adapter with the cone adapter (it should be connected via a tube to the GPFS) to the check valve.
	5.4	Open N_2 bottle valve, then line-in rotary valve. Close N_2bottle valve. Open pressure regulator valve to obtain X [bar] pressure (the absolute pressure is X+1 [bar]). Open shut-off valve. Open the middle flow path selector. The pressure sensor should show X+1 [bar] in the *LabView* code. Close the flow path selector. Undo *TMDA3201950Z* adapter and release the remaining N_2 gas in the tube. If the pressure is higher than X+1 [bar], open VLM valve to release the pressure, let it reach X+1 [bar], and close the valve.
	5.5	Stop the code and close *LabView*
	5.6	Weigh PS and write down the mass value. Place PS back in the vacuum chamber.
	5.7	*This step is removed*
	5.8	*This step is removed*
	5.9	*This step is removed*
	5.10	*This step is removed*
6.		Leak testing:
	6.1	Re-open the *LabView* code immediately after *step 5.6*. Run the code and observe if the pressure changes. If the pressure is dropping at 0.005 [bar/sec] in the first minute of the test, there is an unacceptable leakage. The test should be stopped, the leakage should be localized and removed. Most likely the components need to be tightened better or sealed. If the pressure drops less than 0.005 [bar/sec] in the first few minutes, the test can proceed and be tested for t_L [s].
	6.2	If there is N_2 leakage as described in *step 6.1*, the same *steps 5.4 – 6.1* should be followed.

	6.3	*This step is removed*
7.		*Check Table 3.4*
8.		*Check Table 3.4*
9.		*Check Table 3.4*

3.1.3. TEST-INT-01: Leak Test (Part 3)

Part 3 of TEST-INT-01: Leak Test is detecting and localizing leaks between VLM thruster interface and its solenoid valve.

Methodology

Leak Detection Method: the same *Pressure Change* method is used as for TEST-INT-01: Leak Test (Part 1).

Leak Localization Method: the same leak localization methods are used as for TEST-INT-01: Leak Test (Part 1).

Test Set-Up

Part 3 of TEST-INT-01: Leak Test has exactly the same set-up as *Part 2*. The only difference is that the blocked interface is connected to the VLM solenoid valve. Such a set-up is shown in Figure 3.16 (The orange arrows represent PoIs) and 3.17:

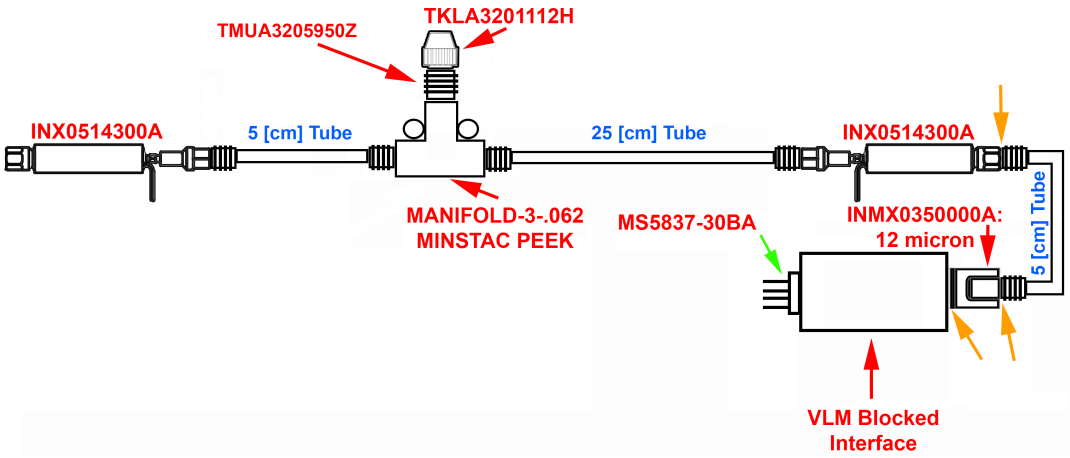

Figure 3.16: Schematic representation of the leak test set-up for TEST-INT-01: Leak Test (Part 3)

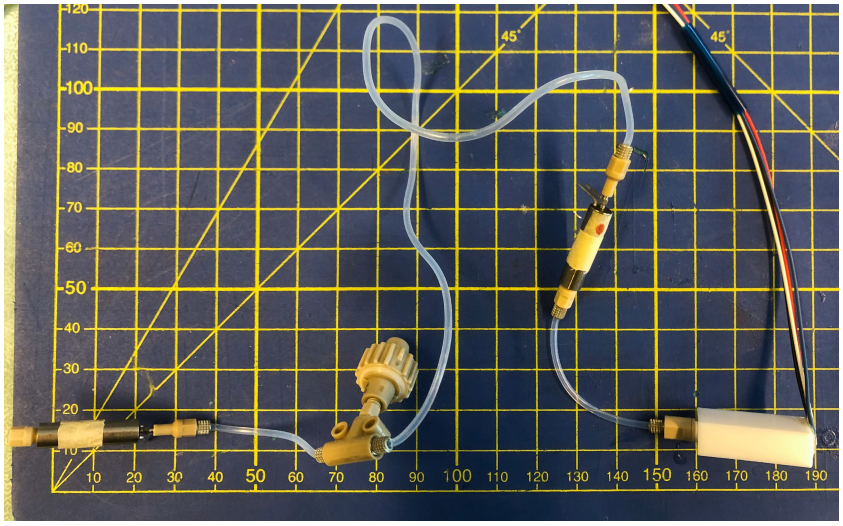

Figure 3.17: The assembled components of the system for TEST-INT-01: Leak Test (Part 3)

The components between the two solenoid valves are used for the same reasons as for *Part 2* test.

Parameters

Part 3 has a similar approach on determining the test parameters. The following Table 3.8 is adapted from Table 3.2:

Table 3.8: Parameters involved in TEST-INT-01: Leak Test (Part 3)

Parameter	Dimension	Description	Range
$P_{st,0}$	[bar]	Initial propellant storage pressure before testing. H_2O is in 5 [cm] tube between valve and interface. N_2 gas is in the rest of PS.	*Controlled parameter*. 1.1 [bar] (final oper. envelope value by [3]). *Accuracy*: $\pm$30 [mbar] (Tech. Data Sheet [40])
M_{PS,H_2O}	[kg]	Initial mass of H_2O in the propellant storage.	*Controlled parameter*. Weighed every time after filling with the nitrogen. *Accuracy*: ±0.003 [g] (Tech. Data Sheet [41])
$M_{PS,0}$	[kg]	Total initial mass of the propulsion system after filling with N_2 and H_2O. The mass of N_2 can be calculated from this parameter value.	*Controlled parameter*. The PS is weighed every time before testing. *Accuracy*: ±0.003 [g] (Tech. Data Sheet [41])

$M_{PS,F}$	[kg]	Final mass of the propellant system after the testing.	*Independent parameter*. The PS is weighed right after the test. It depends on how much of N_2 and H_2O has leaked. *Accuracy*: ±0.003 [g] (Tech. Data Sheet [41])
$V_{H_2O,0}$	$[m^3]$	Initial volume of the water n in the 5 [cm] tube and blocked interface.	*Controlled parameter*. Total volume of tube, safety screen, and interface plenum components. *Accuracy*: N.A.
$V_{H_2O,F}$	$[m^3]$	Final volume of the water in the in the 5 [cm] tube and blocked interface.	*Independent parameter*. Depends on how much H_2O has leaked. *Accuracy*: N.A.

Success Criteria

The success criteria is the same as for TEST-INT-01: Leak Test (Part 1) and can be referred to Table 3.3.

Test Procedure

The procedure steps are adapted from Table 3.4 and 3.7:

Table 3.9: TEST-INT-01: Leak Test (Part 3) procedure

Step	Sub-Step	Description	Performed (Y/N)	Time Stamp
1.		*Check Table 3.4*		
2.		*Check Table 3.4*		
3.		Assemble the propulsion system components:		
	3.1	*Check Table 3.4*		
	3.2	*Check Table 3.7*		
	3.3	Connect the second 5 [cm] *MINSTAC 0.062* tubing w/ *0.138-40 UNF* interface to the outlet *INKX0514300A* (VLM) valve and *INMX0350000A* safety screen. The tightening torque is between 0.35 [Nm] - 0.07 [Nm].		
	3.4	*Check Table 3.7*		
	3.5	*Check Table 3.4*		
	3.6	*Check Table 3.4*		
	3.7	*Check Table 3.4*		
	3.8	Add *TechniRub* O-ring on the *INMX0350000A* safety screen. Don't screw it on the blocked interface until *step 5.*		

4.		*Check Table 3.4*
5.		Fill the propulsion system with the propellants:
	5.1	*Check Table 3.7*
	5.2	*Check Table 3.4 step 5.2*
	5.3	Make sure the 25 [cm] tube, VLM valve, and 5 [cm] tube is pointing downwards. VLM valve should be wired as in step *Check Table 3.4 step 4.2* and the same code used as in *Check Table 3.4 step 4.3*
	5.4	Open the valve using *step 4.3*. Attach the syringe set-up to the check valve and VERY SLOWLY dispense water. The opened valve during this process allows to escape the trapped air in the tube. Close the valve the moment the water reaches safety screen. Remove syringe from the check valve and disconnect the cables from the valve.
	5.5	Fill blocked interface plenum with water using the same syringe.
	5.6	Screw the safety screen on the blocked interface. **NOTE** some water spill frpm the set-up is expected.
	5.7	Attach *TMDA3201950Z* adapter with the cone adapter (it should be connected via a tube to the GPFS) to the check valve.
	5.8	Open N_2 bottle valve, then line-in rotary valve. Close N_2bottle valve. Open pressure regulator valve to obtain X [bar] pressure (the absolute pressure is X+1 [bar]). Open shut-off valve. Open the middle flow path selector. Open VLM valve. The pressure sensor should show X+1 [bar] in the *LabView* code. **NOTE**: due to the water inside the interface, the actual pressure in the system can be different. Close VLM valve. Close the flow path selector. Undo *TMDA3201950Z* adapter.
	5.9	Stop the code and close *LabView*
	5.10	Weigh PS and write down the mass value. Place PS back in the vacuum chamber.
6.		Leak testing:

	6.1	Re-open the *LabView* code immediately after *step 5.10*. Run the code and observe if the pressure changes. If the pressure is dropping at 0.005 [bar/sec] in the first minute of the test, there is an unacceptable leakage. The test should be stopped, the leakage should be localized and removed. Most likely the components need to be tightened better or sealed. If the pressure drops less than 0.005 [bar/sec] in the first few minutes, the test can proceed and be tested for t_L [s].
	6.2	If there is H_2O leakage as described in *step 6.1*, the same *steps 5.4 – 6.1* should be followed.
	6.3	*Check Table 3.7*
7.		*Check Table 3.4*
8.		*Check Table 3.4*
9.		*Check Table 3.4*

3.1.4. TEST-INT-02: Volume and Mass Test

A detailed design and a mass budget of the PPD has been created by *Turmaine* [3]. This design has to meet the propulsion requirements *PROP-SYST-100*, *PROP-SYST-200*, and *PROP-SYST-210*. Furthermore, there was previously only a partial attempt to assemble the whole PPD system. It can be also seen in the report by *Turmaine* [3] that the cage, in which the propulsion system should be fully enclosed, is not entirely complete and has not been produced and assembled using the actual propulsion components. Therefore, the *PROP-SYST-100*, *PROP-SYST-200*, and *PROP-SYST-210* requirements have not been verified, yet.

It is important to know that TEST-INT-02 can be seen as a preliminary test. Since the current design of PPD is a first iteration, it is subjected to changes depending on the outcome of all the tests and other requirements verification.

Methodology

TEST-INT-02 is not an actual test, because instead of a test method an analysis (inspection) method is performed, which is one of the verification methods used in Systems Engineering (SE) approach. TEST-INT-02 requires a user to assemble the propulsion system components according to the design, inspect them visually or with the help of tools/devices, and deduce a conclusion based on the inspection outcome.

Test Set-Up

This inspection requires to assemble or at least gather all the current PPD design components as shown in Section 2.5. To achieve that, the following list of the test components and tools are given:

Table 3.10: List of components, tools and equipment needed for TEST-INT-02: Volume and Mass Test

Component/Tool Name	Amount	Description
TKLA3201112H check valve	1	Check Table 3.1
TMMA3203950Z-3-Boss manifold	1	Check Table 3.1
INKX0514300A solenoid valve	2	Check Table 3.1
TMUA3205959Z male-male adapter	1	Check Table 3.1
INMX0350000A 12 micron safety screen	2	Suggested to be used with 062 MINSTAC components by *The Lee* company
TechniRub O-ring	2	To create a seal between thruster interface and safety screen
5 [cm] MINSTAC 0.062 Tubing w/ 0.138-40 UNF interface	3	Check Table 3.1
25 [cm] MINSTAC 0.062 Tubing w/ 0.138-40 UNF interface	1	Check Table 3.1
TTTA3201243A Torque Wrench	1	Check Table 3.1
Pressure sensor wiring	-	Used to connect to Printed Circuit Board (PCB)
Valve wiring	-	Used to connect to PCB
MS5837-30BA sensor	1	Check Table 3.1
HCLA12X5DU sensor	1	Measures N_2 pressure in LPM plenum
LPM interface	1	-
VLM interface	1	-
Propellant tank housing	1	To store the rolled propellant tubes
Flat bottom small pliers	1	Check Table 3.1
PCB	1	Mock-up of MSP432 μController
PCB connector	4	Mock the interconnection of the other satellite sub-systems
Aluminium plate	1	Base plate for attaching all components
M2 threaded rods	4	Base plate and PCB attached to them
M2 nuts	8	To tighten base plate and PCB to M2 threaded rods
Aluminium spacer tubes	4	Used to keep base plate and PCB board at 30 [mm] distance

PS cage	1	Used to isolate PS from other satellite sub-systems
PocketQube (PQ) satellite side panel	3	To have realistic representation of the satellite
M2 torque screw	8	Used to fix the satellite walls to the cage
Valve support structure	1	To hold 2 solenoid valves in place
ADAM Highland Portable Precision Balances: HCB 123	1	Check Table 3.10
Double sided tape	-	To attach the components temporary

At the current stage of the PPD development, VLM and LPM thrusters have interfaces which are made for testing purposes and do not meet the dimensions requirements. The required size of the thruster interface for both VLM and LPM are *20x20x10* [mm] [42]. The interface mock-ups of these dimensions are produced by *Turmaine* [3] and are used mainly for the purpose of the volume test only:

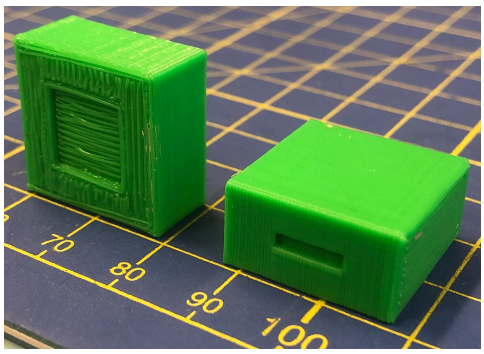

Figure 3.18: 3-D printed VLM and LPM interfaces

However, the same 3D printed interfaces can be used in mass test only if they are considered to be also 3D printed for the flight model. Thus, these printed parts can serve as the preliminary interface mass indicators. One of the most important items in Table 3.10 is the the propulsion system cage. Its purpose is to completely enclose the propulsion sub-system and protect other satellite sub-systems from a leaking propellant contamination. The cage would help to contain any leaked gas or liquid inside it. There was an attempt to create a cage before by *Turmaine* [3]. However, the first design has to many openings and would not meet the protection and containment requirements as stated before. Therefore, it requires an improved version of the propulsion system cage. The driving requirements of the design are given by *Pallichadath* [42] [30], and *Bouwmeester* [43]. After discussing with *Delfi-PQ* team, a killer requirement is created:

PROP-FUN-600: *The propulsion sub-system shall be enclosed and completely sealed to avoid propellant a contamination and damage the rest of Delfi-PQ sub-systems.*

After knowing the driver and killer requirements, a *Design Option Tree* is created and shown in Figure 3.19:

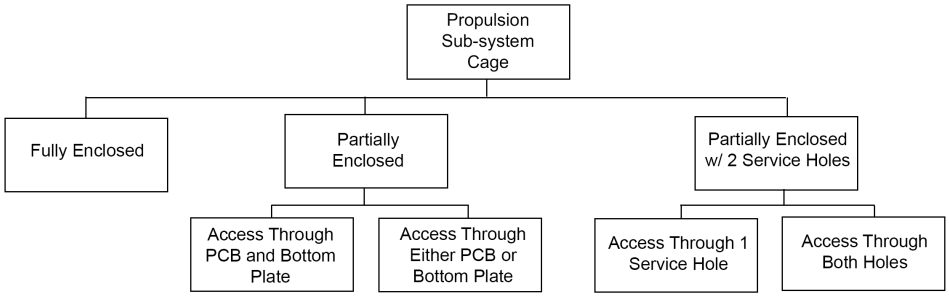

Figure 3.19: Design Option Tree for the improved propulsion sub-system cage

To clarify what each design option is, the explanation and sketches of all options are provided. *Fully Enclosed* option is a cage practically with no openings (all walls are sealed) and looks like a hollow cube. A partially enclosed cage with access through PCB and bottom plate is a design with basically only 4 walls, where top and bottom walls are not present. A partially enclosed cage with access through either PCB or bottom plate is a design with 5 walls and one missing (either top or bottom). A partially enclosed cage with 2 service holes is a design, which has two specially made holes in the cage to comply with service holes made on the satellite side plates. The rest of the cage walls are sealed. The other partially enclosed cage, has just 1 out of the 2 possible service holes. The sketches of the possible cage design options are shown in Figure 3.20:

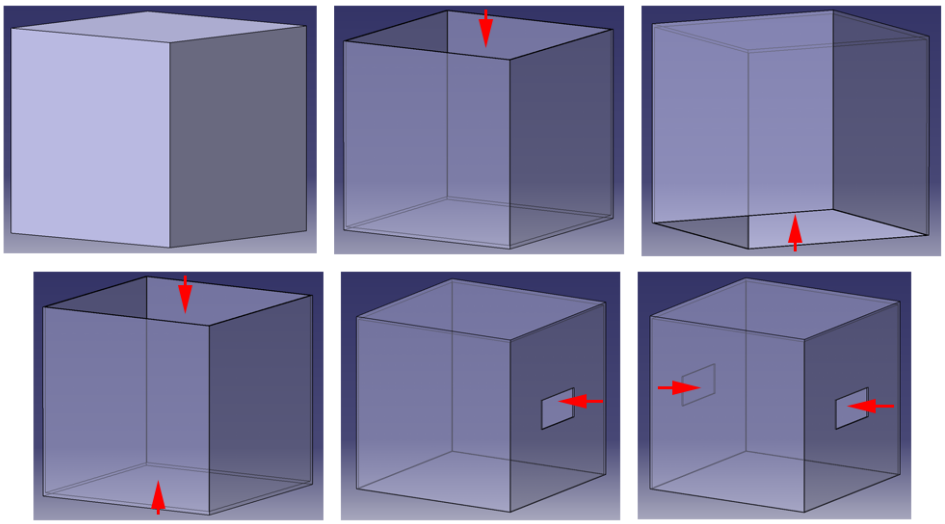

Figure 3.20: Sketches of the all the considered cage design options. Red arrows indicate the access to the inside of the cage. Top left to right: fully enclosed, access through PCB, access through bottom plate. Bottom left to right: access through PCB and bottom plate, access through one of the service holes, access through both of the service holes. Vertical direction of the figures is the directon the satellite units stacking

Normally, only the same level design options from Design Option Tree (DOT) are considered. However, the fully enclosed option does not provide out any more detailed design options into further tiers, but is still a possible design solution on itself. Therefore, it is included in the design trade-off process. The criterion of the trade-off table are the following: *Isolation Performance*, *Mass Performance*, *Development Cost*, *Development Risk*. The weight of each criterion is

defined by the width of its column: Isolation Performance weighs 0.4, Mass Performance weighs 0.3, Development Cost weighs 0.1, and Development Risk weighs 0.2. In total the weights add up to 1. The grades are defined by their color and are explained in the legend of the trade-off table. Green is 10, yellow is 5, and red is 1.

Option \ Criteria	Isolation Performance	Mass Performance	Dev. Cost	Development Risk
Access Through PCB and Bottom Plate	Yellow Possibility of not perfect fit between covers	Green Nominal	Green Zero Delta	Red Interference w/ other components
Access Through Either PCB or Bottom Plate	Yellow Possibility of not perfect fit between one of the covers	Yellow 17% heavier	Yellow Slight Delta	Green No risk
Access Through 1 Service Hole	Green Theoretically perfect seal	Red 32% heavier	Red High Delta	Yellow Not big enough entry
Access Through Both Holes	Green Theoretically perfect seal	Red 30 % heavier	Red High Delta	Yellow Not big enough entry
Fully Enclosed	Green Perfect seal	Red 34% heavier	Red High Delta	Red No retro access to the components

Excellent
Good
Unacceptable

Figure 3.21: Graphical trade-off table of the propulsion system cage design options

The total score of a single design is the sum of each criterion's weight and grade multiplication. The scores for each design option are presented as follows:

- Access Through PCB and Bottom Plate: 6.3
- Access Through Either PCB or Bottom Plate: 6
- Access Through 1 Service Hole: 5.4
- Access Through 2 Service Hole: 5.4
- Fully Enclosed: 4.6

Access Through PCB and Bottom Plate has the highest score, therefore, is the chosen design for the propulsion system cage. The actual design of the chosen cage option is created iteratively. The only extra cage requirements for the design are:

- PROP-INT-600: The cage shall have fixing holes for the satellite panels.
- PROP-INT-700: The cage shall have 2 exit holes for the nozzle exit of VLM and LPM thrusters.
- PROP-INT-800: The cage shall have openings to pass through threaded rods for stacking other sub-systems.

These requirements are devised based on the information provided by *Delfi-PQ* team. These requirements are not hard or fixed and made only for the purpose of the cage design. From the provided information, trade-off, and the previous cage design [3], the following Figure 3.22 shows the comparison between the initial and improved (based on the trade-off winner) design of the cage:

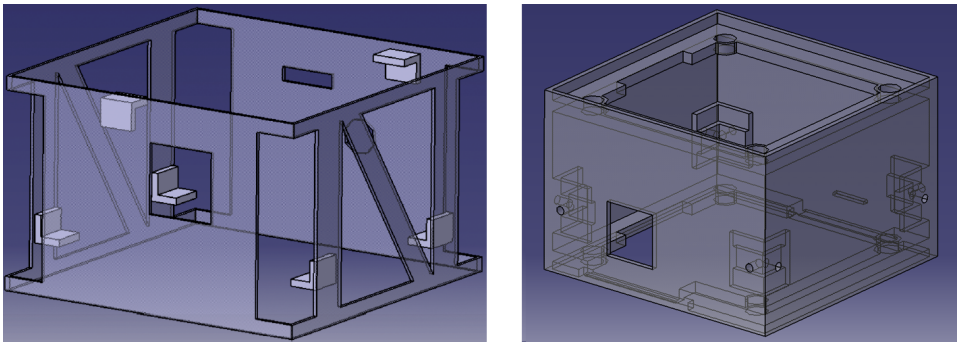

Figure 3.22: Isometric view of the initial (left) [3] and improved (right) PS cage CAD designs

By comparing the initial and the improved cages, there are significant changes in the design. First of all, the improved version has only 2 openings, which are for PCB and bottom plate (NOTE: the extra two small holes on the sides are necessary for the exit of LPM and VLM thruster nozzles as provided by PROP-INT-700 requirement). Second of all, if PCB and bottom plate are attached on the improved cage, theoretically a total mechanical seal is achieved. However, an extra, for example, rubber seal might be necessary to achieve a fluid seal. A further design iteration is needed to achieve a design with a fluid seal. Furthermore, the extra support holes are made to let pass through the threaded rods for stacking the subsystem inside the satellite as required by PROP-INT-800 requirement. Forth of all, the improved cage has also the corner stones integrated already on the sides of the cage, such that the side panels of the satellite can be easily attached with the screws as required by PROP-INT-600. The improved cage is then 3D printed in order to proceed with TEST-INT-02 test:

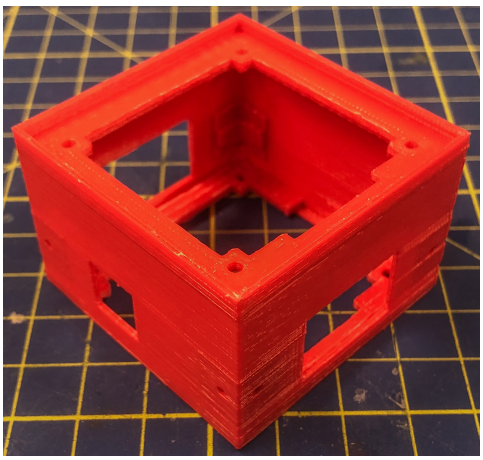

Figure 3.23: 3D printed new (improved version) propulsion system cage

NOTE: it can be seen in the 3D printed cage, there are two extra holes made on the side walls. These two extra holes are made only for the purpose of the showcase such that a person can check how the sealed and integrated cage in the satellite looks like. It also serves as an observation hole to inspect the integration of the propulsion system components from the inside of the cage. Further explanations on the cage design are given in Chapter 4.

Parameters

The parameters which need to be checked for this test can be found in Table 3.11:

Table 3.11: Parameters involved in TEST-INT-02: Volume and Mass Test

Parameter	Dimension	Description	Range
$M_{PPD,dry}$	[kg]	Dry mass of the PPD	Controlled parameter. There is a known number of components with a fixed mass. *Accuracy*: ±0.003 [g] (Tech. Data Sheet [41])
$M_{PPD,wet}$	[kg]	Wet mass of the PPD	Controlled parameter. There is a known number of components with a fixed mass and the required amount of the propellant. *Accuracy*: ±0.003 [g] (Tech. Data Sheet [41])
V_{PPD}	$[m^3]$	The volume of the propulsion components inside a fixed space	Independent parameter. This is more about how and where the components are integrated in the bounded space. *Accuracy*: N.A.

Success Criteria

The success criteria for the volume and mass test is defined as follows:

Table 3.12: Success criteria of TEST-INT-02: Volume and Mass Test

Criteria	Description
SC-TAI02-01	Parameters from Table 3.11 are obtained and documented
SC-TAI02-02	All items in Table 3.10 are present
SC-TAI02-03	The cage integrates with the satellite side panels and feed through rods

Test Procedure

The following test procedure is used to perform TEST-INT-02 test. It can be also considered as an assembly and integration procedure for the flight model version:

Table 3.13: TEST-INT-02: Volume and Mass Test procedure

Step	Sub-Step	Description	Performed (Y/N)	Time Stamp
1.		Verify that all the items described in Test Set-Up are present		
2.		Assemble the the propulsion components:		

	2.1	Insert both solenoid valves into the valve support structure
	2.2	Connect all *The Lee* components as shown in Figure 3.1.
	2.3	Connect the assembly from *Step2.1* to the 3D printed thruster interfaces.
	2.4	Insert both pressure sensors in the thruster interfaces.
3.		Fix the assembly from *Step 2* to the aluminium plate.
	3.1	Attach the 3D printed thruster interfaces to the plate using a double-sided tape
4.		Attach the aliuminium plate and PCB board to the cage
	4.1	The aluminium plate is attached to the bottom of the cage first.
	4.2	The 4 threaded rods are pushed through the 4 fixing holes of the cage and the plate. 4 nuts are attached on the rods.
	4.3	Attach the 3D printed manifold interface to the PCB board with the double sided tape. Attach the *TMMA3203950Z* to the interface
	4.4.	The other 4 nuts are screwed on the 4 threaded rods from the PCB board side.
5.		2x M2 torque screws are screwed through the panel onto the cage.
	5.1	58 [mm] width panel is attached to the wall of the cage where power supply pins are attached
	5.2	2x 48 [mm] width panels are attached to the walls of the cage where the LPM and VLM interfaces are located.
	5.3	1x 50 [mm] width panel is attached to the wall of the cage opposite the 58 [mm] width panel (However, for the purpose of this test, this panel is not attached to the cage).

3.2. Component Tests

3.2.1. TEST-COM-01: Solenoid PWM Test

Following the order of the tests defined in Chapter 2, the Pulse Width Modulated (PWM) signal capabilities of the solenoid valve and its signal characterization is tested. The purpose of this test is to verify Low Pressure Micro-Resistojet (LPM) thruster's performance such that it achieves its operational values in the firing mode. An explicit research of the solenoid valve itself has been previously done by *Silvestrini* [29]. However, the tests have been only performed so far at ambient conditions and not at Final Operational Envelope (FOE) values of the Propulsion Payload Demonstrator (PPD). Furthermore, the solenoid valve has been tested

as a stand alone component and only used with Vaporizing Liquid Micro-Resistojet (VLM). It means it was not integrated with the rest of the propulsion components, which does not represent the actual propulsion system set-up. Furthermore, none of the propulsion sub-system requirements, which are related to this test, given in Table 2.5 are verified, yet.

Methodology

To characterize the performance of the solenoid valve by using PWM mode to achieve FOE values and to verify the requirements from Table 2.5, certain aspects have to be tested:

- Temperature drop in the propellant tank while the nitrogen is being fed to the plenum. A possibility of freezing propellant in the tube.
- Temperature in the plenum and at LPM chip at cold conditions.
- Maximum operational frequency of the solenoid valve. From *The Lee Co* tech. data sheet of the solenoid valve [44]: max. oper. frequency is 1000 [Hz].
- Minimum voltage pulse duration of the solenoid valve. From *The Lee Co* tech. data sheet of the solenoid valve [44]: min. voltage pulse duration is 0.35 [ms].
- A range of operational PWM frequencies and duty cycles for the required plenum pressure (50 - 300 [Pa]) and its stability. According to [29], the optimal operational frequency is 250 [Hz] for such a solenoid valve.
- Ability to empty the propellant tank at the end of LPM performance.
- Total data bit rate and data capacity.
- Coil resistance of the solenoid valve w.r.t. the temperature. From *The Lee Co* tech. data sheet of the solenoid valve [44]: nominal coil resistance is 40 [Ω], and max. coil resistance is up to 66 [^{o}C].

One of the purposes of this test is to characterize the capabilities of the solenoid valve using PWM signal when reduction of the propellant pressure from 20 000 [Pa] [3] to as small as 50 [Pa] is required [1]. PWM signal allows the valve to be at open or closed state at a very fast rates, where its open or closed state is defined by the duty cycle.

In the ideal situation all the mentioned aspects above except the last two should be performed at vacuum conditions. One of the objectives is to perform such a test as close to the real operational conditions in space as possible. Although, it is expected that some parts of the test might be shifted from vacuum to ambient testing conditions. Furthermore, as the main goal of this test is to achieve the required pressure in the plenum, the testing is going to be performed at cold conditions. It means the chip of LPM thruster, and the vacuum chamber are not heated and are at the ambient temperature. Furthermore, the testing requires almost a full assembly of the PPD. A detailed explanation of the components involved in the testing is presented in *Test Set-Up* section.

According to PPD's functional flow diagram [3], first, VLM thruster is going to operate. Afterwards, when VLM is switched off, LPM is operated. This means that water is going to be supplied to VLM first, and then during the operation of LPM, N_2 is going to be supplied. However, it is expected during LPM thrusting there are going to be some water droplets remaining in the propellant tank. Furthermore, these water droplets are allowed to enter LPM thruster. It is possible due to the adiabatic cooling, the droplets can freeze, given that water has a lower freezing temperature than nitrogen. Thus, the pressure and temperature sensor in the

propellant tank, and thermocouples and low pressure sensor in LPM interface would allow to determine the changes in the temperature of the flowing gas of the state of the propellant in the tubes. Furthermore, thermal imaging camera is going to be used as a second measurement and verification tool for such effects.

The maximum operating frequency of 1000 [Hz] is defined by the manufacturer. In order to see if that is correct and to characterize the valve's operating frequencies, the test is going to be performed from 0 to 3000 [Hz]. 3000 [Hz] value is arbitrary and twice than what is recommended by the manufacturer. However, in this way, the valve is tested beyond its limits and a lot of data can be gathered to characterize a full envelope of the valve's capabilities. Similarly, the minimum voltage pulse duration is going to be tested. It is stated that the minimum of 0.35 [ms] voltage pulse signal is required to operate the valve at 1000 [Hz] frequency. This value corresponds to 35% of DC. Thus, a full sweep from 0 to 100% DC at various PWM frequencies is going to be performed.

By knowing the operating limits of PWM and DC values, a combination of the two can be used to achieve the required plenum pressure. However, since the valve is going to operate on a pulsing mode, the stability of the pressure in the plenum is important in order to achieve the required thrust. Thus, a combination of PWM and DC values is checked for every plenum target pressure, which is going to be split to 50, 150, 300 [Pa]. The stability is going to be tested by implementing a static (linear) and dynamic (quadratic) pressure controllers in the test codes. These controllers ensure that a target pressure in the plenum is sustained for a certain time at a fixed propellant tank pressure until the supply of the propellant is insufficient to reach the target pressure.

During the testing and the actual actuation of the valve, certain amount of data is produced. This amount of data and its rate should not exceed the values defined by *Pallichadath* [30]. A preliminary estimation of the amount of data can be deduced from the test by looking at the test data file sizes.

The operational temperature of the solenoid valve is from 4 to 49 [^{o}C] and the nominal coil resistance is 40 [Ω] [44]. The power limit of the propulsion system is 4 [W]. Thus, a coil resistance versus the temperature is going to be tested by measuring the valve connectors' resistance while the valve itself is being heated with a heat gun. The expected temperature range to be tested is from the ambient temperature to 10 degrees above maximum operating coil temperature of 66 [^{o}C] [44].

It is decided to conduct TEST-COM-01 in parts, because it requires to cover various test aspects as shown above. These aspects are included in sub-routines/sub-procedures of TEST-COM-01 test procedure. There are in total 6 sub-procedures: **E**, **F**, **G**, **H**, **I**, and **J**. Further explanation on these sub-routines is given in *Test Procedure* section.

The control of the solenoid valve and the pressure data acquisition is done by μController and *Arduino* compiler. This is done due to the fact that the building of the software code is faster and requires less troubleshooting than with *LabView* software. Moreover, by using a μController, almost an actual set-up of the propulsion system can be represented as shown in Figure 2.7.

Test Set-Up

As it is shown in Section 3.1, *TEST-COM-01: Solenoid Valve PWM Test* has an issue with the compatibility of *The Lee* tubing components and LPM interface. Two compatible LPM interface

versions have been manufactured by DASML, which have *0.138-40 UNF-2B* thread for *The Lee* components. The new LPM interface are shown in Figure 3.24:

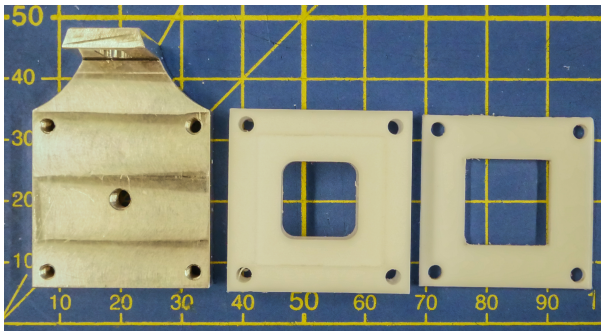

Figure 3.24: New LPM interface with the compatible *The Lee* connection on the aluminium back plate

The second version uses a teflon housing with *0.138-40 UNF-2B* threaded inlet on the back and an aluminium frame around it. The second design is shown in Figure 3.25:

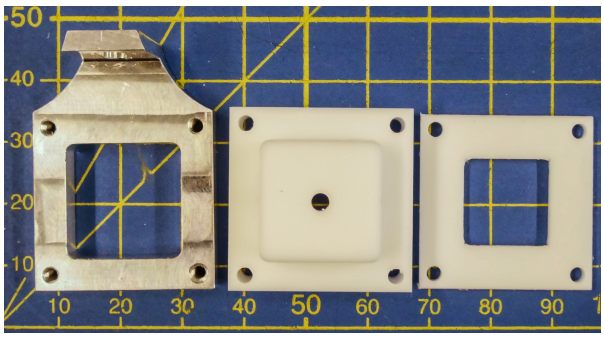

Figure 3.25: New LPM interface with the compatible *The Lee* connection on the teflon frame

It is noticed that the integration of the teflon parts with *The Lee* components does not wear the threads off that fast as compared to the integration of the aluminium parts with *The Lee* components. Therefore, the tests will be performed using the LPM interface with the teflon housing. Furthermore, for the purpose of this test, the teflon protection plate, which was used previously to fix the heater chip and the heater wires in place, is replaced with a simpler one. The reason behind it is that TEST-COM-01 does not require the heating of the chip. Even though, if it is required, the cover plate can be easily modified.

As it was mentioned previously, the theoretical values of PPD system are made for 1.57 [mm] inner diameter tubes. However, due to to the miscommunication and order mistakes from the previous student, the available tubes were with 0.81 [mm] inner diameter and were used initially for the leak test. For this test the new tubes with the correct 1.57 [mm] inner diameter from *The Lee* manufacturer are used. Therefore, the test data can be compared more closely to the theoretical values calculated by *Turmaine* [3]. Furthermore, the performance of the new tubes can be checked during this test. The following Table 3.14 shows all the components which are necessary to perform the whole TEST-COM-01 test:

Table 3.14: List of components, tools and equipment needed for TEST-COM-01: Solenoid Valve PWM Test

Item	Component/Tool Name	Amount	Description
1.	TKLA3201112H check valve	1	Check Table 3.1
2.	TMMA3203950Z-3-Boss manifold	1	Check Table 3.1
3.	NKX0514300A solenoid valve	2	Check Table 3.1
4.	TMUA3205959Z male-male adapter	1	Check Table 3.1
5.	INMX0350000A 12 micron safety screen	1	Check Table 3.10
6.	*TechniRub* O-ring	2	To create a seal between thruster interface and safety screen
7.	5 [cm] MINSTAC 0.062 Tubing w/ 0.138-40 UNF interface	2	The new 1.57[mm] Inner Diameter (I.D.) tube is used
8.	25 [cm] MINSTAC 0.062 Tubing w/ 0.138-40 UNF interface	1	The new 1.57[mm] I.D. tube is used
9.	Pressure sensor wiring	-	Used to connect to PCB
10.	Valve wiring	-	Used to connect to PCB
11.	GPFS	-	To provide nitrogen for the PPD
12.	MS5837-30BA sensor	1	Check Table 3.1
13.	HCLA12X5DU sensor	1	Measures N_2 pressure in LPM plenum
14.	LPM interface	2	To create plenum environment, connect propellant tubes, integrate sensors
15.	LPM chip	1	Used to replicate real plenum and thruster set-up
16.	Silicon tube	1	To connect HCLA12X5DU sensor to LPM interface
17.	Kapton/Duct tape	-	To attach the components temporary
18.	IECX0501350AA Spike and Hold Electrical Driver	1	To provide power and control solenoid valve
19.	*MEGA 2560 R3* μController	1	To send signal to the solenoid valve, receive data from the sensors
20.	*Arduino* code and compiler	-	To configure and upload the routines onto the μController

21.	*Tera Term* software	-	To control *MEGA 2560 R3* and save test data into a file
22.	Negative Temperature Coefficient (NTC) thermistor	1	To measure reference ambient temperature
23.	10k [Ω] resistor	2	For P/T sensor circuit wiring
24.	5k [Ω] resistor	1	For NTC thermistor circuit wiring
25.	0.1 [μF] capacitor	2	For voltage regulation both pressure sensors
26.	*LabView 2016* software and code	-	To read and save thermocouple data
27.	NI USB-9162 DAQ	1	To obtain the readings of the thermocouples in the LPM interface
28.	K-type thermocouple	2	To obtain the temperature at the plenum and LPM chip
29.	*FLIR AX-15 Series* thermal imaging camera	1	To record temperatures at various locations of the solenoid valve
30.	*Research IR* software	-	To control *FLIR* camera and record its images and data
31.	*Heraeus vacuutherm* vacuum oven	1	To create a vacuum environment for the test
32.	*Vacuubrand RZ 6* rotary vacuum pump	1	To pump the air out of the vacuum oven
33.	*VC 837* multimeter	1	To read temperature of the thermocouple
34.	*TENMA 72-7770* multimeter	1	To measure the coil resistance
35.	*Steinel HL 2010 E* heat gun	1	To heat up the solenoid valve
36.	Jumper wires	-	To connection various components
37.	E030-10 & D030-10 PSU	2	Check Table 3.1

The graphical representation of the Propulsion System (PS) hardware set-up for **E** to **I** sub-routines of TEST-COM-01 is shown in Figure 3.26:

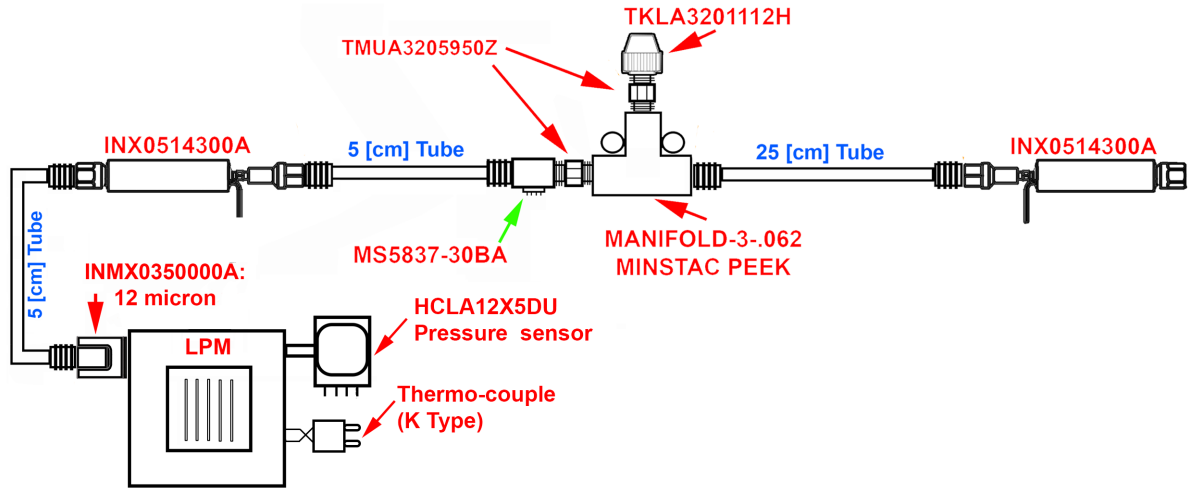

Figure 3.26: The graphical representation of the propulsion system hardware test set-up part of TEST-COM-01 for **E** to **I** sub-routines

The graphical representation of the whole TEST-COM-01 test hardware set-up for **E** to **I** sub-routines is shown in Figure 3.27:

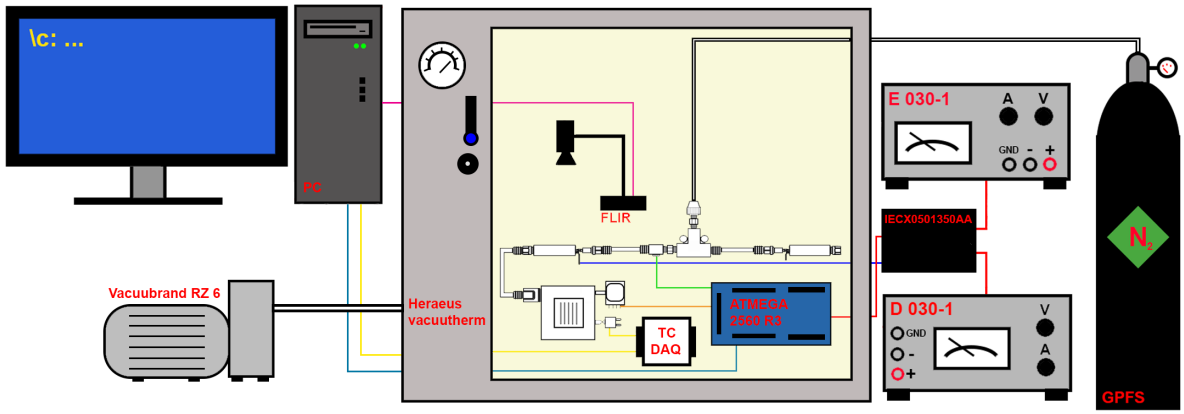

Figure 3.27: The graphical representation of the whole TEST-COM-01 test hardware set-up for **E** to **I** sub-routines

The graphical representation of TEST-COM-01 test hardware set-up for **J** sub-routine is shown in Figure 3.28:

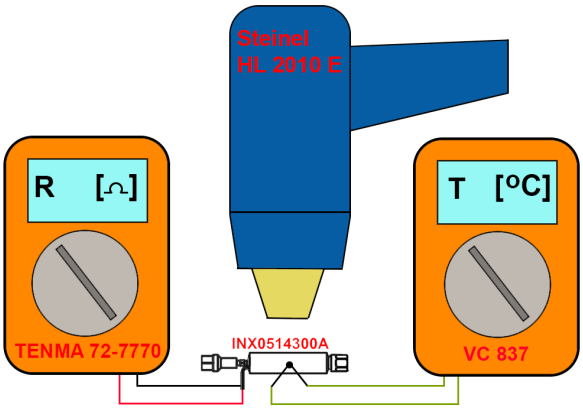

Figure 3.28: The graphical representation of TEST-COM-01 test hardware set-up for **J** sub-routine

In addition to the pressure measurements, the temperature at various locations is also going to be measured, because there is no sufficient information about its effects on the propellant feed from the tank to the plenum or how the temperature change affect the solenoid valve's performance. Furthermore, such an information would also help to verify the requirements presented in Table 2.5. One temperature sensor is located in the propellant tank and is embedded in MS5837-30BA sensor. The other temperature measurements are obtained by using K-type thermocouples in the plenum of the thruster. One is located very close to the inlet of the plenum, the other is close to LPM chip. A thermocouple is a device where the temperature is measured at a junction of two different types of alloy wires by applying the thermoelectric, and Seeback effects [45]. The thermocouple junction has a very small size, which can be easily implemented virtually anywhere and helps to determine the temperature with a high precision at a given location.

For the purpose of this test it is decided to use open source data acquisition hardware and software. The reason behind it is that the open source data acquisition is more flexible, faster and easier to implement in the hardware. It is also noticed from the previous tests that troubleshooting *LabView* code requires quite some effort, if a previous code is reused. Only the thermocouples will be connected to National Instruments (NI) Data Acquisition (DAQ) and their data obtained via *LabView* software. Therefore, all the pressure sensors, and tank temperature data is collected via *Arduino* type *MEGA 2560 R3* μController and using *Tera Term* software. The same μController is also used to send PWM signal to the solenoid valve. *Arduino* compiler is used to generate the required code and upload onto the micro-controller. The electric wiring diagram of the micro-controller and the mentioned sensors can be found in Figure 3.29:

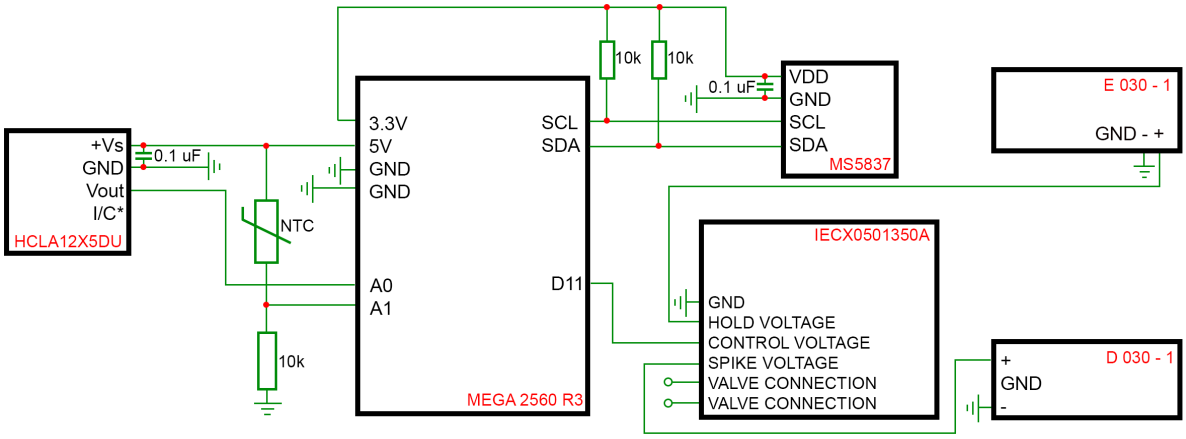

Figure 3.29: Electric diagram used to control the solenoid valve and obtain sensor data

Parameters

In order to obtain a quantifiable data during the test, the following parameters in Table 3.15 are determined during TEST-COM-01:

Table 3.15: Parameters involved in TEST-COM-01: Solenoid Valve PWM Test

Parameter	Dimension	Description	Range
DC	[%]	Duty Cycle of the PWM signal of the solenoid valve	*Controlled parameter*. Range is from 0 to 100% (translated to 1 - 255 [-] values). 0% is 1 [-] and 100% is 255 [-] setting in the valve. Valve is fully closed at 0% and fully open at 100%. The value is adjusted w.r.t. the pressure in the tank over the time. *Accuracy*: min. DC of 35% at 1000 [Hz] (Tech. Data sheet [44])
f_{PWM}	[Hz]	Pulse Width Modulated PWM frequency	*Controlled parameter*. The test frequency range is 1 - 3000 [Hz]. The value is adjusted w.r.t. the pressure in the tank over the time. *Accuracy*: max. operating frequency is 1000 [Hz] (Tech. Data Sheet [44])
$\dot{m}_{N_2}$	[kg/s]	Mass flow of nitrogen gas from the tank to the plenum	*Independent parameter*. Depends on the pressure and temperature data, and it is determined indirectly by calculating. *Accuracy*: N.A.

t_s	[s]	Sampling time of the test	*Independent parameter*. Depends on how fast the nitrogen gas travels to the plenum and the required pressure is achieved, and the size of the tank volume. *Accuracy*: N.A.
$P_{st,0}$	[bar]	Initial propellant storage pressure	*Controlled parameter*. The required N_2 pressure is 20 100 [Pa] or 0.201 [bar]. *Accuracy*: ±1 [mbar] (in-built in *Arduino* code)
P_{pl}	[bar]	The pressure measured just at the inlet of LPM interface plenum	*Independent parameter*. Depends on the PS performance. Maximum allowable P_{pl} is 300 [Pa]. *Accuracy*: depends on the low pressure sensor (no data from the manufacturer)
T_{amb}	[K]	The temperature at ambient inside the vacuum oven.	*Independent/Controlled* parameter. The ambient temperature normally is fixed to the temperature in the clean-room at that moment. However, it can be regulated between 5 - 85 [^{o}C] (inside the vacuum oven) to meet PROP-INT-200 requirement. *Accuracy*: ±4 [^{o}C] (Tech. Data Sheet [46])
T_{pl}	[K]	The temperature measured at the inlet of LPM plenum	*Independent parameter*. The value depends on the flow of the nitrogen gas and the ambient temperature. The temperature is measured by K-type thermocouple. *Accuracy*: ±0.75 - 2.2 [^{o}C] (Tech. Data Sheet [47])
$T_{st,0}$	[K]	The temperature measured in the propellant storage tank	Independent parameter. The value depends on the ambient temperature. *Accuracy*: $\pm$30 [mbar] (from the technical data sheet of the sensor [40])

T_{sv}	[K]	The temperature of the solenoid valve	Controlled parameter: By heating the valve with a heat gun at a fixed temperature. The range is 25 - 70 [°C]. *Accuracy*: depends on the multimeter (no data available)
R_{coil}	[Ω]	The coil resistance of the solenoid valve	Independent parameter: Its value depends on the temperature of the coil temperature, which is the temperature of the valve. *Accuracy*: ±1% + 2 (Tech. Data Sheet [48])

Success Criteria

The following criteria is used to defined whether the test has been successfully performed, but also whether the system performs according to the requirements:

Table 3.16: Success criteria of TEST-COM-01: Solenoid Valve PWM Test

Criteria	Description
SC-TC01-01	Parameters from Table 3.15 are obtained and documented
SC-TC01-02	All items in Table 3.14 are present
SC-TC01-03	The temperature influence on the solenoid valve coil resistance is analyzed
SC-TC01-04	The PWM mode leaves enough power for heating the thruster chip
SC-TC01-05	The pressure drop in the propellant tank is negligible for the required pressure in the tank during the actual testing
SC-TC01-06	The sensor test data is obtained, saved in a file, and backed up

Test Procedure

The whole TEST-COM-01 test procedure is split into a number of sub-procedures. As it was introduced previously, each sub-procedure covers a certain aspect of the test presented in the *Methodology* section. A general test procedure including all sub-procedures is given in Table 3.17:

Table 3.17: TEST-COM-01: Solenoid Valve PWM Test general procedure

Step	Sub-Step	Description	Performed (Y/N)	Time Stamp
1.		Perform sub-procedure **E**: *0.2 [bar] system pressurization*		

2.	Perform sub-procedure **F**: *Maximum operating frequency*
3.	Perform sub-procedure **G**: *Minimum voltage pulse duration*
4.	Perform sub-procedure **H**: *Plenum pressure stability at various PWM frequencies*
5.	Perform sub-procedure **I**: *Plenum pressure stability with FOE values in a closed system*
6.	Perform sub-procedure **J**: *Coil resistance of the valve due to the temperature increase*

Each sub-procedure from Table 3.17 is described in detail below:

Table 3.18: Test procedure of sub-procedure **E**: *0.2 [bar] system pressurization*

Step	Sub-Step	Description	Performed (Y/N)	Time Stamp
1.		Check if items 1 - 28, 31, 32, 35, and 36 are present from Table 3.14		
2.		Assemble the propulsion system components as shown in Figure 3.26		
3.		Assemble all the components as shown in Figure 3.29		
4.		Check if all hardware is connected as shown in Figure 3.27 (*FLIR* camera is not necessary)		
5.		Turn on *E030-10* and *030-10* PSUs and wait around 30 min. to warm up		
6.		Launch *LabView* code called *TC_readout.vi*:		
	6.1	Create a file with *.lvm* extension, name it, and save it in the wanted directory. Specify the file's directory path in *TC_readout.vi*		
	6.2	Run *TC_readout.vi* code to check if the temperature readings of the thermocouples are registered.		
7		Check if GPFS has sufficient N_2 gas. Otherwise follow the procedure from *Step 4.4* (Table 3.4)		
8.		Launch *Arduino* code called *A_Standby.ino* and upload the code to the μController		
9.		Launch *Tera Term* software:		
	9.1	Create *.log* type of file, name it, and save it in the wanted directory		
	9.2	Specify that same directory path in *Tera Term* software		

	9.3	Specify from which port to read data (μController's port should be recognized in the selection list)
	9.4	Execute the functions of the uploaded *A_Standby.ino* code and check if the valve is responding and all sensors' data is being read
10.		Pressurization:
	10.1	Check if the gas feed line going to the vacuum oven is connected to the middle section pipe of the GPFS
	10.2	Connect the feed-through tube inside the vacuum oven to the oven's adapter and the other end to the check valve of PS
	10.3	Set the pressure regulator to around 0.5 [bar], open the shut-off valve, and then the middle flow path valve.
	10.4	Open the solenoid valve using *Tera Term* for some time to release the trapped air inside PS tubes. Close the solenoid valve
	10.5	Read the pressure sensor inside the propellant tank tube until the pressure is above 1.2 [bar]. Then remove the gas feed line from the check valve
	10.6	Disconnect the gas feed line from the inside of the vacuum oven
11.		Vacuum creation:
	11.1	Close the vacuum door and move the door handle completely down
	11.2	Turn the drain valve on the vacuum oven such that it is closed
	11.3	Open the vacuum oven valve which is connected to the vacuum pump
	11.4	Turn on the vacuum pump and observe if no pump irregularities are present
	11.4	Sufficient vacuum is achieved at around 0.01 - 0.04 [mbar] pressure
12.		Execution:
	12.1	After the pressure inside the vacuum oven drops to around 0.01 - 0.04 [mbar], code *E.ino* is uploaded via *Arduino* compiler
	12.2	*E.ino* is executed using *Tera Term*

	12.3	The code automatically removes any excess of the nitrogen above 0.2 [bar] in the propellant tank by opening/closing the valve and reading the sensor data in the propellant tank. When the pressure reaches 0.2 [bar] , the code stops
	12.4	Code *A_Standby.ino* is re-uploaded and the pressure in the propellant tank is checked for some time
	12.5	If the pressure stays stable for around 10 [s], the test is stopped and data is saved
13.		Vacuum oven pressurization:
	13.1	The valve connecting the vacuum oven and the pump is closed
	13.2	The vacuum pump is switched off
	13.3	The vacuum oven drain valve is opened
	13.4	After the vacuum oven's pressure gauge reaches 101 000 [Pa], the oven's door can be opened
14.		The solenoid valve is opened shortly to release the rest of the nitrogen and balance the pressure inside the tube with the ambient pressure
15.		Disconnect all the wires from the PS, μController, and switch off the PSUs. Close *LabView*, *Tera Term*, and *Arduino*.

Table 3.19: Test procedure of sub-procedure **F**: *Maximum operating frequency*

Step	Sub-Step	Description	Performed (Y/N)	Time Stamp
1.		Check if items 1 - 31, 36, and 37 are present from Table 3.14		
2.		The same as *Step 2.* in Table 3.18		
3.		The same as *Step 3.* in Table 3.18		
4.		Check if all hardware is connected as shown in Figure 3.27		
5.		The same as *Step 5.* in Table 3.18		
6.		The same as *Step 6.* in Table 3.18		
7.		The same as *Step 7.* in Table 3.18		
8.		The same as *Step 8.* in Table 3.18		
9.		The same as *Step 9.* in Table 3.18		
10.		Pressurization:		
	10.1	The same as *Step 10.1.* in Table 3.18		

	10.2	Connect the feed-through tube inside the vacuum oven to the oven's outlet adapter and the other end screw onto the check valve (remove the yellow plastic adapter)
	10.3	Set the pressure regulator to 1 [bar] (which is 2 [bar] in the tube), open the shut-off valve, and then the middle flow path valve
	10.4	The same as *Step 10.4* in Table 3.18
	10.5	Leave the nitrogen feed line attached to the check valve. Using the pressure regulator, adjust the pressure to be as close as possible to 2 [bar]
11.		Camera set-up:
	11.1	Connect the cables of *FLIR* according to the instructions
	11.2	Launch *ResearchIR* software and connect camera
	11.3	Adjust the camera stand or use the lens focus adapter to have a whole and sharp view of the solenoid valve
	11.4	Define the directory path for the video file to be saved at
13.		Execution
	13.1	Upload *Arduino* code called *F.ino*
	13.2	Start recording the temperature data with *TC_readout.vi*
	13.3	Start recording the video with *FLIR* camera
	13.4	Execute *F.ino* via *Tera Term*
	13.5	When the frequency sweep is over, stop *LabView* code and *FLIR* camera recording. Immediately after that re-upload *Arduino* code *A_Standby.ino*
14.		Check if all the test data is saved accordingly
15.		Disconnect all the wires from the PS, μController, *FLIR* camera, and switch off the PSUs. Close *LabView*, *Tera Term*, *ResearchIR*, and *Arduino*.

Table 3.20: Test procedure of sub-procedure **G**: *Minimum voltage pulse duration*

Step	**Sub-Step**	**Description**	**Performed (Y/N)**	**Time Stamp**
1.		The same as *Step 1.* in Table 3.19		
2.		The same as *Step 2.* in Table 3.19		
3.		The same as *Step 3.* in Table 3.19		

4.		The same as *Step 4.* in Table 3.19
5.		The same as *Step 5.* in Table 3.19
6.		The same as *Step 6.* in Table 3.19
7.		The same as *Step 7.* in Table 3.19
8.		The same as *Step 8.* in Table 3.19
9.		The same as *Step 9.* in Table 3.19
10.		The same as *Step 10.* in Table 3.19
11.		The same as *Step 11.* in Table 3.19
12.		Set the frequency to *XX* [Hz] value in *G.ino*. Upload the code to the μController
13.		Execution:
	13.1	The same as *Step 13.1* in Table 3.19
	13.2	The same as *Step 13.2* in Table 3.19
	13.3	Execute *G.ino* via *Tera Term*
	13.4	When the voltage pulse sweep is over, stop *LabView* code and *FLIR* camera recording. Immediately after that re-upload *A_Standby.ino*. Change the frequency value in *G.ino* for a new run, accordingly
	13.5	Wait for around 5 minutes for the solenoid valve to cool down
	13.6	Create new *LabView*, *ResearchIR*, and *Tera Term* files for each new set frequency
	13.7	Repeat *Steps 13.1 to 13.6*
14.		The same as *Step 14.* in Table 3.19
15.		The same as *Step 15.* in Table 3.19

Table 3.21: Test procedure of sub-procedure **H**: *Stability of the plenum pressure at a fixed PWM frequency*

Step	**Sub-Step**	**Description**	**Performed (Y/N)**	**Time Stamp**
1.		The same as *Step 1.* in Table 3.19		
2.		The same as *Step 2.* in Table 3.18		
3.		The same as *Step 3.* in Table 3.18		
4.		The same as *Step 4.* in Table 3.18		
5.		The same as *Step 5.* in Table 3.18		
6.		The same as *Step 6.* in Table 3.18		

7.		The same as *Step 7.* in Table 3.18
8.		The same as *Step 8.* in Table 3.18
9.		The same as *Step 9.* in Table 3.18
10.		Pressurization:
	10.1	The same as *Step 10.1* in Table 3.18
	10.2	The same as *Step 10.2* in Table 3.19
	10.3	The same as *Step 10.2* in Table 3.19
	10.4	The same as *Step 10.4* in Table 3.18
	10.5	Leave the nitrogen feed line attached to the check valve
11.		The same as *Step 11.* in Table 3.18
12.		The same as *Step 12.1 - 12.4* in Table 3.18. Except the target propellant tank pressure is set by the user. Wait until the vacuum drops to 0.01 - 0.04 [mbar] after stabilizing the pressure in the tank.
13.		Execution:
	13.1	Set the target plenum pressure, and PWM frequency in *H.ino*, accordingly
	13.2	Upload *H.ino* to the μController
	13.3	Start recording the temperature data with *TC_readout.vi*
	13.4	Execute *H.ino* via *Tera Term*
	13.5	When *H.ino* has finished, stop *LabView* code and re-upload *E.ino*
	13.6	Repeat *Step 12. - 13.5* for the required plenum pressures and PWM frequencies
14.		The same as *Step 14.* in Table 3.19
15.		The same as *Step 13.* in Table 3.18
16		The same as *Step 14.* in Table 3.18
17.		The same as *Step 15.* in Table 3.19 (Ignore *FLIR* and *ResearchIR*)

Table 3.22: Test procedure of sub-procedure **I**: *Final Operational Envelope pressure at closed conditions*

Step	**Sub-Step**	**Description**	**Performed (Y/N)**	**Time Stamp**
1.		The same as *Step 1.* in Table 3.19		

2.		The same as *Step 2.* in Table 3.18
3.		The same as *Step 3.* in Table 3.18
4.		The same as *Step 4.* in Table 3.18
5.		The same as *Step 5.* in Table 3.18
6.		The same as *Step 6.* in Table 3.18
7.		The same as *Step 7.* in Table 3.18
8.		The same as *Step 8.* in Table 3.18
9.		The same as *Step 9.* in Table 3.18
10.		Pressurization:
	10.1	The same as *Step 10.1* in Table 3.18
	10.2	The same as *Step 10.2* in Table 3.19
	10.3	The same as *Step 10.2* in Table 3.19
	10.4	The same as *Step 10.4* in Table 3.18
	10.5	Leave the nitrogen feed line attached to the check valve
11.		The same as *Step 11.* in Table 3.18
12.		The same as *Step 12.1 - 12.4* in Table 3.18. Wait until the vacuum drops to 0.01 - 0.04 [mbar] after stabilizing the pressure in the tank.
13.		Execution:
	13.1	Set the target plenum pressure, and PWM frequency in *I.ino*, accordingly
	13.2	Upload *I.ino* to the μController
	13.3	Start recording the temperature data with *TC_readout.vi*
	13.4	Execute *I.ino* via *Tera Term*
	13.5	When *I.ino* has finished, stop *LabView* code and re-upload *E.ino*
	13.6	Repeat *Step 12. - 13.5* for the required plenum pressures and PWM frequencies
14.		The same as *Step 14.* in Table 3.19
15.		The same as *Step 13.* in Table 3.18
16		The same as *Step 14.* in Table 3.18
17.		The same as *Step 15.* in Table 3.19 (Ignore *FLIR* and *ResearchIR*)

Table 3.23: Test procedure of sub-procedure **J**: *Coil resistance of the valve due to the temperature increase*

Step	Sub-Step	Description	Performed (Y/N)	Time Stamp
1.		Check if items 3, 17, and 33 - 36 are present from Table 3.14		
2.		Attach the thermocouple		
	2.1	Use Kapton tape to attach the measuring part of the thermocouple on the cylindrical part of the solenoid valve		
	2.2	Connect the thermocouple to the multimeter and set the multimeter to [^{o}C] function		
3.		Connect the other multimeter to the valve connection pins and set it to measure the resistance		
4.		Measure and note down:		
	4.1	Thermocouple temperature: ... [^{o}C]		
	4.2	Valve resistance: ... [Ω]		
5.		Start heating the valve with the heat gun until the thermocouple reaches 35 [^{o}C]		
	5.1	Perform *Step 4.*		
6.		Start heating the valve with the heat gun until the thermocouple reaches 45 [^{o}C]		
	6.1	Perform *Step 4.*		
7.		Start heating the valve with the heat gun until the thermocouple reaches 55 [^{o}C]		
	7.1	Perform *Step 4.*		
8.		Start heating the valve with the heat gun until the thermocouple reaches 65 [^{o}C]		
	8.1	Perform *Step 4.*		
9.		Start heating the valve with the heat gun until the thermocouple reaches 70 [^{o}C]		
	9.1	Perform *Step 4.*		
10.		Disassemble the components and turn off the devices		

3.2.2. TEST-COM-04: Heater Efficiency Test

Methodology

TEST-COM-04 is a preliminary test. The most important goal is to obtain the required heater power and relate it to the chip pressure data. Such data can be compared to the Final Oper-

ational Envelope (FOE) numerical analysis values found by *Turmaine* [3], and help to verify PROP-FUN-100 and PROP-SYST-300 requirements. The selection of the Vaporizing Liquid Micro-Resistojet (VLM)thruster chips is based on the results provided by *Silva* [2]. Currently, there are 4 first generation operational VLM thruster chips:

Table 3.24: First generation operational VLM chips

-	Code	Nozzle Shape	Channel Shape	Heater Configuration
1.	01-LS1-01	Long	Large serpentine	21 Lines
2.	01-Ld1-01	Long	Small diamond	21 Lines
3.	01-WD2-01	Wide	Large diamond	30 Lines
4.	01-BS2-01	Bell	Large serpentine	30 Lines

To obtain the power and pressure readings, each thruster is placed in a stationary location by using the third hand stand. The power to the heaters is provided by a power supply unit. Its voltage and current is controlled by the user. The water is injected to the plenum either by the water syringe pump or by a dedicated water tank connected to the pressurized nitrogen gas tank. The pressure inside the plenum is measured by a pressure/temperature sensor and its readings are sent to the computer. The increase/decrease of the power input is done in small steps until the thruster is not able to vaporize the water inside the chip and it overflows. All 4 thruster chips are tested using the same method.

To represent the actual propellant feeding process, the pressurized water tank with a solenoid valve connection to the thruster interface would be ideal. During the design of a such set-up, it is noticed that the control of the nitrogen gas from General Purpose Feed System (GPFS) is complicated and inaccurate for such a test, and requires additional hardware. Therefore, it is decided to use a dedicated water mass flow sensor, to measure the exact water flow speed and determine the pressure. *Sensirion SLI-C 430* water mass flow sensor can be used for such an application. To check how accurate *Sensirion SLI* sensor itself is, it is connected to the *NE-1000X2* syringe pump. The pump flow speed is matched to a measurable speed of the water mass flow sensor. However, after a few trials with different mass flow velocities, it is noticed that the *Sensirion SLI* sensor is not matching the flow set in the syringe pump. It is possible that the water mass flow sensor is damaged, dirty from the previous usage, or needs re-calibration. Due to the test time constraints it is decided to use only a syringe pump as a mean of propellant feed to the thruster's interface.

The current version of VLM interface does not have the temperature sensor inside the chip. Two methods can be used to determine the temperature. A thermal imaging camera is used to approximately determine the temperature of the chip and the interface. By using the in-built tools from the camera software, certain temperature spots of the thruster can be measured precisely. Although, a reflectivity of secondary surfaces has to be taken into account. Another option is to calculate the temperature from the measured resistance of the heaters. However, from the observed initial damage of the heaters and conditions of the heating chambers of the chips, it is decided not to use this option in order to minimize the error in the obtained data. An optical micro-scope camera is used to visualize the flow and water vaporization inside VLM chip. The camera is also used as an optical indicator to spot the overflow of the water inside the interface.

As an extra objective for this test a thrust bench test can be performed to validate the obtained

power measurements from the above method. The validation is done by comparing the static chip power-pressure measurement data with the displacement of the thrust bench using the same chip. It means if a displacement is registered, a vaporization of the water is created and a force is expelled. That vaporization corresponds to the same static vaporization at a set power level. A pendulum thrust bench *AE-TB-5m* is used to measure the displacement created by the VLM thruster. In this case, only the magnitude of the thrust force is needed to be measured. Thus, no calibration of the pendulum is needed. Although, it might be difficult to perform such a task, because it is hard to visually observe how the thruster is performing. Thus, a good characterization of the power and pressure is required beforehand to do a thrust bench testing. Since TEST-COM-04 is a preliminary test and certain hardware is not allowed to be in vacuum, the thrusting would be performed at ambient conditions.

Test Set-Up

Table 3.25 represents all the hardware and software equipment, and tools required for TEST-COM-04:

Table 3.25: List of components, tools and equipment needed for TEST-COM-04: Heater Efficiency Test

Item	Component/Tool Name	Amount	Description
1.	INMX0350000A 12 micron safety screen	1	To connect MINSTAC 0.062 tube to VLM interface
2.	XX [cm] *0.062 MINSTAC* tube w/ 0.138-40 UNF interface	2	To connect syringe to the safety screen
3.	MS5837-30BA sensor	1	Check Table 3.1
4.	MS5837-30BA sensor wiring	-	To connect the sensor to PCB
5.	Syringe needle with *Luer* lock	1	To provide water for VLM thruster and connect to the *0.062 MINSTAC* tube
6.	*Kapton* duct tape	-	To attach the components temporary
7.	*Heraeus Vacutherm* vacuum oven	1	Check Table 3.1
8.	NI *LabView* 2015 software and code	-	Check Table 3.1
9.	Data Acquisition (DAQ) devices	2	Check Table 3.1
10.	NI USB-9162 DAQ device	1	To measure the temperature at the thruster outlet (if necessary)
11.	De-mineralized water	-	Used as a propellant in VLM thruster and stored in the water tank

12.	*AE-TB-5m* pendulum thrust bench	1	A swing where a pendulum is used to create a swivel by firing VLM thruster. At a fixed location is static displacement sensor, which measures the distance the pendulum moves from the sensor. That distance in converted to the thrusting force of the thruster
13.	*DSU 030-5* Power Supply Unit (PSU)	1	To provide voltage at a fixed current for the heater pins in VLM interface
14.	NI Micro-Epsilon DAQ	1	Register data of the displacement sensor and send to Personal Computer (PC)
15.	*SM7020-D* PSU	1	It is used to power the calibration coil
16.	*FLIR AX-5* series thermal imaging camera	1	To record the temperatures during the vaporization of the water in the thruster
17.	*ResearchIR* software	-	To control *FLIR* camera and record its images and data
19.	*Dino-Lite* Microscope camera	1	To record the vaporization of the water in the thruster
20.	*Dino-Lite Capture* software	-	To record videos of the microscope camera
21.	*TENMA 72-7770* multimeter	1	To check the resistivity of the VLM heaters
22.	Jumper wires	-	To connect various components
23.	*NE-1000X2* syringe pump	1	To feed water to VLM at a fixed mass flow rate
24.	Personal Computer (PC)	1	To execute *LabView* code, connect DAQ, and store test data
25.	Third hand stand	1	To hold in place VLM thruster
26.	Mirror on a stick	1	To visually inspect the exhausting steam at the nozzle exit
27.	*Prosat PS-911* wipes	-	to clean VLM chips, interface, and its glass
28.	*Polyco Bodyguards* Finite P Indigo AF Nitrile examination gloves	-	To prevent touching VLM chip and interface with bare hands and contamination
29.	TMMA3203950Z – PEEK 3-boss manifold	1	To use as an extension connector between thrust bench and syringe pump tube
30.	TMPA3201919Z – PCTFE boss plug	1	To plug the remaining inlet in the 3-boss manifold

Figure 3.30 and 3.31 show the test set-ups for both parts of TEST-COM-04:

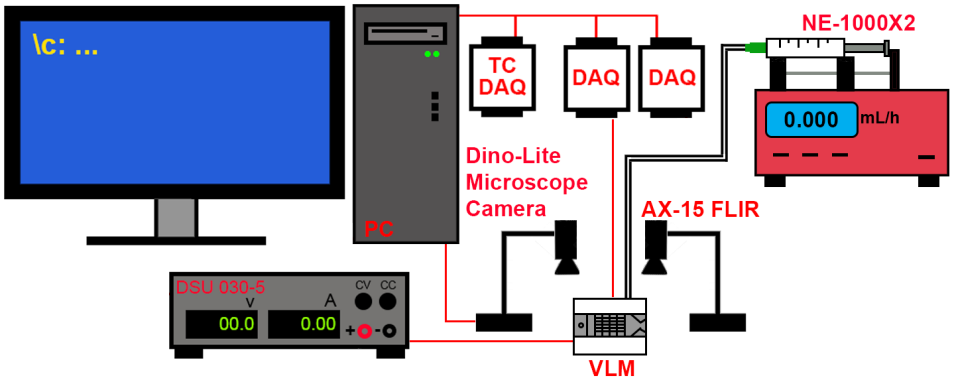

Figure 3.30: TEST-COM-04 test set-up for power and pressure testing part

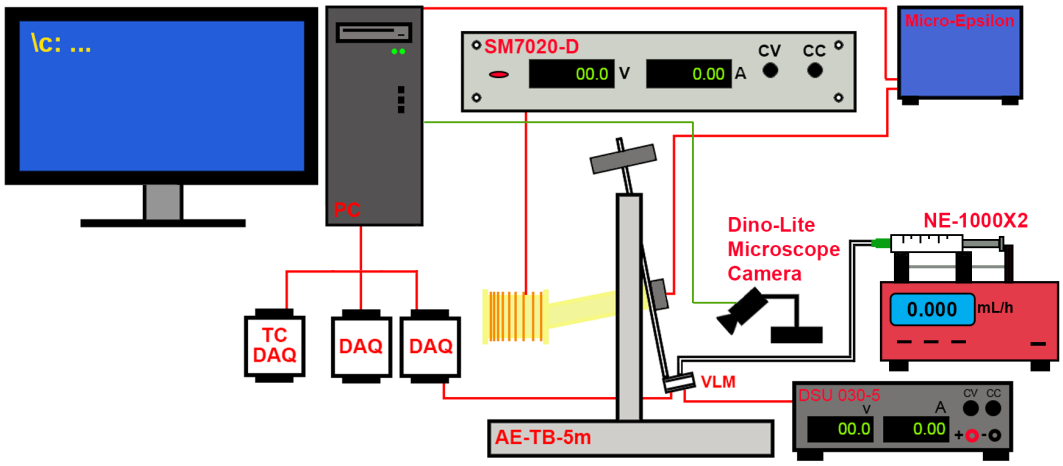

Figure 3.31: TEST-COM-04 test set-up for thrust bench testing part

A photo from the actual test set-up is shown in Figure 3.32:

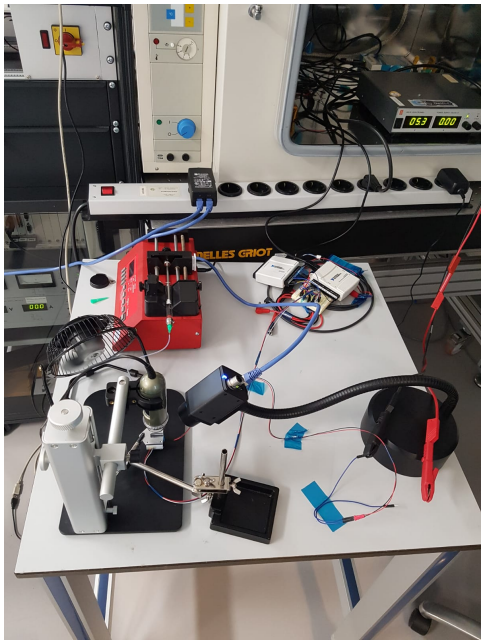

Figure 3.32: Actual representation of the TEST-COM-04 test set-up

Parameters

The test parameters, which need to be quantified and are necessary to obtain test data, are defined in this section. Two sets of parameters are provided: theoretical (predefined by the numerical analysis), and the intended during the testing. A summary of the FOE parameters (theoretical) calculated by *Turmaine* [3] is given in Table 3.26:

Table 3.26: The theoretical values of pressure, power, and mass flow for FOE determined by [3]

Parameter	Value	Units	Description
P_{c0}	$1.1 \cdot 10^5$	[Pa]	Initial pressure of the propellant
$P_{c\text{end}}$	$0.201 \cdot 10^5$	[Pa]	Final pressure of the propellant
$\dot{Q}_{\text{min}}$	0.4	[W]	Final required power by the propellant
$\dot{Q}_{\text{max}}$	2.2	[W]	Initial required power by the propellant
$\dot{m}_{\text{min}}$	0.5	[mL/h]	Final propellant mass flow rate
$\dot{m}_{\text{max}}$	2.8	[mL/h]	Initial propellant mass flow rate

The following parameters involved in the test are shown in Table 3.27:

Table 3.27: Parameters involved in TEST-COM-04: Heater Efficiency Test

Parameter	Dimension	Description	Range

P_c	[mbar], [Pa]	Plenum pressure inside VLM thruster interface	*Independent parameter*: depends on the water mass flow and vaporization inside the chip. *Accuracy*: $\pm$30 [mbar] (Tech. Data Sheet [40])
T_0	[^{o}C]	Plenum temperature inside VLM thruster interface	*Independent parameter*: depends on the water mass flow and vaporization inside the chip. *Accuracy*: $\pm$0.003 [g] (Tech. Data Sheet [40])
T_c	[K], [^{o}C]	Temperature at the chip chamber	*Independent parameter*: its value is determined from the thermal imaging camera. Range: depends on the chip performance. *Accuracy*: ±5 [^{o}C] (Tech. Data Sheet [49])
V_i	[V]	Input Voltage from the PSU	*Controlled parameter*: user sets the value. It depends on the heater resistance. Increased in steps of 0.1 - 0.5 [V] until there is overflow. Range is 0-12 [V]. *Accuracy*: ±0.1 [V] (Device's display scale)
I_i	[A]	Input current from the PSU	*Controlled parameter*: user sets the value. Its maximum value is set according to the heater resistance and power required. It is always in a range of milli-amperes. Range is 0 - 1 [A]. *Accuracy*: ±0.01 [A] (Device's display scale)
R_h	[Ω]	Heater resistance	*Independent parameter*: the resistance depends on the heater configuration and amount of heaters. *Accuracy*: ±1% + 2 (Tech. Data Sheet [48])
P_i	[W]	Input power to the heaters. Defined by the voltage and current	*Controlled parameter*: dependent on the voltage and current input. *Accuracy*: N.A.

$\dot{m}_{H_2O}$	[mL/h]	Mass flow from the syringe pump	*Controlled parameter*: user sets the value in steps of 0.5 [mL/h] per test. The range is 0.5 - 3 [mL/h] derived from Table 3.26. *Accuracy*: N.A.
t_s	[s]	Sampling time of the test	*Independent parameter*: the testing time depends on when the overflow is reached. The sampling frequency of the sensors is 0.28 [s]. *Accuracy*: N.A.
Δ_{displ}	[μm]	Pendulum displacement	*Independent parameter*. The description is found in [34]
F_t	[N]	Thrust	*Independent parameter*. The description is found in [34]

Success Criteria

The following criteria is used to define whether the test has been successfully performed, but also whether the system performs according to the requirements:

Table 3.28: Success criteria of TEST-COM-04: Heater Efficiency Test

Criteria	Description
SC-TC04-01	Parameters from Table 3.27 are obtained and documented
SC-TC04-02	All items in Table 3.25 are present
SC-TC04-03	The power-pressure test part using the syringe pump is performed and at least one of the mass flow values is used
SC-TC04-04	The thrust bench test part is conditionally performed (it can be considered as a bonus result of the whole test)
SC-TC04-05	A full vaporization of the water is achieved inside the chip
SC-TC04-06	The sensor test data is obtained, saved in a file, and backed up
SC-TC04-07	The video footage is obtained, saved in a file, and backed up
SC-TC04-08	The log of the observation comments is documented, saved in a file, and backed up
SC-TC04-09	At least 2 mass flow values are tested
SC-TC04-10	The required power to vaporize the water is according to the requirements

Test Procedure

The test procedure is split into two parts. One part describes the power-pressure measurements using the set-up as shown in Figure 3.30. The second part describes the thrust bench set-up testing as shown in Figure 3.31.

Table 3.29: Test procedure of the power-pressure measurements

Step	Sub-Step	Description	Performed (Y/N)	Time Stamp
1.		Check if the items 1 - 11, 13, 16 - 28 are present from Table 3.25		
2.		Turn on PC and connect DAQ to USB		
3.		Turn on *DSU 030-5* PSU:		
	3.1	Make sure the voltage and current values are set to zero		
	3.2	Connect the jumper wires accordingly		
4.		Connect microscope camera:		
	4.1	Connect *Dino-Lite* camera to front USB port of the PC (avoid connecting it to the USB hub, due to the required stable power input for the camera)		
	4.2	Launch *Dino-Lite Capture* Software (SW) and create file directories to save the footage accordingly		
5.		Connect thermal imaging camera:		
	5.1	Connect *FLIR AX-5* camera to the Ethernet port on the PC If the PC next to the vacuum oven is used, the displacement sensor cable has to be removed and camera's cable is inserted instead		
	5.2	Launch *ResearchIR* SW and creat file directories to save the footage accordingly		
6.		Launch *LabView* and set the file directories to save the data accordingly		
7.		Syringe pump set-up:		
	7.1	Turn on *NE-1000X2* syringe pump and set the mass flow to [mL/h]		
	7.2	Fill the syringe with the de-mineralized water such that the water reaches maximum syringe volume		
	7.3	Attach *0.062 MINSTAC* tube to the syringe via the *Luer* lock and make sure the tube is filled with water until the outlet (saves time when need to fill the plenum with water)		
	7.4	Place the syringe in the pump and fix it accordingly. Connect the tube end to the safety screen inlet		
8.		Placement of VLM thruster:		
	8.1	The thruster interface is placed on the table and clamped with the third hand stand.		

	8.2	The thruster should be directly under the microscope camera. The outlet of the thruster is facing the thermal imaging camera
	8.3	Pressure sensor wires are connected to the DAQ
	8.4	The heater wires are connected to the jumper wires leading to the *DSU 030-5* PSU
9.		Execution:
	9.1	If the chip and the interface are used for the first time, they need to be filled with water first. Set the pump mass flow value to 1.5 [mL/h] and start pumping. When the water reaches the plenum it can be observed via microscope camera footage. The pump is stopped when the water just hits the plenum
	9.2	Set the mass flow value according to the given values in Table 3.27 for the actual testing
	9.3	Set the current value on *DSU 030-5* PSU to the maximum required power according to the chip heater resistance. Voltage should be set to zero at the moment
	9.4	Start the recordings of both cameras one after another. Start *LabView* code immediately after that. Write a time-stamp down
	9.5	Increase voltage to the maximum power requirement and wait until the chip reaches 80 - 90 [^{o}C]
	9.6	Start the pump
	9.7	Observe via *Dino-Lite Capture* software the behavior of the vaporization
	9.8	Decrease the voltage and comment for every voltage step the behavior of the chip
	9.9	When an overflow inside the chip is reached, the power from PSU is cut-off and the pump is stopped immediately
	9.10	The camera recordings and *LabView* code is stopped
10.		Re-run of the test:
	10.1	After *Step 9.10* let the thruster cool down to 36 [^{o}C] and removed from the third hand clamp
	10.2	The user should wear latex gloves and unscrew 4 interface screws such that the glass and the chip can be easily removed

	10.3	Using the pre-saturated wipes the water excess is cleaned off from the chip, the glass, and inside the interface where the chip is placed
	10.4	Inspect the chip for any damage on the heater side. If the heaters seems to be damaged, measure their resistance with the multimeter and note its value down
	10.5	Re-assemble the interface and set it up as explained in *Step 8.*
	10.6	Follow the procedure as explained in *Step 9.* for different mass flow values
11.		Make a log of the comments for every voltage step and mas flow trials for each thruster chip accordingly. Save the log and back it up
12.		Close all the software, back up all the footage, switch off all the equipment, remove the residue water from the interface and syringe

Table 3.30: Test procedure of the thrust bench measurements

Step	Sub-Step	Description	Performed (Y/N)	Time Stamp
1.		Check if the items 1 - 15, and 19 - 30 are present from Table 3.25		
2.		The same as *Step 2.* in Table 3.29		
3.		The same as *Step 3.* in Table 3.29		
4.		The same as *Step 4.* in Table 3.29		
5.		The same as *Step 6.* in Table 3.29		
6.		Place the thrust bench inside the vacuum chamber (the thrusting side of VLM should be facing the right side of the vacuum oven)		
7.		Placement of VLM thruster:		
	7.1	The thruster is screwed on the pendulum and using a corner alignment tool its position is made straight to obtain the best displacement measurements		
	7.2	All the heater and sensor wiring must be coiled around the pendulum's rod (NOTE: make sure none of the wires are touching pendulum's frame)		
	7.3	Pressure sensor wires are connected to the DAQ		
	7.4	The heater wires are connected to the jumper wires leading to the *DSU 030-5* PSU		
8.		Syringe pump set-up:		

	8.1	The same as *Step 7.1* in Table 3.29
	8.2	The same as *Step 7.2* in Table 3.29
	8.3	Screw the tube from the syringe and thrust bench to the manifold. Seal it with the 3-boss plug
	8.4	The same as *Step 7.3* in Table 3.29
	8.5	The same as *Step 7.4* in Table 3.29
	8.6	Screw the other end of the tube onto the safety screen
9.	Execution:	
	9.1	Connect the jumper wires from the heater wires to the PSU
	9.2	Start the recordings of both cameras one after another. Start *LabView* code immediately after that. Write a time-stamp down
	9.3	Set the current and voltage to the maximum power requirement according to the heater resistance and start heating the thruster
	9.4	Start the pump with the mass flow value according to the given values in Table 3.27
	9.5	As there is no way to observe when the water reaches the plenum, the user can observe the pressure jump on the *LabView* code (most likely a turbulent increase in pressure is visible)
	9.6	Observe via *Dino-Lite Capture* software the outgoing gas or water from the nozzle exit
	9.8	Decrease the voltage and comment for every voltage step the behavior of the chip
	9.9	When an overflow inside the chip is reached, the power from PSU is cut-off and the pump is stopped immediately
	9.10	The camera recordings and *LabView* code is stopped
10.		Re-run of the test:
	10.1	After *Step 9.10* let the thruster cool down to 36 [^{o}C] and removed from the thrust bench
	10.2	The same as *Step 10.2* in Table 3.29
	10.3	The same as *Step 10.3* in Table 3.29
	10.4	The same as *Step 10.4* in Table 3.29
	10.5	Re-assemble the interface and set it up as explained in *Step 7.*
	10.6	The same as *Step 10.6* in Table 3.29

11.	The same as *Step 11.* in Table 3.29
12.	The same as *Step 12.* in Table 3.29

4

Results Analysis

In this chapter the results of the testing campaign and PPD design improvements are discussed.

4.1. TEST-INT-01: Leak Test

In Section 3.1 it is shown that the leak tests are split into three parts. Each part had a number of attempts. The reasons for each attempt are given at each leak test part results analysis in this section. An rundown of all the leak tests, which were performed on the PPD, are shown in Table 4.1:

Table 4.1: Overview of all performed TEST-INT-01 tests

Date	Test Part	P_0 [bar]	Condition	Duration [h]	Comments
03/01/2019	Part 1	5	Ambient	24	Check valve issues at 5 [bar]. 2.47 [bar] achieved as P_0
07/01/2019	Part 1	1.5	Ambient	24	1.49 [bar] achieved as P_0
09/01/2019	Part 1	3.5	Ambient	24	Only N_2 is used. 3.63 [bar] achieved as P_0
16/01/2019	Part 1	2	Ambient	48	No plugs. Reference test
19/01/2019	Part 1	2	Ambient	48	Plug on the check valve
21/01/2019	Part 1	2	Ambient	48	Plug on the LPM valve
24/01/2019	Part 1	2	Ambient	48	All plugs
25/01/2019	Part 1	2	Ambient	48	Plug on the VLM valve
30/01/2019	Part 1	1.1	Ambient	24	All plugs. Final Operational Envelope
15/02/2019	Part 1	1.1	Vacuum	24	All plugs. Final Operational Envelope

21/02/2019	Part 2	1.1	Vacuum	24	Plug on the check and the VLM valves. Final Operational Envelope
22/02/2019	Part 3	1.1	Vacuum	24	Plug on the check and the LPM valves. Final Operational Envelope

4.1.1. Leak Test Part 1 Results

In this section all the leak test attempts for *TEST-INT-01: Leak Test (Part 1)* as described in Section 3.1.1 are presented here. A total of 10 test runs have been attempted.

The first 3 test runs from Table 4.1 can be considered as the preliminary tests. Since there is no data available on how the pressurized propellant tank would behave, it is decided to pressurize the system with nitrogen at various different initial pressures.

The first run is at 5 [bar] initial pressure. It is just below 5.17 [bar] maximum pressure of the check valve [50], where the solenoid valve can operate up to 120 [psig], which is equivalent to around 8.27 [bar] [44]. The very first pressurization has failed what is thought due to the malfunctioning of the check valve. Following the test procedure described in Section 3.1.1, it is noticed that the check valve releases N_2 through its inlet. Normally a check valve is designed to create a uni-directional flow. It is decided to check manually if the check valve actually closes at lower level pressures. A nitrogen gas has been fed at 4 [bar], 2 [bar], and 1 [bar] against the indicated flow direction on the check valve. The valve just opened up and let the gas out at all three tries. It is thought that this valve is malfunctioning due to the manufacturing inaccuracies. Therefore, it was replaced with an identical, but a new check valve. However, the initial pressure was lowered to 2.5 [bar] (half the original intended). In this case, the check valve was behaving the same as the first one.

At this moment, it is doubtful that both check valves are flawed. Th cause of the malfunctioning could be its wrong operation by the user. Since there is no manufacturer's manual on how to operate the check valve, it is decided to determine what type of the check valve it is such that the working principle could be understood. There are various types of check valves: *Swing (Top Hinged, Tilting Disk) Type*, *Lift (Piston, Ball) Type*, *Dual Plate Type*, or *Stop Type* [51]. After inspecting *The Lee* check valve visually, it is hard to deduce what type it is (**NOTE**: *up to this time there is no provided information from the manufacturer on how to operate the check valve and what type it is*). From the current experience on operating *The Lee* check valve, it is noticed that for the check valve in order to close and not release the gas, the filling of the gas has to be performed at least few times until at a certain attempt it seals itself and the pressure is maintained after filling. It can be assumed that the certain latching device inside the check valve needs to be either stretched or "warmed up" (assuming it has a spring) before it can work efficiently.

The test proceeded according to the test procedure when the check valve closed properly. The results of the first attempt are presented in Figure 4.1.

The second attempt is set to 1.5 [bar] initial pressure. This is done to check what is the behavior of the leak at different initial pressures and help to characterize the leak, since there is no other similar test data available. Furthermore, the 1.5 [bar] pressure is used due to the same check valve gas filling problems. The results of the second attempt are presented in Figure 4.1.

The third attempt is performed at a higher initial pressure with only N_2 gas inside the tube. The chosen initial pressure is 1 [bar] higher than the 2.5 [bar] attempt. This is done to check whether the check valve can actually hold at a higher pressure, since the first check valve broke due to the assumed reasons. At the same time only nitrogen is injected in the tube. It is done to check whether by replacing the water, the leak would increase and would mean there is also a leak at PoIs where the water is stored. The results of the third attempt are presented in Figure 4.1.

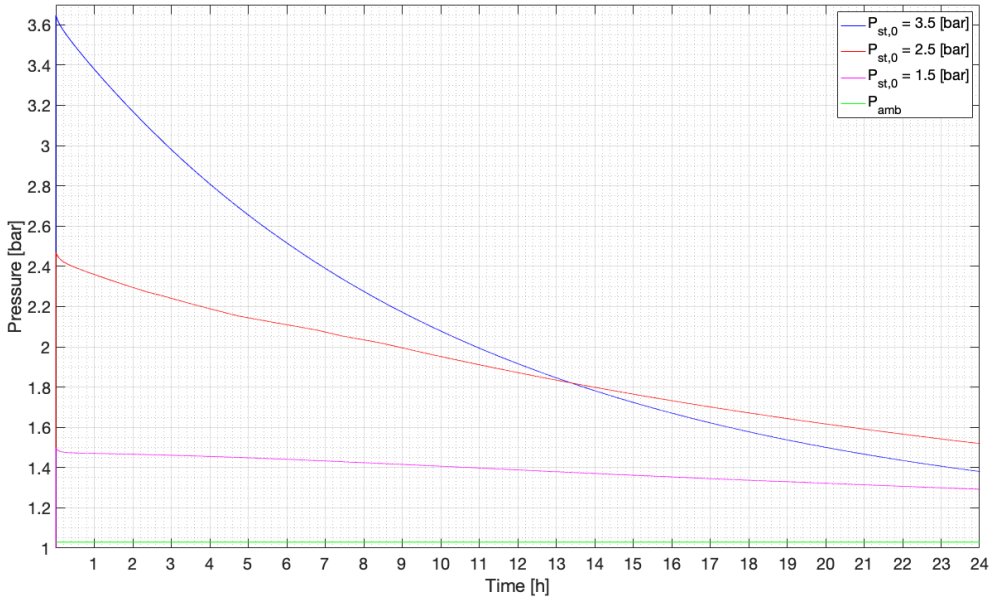

Figure 4.1: Preliminary leak tests with 1.5, 2.5, and 3.5 [bar] initial pressures

During the test procedure step of the nitrogen filling, it is noticed that to reach the exact intended initial pressure is very hard due to the mechanical pressure regulator in the GPFS. The intended initial pressure of the first attempt is 2.5 [bar], but the actual achieved pressure is 2.47 [bar]. For the second attempt the intended initial pressure is 1.5 [bar], but the actual is 1.49 [bar]. For the third attempt the intended initial pressure is 3.5 [bar], but 3.63 [bar] is achieved. Since the initial pressure values are not hard requirements for these preliminary tests, it is decided that the approximate pressure is good enough at this stage of the testing.

Swiping through the data points of all 3 attempts, it is noticed that the pressure does not gradually decrease over the time. There are small peaks in every time step, where the variations are in a range of 0.01 [bar]. This happens due to the signal noise in the sensor. Such a noise increases the error in the data over the time. It is decided to reduce this error by *smoothing* the data. It is done by applying *smooth* function in *MatLab*. For the *smooth* function the *moving average filter* method is used. It is one of the most popular methods for signal processing and it doesn't downgrade the original signal properties [52]. As an example of the raw and smoothed data of the first attempt is shown in Figure 4.2:

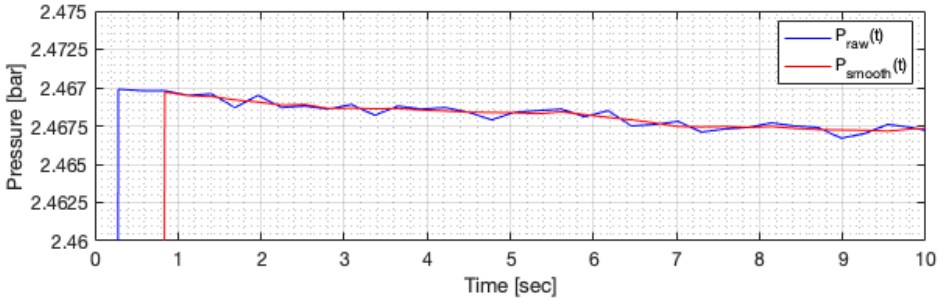

Figure 4.2: First 10 [s] of the first attempt leak test to show raw and smooth data

Figure 4.1 shows the smoothed data for all three preliminary tests. As it can be seen, there are obvious leaks for all shown attempts. The total drop of pressure inside PS in 24 hours is determined by Equation 4.1:

$$\Delta P = P_{ST,0} - P_{ST,F} \tag{4.1}$$

$P_{st,0}$ is the first data point entry of the pressure [Pa], and $P_{st,F}$ is the last data point entry [Pa]. Furthermore, the average pressure drop per second is determined. Using *MatLab* function *diff*, the sampling rate of the *MS5837-30BA* sensor data in *LabView* code is determined. The result is 0.281 [s]. The sampling frequency is calculated using Equation 4.2:

$$f_s = \frac{1}{t_s} \tag{4.2}$$

t_s is 0.281 [s], which gives f_s of around 3.5 [Hz] (0.281 [s] is set by the user in DAQ settings and *LabView* code. After checking the pre-built code by a previous student, the same 0.281 [s] value is found). The sampling frequency here is used only for the purpose to determine the pressure change every second. Thus, it is easier to translate this time and pressure data over long time spans. The same *MatLab* function *diff* is used to calculate pressure change every 0.281 [s] (ΔP_{avg}), which is averaged using *MatLab* function *mean* over the whole test data (assuming the data is quasi-linear). To know what is the average pressure change every second, the following expression is used:

$$P_{avg}(t) = f_s \cdot \Delta P_{avg} \tag{4.3}$$

The summarized results of the three preliminary tests using Equations 4.1 to 4.3 are shown in Table 4.2:

Table 4.2: Results of the three preliminary leak tests

Parameter	$P_{st,0}$ [mbar]	$P_{st,F}$ [mbar]	ΔP [mbar]	t_s [s]	f_s [Hz]	ΔP_{avg} [mbar]	$P_{avg}(t)$ [mbar/s]
1.5 [bar] Test	1497.0	1292.6	204.4	0.281	3.5	0.0007	0.00245
2.5 [bar] Test	2469.9	1512.1	957.8	0.281	3.5	0.0031	0.01085
3.5 [bar] Test	3648.2	1378.2	2270.0	0.281	3.5	0.0073	0.02555

From Figure 4.1 and Table 4.2 can be seen that there is an obvious leak. The most noticeable feature from the data is the increase of thre pressure change gradient with the increasing initial pressure in the system. However, the three preliminary leak tests do not reach the ambient pressure (green line) in Figure 4.1. The behavior of the leak when it would reaching the ambient pressure is not known. Therefore, 48 [h] leak tests are performed.

In the 48 [h] trials a leak detection is also implemented. As there are doubts about the tightness of the check valve membrane, a special plug is made for its inlet. The same is done for the outlets of both solenoid valves. There is a possibility that the leakages are located there and whether the plugs can prevent them. The plugs are made from a re-moldable thermoplastic, which is used for a rapid prototyping. It is called *Gorilla Plastic*, which can be ordered on-line via *Conrad* website. Furthermore, the nitrogen feed line in the vacuum chamber is equipped with *TMDA3201950Z* adapter. This adapter is from the same *062 MINSTAC* family of the *The Lee* parts. Therefore, it fits the inlet of the check valve. However, it is noticed during the set-up of the previous 3 preliminary leak tests, that one of the probable reasons why the nitrogen escapes so fast via inlet of the check valve is that the unscrewing of the adapter takes a lot of time. It is assumed that due to the outgoing gas from the feed line while the adapter is being removed, its pressure somehow keeps the membrane of the check valve open, thus the gas from the PS escapes immediately. Furthermore, it is noticed that by unscrewing the feed line adapter from the check valve really fast, it prevents the escape of the gas from the PS. Therefore, a special adapter from the same thermoplastic is made, which requires only sliding it on the check valve when in use. Thus, the feed line can be removed in a fraction of the second. The adapter and the plugs are shown in Figure 4.3 and 4.4:

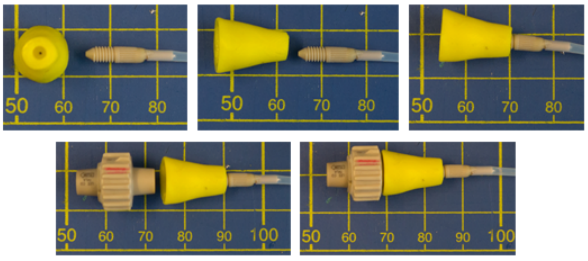

Figure 4.3: The adapter made to connect the nitrogen feed line adapter and the check valve

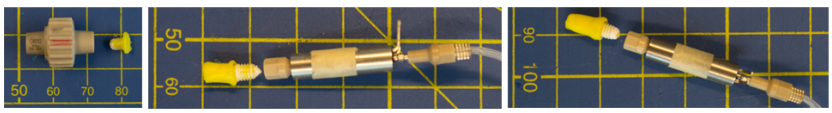

Figure 4.4: Plugs for the check and solenoid valves used in the leak tests

A slightly lower initial pressure in the propellant tank is chosen for these tests. It would give extra information on the leak behavior at various initial pressures. Therefore, for the second set of attempts an initial pressure of 2 [bar] is selected.

There are in total of 5 attempts at 2 [bar] initial pressure. The first one is performed without any plugs as a reference test. The second one is performed with a plug on the check valve. The third one is with the plug on the LPM valve. The fourth one is with the plug on the VLM valve. Finally, the fifth one is performed with the plugs on the check, LPM, and VLM valves. The outcome of all 5 attempts are shown in Figure 4.5:

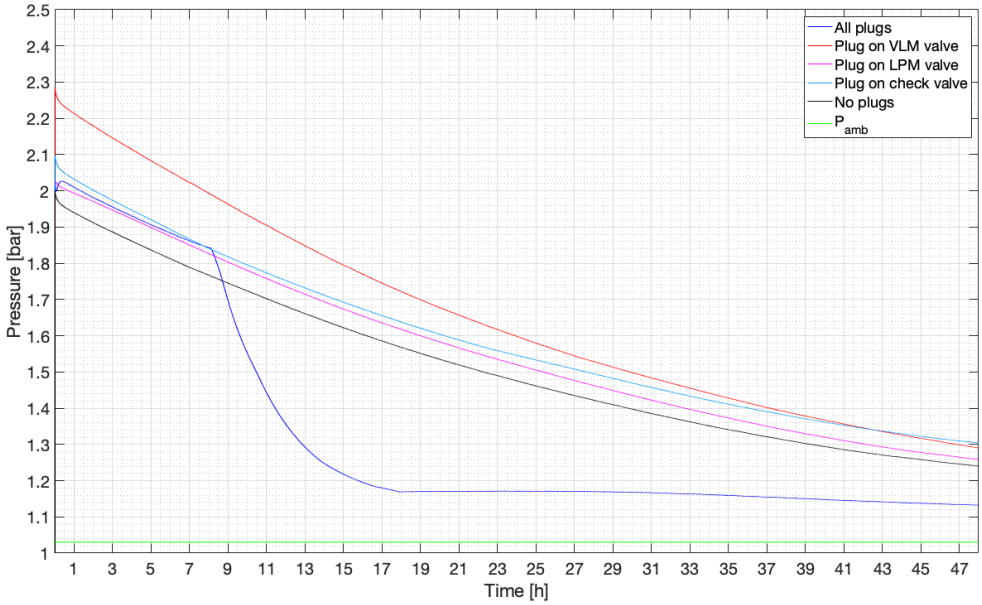

Figure 4.5: The leak tests results at initial pressure of 2 [bar] using the plugs

It can be seen not all the attempts have reached initial pressure of 2 [bar] during the pressurization. There is obviously a leak in the system somewhere not matter if the plugs are used. The data behavior of each run is very similar to the rest. There are slight variations in the pressure drop rate for each run. Thus, plugs do not improve the system's leakage. Furthermore, looking at Figure 3.1 from the outlet of the LPM and VLM valve and onwards, the system is open until the thruster. It is not possible to use a plug or a seal during the *Idle* mode of the PS in real space case. During the test with all plugs, a sudden drop in pressure appeared between the 8th and 18th hours of test. As the PS was all the time in the vacuum chamber with closed door, it does not seem that the sudden pressure loss is due to some external forces. Furthermore, there was no water residue outside the propellants, so it is most likely that only the nitrogen leaked and it leaked on the side of the PS where the gas could only be stored. Moreover, it is thought that the sensor has broken or its interface is leaking, but the it is known that the test with the plug on VLM is performed after the test with all the plugs, and its data seems to be fine as expected. The same Equations 4.1 to 4.3 are used to characterize these 5 attempts. The results are shown in Table 4.3:

Table 4.3: Results of the five leak tests at 2 [bar] initial pressure and using the plugs

Parameter:	$P_{st,0}$ [mbar]	$P_{st,F}$ [mbar]	ΔP [mbar]	t_s [s]	f_s [Hz]	ΔP_{avg} [mbar]	$P_{avg}(t)$ [mbar/s]
No plugs test	2001.6	1235.3	766.3	0.281	3.5	0.0012	0.0042
Plug on Check Valve Test	2097.9	1302.2	795.7	0.281	3.5	0.0013	0.00455
Plug on LPM Valve Test	2026.9	1258	768.9	0.281	3.5	0.0012	0.0042
Plug on VLM Valve Test	2284.1	1287.7	996.4	0.281	3.5	0.0016	0.0057
All Plugs Test	2000	N.A.	N.A.	0.281	3.5	N.A.	N.A.

Finally, the rest of the leak tests are performed using the FOE pressure values suggested by *Turmaine* [3] at various conditions. Two tests are done at ambient and vacuum conditions using the initial pressure of 1.1 [bar]. The outcome is presented in Figure 4.6:

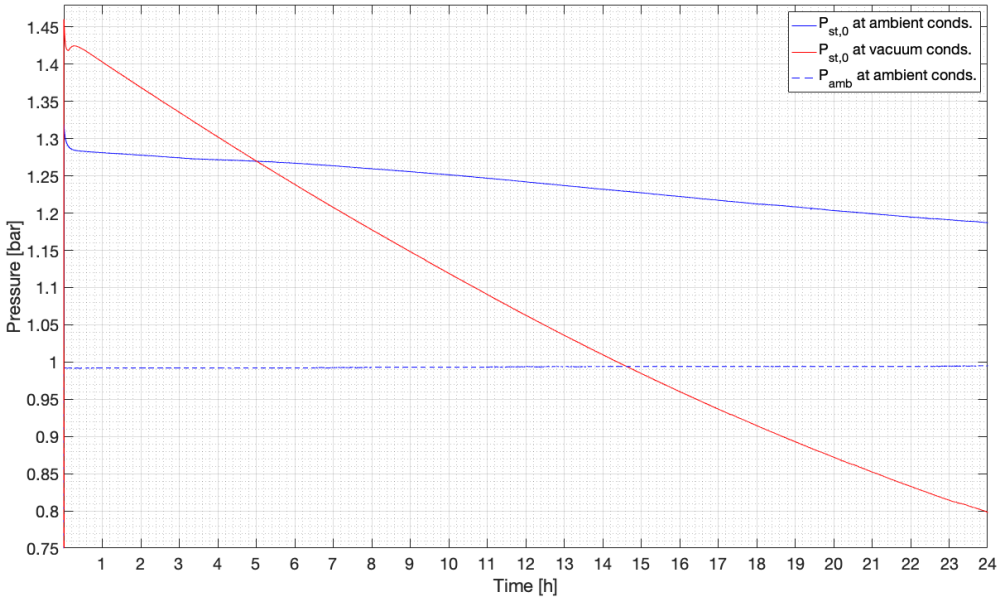

Figure 4.6: The leak tests results of the *Final Operational Envelope* at ambient and vacuum conditions

It can be seen that for both testing conditions the exact initial pressure of 1.1 [bar] is not achieved. It has to do with the technical limitations of the GPFS and the existing issues of the check valve. The pressure regulator on the GPFS has marked the increments of 0.5 [bar] on the dial, which makes it hard to pin-point smaller increments than 0.5 [bar]. The main issue lies behind the check valve during the filling of the nitrogen. As it was mentioned previously, the check valve randomly closes during the removal of the gas feed line with the adapter (ref. Figure 4.3). NOTE: In Figure 4.6 only the ambient pressure at ambient conditions is provided. The ambient pressure in the vacuum oven during the vacuum test is not provided, because due to the resolution of *MatLab* graph, the combined data from ambient test run would not be representable in single plot. However, the ambient pressure at vacuum conditions ranges from 1.03 [bar] to 0.005 [bar].

Furthermore, due to the *Matlab* graph resolution limit, the ambient pressure at vacuum conditions is excluded from Figure 4.6. A maximum of 0.000075 [bar] vacuum pressure has been achieved in the vacuum oven. Due to the safety regulations, the vacuum pump has only been turned on for the first 9 hours of the test (it is not allowed to keep the pump running during the night). As it is expected there is a small leak in the vacuum oven itself. Thus, the vacuum pressure decreased up to 0.005 [bar] at the end of the test. It gives a vacuum drop in the oven of $4.925 \cdot 10^{-3}$ [bar] over 24 [h] time period. This range falls under the low and medium vacuum class [53]. The maximum achievable vacuum by the clean-room vacuum oven is in the range of 10^{-4} [mbar], which would be considered as a high vacuum [53]. Thus, the reduction of $4.925 \cdot 10^{-3}$ [bar] in pressure is negligible compared to the final pressure of N_2 in the tank,which is 770.7 [mbar].

After applying the Equations 4.1 to 4.3, the results can be seen in Table 4.4:

Table 4.4: Results of TEST-INT-01: Leak test *Part 1* at the *Final Operational Envelope* values, and ambient and vacuum conditions

Parameter:	$P_{st,0}$ [mbar]	$P_{st,F}$ [mbar]	ΔP [mbar]	t_s [s]	f_s [Hz]	ΔP_{avg} [mbar]	$P_{avg}(t)$ [mbar/s]
FOE at Ambient Test	1318.7	1069.9	248.8	0.281	3.5	0.0002	0.0007
FOE at Vacuum Test	1460	770.7	689.3	0.281	3.5	0.0021	0.00735

The tests results presented in Figure 4.6 and Table 4.4 show that there are leaks at both conditions. The test at ambient conditions has a similar behavior of the test at 1.5 [bar] in Figure 4.1. It can be considered as a continuation of the preliminary test. However, the pressure change at vacuum conditions is extremely different than at ambient. This can be probably explained by understanding how the gas behaves in vacuum. Since there is a leak present somewhere in the system anyway, the pressure change is increased due to the sudden vacuum creation. By looking at the data of the vacuum oven pressure sensor, the vacuum in the order of 10^{-1} [mbar] is created within the first hour. It creates a pressure difference of 1.45 [bar] between the nitrogen in the tank and the ambient. Thus, the pressure change seen in Figure 4.6 at vacuum conditions is somewhat similar to the behavior of the leak test at 3.5 [bar] shown in Figure 4.1. There the pressure difference is around 2.4 [bar].

4.1.2. Leak Test Part 2 and Part 3 Results

The last two leak tests are performed for *Part 2* and *Part 3* of the TEST-INT-01 test. These two tests are performed at the *Final Operational Envelope* conditions as well. The leak test for *Part 2* considers a 1.1 [bar] initial nitrogen pressure in the tube. However, while performing these tests, there were mistakes found in the tube inner diameter size. Although, due to the unknown influence of it on the initial pressure at this moment, it is still decided to use a 1.1 [bar] pressure.

The leak test *Part 3* considers a water in the tube at 1.1 [bar] initial pressure. Since these two tests are similar in the set-up, they are presented in the same section. The outcome of the two tests is shown in Figure 4.7:

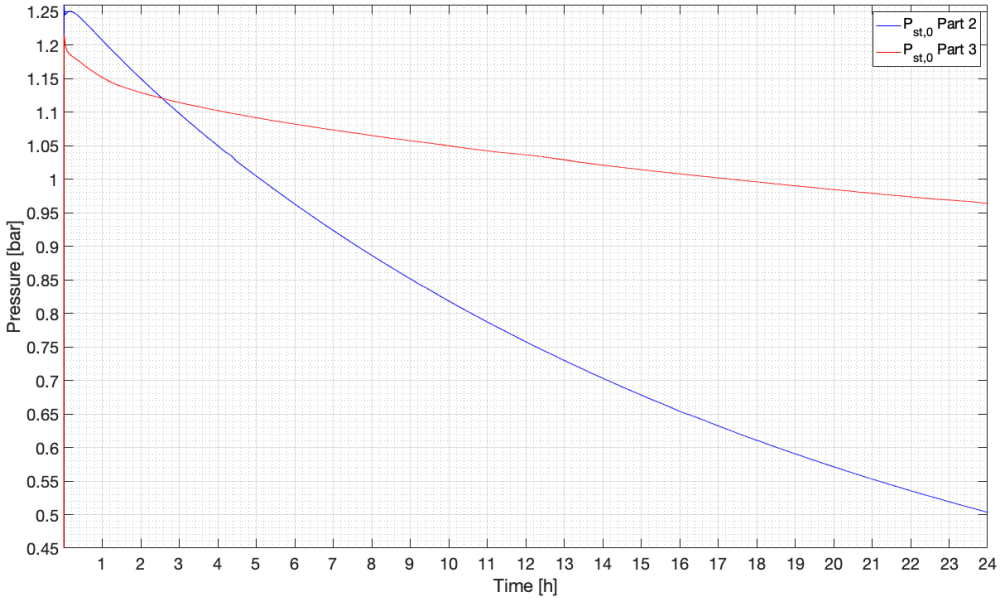

Figure 4.7: *Part 2* and *Part 3* of TEST-INT-01 leak tests results at the *Final Operational Envelope* and vacuum conditions

In Figure 4.7 can be seen that the initial pressures are slightly higher than the intended 1.1 [bar] (NOTE: the ambient pressure at vacuum conditions is not included in the plot, because of the graph resolutions limitations in *MatLab*. The ambient pressure at vacuum conditions for these two runs ranges from 1.03 [bar] to 0.005 [bar]). This is due to the same technical difficulties of the GPFS. The pressure change of *Part 2* leak test is very similar to the leak test wit the initial pressure of 1.45 [bar] in Figure 4.6. It means there is a similar size leak orifice at the PoIs. However, in this case a safety screen is used which can create an extra leak. This has to be investigated further, because at the moment it is also not known whether the safety screen is necessary for the LPM interface.

Part 3 leak test results in Figure 4.7 show a slightly different pressure change behavior. It is more gradual than the *Part 2* test. It most likely has to do with the substance in the tube and its properties. For *Part 3* leak test, the tube between the solenoid valve and the VLM interface is filled with water and pressurized with the nitrogen gas up to 1.1 [bar]. It is done to mimic the PS operational mode when in orbit. Since water molecules are bigger and water itself is much more viscous than nitrogen, it is harder for it to escape through the leak orifice. On the other hand, the gradual leak can be due to the not enough water pressure in the tube. After applying Equations 4.1 to 4.3 the overview of the discussed results can be found in Table 4.5:

Table 4.5: Results of TEST-INT-01: Leak test *Part 2* and *Part 3* at the *Final Operational Envelope* values, and vacuum conditions

Parameter:	$P_{st,0}$ [mbar]	$P_{st,F}$ [mbar]	ΔP [mbar]	t_s [s]	f_s [Hz]	ΔP_{avg} [mbar]	$P_{avg}(t)$ [mbar/s]
Part 2 Test	1266.8	501.8	765	0.281	3.5	0.0025	0.00875
Part 3 Test	1213.4	961.7	251.7	0.281	3.5	0.0008	0.0028

Another possible leak explanation for *Part 3* test is due to the water phase change while reducing the pressure in the vacuum oven. Water phase diagram is shown in Figure 4.8:

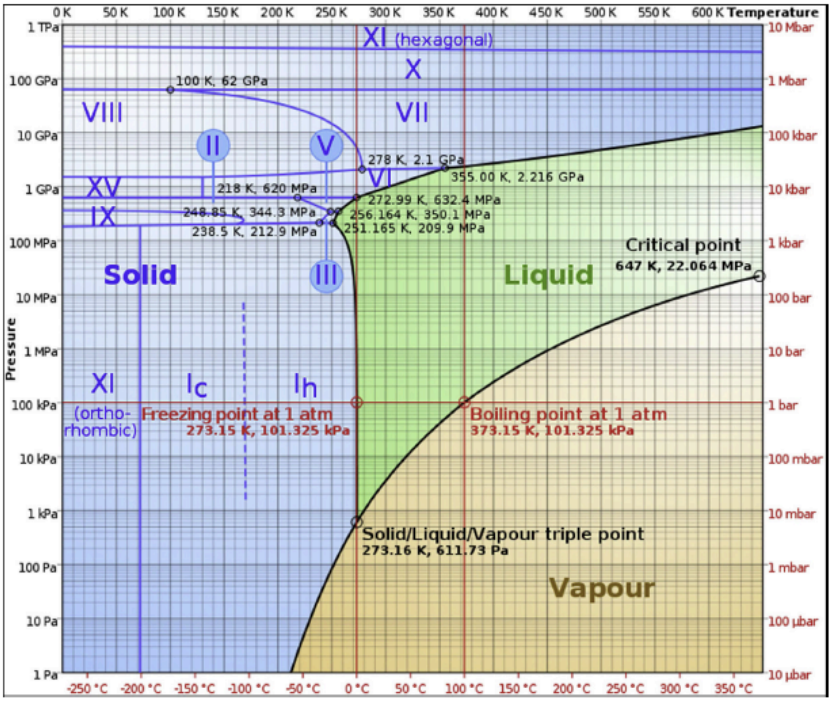

Figure 4.8: Water phase diagram [54]

From the given water phase diagram by [54], it can be seen that the water can transit from a liquid state region to vapour state region if the ambient temperature is kept constant and the ambient pressure is reduced. From the obtained *Part 3* test data it is known that the ambient pressure has been reduced from 1.03 [bar] to $7.83 \cdot 10^{-5}$ [bar]. The temperature in the cleanroom and, therefore, in the vacuum oven is around 20 [^{o}C]. Thus, by looking at Figure 4.8 it can be seen that water in the tank could possibly start vaporizing. This vaporizing gas is less dense and viscous, thus the water vapour molecules can easier escape through a leak orifice.

4.1.3. Leak Rate Definition

As one of the goals of TEST-INT-01 Leak tests is to validate PROP-PERF-300 requirement, a leak rate at the propellant storage has to be found. Therefore, the leak rate of the *Part 1* tests are considered. The results presented in Tables 4.2, 4.3, and 4.4 only show the pressure change, it does not define the actual leak rate. The leak rate can be calculated using 3 different methods according to *Zandbergen* [38]:

1. Molar Leak Rate (Q_m)
2. Volumetric Leak Rate [a.k.a. throughput] (Q_V)
3. Mass Leak Rate (Q_M)

It is decided to use *Mass Leak Rate* method. The mass leak rate is only considered for the nitrogen inside the tube. It can be determined by using the following Equation 4.4:

$$Q_M = \frac{\Delta M}{t} \tag{4.4}$$

It describes the mass change over the time. The time in this case would be the leak time(t_L). (ΔM) in the above equation is a mass change of the pressurant gas in the tank and is calculated using Equation 4.5:

$$\Delta M = \frac{V_{st}}{R} \cdot \left(\frac{P_{st,F}}{Z \cdot T_{st,F}} - \frac{P_{st,0}}{Z \cdot T_{st,0}} \right) \tag{4.5}$$

V_{st,N_2} is the volume that gas occupies in the storage. This volume is calculated using the following expression:

$$V_{st} = l_{st,total} \cdot \pi \cdot \left(\frac{D_{st}}{2} \right)^2 \tag{4.6}$$

Length of the propellant storage tank is $l_{st,total}$ [m]. The inner diameter (D_{st}), which is considered constant throughout all the components and is equal to $8.1 \cdot 10^{-4}$ [m] (the old, not correct value is used from [3]). All *Part 1* leak tests use the same $l_{st,total}$. The total storage length for *Part 1* tests comprises of the following components:

- *062 MINSTAC* tube - 5 [cm] (NOTE: its length is actually 6 [cm]).
- 2x *062 MINSTAC Male to Male* adapter
- The pressure sensor interface
- 3-Boss *062 MINSTAC* manifold
- Check valve
- LPM valve

These components and their configuration can be referred to Figure 3.3. However, the actual storage length is not from end to end of the component. Some of the components when they are assembled take up the volume of the other component, e.g. when a male-male adapter is screwed inside the pressure sensor interface. Thus, the following description is about the actual true total length of the volume which nitrogen occupies.

The channel length inside the manifold is assumed to be negligible, because no actual lengths are provided (see Figure 3.4). The same applies to the check valve. Although, it is not known how much gas would go inside the solenoid valve. It is assumed that the gas does not go further than the tube end inside the solenoid valve. The pressure sensor interface has a length of 14 [mm] (NOTE: it is 2 [mm] shorter than the one designed and produced in Figure 3.6 and 3.7). Furthermore, from Figure 3.5 can be seen that on the one side of the interface the male-male adapter is connected, and on the other side the *062 MINSTAC* tube. This reduces the internal volume of the interface. Since it is noticed that the tube and the adapter are not fully inside the interface, there is more internal volume left in the interface. The approximation of the pressure sensor interface actual length left inside is made accordingly:

- First, the threaded part of the *062 MINSTAC Male to Male* adapter together with the conical end is calculated. Using Figure D.1 from Appendix D, one threaded side with the conical end is equal to 6.65 [mm].

- Second, the length of the threaded part of the *062 MINSTAC* tube (ref. Figure D.2) is measured, since there are no actual dimensions. After measuring it with te calliper, the length is approximately 4 [mm].The conical end of the tube is 1.4 [mm]. The total length of 5.4 [mm] is calculated that can be inserted in the interface.
- Third, the actual length of the *062 MINSTAC Male to Male* adapter that is inside the interface is measured, as it is shown in Figure 3.5. Around 1 [mm] of the adapter thread is sticking out. It means the threaded part occupies 5.65 [mm] inside the interface.
- Fourth, the actual length of the *062 MINSTAC* tube that is inside the interface is measured, as it is shown in Figure 3.5. Only around 1 [mm] of the threaded part is inside. Adding the conical part of the tube, gives approximately 2.4 [mm] inside the interface.
- Finally, the length left inside the interface is calculated, where the lengths in step three and four are subtracted from the total length of the interface. The length left becomes approximately 5.95 [mm].

After defining all the lengths of the components, $l_{st,total}$ becomes 99 [mm] or 0.099 [m]. The final values of the storage volume determined by Equation 4.6 can be found in Table 4.6.

Next, R_{N_2} from Equation 4.5 is calculated using the following expression [55]:

$$R = \frac{\bar{R}}{M} \tag{4.7}$$

$\bar{R}$ has a value of 8.314 [kJ/(mol · K)] [55]. M has a value of 28.02 [g/mol] for N_2 [56]. Nitrogen gas constant (R_{N_2}) becomes 296.72 [J/(kg · K)]. Then, the compressibility factor (Z) value is taken as an average of 1 [bar] and 5 [bar] at 300 [K] [56] for initial and final conditions. Z value at 1 [bar] (300 [K]) is 0.9998 [-] and at 5 [bar] (300 [K]) is 0.999 [-], which gives an average value of 0.9994 [-]. The initial temperature ($T_{st,0}$) and the final temperature ($T_{st,F}$) of the propellant storage is taken from the measurement data, which needs to be converted to Kelvin degrees using the following expression [56]:

$$T[K] = T[^oC] + 273.15 \tag{4.8}$$

From all the plots of *Part 1* tests can be seen that the pressure change is non-linear globally, but looking at the local portions, the behavior tends to be more quasi-linear (this has to do due to the very long test runs of 24 [h] or 48 [h]). It can be assumed that the pressure change is constant. Thus, the duration of the leak is the test time, which is either 1 day (24 [h] = 86 400 [s]) or 2 days (48 [h] = 172 800 [s]) depending on the performed test. A summary of the intermediate parameters and the final mass leak rate for all *Part 1* leak tests is given in Table 4.6:

Table 4.6: Summary of the mass leak rate parameters of *Part 1* leak tests

Constants:	M [g/mol]	$\bar{R}$ [kJ/mol K]	D_{st} [m]	Z [-]	V_{st,N_2} [m^3]	R_{N_2} [J/kg K]	
	28.02	8.314	$8.1 \cdot 10^{-4}$	0.9994	$5.1 \cdot 10^{-8}$	296.72	
Inputs:					**Outputs:**		
Parameter	$P_{st,0}$	$P_{st,F}$	$T_{st,0}$	$T_{st,F}$	t_L	ΔM	Q_M

	[bar]	[bar]	[K]	[K]	[s]	[mg]	[mg/s]
2.5 [bar] Test	2.4699	1.5121	297.07	294.42	86 400	$5.468 \cdot 10^{-7}$	$6.33 \cdot 10^{-12}$
1.5 [bar] Test	1.497	1.2926	298.28	294.88	86 400	$1.093 \cdot 10^{-7}$	$1.26 \cdot 10^{-12}$
3.5 [bar] Test	3.6482	1.3782	296.65	294.96	86 400	$1.31 \cdot 10^{-6}$	$1.52 \cdot 10^{-11}$
No Plugs Test	2.0016	1.2353	297.35	294.88	172 800	$4.37 \cdot 10^{-7}$	$2.53 \cdot 10^{-12}$
Plug on Check Valve Test	2.0979	1.3022	296.37	294.32	172 800	$4.57 \cdot 10^{-7}$	$2.64 \cdot 10^{-12}$
Plug on LPM Valve Test	2.0269	1.258	296.4	294.27	172 800	$4.41 \cdot 10^{-7}$	$2.55 \cdot 10^{-12}$
Plug on VLM Valve Test	2.2841	1.2877	296.4	294.5	172 800	$5.72 \cdot 10^{-7}$	$3.31 \cdot 10^{-12}$
All plugs Test	N.A.	N.A.	N.A.	N.A.	N.A.	N.A.	N.A.
FOE at Ambient Test	1.3187	1.0699	299.23	294.19	86 400	$1.32 \cdot 10^{-7}$	$1.53 \cdot 10^{-12}$
FOE at Vacuum Test	1.46	0.7797	298.42	295.63	86 400	$3.93 \cdot 10^{-7}$	$4.55 \cdot 10^{-12}$

4.1.4. Leak Detection and Localization

Since there is an obvious leak somewhere in the system, the next step is to localize the leak. There is a number of leak detection and localization techniques described in 3.1.1. Five different techniques have been used.

Foam Application Method

One of the simplest and cheapest methods to detect and localize gas leak is using *Bubble* Method [38], also called *Soap Bubble Screening* [36], and *Foam/Liquid Application* [35]. This method is described in Section 3.1.1.

In the clean room there is a special soap solution spray flask called *Electrolube The Solutions People* (ref. Appendix C) which can be used specifically for such applications. The following leak detection procedure is applied to the PPD using *Soap Liquid* method:

1. The PPD pressure sensor is connected to the DAQ and the same *LabView* code as in *TEST-INT-01: Leak Test (Part 1)* is used.
2. The PPD is filled with around 2.6 [bar] nitrogen gas only and detached from GPFS.
3. To protect the electronic components, DAQ, and open wires from short circuiting, clean room dry wipes are used as a shield and absorber for the excess of the liquid.
4. The soap liquid flask is shaken, first, and, then, sprayed on the location where PoI is.
5. The PoI is inspected visually from all sides if there are bubbles forming and rising to the surface.
6. If no leak is detected on the sprayed PoI, the next following PoI is tested. The previous location is wiped off and dried with the wipes.

7. If a leak is detected at the sprayed location, it should be noted down. It is useful to note down the size of the bubbles and how fast they are forming. It can be also useful to take a short video with a camera to re-investigate the leak later if it is needed.
8. At the end of this inspection, the whole PPD should be cleaned and dried with the wipes. The remaining gas in the tube is released to the ambient.

It is noticed that the soap foam reduces to a liquid state in a matter of tens of seconds if the foam layer is very thin. Various thicknesses of the foam layer are tried. However, the leak cannot be detected easily and fast. Furthermore, the leak is most likely very small and it takes longer for the gas to form the bubbles before the foam reduces to liquid state completely. The *Foam Application* method did not yield any results as the leak detection and localization method.

Immersion Method

After it is decided that the *Foam Application* method does not work in this case, it is suggested to apply second part of the *Bubble* Method [38], or also known as *Immersion* method [35]. It is known from Section 3.1.1, such a method is more for localizing the source of the leak than quantifying it. The quantification can be implemented to a certain level of accuracy. The following leak detection procedure is applied to the PPD using *Bubble* method:

1. A glass beaker of 600 [mL] is filled with approximately room temperature water from the tap. It is placed on the table in the clean-room.
2. The PPD pressure sensor is connected to the DAQ and the same *LabView* code as in *TEST-INT-01: Leak Test (Part 1)* is used.
3. The PPD is filled with 2.6 [bar] nitrogen gas only and removed from GPFS.
4. The PPD is submerged completely in the beaker with the water. None of its components should stick in the air, which means all PoI are under the water. The wires together with the connector of the pressure sensor can be left hanging in the air.
5. It is possible that the light or reflections behind the beaker is too bright. The observer can put some dark cover behind the beaker to reduce the light intensity. This might help to notice the bubbles better, because the bubbles are transparent and are less visible in the white or bright background.
6. It is possible that some air is trapped in the form of bubbles at various locations on the PPD. The user can either shake them off, while the system is still in the water or use a q-tip to break the air bubbles or remove them from the components.
7. if the leak is detected, the bubble(s) size and their frequency should be noted down.
8. After the inspection is over, remove the PPD from the beaker and dry it with the wipes.
9. Drain the water in the beaker to the sink and clean it with the wipes.

This method might have possibly yielded some results. The following Figure 4.9 shows the bubble propagation at the outlet of the LPM solenoid valve (encircled in red color) during the *Immersion* method:

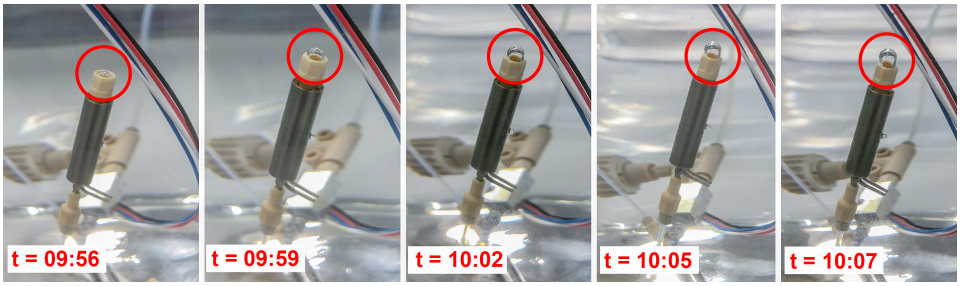

Figure 4.9: Nitrogen gas bubble propagation over time at the outlet of LPM solenoid valve

As there is no technical data about the leak of the solenoid valves from the manufacturer, it is thought that the solenoid valve in Figure 4.9 is malfunctioning due to the manufacturing faults or inaccuracies. Therefore, the same *Immersion* method is applied using other two solenoid valves. One valve is also brand new, and the other one is from the experiments used by *Makhan* [34]. Following the same procedure described above, there was no bubble emerging from the valve outlet. Nonetheless, after connecting the PS to the computer, a reduction in the pressure is observed for both alternative valves. It means that the leak is somewhere else than in the solenoid valve itself. After that, the same valve shown in Figure 4.9 is re-tested again and no observable bubble coming from the same outlet is observed. The only explanation of the emerging bubble in Figure 4.9 is that there was a considerable amount of trapped air inside the solenoid valve which was slowly creeping out. However, the leak at that location cannot be completely dismissed. Such a bubble formation can be random due to the same problem as the check valve have. It is possible that the solenoid valve does not close completely when it is not connected to the power supply.

Dye Penetration Method

After the *Immersion* method failed to localize the leak in the PS, another method is considered. It is called *Dye Penetration* method [38]. In this case, the dye or a colored viscous liquid is replaced with a smoke. The idea is that by injecting the smoke inside the system at a slightly higher pressure than the ambient, it would come out through the leak location and can be visually detected. One way to do it is to use CO_2 dry-ice. Such a fog/smoke is created by a *heat-transfer* process, where a sublimation of the CO_2 dry-ice in the water takes place. This fog/smoke is created by a mixture of the CO_2 vapour and condensed H_2O vapour in the water [57]. The phenomena is shown in Figure 4.10:

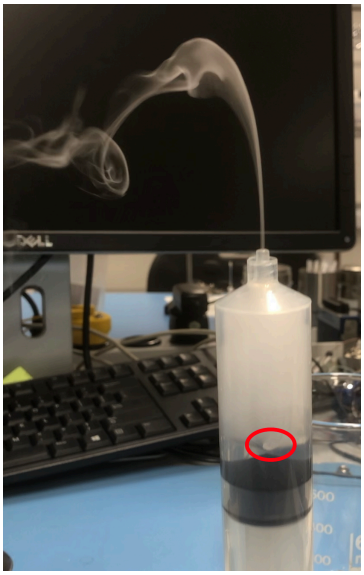

Figure 4.10: Sublimating dry-ice pellet (red circle) in the water inside the syringe

Such a method is apparently difficult to implement. Two issues are observed. One is very hard to sustain the fog for a long time. Due to a very big temperature difference between the dry-ice/water vapour and the ambient, the smoke dissipates very fast. Dry-ice sublimates at -78.5 [^{o}C] [57] and the ambient temperature is around 20-22 [^{o}C] in the clean-room. The second issue is during the sublimation of the dry-ice, where the escaping CO_2 gas creates pressure inside the container. If enough pressure is created in the enclosed volume, the container can burst/explode. Due to the technical limitations of this method, it is hard to measure the created pressure inside the syringe. Thus, only small amounts of gas has been injected in the PS. This lead to the first issue described above. Therefore, this dry-ice steam method is abandoned for the leak detection and localization. Nonetheless, if dry-ice is ever again needed, it can be obtained from *Logistiek en Milieu* building at TU Delft.

Optical Method

Since the clean-room is equipped with a thermal imaging camera, it can be used as an optical leak detection and localization method. The camera in use is *FLIR AX-15 series*. With the help of *FLIR* camera software the observed area can be shown in various color patterns and using the pin pointing tool a single spot on the observed area can be picked and its temperature shown. The sample image of the thermal camera is shown in Figure 4.11:

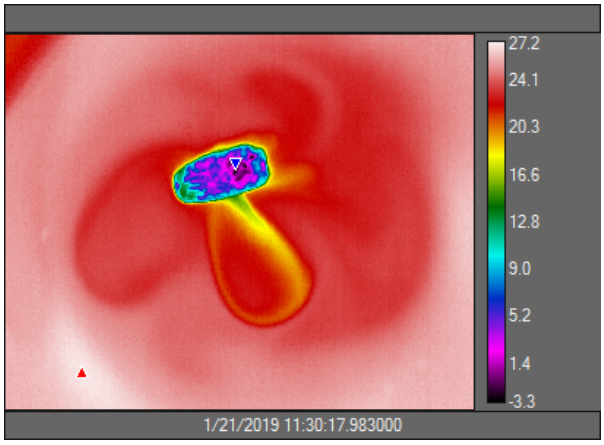

Figure 4.11: FLIR thermal camera image of the sublimating dry-ice pellet in the water

The sublimating dry-ice can be clearly seen in the yellow and green colors. The observed temperature range is shown on the right of Figure 4.11. A similar image is expected when a gas is escaping through the leak orifice in the PS. However, to see such an image the gas has to be at a lower or higher temperature than the ambient. Two different attempts have been tried. One, where the propellant tank has been filled with nitrogen at a pressure of 2 [bar]. Then the propulsion system was put in the clean-room's freezer for 5 minutes. After that it is taken out and observed with *FLIR* camera. No leak has been detected or it was hard to do it, because the cold components were warming up the air around it so the cold air swirls were everywhere in the thermal image.

The second attempt was by using the cold gas produced by the dry-ice pellet in the water. However, the produced CO_2 steam warms immediately in the tank tube. So no cold gas leak is observed with the camera. Nonetheless, at that moment it is believed that the leak could be very small and it is not possible to observe or detect with the proposed methods.

Mass Spectrometry Method

The last leak detection and localization method that is implemented is the *Mass Spectrometry*. A so called *sniffer* is used to detect a leaking helium gas [38]. The good part about using helium as a pressurant gas that it is relatively smaller particle than nitrogen, which means it would escape more easily through a gap. Since there is available helium sniffer at the *Aerospace Engineering* faculty, one is arranged from the *Applied Sciences* faculty:

Figure 4.12: BOC Edwards helium sniffer

However, to be able to use the helium sniffer from Figure 4.12, it is important to define a possible volumetric leak rate in the PS if helium is used instead of nitrogen. This is done

because the smallest detectable volumetric leak rate that *BOC Edwards* helium sniffer can detect is in the range of 10^{-5} [ml/s]. The volumetric leak rate can be calculated using the approach described by [38]. First, the equations 4.4, 4.5, and 4.6 are applied. The storage volume stays the same, which is $5.1 \cdot 10^{-8}$ [m^3]. The nitrogen gas constant in Equation 4.5 is replaced with helium's. M of helium is 4 [g/mol] [56]. Helium gas constant (R_{He}) becomes 2078.5 [J/kg·K] after applying Equation 4.7. The volumetric leak rates are performed on the three preliminary leak tests at 1.5 [bar], 2.5 [bar], and 3.5 [bar]. Therefore, the compressibility factor (Z) is around 1 for the considered pressures as taken from [58].

The leak rate in terms of moles per second is calculated using the following Equation 4.9:

$$Q_m = \frac{Q_M}{M} \tag{4.9}$$

For any given gas, 1 [mol] is equal to 22.414 [L] of gas (at 1.013 [bar] and 0 [°C]) [38]. By multiplying this value with Q_m, the volumetric gas leak rate (Q_V) is found. The volumetric leak rate is adjusted to the ambient temperature by using *Charle's law*, where the ambient pressure is constant [59]:

$$\frac{V_1}{T_1} = \frac{V_2}{T_2} = const \tag{4.10}$$

The volume variables in Equation 4.10 can be replaced with the volumetric leak rate constants. The ambient temperature (T_{amb}) is considered to be 22 [°C] . The corrected volumetric leak rate is called Q_{Vc}. The summary of the parameters is given in Table4.7:

Table 4.7: Summary of the volumetric leak rate parameters

Parameter:	V_{st,N_2} [m_3]	R_{He} [J/kg·K]	Z [-]	$T_{st,0}$ [K]	$T_{st,F}$ [K]	$P_{st,0}$ [bar]	$P_{st,0}$ [bar]
1.5 [bar] Test:	$5.1 \cdot 10^{-8}$	2078.5	1	298.28	294.86	1.497	1.2926
2.5 [bar] Test:	$5.1 \cdot 10^{-8}$	2078.5	1	297.42	294.42	2.4699	1.5121
3.5 [bar] Test:	$5.1 \cdot 10^{-8}$	2078.5	1	296.65	294.96	3.6482	1.3782

Parameter:	T_{amb} [K]	ΔM [mg]	Q_M [mg/s]	Q_m [mol/s]	Q_V [L/s]	Q_{Vc} [ml/s]
1.5 [bar] Test:	295.15	$1.559 \cdot 10^{-8}$	$1.805 \cdot 10^{-13}$	$4.512 \cdot 10^{-20}$	$1.011 \cdot 10^{-18}$	$1.093 \cdot 10^{-15}$
2.5 [bar] Test:	295.15	$7.801 \cdot 10^{-8}$	$9.029 \cdot 10^{-13}$	$2.257 \cdot 10^{-19}$	$5.059 \cdot 10^{-18}$	$5.47 \cdot 10^{-15}$
3.5 [bar] Test:	295.15	$1.872 \cdot 10^{-7}$	$2.166 \cdot 10^{-12}$	$5.415 \cdot 10^{-19}$	$1.214 \cdot 10^{-17}$	$1.312 \cdot 10^{-14}$

The corrected volumetric leak rates in Table 4.7 show that *BOC Edwards* helium sniffer could theoretically detect the leak in the PS. However, this would be on the extreme end of its detection range. The volumetric leak rates have been also calculated for the rest of the leak tests shown in Table 4.1. All the tests are at the 10^{-15} [ml/s] rate range. It is decided not to implement this method.

4.2. Leakage Simulation

In this section a leakage model is presented. The goal is to characterize the leak properties and the process behind the leak. It helps to understand at what conditions the leak appears, how big is the possible leak hole, and how the leak could possibly be prevented or minimized. The leak simulation is performed for FOE conditions only.

4.2.1. Simulation Assumptions

Before constructing the leakage model, certain assumptions are made to define the system boundaries and simplify real-life conditions. The assumptions are:

- Nitrogen is considered as the test substance and used in a gas state to pressurize the storage tank.
- The ambient temperature of the outside environment is constant and at 293.15 [K]. The leak simulation is based on *isothermal* conditions.
- The control volume is constant and has a value of $5.1 \cdot 10^{-8}$ [m^3].
- The inner diameter of the tube is 0.81 [mm].
- There is no water leak on the VLM side of the propellant tank.
- The simulation run time is 24 [h].
- The gas leak is considered at two cases: *subsonic* and *supersonic* flow.

4.2.2. Methodology

The model creation is based on the two gas flow conditions: *subsonic* and *supersonic*. Each condition is described by a number of equations.

Supersonic Leak Flow

To model the time dependent pressure change, first, the initial system conditions are defined. From the assumptions it is known that the process is *isothermal*. So the initial mass density of the nitrogen in the tube is calculated using Equation 4.11 [60]:

$$\rho = \frac{P}{T \cdot R} \tag{4.11}$$

Equation 4.11 is the ideal gas law equation expressed in terms of the density ρ [kg/m^3]. P is the initial pressure of N_2 in the tube [Pa], T is the room temperature [K], which is given in the assumptions: 293.15 [K], and R is the universal gas constant. R_{N_2} is converted to specific gas constant, in this case for nitrogen, where equation 4.7 is applied. The initial mass of the nitrogen in the tube is calculated using Equation 4.12 [55]:

$$m = \rho \cdot V \tag{4.12}$$

V [m^3] is in this case V_{st,N_2} and its value is given in the assumptions. After that, the initial mass flow of the leak is calculated from Equation 4.13 [60]:

$$\dot{m}_{real} = \frac{C_d \cdot P \cdot A_l}{c^*} \tag{4.13}$$

c^* is a characteristic velocity [m/s]. It is a relation between the chamber temperature, gas constant and gas specific heat ratio [60]:

$$c^* = \frac{1}{\gamma} \cdot \sqrt{R \cdot T_c} \tag{4.14}$$

R is R_{N_2} in this case, and T_c is 293.13 [K]. γ is the specific heat ratio of nitrogen, which is 1.404 [-] [56] (or can be calculated from Eqution 4.33). A_l [m^2] is the cross-sectional area of the leak orifice and is calculated using the following expression:

$$A_{leak} = \pi \cdot \frac{d_l^2}{4} \tag{4.15}$$

d_l [m] is the diameter of the leak orifice. C_d [-] is the discharge coefficient. It is used in non-ideal (real) case to give a relation between the area of the orifice and substance discharge due to the friction or flow separation. C_d is calculated from Equation 4.16 [60]:

$$C_d = \sqrt{\frac{1}{\zeta}} \tag{4.16}$$

ζ [-] is a total loss factor. It is a relation between the loss factor for a sudden contraction and a loss factor for a sudden expansion in the flow [60]:

$$\zeta = \zeta_c + \zeta_e \tag{4.17}$$

ζ_c [-] is the loss factor due to the sudden contraction and is calculated using Equation 4.18 [60]:

$$\zeta_c = 0.5 \cdot \left(1 - \frac{A_s}{A_l}\right)^{3/4} \tag{4.18}$$

ζ_e [-] is the loss factor due to the sudden expansion and is calculated using Equation 4.19 [60]:

$$\zeta_e = \left(1 - \frac{A_s}{A_l}\right)^2 \tag{4.19}$$

A_s is in this case the A_l [m^2] (cross-sectional area of the leak) and A_l is A_t [m^2] (cross-sectional area of the inner diameter of the tube). A_t can be calculated using the following expression:

$$A_t = \pi \cdot \frac{D_{st}^2}{4} \tag{4.20}$$

D_{st} is used with the value of 0.81 [mm]. The relation between the areas of the tube and leak orifices and loss factors can be shown in the following Figure 4.13:

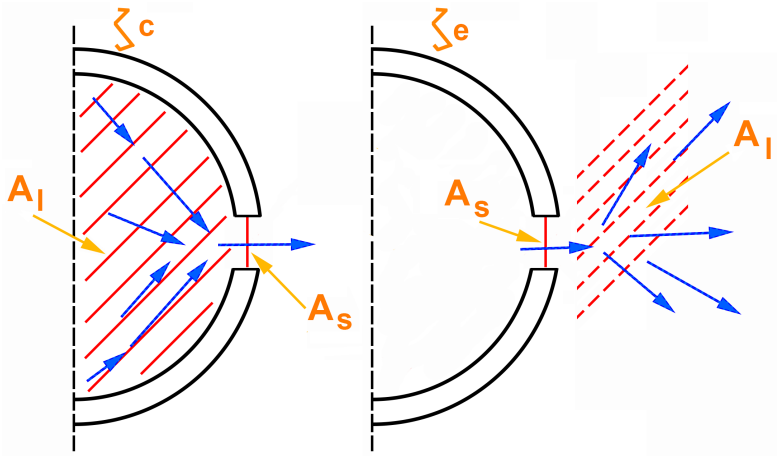

Figure 4.13: Gas flow representation at a sudden contraction and sudden expansion in the tube. Blue arrows are the gas flow direction. Red diagonal lines are the cross-sectional areas.

After defining the initial simulation conditions for the supersonic flow case, the iteration process is outlined. Every iteration has a defined time step (Δt), which is 1 [s]. The total time of the simulation is 24 [h], which is 86400 [s] in total. For every time step the iterations have to follow a chronological order of the calculations:

1. Every consecutive mass of the gas in the tube is calculated as follows:

$$m_i = m_{i-1} - \dot{m}_{i-1} \cdot \Delta t \tag{4.21}$$

2. Every consecutive mass density of the gas in the tube is calculated from the following expression:

$$\rho_i = \frac{m_i}{V} \tag{4.22}$$

3. Every consecutive mass flow rate of the gas is calculated as follows:

$$\dot{m}_i = \frac{C_d \cdot P_{i-1} \cdot A_{leak}}{c^*} \tag{4.23}$$

4. Every consecutive pressure of the gas in the tube is calculated using isothermal (T=const) gas law expression:

$$P_i = \frac{P_{i-1}}{\rho_{i-1}} \cdot \rho_i \tag{4.24}$$

Subsonic Leak Flow

For the *subsonic* leak flow, the initial conditions have to be calculated first. The approach is similar to the *supersonic* initial conditions calculations. Same Equations 4.11 and 4.12 are used to find initial gas density and mass in the tube. Additionally, the injection velocity and

mass flow rate has to be calculated. The initial injection velocity (v_i) [m/s] [60] is determined as follows:

$$v_i = \sqrt{\frac{1}{\zeta}} \cdot \sqrt{\frac{2 \cdot \Delta p}{\rho}} \tag{4.25}$$

Δp is the pressure difference between the initial pressure in the tube and the outside pressure (P_a) [Pa]. The injection velocity is measured between the entrance and exit of the leak orifice. This velocity is used to determine the initial mass flow rate of the gas leak [60]:

$$\dot{m} = \rho \cdot v \cdot A \tag{4.26}$$

A is the cross-sectional area of the leak (A_l) [m^2] in this case. As it can be seen for the *subsonic* flow, the mass flow rate only depends on the injection velocity, mass density of the gas inside the tube and the leak cross-sectional area.

After defining the initial conditions for the *subsonic* leak flow, the iterative method is described. The time step and iteration length stays the same as for the *supersonic* leak flow condition. The following chronological order of the iterations is given below:

1. Every consecutive mass of the gas in the tube is calculated as follows:

$$m_j = m_{j-1} - \dot{m}_{j-1} \cdot \Delta t \tag{4.27}$$

2. Every consecutive mass density of the gas in the tube is calculated from the following expression:

$$\rho_j = \frac{m_j}{V_t} \tag{4.28}$$

3. Every consecutive pressure of the gas in the tube is calculated using isothermal (T=const) gas law expression:

$$P_j = \frac{P_{j-1}}{\rho_{j-1}} \cdot \rho_j \tag{4.29}$$

4. Every consecutive injection velocity of the gas is calculated from the following expression:

$$v_j = \sqrt{\frac{1}{\zeta}} \cdot \sqrt{\frac{2 \cdot (P_j - P_a)}{\rho_j}} \tag{4.30}$$

5. Every consecutive mass flow rate of the gas is calculated as follows:

$$\dot{m}_j = \rho_j \cdot v_{i_j} \cdot A_{leak} \tag{4.31}$$

After defining the mathematical relations and implementation process of the iterations, the simulation code is written and executed in *Matlab*.

Critical Conditions

According to [60], the sonic conditions at the throat and supersonic conditions at the divergent part of the nozzle are not necessarily achieved by default. So called *Critical Conditions* have to be met. One of them is the pressure ratio between the upstream and the downstream flow pressures. The supersonic conditions only achieved if the ratio between the upstream flow pressure and the downstream flow pressure is higher than the inverse of the critical ratio. The critical pressure ratio is found by applying Equation 4.32:

$$\left(\frac{P_{th}}{P_c}\right)_{cr} = \left(\frac{2}{\gamma+1}\right)^{\left(\frac{\gamma}{\gamma-1}\right)} \tag{4.32}$$

Equation 4.32 is derived from *Continuity* Equation 4.26 and following *Ideal Rocket Theory* in [60]. The pressure downstream can be considered as the pressure in the throat, and the pressure upstream can be considered as the chamber pressure in the nozzles. γ is the specific heat ratio of the gas [-], where in this case it is a nitrogen gas. The value can be obtained from [56] or calculated as follows:

$$\gamma = \frac{C_P}{C_V} \tag{4.33}$$

Molar specific heat of nitrogen at constant volume (C_V) is defined as:

$$C_V = \frac{5}{2}R \tag{4.34}$$

Equation 4.34 is used for diatomic gases, such as nitrogen [61]. R is the universal gas constant 8.314 4598 [J/mol K] [62]. 20.786 [J/mol K] is obtained for C_V value. Molar specific heat of nitrogen at constant pressure (C_P) is calculated as follows [61]:

$$C_P = C_V + R \tag{4.35}$$

29.1 [J/mol K] is obtained for C_P value. After substituting both values of the molar specific heats into Equation 4.33, 1.4 [-] is obtained for γ. 1.4 [-] is substituted into Equation 4.32. A critical pressure ratio of 0.528 [-] is found. It means that the sonic flow at the throat is achieved at around half the chamber pressure. The supersonic condition is only achieved if the pressure ratio between the throat and the chamber pressure is lower than the critical ratio.

The *Critical Conditions* results can be applied for the leak simulation model. In this case the throat pressure would be the leak hole pressure and the chamber pressure would be the pressure of the nitrogen in the tube. This means that at *ambient* conditions to have a sonic flow at the throat, the chamber pressure (nitrogen pressure in the tube) must be at least 2.14 [bar]. Below this value the flow at the throat is subsonic. At *vacuum* conditions there would, virtually, always a supersonic flow at the throat.

4.2.3. Simulation Results

First, the leak simulation model is applied for the FOE leak test data at ambient conditions. The results are shown in Figure 4.14:

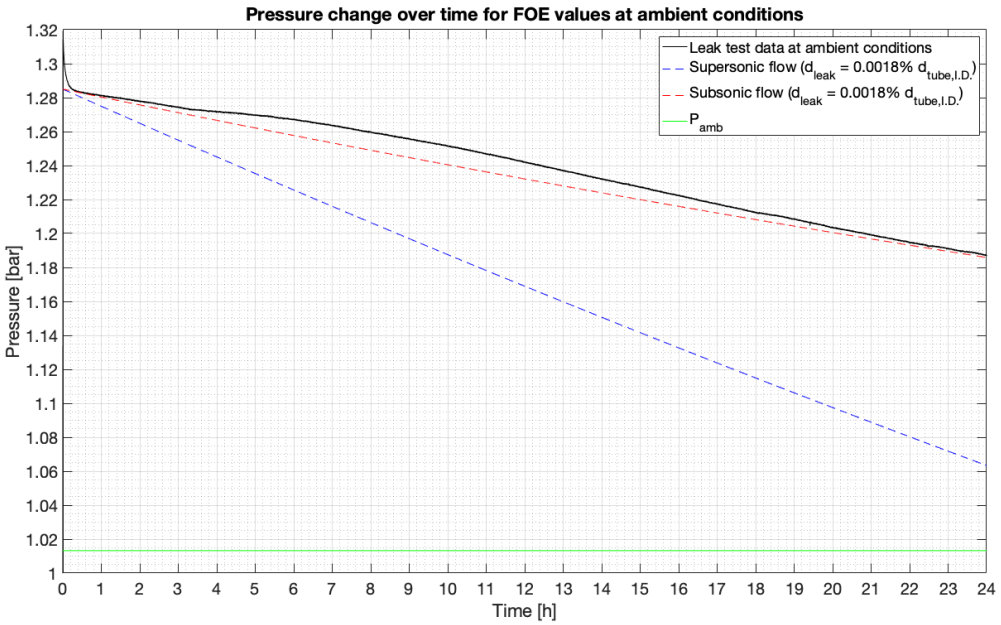

Figure 4.14: Leak model simulation results compared to the Final Operational Envelope leak test data at ambient conditions

Since the initial pressure in the tube is around 1.28 [bar], it does not meet the critical pressure condition, thus, the leak is subsonic. Keeping that in mind after a few code runs in Matlab, the size of the leak orifice is found. The closest fit of the possible leak hole for the subsonic flow (red dotted line) is found. The diameter of the leak orifice corresponds to 0.0018% of the inner tube diameter. This translates to a leak hole diameter of $1.458 \cdot 10^{-3}$ [mm]

Then, the leak simulation model is applied for the FOE leak test data at vacuum conditions. The results are shown in Figure 4.15:

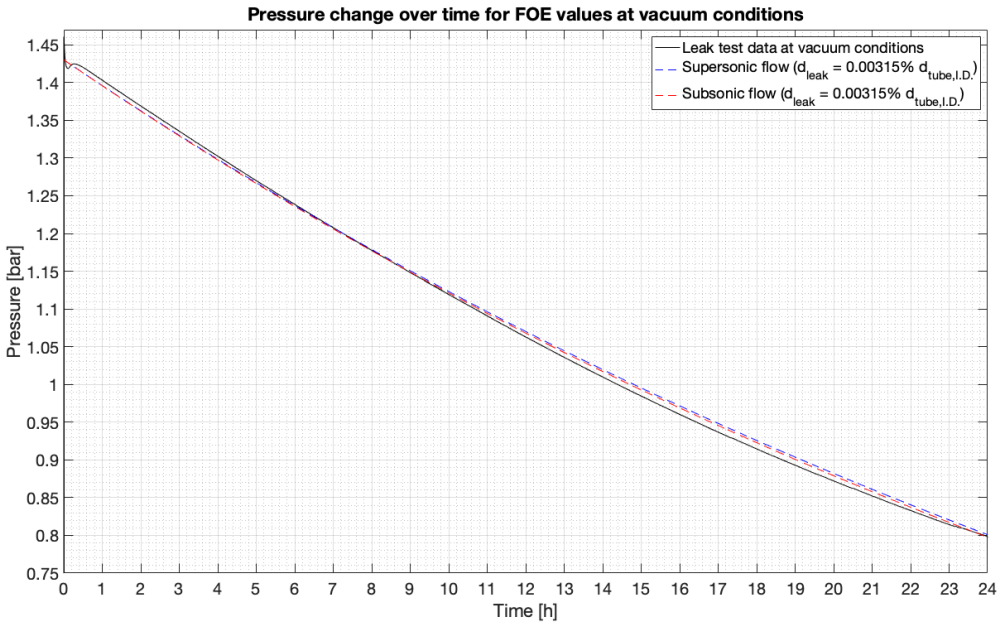

Figure 4.15: Leak model simulation results compared to the Final Operational Envelope leak test at vacuum conditions

From the defined critical conditions at vacuum, the leak in Figure 4.15 should always be supersonic. Although, it can be seen that the subsonic flow (red dotted line) is almost identical to the supersonic flow (blue dotted line). Furthermore, the leak orifice is found to be bigger than for the ambient conditions. Its diameter corresponds to 0.00315% of the inner diameter of the tube, which is equivalent to $2.55 \cdot 10^{-3}$ [mm]. It is around 1.7 times bigger than the hole at ambient condition. Although, due to the made assumptions and first order approximations, these results can be considered as similar for the same order of magnitude. However, the hole/slit difference is rather unexpected, since it is anticipated that the leak orifice should remain the same at both test conditions. It is possible that due to the handling of the PS components during the set-up of the tests, some of them got loose. Therefore, it can possibly increase a chance of enlarging the size of the leak orifice. The other explanation for the leak hole size difference can be due to the uneven closure of the solenoid valve or check valve every time they are used.

The created leak model uses first-order approximations and basic level assumptions. If the leak model is going to be improved in the future, a better understanding of what mechanisms behind the leak are is needed. A possible method to characterize a pressure loss due to the friction in the propulsion components is by using *Darcy-Weisbach* equation [60]:

$$\Delta p = f \frac{L}{D} \frac{1}{2} \rho V^2 \tag{4.36}$$

f is the Darcy friction factor [-], L is the length of the pipe [m], D is the diameter of the pipe [m], ρ density of the fluid [kg/m^3], V is the fluid velocity [m/s]. The above Equation 4.36 takes into account a friction factor which can be related through the Reynolds number. This friction factor represents the roughness of the tube surfaces. However, a further analysis of the friction effect is not performed in this thesis due to the time constraints. Furthermore, the leak can

be further characterized in terms of what type the flow is: *continuum flow*, *molecular flow*, or *transition flow*. The Knudsen values corresponding each flow is given in Table 4.9:

Table 4.9: Types of flow for a given Knudsen number

Type of flow	**Knudsen number**
Continuum	Kn < 0.01
Molecular	Kn > 1
Transition	0.01 < Kn < 1

Knudsen number is described by a ratio of the mean free path of the molecule and the characteristic channel length [60] [1]:

$$Kn = \frac{\lambda}{L} \tag{4.37}$$

λ is the mean free path and its units are [nm], L is the characteristic channel length and its units are [mm]. Using the current version of the leak model, there are two possible characteristic channel lengths. These correspond to the leak orifices (d_{leak}) at ambient and vacuum conditions found from the simulation. The mean free path value is taken from a reference data, which in this case is nitrogen at 1 [bar] [63]. The calculations and definition of the type of flow for the simulation results is given in Table 4.10:

Table 4.10: Type of leak flow for the found model results

Conditions	d_{leak} [mm]	λ [nm]	Kn [-]	**Type of flow**
Ambient	$1.458 \cdot 10^{-3}$	67	0.046	Transition
Vacuum	$2.55 \cdot 10^{-3}$	67	0.026	Transition

After dis-mantling the assembly used for the leak tests, the converging outlet on the side of the check valve is compressed. A possible leak cause and its location could be the deformed male-male adapter used between the check valve and the 3-boss manifold. Figure 4.16 shows the comparison between a brand new and the used male-male adapters:

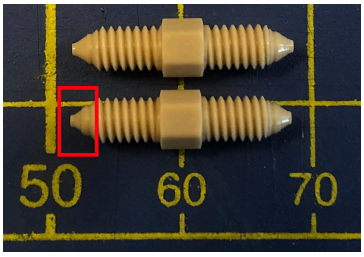

Figure 4.16: A brand new (top) and used (bottom) male-male adapters. The deformation is shown in the red rectangular

The deformation or wearing of the parts is expected if they are often assembled and dis-

assembled. Therefore, a component cycle requirement should be created. This requirement would define the amount of how many times the component can be used for the testing before it is replaced with a new component. Further tests of the testing campaign, which require a frequent assembly and disassembly of the PS components, should consider such a requirement.

All *MatLab* codes used for the results analysis can be found in Appendix F.

4.2.4. Design and Requirements Verification

One of the main goals of TEST-INT-01 is to verify the propulsion system requirements: PROP-PERF-300, PROP-FUN-300, PROP-FUN-500, PROP-RAMS-200, and PROP-RAMS-310. From Table 2.5 can be seen that PROP-PERF-300 has no value for the maximum leak rate at the maximum operational pressure. For the *Final Operational Envelope* values calculated by [3], the maximum operational pressure of the nitrogen in the propellant tank is 1.1 [bar]. There is no exact information yet on how long does the propulsion system has to idle from the moment of finishing the filling of the propellants to thrusting one of thrusters. After discussing with the academic staff who had experience with the CubeSat integration in the rack and launching the satellite, the time frame can be from 1 month up to 12 months. The time span depends on the contract between the launcher provider, satellite integration provider, and the type of satellite launch method. Assuming the satellite is immediately inserted into its orbit after the launch, the 1 - 12 months is the only time the satellite is unserviced by the user. From the results of the leak test performed at FOE ambient conditions, the pressure drop is 248.8 [mbar] in 24 [h]. It means that the pressure inside the propellant tank would reach ambient pressure within 48 [h]. Where the pressure drop at FOE vacuum conditions is 689.3 [mbar] in 24 [h]. The whole pressurant would like out in 48 [hrs] if the leak only happens in space.

Assuming the satellite is idling for 1 month (from filling propellant to thrusting in space) and the maximum operational pressure has to remain 1.1 [bar] when in space, the propulsion system can be filled with 1.2 [bar] pressure, and assuming the pressure drop is 0.1 [bar] over 1 month. This would lead to 0.003 [bar] or 3 [mbar] drop per day. Comparing this value to the test results at ambient conditions, the leak rate is 83 times higher than the assumed.

However, assuming the satellite has to idle for 12 months and it is filled with 0.1 [bar] above the maximum operational pressure of 1.1 [bar]. The pressure drop of 0.0083 [bar] per month can be reached. it leads to 0.00028 [bar] or 0.28 [mbar] drop per 24 [h]. It is a difference of 888 times less than the leak test results at ambient conditions.

Of course these leak rates are just the estimates. However, a first order approximation of the leak rate can be defined for the given requirement, based on the leak test results analysis and the information on the satellite integration and launch time frames. The estimated leak rates are split into two parts: worst case scenario (12 months) and best case scenario (1 month). Their values are put in the definition of PROP-PERF-300 requirement and TBC is added next to it (first value is the best case, and the second is for the worst case):

***PROP-PERF-300**: The maximum leak rate shall be Δp = 3 [mbar] per 24 [h] <TBC> at a maximum operating pressure.*

***PROP-PERF-300**: The maximum leak rate shall be Δp = 0.2 [mbar] per 24 [h] <TBC> at a maximum operating pressure.*

Further investigation in the leak of the propulsion system needs to be done. The defined leak rates for the requirement needs to be adjusted depending on the further leak analysis.

PROP-FUN-300 requirement is partially verified while the leak tests were conducted. All of the leak tests did not require active control of the propulsion system. None of the test which used water inside the propellant tube showed any water residue outside the propulsion system. Although, it is possible that the water was in the crevices between the connection points of the components. If the water is sustained there and it does not endanger other propulsion system components, then it is not an issue. On the other hand, the leak is caused mos likely by the nitrogen gas coming out of the propulsion system, which would definitely leave the propulsion system to the ambient. Due to this reason PROP-FUN-300 requirement cannot be verified. However, if the propulsion system uses a cage presented in TEST-INT-02 test and it is assumed to stop any other subsystems contamination, then PROP-FUN-300 can be verified by extensively testing the cage.

PROP-FUN-500 requirement cannot be verified at this moment using the leak tests. During the leak tests it was found that the tube size is not correct. It means that the initial pressure of the nitrogen is not correct for the *Final Operational Envelope*. However, by using 1.5 [bar] and 2 [bar] as the initial pressure for nitrogen in the propellant tank during the leak tests, the whole water did not come out of the tube when the solenoid valve was opened to remove the water for a new test trial. Although, the water release is performed at ambient conditions. It is possible that there is not enough pressure inside the tube to push out all the water due to the present ambient pressure. PROP-FUN-500 requirement can only be fully verified when TEST-PRO-02 is conducted.

Throughout the leak testing of the propulsion system the maximum achieve pressure is with 3.5 [bar] test. The very first attempt of the leak test was to pressurize the system with 5[bar] nitrogen pressure, which has failed. However, the defined maximum propellant storage pressure is only 1.1 [bar]. Therefore, in any case PROP-RAMS-200 requirement was never violated.

PROP-RAMS-310 requirement is also met. The tubes are made from Polychlorotrifluoroethylene (PCTFE) material. Check valve is made from Polyetheretherketone (PEEK) (body) and Perfluoroelastomer (FFKM) (diaphragm). 3-boss manifold, safety screen, and male-male adapter is also made from PEEK material. All of them are compatible with nitrogen, water, and air.

NOTE: During TEST-COM-01 testing, new tubes with the correct inner diameter have been used. During this test there was no obvious leak detected for a short period of time. However, they should be tested in the future and compared to a smaller diameter ones. It is important to check that, because it is noticed that the new tube walls are thinner, which affects the stretching of the tube. It is thought that the thinner walls expand more easily at vacuum due to the pressure difference inside the tube and the vacuum oven, and results in blocking any leak hole/slit in the propulsion system.

4.3. TEST-INT-02: Volume and Mass Test

4.3.1. Preliminary TEST-INT-02 Volume Test

First, the preliminary TEST-INT-02 test for volume check is performed based on the detailed design by *Turmaine* [3]. However, by looking at the produced Computer Aided Design (CAD) files, manufactured and 3D printed parts, there are already some design inconsistencies:

- The tubes in the 3D printed assembly do not have the threaded spherules to connect them to other components.

- The 3D printed and milled tank, which is used to keep the tubes rolled inside, are not the same. The comparison of the two parts is shown in Figure 4.17:

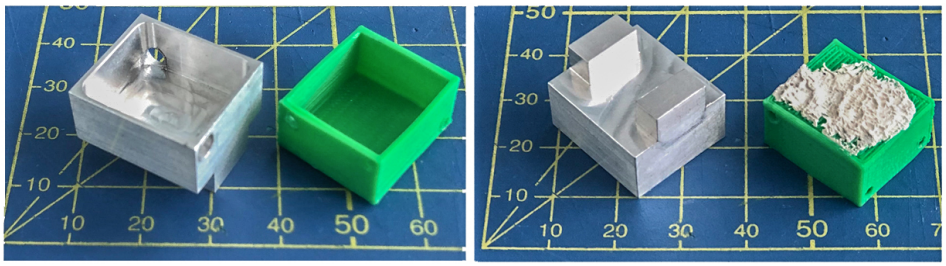

Figure 4.17: Comparison of the milled and 3D printed propellant tank (white stain on the 3D printed tank is glue used for assembly of the propulsion system)

  The milled tank has two legs and their purpose is not defined [3]. The size of the legs is big and takes up a substantial amount of free space in the 42x42x30 [mm] (ref. PROP-SYST-200 requirement) compartment.

- *The Lee* safety screens (INMX0350000A) are not considered as part of the assembly. However, there is no verified information that they are needed for LPM or VLM interfaces. Only *The Lee* website it says that the safety screen is recommended to be used with 062 MINSTAC tubes.
- In the CAD design of the flight model the currently used pressure sensor (HCLA12X5DU) is excluded. Its size is relatively big compared to the other propulsion components.
- In the CAD design of the flight model there is only 3-Boss manifold (TMMA3203950Z). It means a plug based version of the propulsion system is considered. However, the plug itself is not present in the model. Therefore, it is hard to estimate if the manifold and the plug would fit in the assembly.
- A check valve (TKLA3201112H) and its adapter (TMUA3205950Z) are not included in the final version of the design, while the check valve is part of the mass budget.

Furthermore, the PS cage design by *Turmaine* [3] has not been produced and not used anywhere else. Therefore, it is left out from the preliminary test. The following Figure 4.18 shows the first attempt of the PPD assembly according to the proposed flight model design by *Turmaine* [3]:

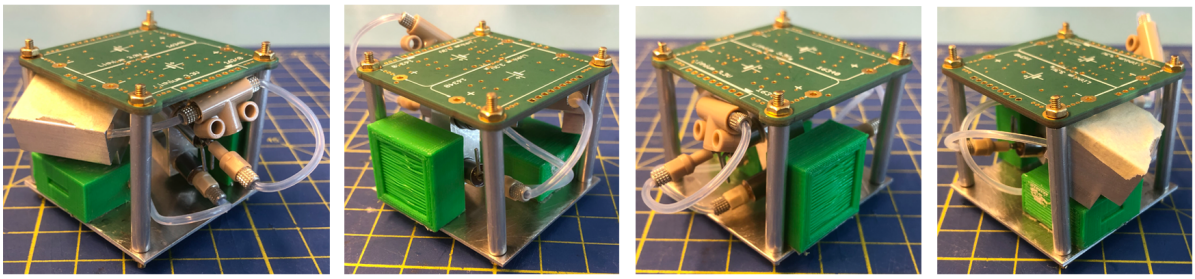

Figure 4.18: The preliminary TEST-INT-02 assembly of the PPD flight model version

According to [3] and [30], both thrusters are placed on the opposite sides of the base plate where the propulsion components are integrated on. In this case, it is the aluminium plate.

During the test procedure *Step 2.2* and *2.3* the connection of 5 [cm] tubes to the valves proven to be difficult. In the detailed design part by *Turmaine* [3] it is stated that the distribution of the propulsion components and support structures inside the required volume would prevent the kinks or blockages of the propellant tubes. Due to the stiffness of the tubes, which are made of PCTFE material, and including the threaded tube spherules, the kinks have been made while integrating the components. The kinks are visible in Figure 4.18 at the connection points of the valves.

Furthermore, due to the same tube stiffness, a tension or compression is created on the rest of the components connected to the tubes. For the purpose of this test, only the interfaces of LPM and VLM are screwed to the base plate with a M2 torque screws. Although, it is clear that, for example, the components such as the 3-Boss manifold, tube tank, and the valve support structure are going to be also fixed either by gluing, clamping, or using screws. Nonetheless, that same tension/compression slowly loosens the threaded spherules connected to propulsion components. This issue needs to be addressed in the further development of the PPD.

4.3.2. Actual TEST-INT-02 Volume Test

The PS components between the PCB and aluminium base plate needs a reconfiguration based on the outcome of the preliminary test results. First, it is done by creating a CAD assembly model in *CATIA*. The CAD model of such reconfiguration is shown in Figure 4.19:

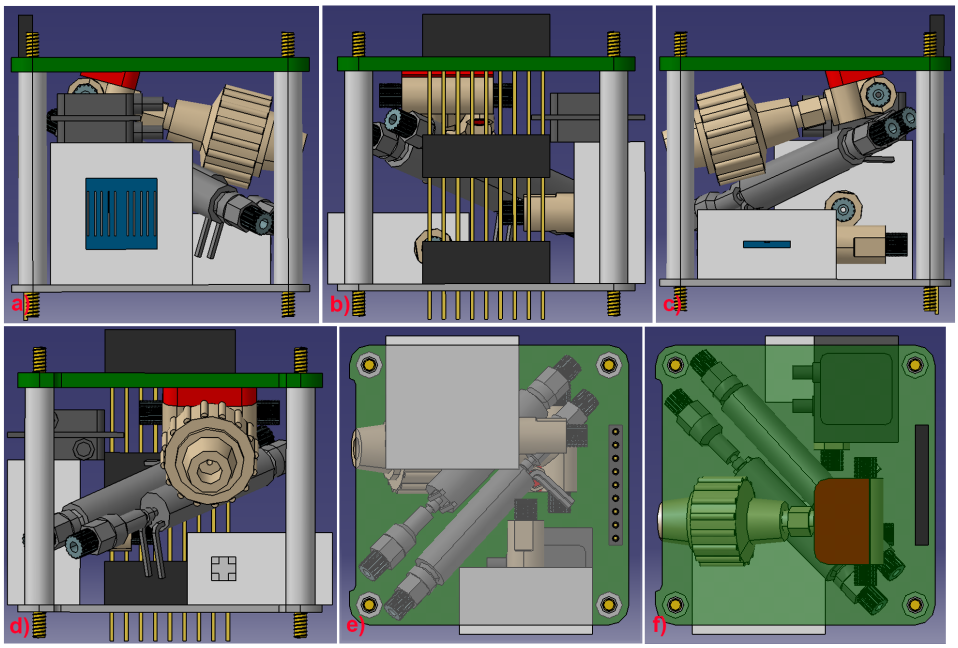

Figure 4.19: Front (a), back (b), VLM (c), LPM (d), bottom (e), and top (f) view of the reconfigured PS components

In the new configuration presented in Figure 4.19 there are a few updates:

- 2 safety screens (INMX0350000A) are included for LPM and VLM interfaces.
- LPM pressure sensor (HCLA12X5DU) is included.
- PCB pins going from the PCB until the aluminium base plate are included.

- The valve support structure is removed, because it interferes with the other components. This affects the position and location of the two solenoid valves. At the moment, they are temporarily placed as shown in Figure 4.19. It can be seen there is no valve support structure. It is decided to not include it, because the valves are placed in such a way that they just fit in the given volume. It means lengthwise they fit in the compartment and the tube spherules can be connected to the valves. However, the kinks of the tubes ar expected. Furthermore, any additional parts or removal of any other part will explicitly affect the orientation and location of the valves as well as the other components. A good example of such a case is the introduction of the check valve in the assembly. Its orientation and location is aligned to one of the service holes in the cage. In such a case there is an easy access to service the propulsion system. On the other hand, it affects the positioning of the solenoid valves.
- The threaded spherules of the tubes are included. Since they are rigid bodies, it is easy to implement in *CATIA* model.
- The male-male adapter (TMUA320590Z) for the check valve (TKLA3201112H) and a newly created its support structure are included. The check valve is placed on an angle and attached to the PCB. It is aligned with the service hole on the cage. A small adapter (red colored part in Figure 4.19) is created. It is used to fix the manifold and achieve a certain angle that the check valve can be easily serviced. However, such a placement of the check valve influences the design and infrastructure of PCB components.

The new configuration from Figure 4.19 can meet at least PROP-SYST-200 requirement. Then the updated PS cage is created and integrated as shown in Figure 4.20:

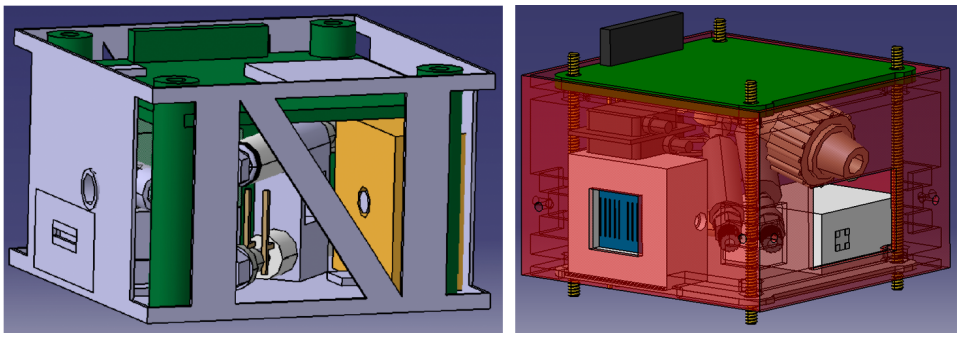

Figure 4.20: The initial final flight model assembly by [3] (Left) and the updated assembly (Right). The updated cage is shown in transparent red. NOTE: the aluminium rod spacers are not required when a cage is used

The cage design is used from the outcome of the trade-off process as described in Chapter 3. A final step is to check whether the assembly and the cage fit within the enclosed volume by the satellite panels. This is represented in Figure 4.21:

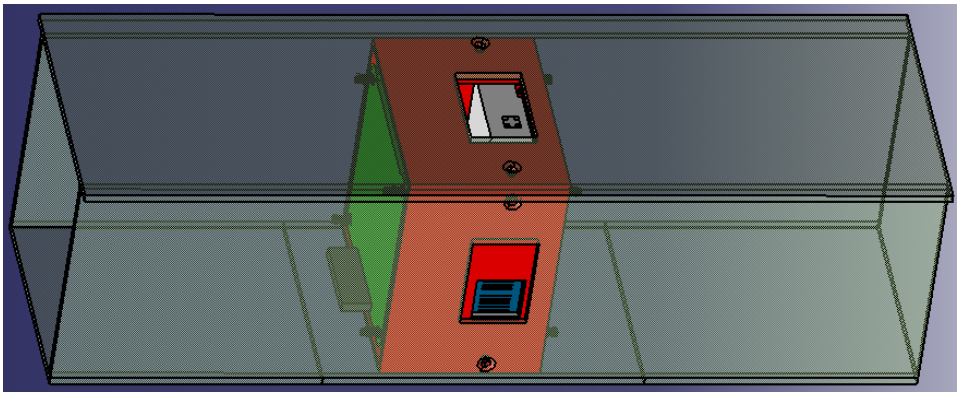

Figure 4.21: PS and satellite panels assembly

Each satellite panel has a rectangular (20.3x13.5 [mm]) opening in the middle. It is specifically made to either access the PS, e.g. to fill or drain the propellant, or have an exit area for the thrusters. For the purpose of the testing phase, only the openings on the LPM and VLM sides are fully covered with only holes left for thruster chip exit nozzles. As a proof of concept and to visually inspect the design in reality, the cage is 3D printed as shown in Figure 3.23 and integrated with 3 satellite panels, PCB board, and aluminium base plate:

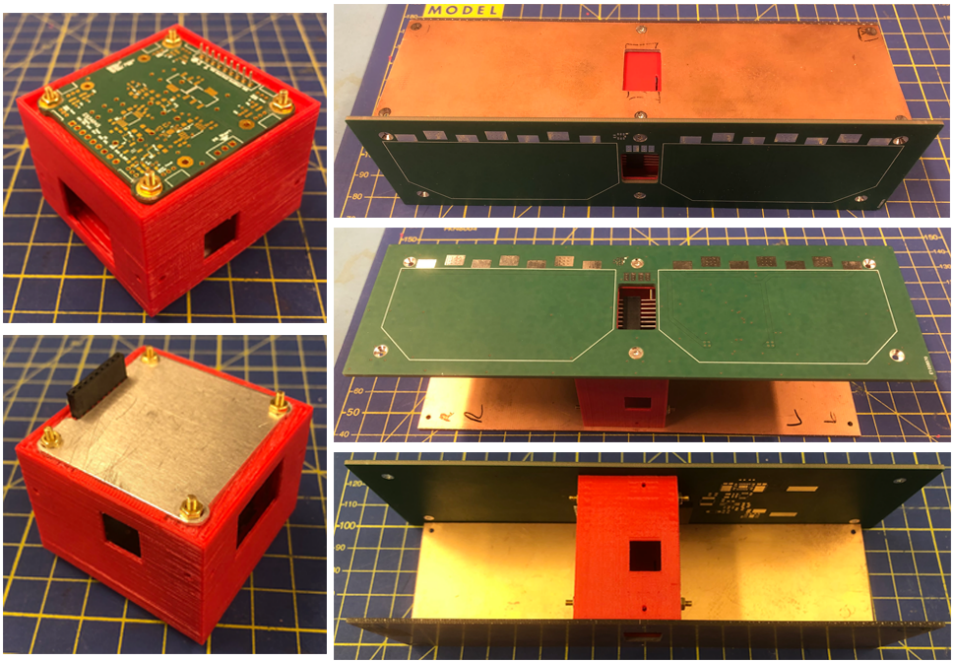

Figure 4.22: Cage, PCB, and satellite panels assembly. NOTE: 3D printed cage has two extra holes aligned with the satellite panel holes. They are made only for the purpose of the demonstration

By introducing the PS cage, the maximum internal volume, which propulsion components can occupy, can be increased from 42x42x30 [mm] to 46x44.5x30 [mm]. If these dimensions can become a new PROP-SYST-200 requirement, it might help to avoid the kinks in the tubes by placing the components differently. Therefore, the provided configuration in Figure 4.19 can be actually realized.

The new configuration presents an issue. If both safety screens are used in the flight model version of the thruster interfaces, they reduce plenum's volume considerably. It has to do with the threaded part of the safety screen which goes inside the interface. The current requirement of the interface size is 20x20x10 [mm] for both thrusters [42]. The 10 [mm] is the depth of the interface. For example, the inlet for the tube in LPM's housing is perpendicular to the thruster chip. The length of the threaded part of the safety screen (INMX0350000A) is around 6.15[mm]. This is 60% of the depth of the LPM's interface depth. Currently there is no explicit analysis done on the size of the LPM's plenum size and its relation to the performance of the thruster and propellant feed. The representation of the issue is presented in Figure 4.23:

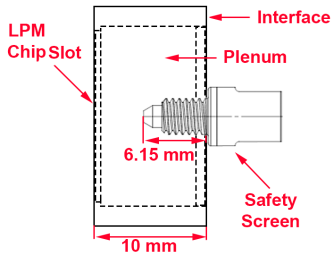

Figure 4.23: Side view of LPM interface and *The Lee* safety screen integration

A possible issue is observed for VLM's interface and safety screen integration. However, in this case, the safety screen is connected on the side of the current thruster housing version. The plenum is along the 20 [mm] dimension of the interface. There is also no explicit analysis of the effect of using the safety screen. Although, in Figure 4.24 can be seen that there is a tubular geometry created for an adapter by *Silva* [2], assuming such a design is also used in the flight model housing version:

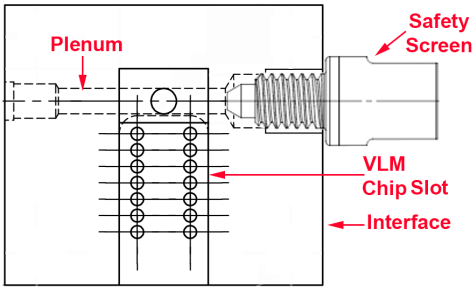

Figure 4.24: Back view of the VLM interface and *The Lee* safety screen integration

The biggest concern with the plenum size is for LPM thruster. At the moment, there is no model created to check the effects of the plenum size on the performance of the thruster. According to [1] the optimal LPM thruster design requires a heat chip area of 593.8 [mm^2] for the PocketQube application, the plenum pressure no bigger than 300 [Pa] and heater chip temperature between 300 [K] and 700 [K]. Furthermore, there is no information on how the heating of the chip affect the temperature and the pressure of the plenum and its size. Therefore, it is recommended to create a model and devise a test for effect of the plenum size on LPM thruster performance.

4.3.3. TEST-INT-02 Mass Test

According to [3], a preliminary estimation of the mass budget based on the created PPD detailed design is performed. The estimated mass budget is missing certain detailed design components. Thus, they are included in this budget analysis. The mass budget is split into 3 parts: *Structural components*, *Electrical Components*, and *Propulsion Components*. The split helps to identify which components of the whole propulsion system belongs to specific part of the system. Furthermore, it provides a mass budget breakdown for the future *PocketQube* mission studies, which can be used a reference information. The comparison between the estimated and the actual mass budget for the current detailed design is given in Tables 4.11, 4.12, 4.13.

Some of the newly added components have the estimated values either from *CATIA* models or the manufacturer data sheet. However, some of the components can be considered as 3D printed parts. For example, the cage or the interfaces of the thrusters can be opted for 3D printed version or machined from aluminium (cage) or ceramics (interfaces). Therefore, both version if applicable are considered in the mass analysis.

The aluminium spacers, which are used to separate the PCB and aluminium base plate at a distance of 30 [mm], are conditionally considered as part of the mass budget. It is known if the cage is used, the spacers are not required. Similarly, if only the spacers are used, the cage should not be included. Thus, two options are considered in the mass budget analysis. In such a way a distinction can be made, which option is lighter if the mass becomes a critical selection factor.

Furthermore, there is nothing mentioned about fixing elements (e.g. screws, bolts, clamps) for valve support structure, tube tank, check valve, and the 3-Boss manifold in the estimated mass budget. At this moment, only 3x M2 torque screws are considered for fixing the thrusters and the valve support structure on the aluminium base plate. A mount is 3D printed to attach the assembly of 3-Boss manifold and the check valve.

Table 4.11: Mass budget of the structural components

Component	Estimated Mass [g]	Actual Mass [g]	Comments
Aluminium metal plate	4	4.54	-
*Delfi-P*Q interface structure	5	0.568	Assuming these are the thruster support structures. Actual value is of the 3D printed parts
Valve support structure	1	1.816	-
Propellant tube storage container	2	4.139	-
M2 torque screws (3x)	-	0.616	Estimated value N.A.. The actual items are used from SSE department workshop

PS cage	24 (11)	- (9.221)	Estimated value is from the *CATIA* model design, where aluminium is used as a material. The estimated value in the brackets is from the *CATIA* model design, where plastic is used as a material. The actual value in the brackets is the 3D printed version of the part.
Total	**36 (23)**	**11.679 (20.9)**	The values in brackets are considered for all the component values given in the brackets above.

If 4 *ART Elektromechanik* aluminium spacers are considered instead of the cage, the total actual mass of the components would be 14.264 [g] (4 spacers weigh 2.585 [g]). The total estimated mass would be 12 [g] (there is no data on the estimated value of the spacers from the manufacturer's data sheet). It can be seen that the structural components are within the estimated mass margin. Aluminium panel, solenoid valve support structure and the propellant storage components are overestimated 80%, 14%, and 200% respectively.

Table 4.12: Mass budget of the electrical components

Component	Estimated Mass [g]	Actual Mass [g]	Comments
Sensors, PCB, electronics	15	9.524	The actual mass of the VLM pressure sensor is 0.063 [g], PCB board (no SMD components) is 7.2 [g], PCB pins are 0.732 [g], LPM pressure sensor is 1.529 [g]
Wiring	5	2	Actual mass is for the currently used components only
Total	**20**	**11.524**	

It can be seen that around 5.5 [g] over-estimation is made on the sensors, PCB, and electronics. However, the actual mass of these items are only provided from the testing phase. It means that these components are might be used only for the testing campaign and subdue to the changes in the optimized design of the PPD.

Table 4.13: Mass budget of the propulsion components

Component	Estimated Mass [g]	Actual Mass [g]	Comments
VLM thruster interface	10	4.124	Estimated value is from [42]. Actual mass is assuming 3D printed version is used for actual part

LPM thruster interface	10	3.597	Estimated value is from [42]. Actual mass is assuming 3D printed version is used for actual part
INKX0514300A solenoid valve (2x)	3.6	3.754	-
062 MINSTAC Tubes	2	2.415 (2.26)	Assuming 3x 5 [cm] and 1x 25 [cm] length tubes with I.D. 0.81 [mm]. Value in the bracket is tubes with 1.57 [mm] I.D..
TMMA3203950Z 3-Boss manifold	1	0.437	-
TKLA3201112H check valve	1.5	1.622	-
Propellant	0.5	0.146 (0.201)	Water only in the 25 [cm] tube is considered for the actual value. The value in the brackets is for the tube with 1.57 [mm] I.D.
TMUA3205950Z-PEEK male-male adapter (1x)	-	0.15	No data on the estimated value from the manufacturer's data sheet
INMX0350000A: 12 micron safety screen (2x)	-	0.416	No data on the estimated value from the manufacturer's data sheet
Total	**28.6**	**16.661 (16.561)**	

All the components in Table 4.13 are only related to the propellant, thrusting, storage, and feed system of the PPD.

Table 4.14: Total mass budget of all components added together

Component	Estimated Mass [g]	Actual Mass [g]	Comments
Structural	36 (23)	11.679 (20.9)	-
Electrical	20	11.524	-
Propulsion	28.6	16.661 (16.561)	-
10% Contingency	8.46 (7.16)	3.99 (4.89)	-
Total	**93.06 (78.76)**	**43.85 (53.875)**	

The estimated mass budget with the included remaining components varies between 78.76 and 93.06 [g]. The variation of the values is due to the fact of what material should be the cage made of. Nonetheless, the estimation is around 3.76 - 18.06 [g] higher than the maximum allowable 75 [g]. However, if instead of the cage only the spacers would be used, the total

estimated mass would be 66.66 [g], which is around 8.34 [g] less than the maximum allowable mass.

By looking at the actual mass budget of the current design, the values vary between 43.85 to 53.875 [g]. The difference in the values has to do with the fact whether the cage is opted for 3D printed or machined version, and whether the inner diameter of the tube size is increased, which consequently affect the amount of the propellant. Although, the actual mass of the current version of the design is within the limit of the maximum allowable mass. It is around 58 - 71% of the max. allowable 75 [g] limit. Again if the spacers are used instead of the printed cage, the total actual mass would be 46.69 [g]. However, for example, a fill/drain valve and its support structure is missing. Thus, they should weigh no more than the remaining 31.15 - 29.15 [g] of the total actual mass budget. Furthermore, it is plausible that extra fixing/clamming components are necessary for the remaining parts if the newly introduced parts require a relocation of the those remaining parts. A sensitivity check should be performed.

4.3.4. Design and Requirements Verification

TEST-INT-02 results provide a useful information needed to verify PROP-SYST-100 and PROP-SYST-200 requirements. After performing the preliminary volume test while using the actual design created by *Turmaine* [3], PROP-SYST-200 requirement theoretically cannot be met. The biggest issue encountered during this test was the tubes. They have kinks at the connection points of the solenoid valves. The tube metal spherules have not been taken into the account by *Turmaine* [3], thus the solenoid valve support structure could not be fitted anymore inside the required volume (ref. Figure 4.19). Furthermore, the propulsion cage requires to protect the other satellite sub-systems from the leak of the propellant. The initial cage design by *Turmaine* [3] was not fully enclosing the PS assembly. New CAD design of the updated propulsion system assembly and cage was designed to meet PROP-SYST-200 requirement. The propulsion system theoretically fits inside the 42x42x30 [mm] volume, but without the solenoid valve support, the aluminium spacers, and the propellant tube container. Moreover, an issue is encountered by using the safety screens for both of the thrusters. Due to its size the plenum of the LPM thruster might reduce, but also reduce the volume left for other components inside the required volume.

The estimated mass budget with the included missing parts of the propulsion system does not meet PROP-SYST-200 requirement. The estimated total mass is 5 - 24% higher than the maximum allowable. The total actual mass budget of the propulsion system meets PROP-SYST-200 requirement. Despite it, the current version of the propulsion system still does not even have a fill/drain valve, solenoid valve support structure, and a container for the propellant tubes, or even an optimized thruster interface. For a future development of the system, these results and mentioned aspects should be taken into account. For example, it is suggested by *Guerrieri* [1] that a ceramic based LPM interface can be used a further step in the design. By using the additive manufacturing technology from [64], it can be easily achieved.

One of the biggest challenges remains unsolved, which is the kinks in the tubes. It was found out during the testing campaign that an incorrect size of the inner diameter of tubing has been used. By increasing the inner diameter of the tube, the kinks are more expected than ever. The bigger diameter tubes are more rigid and their walls are thinner. This increases the chance of the kinks under the extreme bending. An optimization of the components integration is required for the current design of the propulsion system.

4.4. TEST-COM-01: Solenoid Valve PWM Test

In this section the results of TEST-COM-01 are going to be analyzed. The analysis follows the same order as the test procedures presented in Table 3.17. At the end, the design and requirements verification related to this test is discussed.

4.4.1. 0.2 [bar] System Pressurization

For the 0.2 [bar] system pressurization test there is no actual test data collected. It is a check test to see if the required pressure inside the propulsion system tank as a closed system can be achieved at vacuum conditions. The GPFS is only accurate to provide the nitrogen gas up to 0.5 [bar]. It means there is an excess of 0.3 [bar] pressure inside the propellant tank compared to the required 0.2 [bar] FOE value. At that point, the excess of the gas inside the propellant tank is regulated by using *Arduino* code *E.ino*. It has a function which uses PWM mode to dump the gas out of the propellant tank and stop at 0.2 [bar]. To overcome the ambient pressure outside the tank, the vacuum oven is used to reach sub-atmospheric pressure. At the moment of the residual pressure dump, the vacuum oven reduced pressure up to 0.35 [mbar]. At this pressure level it is considered to be sufficient to reach 0.2 [bar] in the tank, and the vacuum oven from around this point sucks out air 0.1-0.2 [mbar] every 20-30 [min]. Thus, to save time it is considered a sufficient vacuum level inside the oven.

After reaching 0.2 [bar] value, intermediate readings of the tank pressure are checked. The purpose is to check if the tank is not leaking for a sufficient time. Furthermore, the new tubes with the 1.57 [mm] inner diameter are used for this test. It is noted that the pressurization and the pressure stability of the propulsion system is performing better than with the previous tubes with 0.81 [mm] inner diameter. As the leak test is not the purpose of this test, the long term leak test is not performed.

After around 5 [min] time period with every 30 [s] interval check on the gas pressure inside the tube, it was noted that the system does not leak and no significant variations in the pressure level are observed. It is concluded as a successful test.

4.4.2. Maximum Operating Frequency

According to the manufacturer, *INKX0514300A* solenoid valve has a maximum operating frequency of 1000 [Hz] at 12 [VDC] (although, the required spike voltage according to the technical data sheet is 24 [VDC]) [44]. The intention to use this solenoid valve is at the sub-atmospheric pressures and there is nothing known at what PWM frequency it needs to operate at such conditions. Therefore, the frequency sweep is performed. Its goal is to know what is the minimum and maximum operating frequencies the valve can handle. The frequency sweep is done from 0 [Hz] to 3000 [Hz] at a fixed duty cycle of 128 [-] (it corresponds to 50% of 255 [-] DC). 3000 [Hz] upper limit is selected to make sure that the solenoid valve fails to operate above 1000 [Hz] limit and help to characterize the full operational spectrum of the valve. The 50% duty cycle is selected, because it lets to achieve the maximum frequency and is the half time required to open and close the valve (assuming it takes the same amount of time to open and close the valve's latch). For this test it is decided to have an infinite amount of nitrogen gas supply at a fixed pressure, which is 2 [bar]. During this test the behavior of the gas inside the tank is also tested, such as the pressure and the temperature. In Figure 4.25, the snapshots from *FLIR* camera show the temperature effect on the valve:

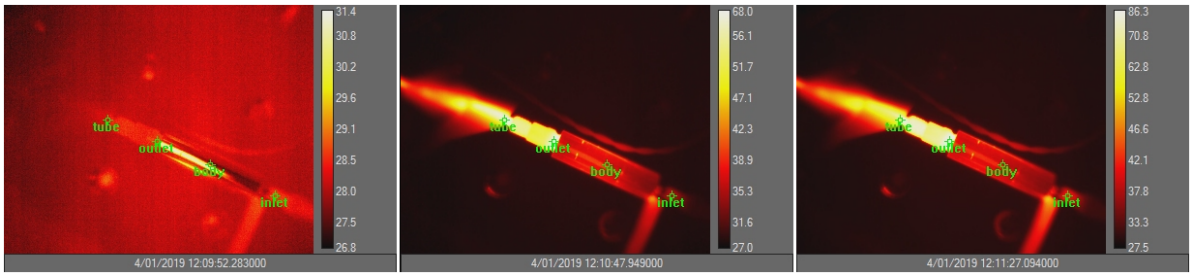

Figure 4.25: Snapshots of the solenoid valve temperature during the frequency sweep. Starting from the left image: at 0 [Hz], 1500 [Hz], and 3000 [Hz].

There are 4 spots at which the temperature values are obtained from *ResearchIR* software. Those spots (green ROI cursors as shown in Figure 4.25) are:

- Tube at the outlet of the valve
- Outlet of the valve
- Body of the valve (around the middle of the valve)
- Inlet of the valve

Table 4.15: Temperature values at ROIs during 0 [Hz], 1500 [Hz], and 3000 [Hz] sweep

	Tube at the outlet	**Outlet of the valve**	**Body of the valve**	**Inlet of the valve**
			0 [Hz]	
Temperature [^{o}C]	28.2	28.8	28.4	28.9
			1500 [Hz]	
Temperature [^{o}C]	59.4	63.8	36.6	34.3
			3000 [Hz]	
Temperature [^{o}C]	68.8	83.3	38.4	40.7

Figures 4.26, 4.27, 4.28, and 4.29 show the full temperature change during the frequency sweep at 4 ROI spots:

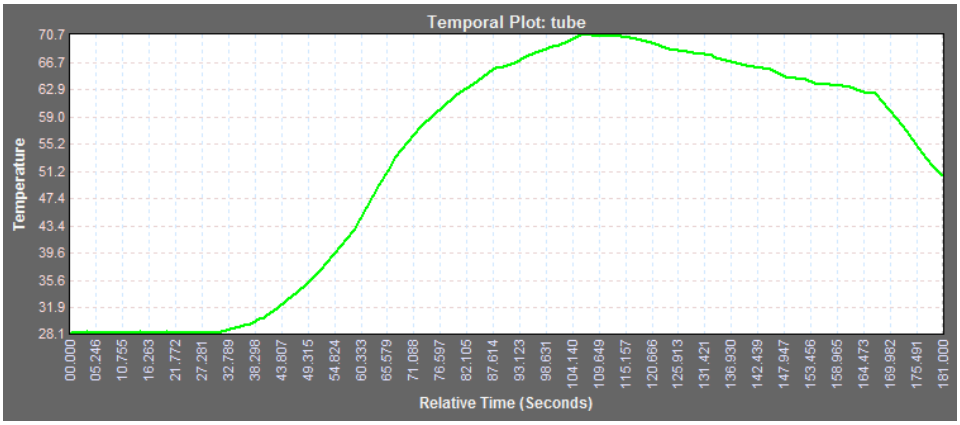

Figure 4.26: Temporal plot of the temperature change at the *tube* ROI

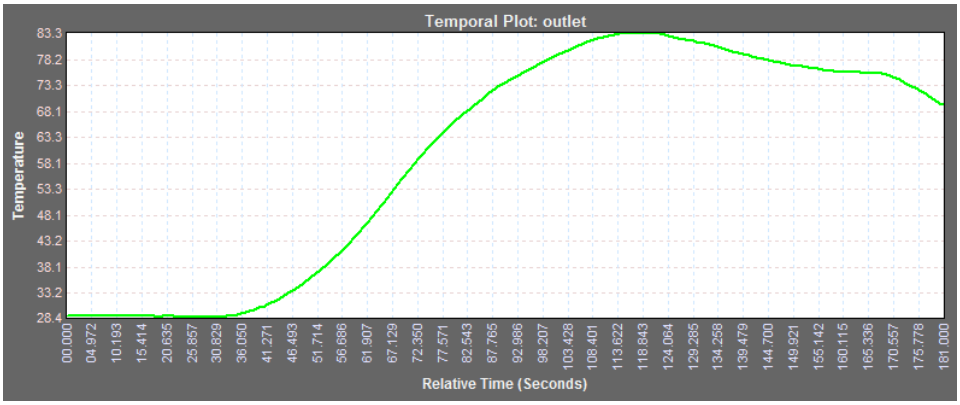

Figure 4.27: Temporal plot of the temperature change at the *outlet* ROI

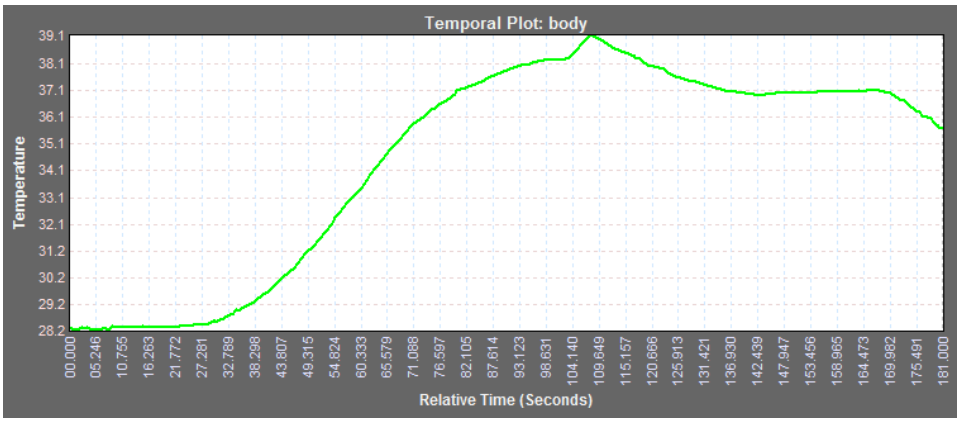

Figure 4.28: Temporal plot of the temperature change at the *body* ROI

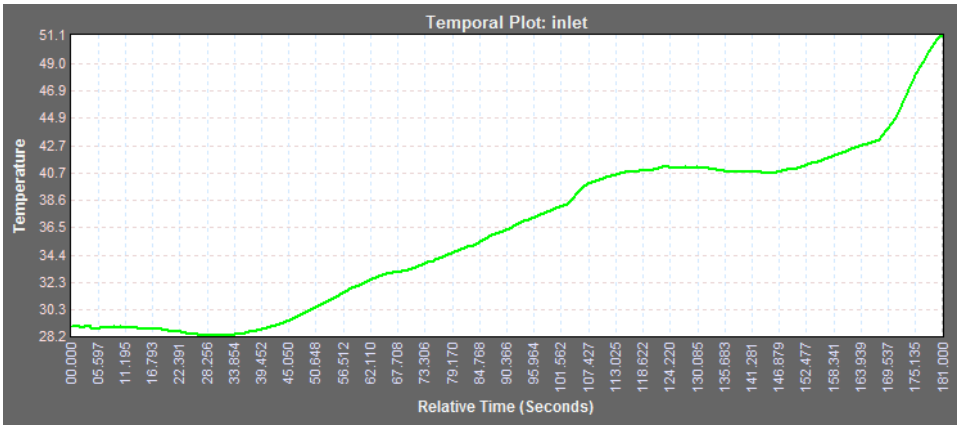

Figure 4.29: Temporal plot of the temperature change at the *inlet* ROI

It can be seen from Figure 4.26 and 4.27 there is a highest surge of heat around the tube and the outlet of the valve. The maximum temperature increase around the tube and outlet of the valve is 70.7 and 83.3 [^{o}C], respectively, which corresponds to 3000 [Hz]. However, from the snapshots provided in Figure 4.25, the temperature at the tube at 3000 [Hz] is 68.8 [^{o}C]. The almost 1 degree difference could be due to *ResearchIR* software or a delayed heat transfer from the hotter spot at the valve outlet, since there was gas in the tank at a higher pressure and it was coming out to the ambient due to the opening and closing of the valve. Similar phenomenon is registered a the inlet of the valve. There is an increase of temperature of around 23 [^{o}C]. Such a temperature jump has an impact on the nitrogen gas temperature inside the tube. Moreover, it can be seen from Figure 4.29 that the highest temperature value is achieved after 3000 [Hz]. It means that the heat dissipation from the valve has been transferred to the nitrogen gas and tank tube. At 1000 [Hz], which is the maximum operating frequency of the valve, the temperatures are vary between 30 [^{o}C] at the inlet and body of the valve, and 60 [^{o}C] at the outlet and tube at the outlet of the valve. At the max. oper. frequency the temperature increase is around 30 degrees from the initial valve conditions at the outlet area. The temperature increase at the inlet area for the same conditions is only a couple of degrees. This temperature distribution between the two areas of the valve has to do with the flow of the gas. The gas moves from the inlet of the valve to the outlet, which transfers the produced heat in the same direction. The change of the gas temperature inside the propellant tank and the plenum during the frequency sweep can be seen in Figure 4.30 and 4.31:

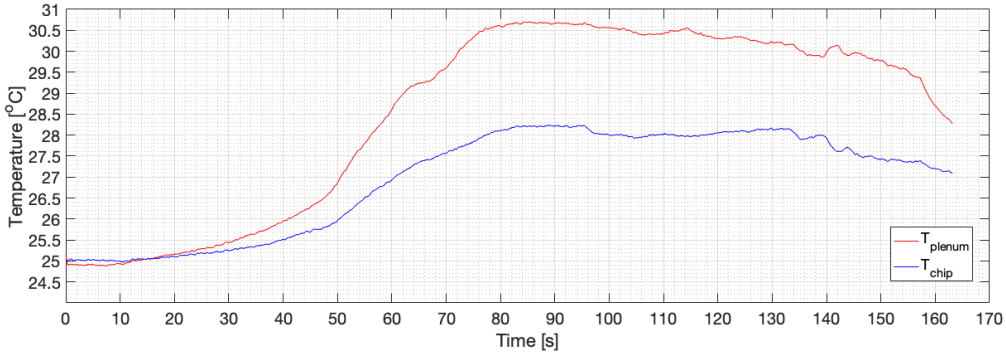

Figure 4.30: Plenum and LPM chip temperatures during the frequency sweep

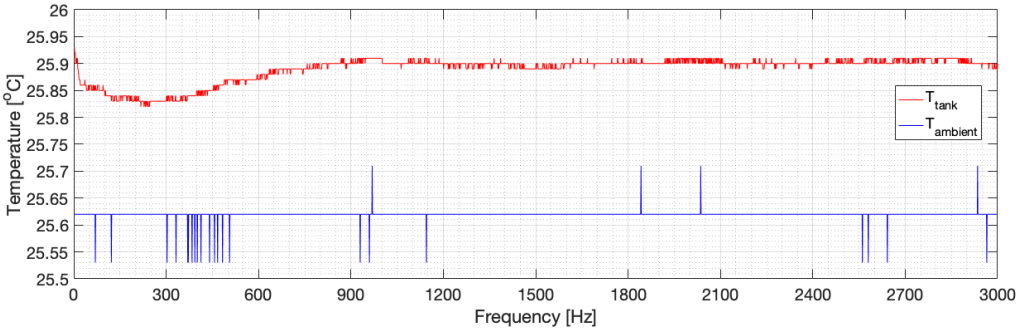

Figure 4.31: Propellant temperature inside the tube during the frequency sweep. The ambient temperature is added for comparison

From Figure 4.30 can be seen that there is jump of around 5 degrees inside the plenum and 3 degrees at LPM chip (NOTE: Figure 4.30 is plotted against time and 4.31 against frequency.This due to two different DAQ devices used in obtaining the data at different frequencies. There is not enough data points to extrapolate temperature at the plenum and chip with respect to the PWM frequency to match the frequency range in Figure 4.31). However, by looking at Figure 4.31, there is no significant changes in temperature inside the tank at any frequency. The slight dip at around 300 [Hz] can be due to the incoming gas from further in the tank while the valve is still relatively cold. Furthermore, the pressure sensor in tank is placed at around 6 [cm] from the valve, which means there is not enough heat to reach that far.

From Figure 4.28 can be seen that there is an increase in the temperature of 10 [^{o}C]. This would definitely affect the coil resistance and the power input. A further discussion on the coil temperature and resistance is presented in Section 4.4.6.

To know at what frequencies the solenoid is performing and at where it is failing, Figure 4.32 shows the relation between the plenum pressure and the frequency:

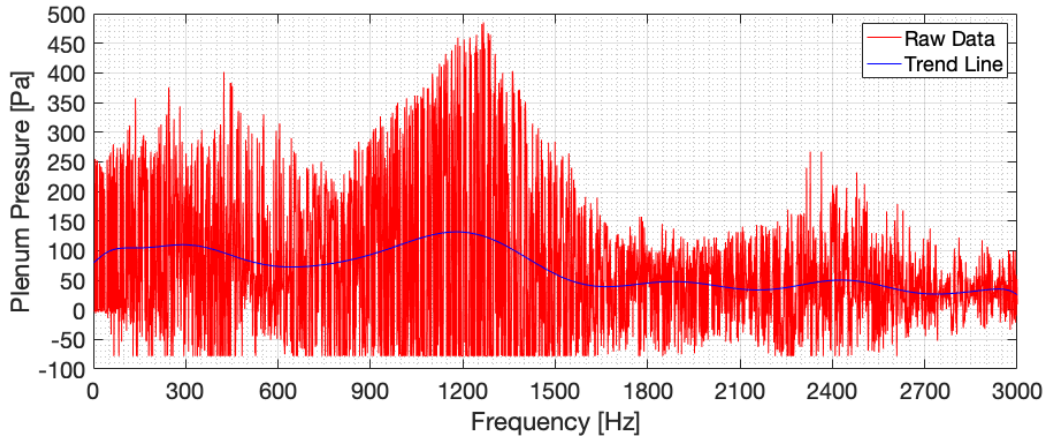

Figure 4.32: The performance of the solenoid valve for 1 - 3000 [Hz] frequency sweep w.r.t. the plenum pressure

Figure 4.32 shows that from around 0 - 500 [Hz] the pressure is more or less stable. There is an increase in pressure around 900 - 1200 [Hz], but with a lot of noise. The solenoid valve struggles to actuate from around 1300 [Hz] and onwards, meaning the frequency between full

open and partially open states of the valve is too fast to release sufficient gas through the valve's outlet. Thus, the low pressure sensor barely registers any gas input in the plenum. The noise in the data can be explained due to the fact that the low pressure sensor measurements are discrete and not continuous. Thus, it is possible that some measurements (negative values) are done when the valve is closed. The smoothed data (blue line in Figure 4.32) is provided to show a trend between the noisy data.

4.4.3. Minimum Voltage Pulse Duration

According to the manufacturer, the minimum voltage pulse duration of *INKX0514300A* solenoid valve is 0.35 [ms] at 12 [VDC] (although, the required spike voltage according to the technical data sheet is 24 [VDC]) [44]. The pulse duration can be determined by using Equation 4.38:

$$t_{pd} = \frac{1}{f_{PWM}} \cdot DC/255 \cdot 1000 \tag{4.38}$$

The voltage pulse duration is related through the valve's duty cycle and PWM frequency. It is decided to perform duty cycle sweeps at fixed PWM frequencies. Such tests provide knowledge on how the valve performs at its boundaries, but also an optimal duty cycle can be selected to achieve the required plenum pressures. Six fixed PWM frequencies are selected based on the outcome of the maximum operating frequency results. The values are 25, 50, 125, 250, 500, and 750 [Hz]. The duty cycle range is from 1 to 255, where 1 is 0 % and 255 is 100% (1 corresponds to fully closed valve, and 255 is fully opened valve). The supply of the nitrogen gas is infinite and is fixed at 2 [bar] as in the previous test. The target pressure inside the plenum is set to 150 [Pa]. That is why during the duty cycle sweep the plenum pressure values vary averagely around 150 [Pa]. Figures 4.33, 4.34, 4.35, 4.36, 4.37, 4.38 show the duty cycle sweeps at fixed PWM frequencies w.r.t. the plenum pressure:

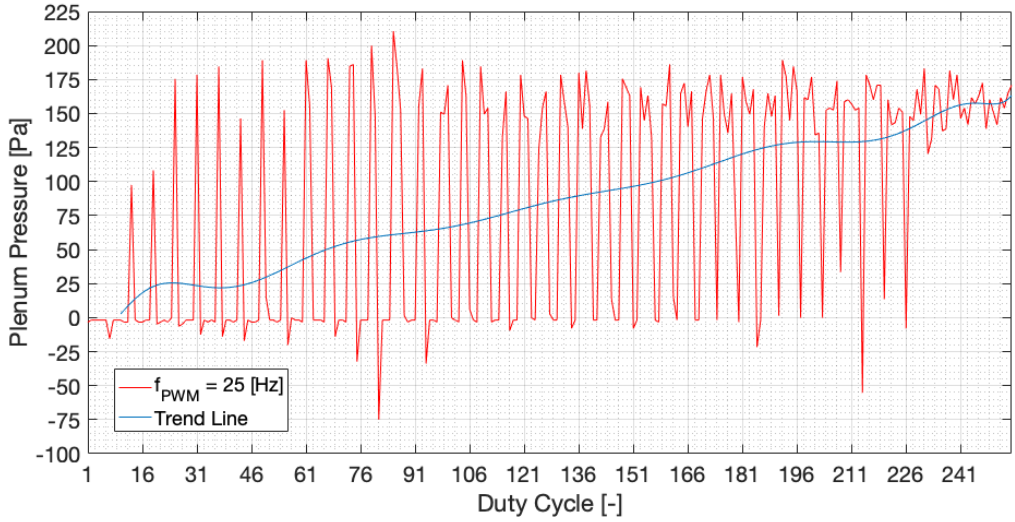

Figure 4.33: Plenum pressure and duty cycle sweep at 25 [Hz]

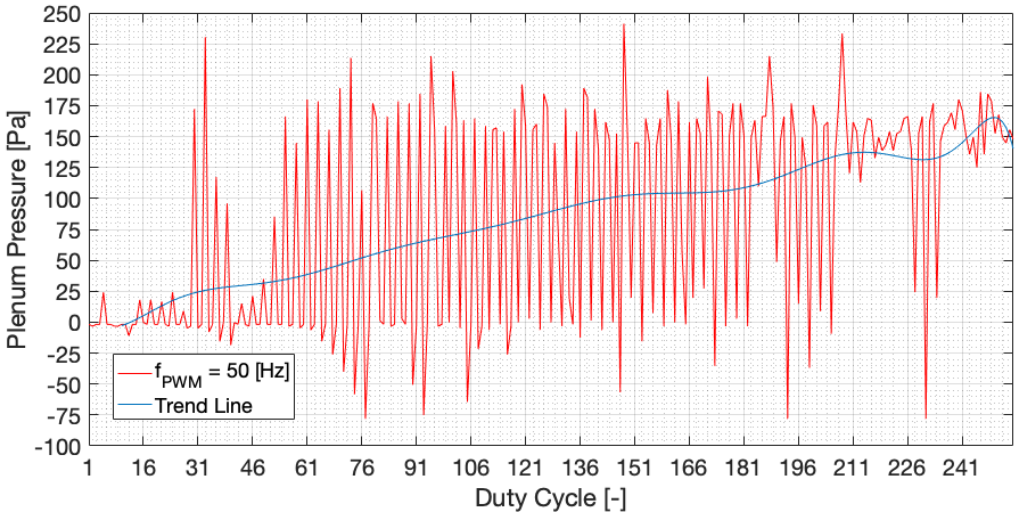

Figure 4.34: Plenum pressure and duty cycle sweep at 50 [Hz]

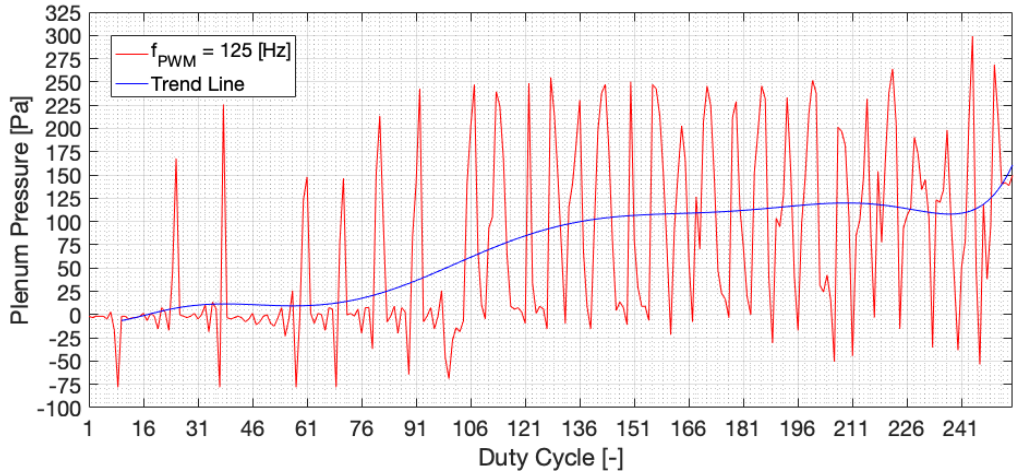

Figure 4.35: Plenum pressure and duty cycle sweep at 125 [Hz]

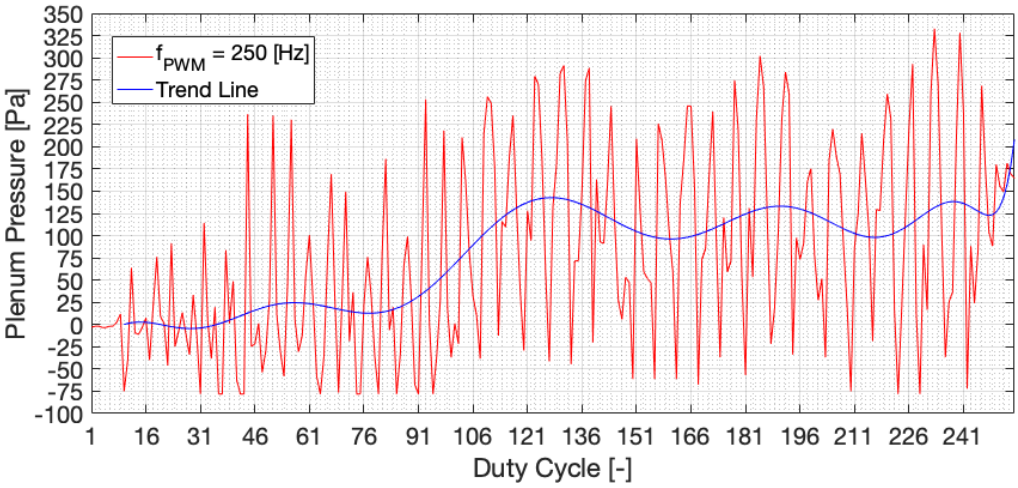

Figure 4.36: Plenum pressure and duty cycle sweep at 250 [Hz]

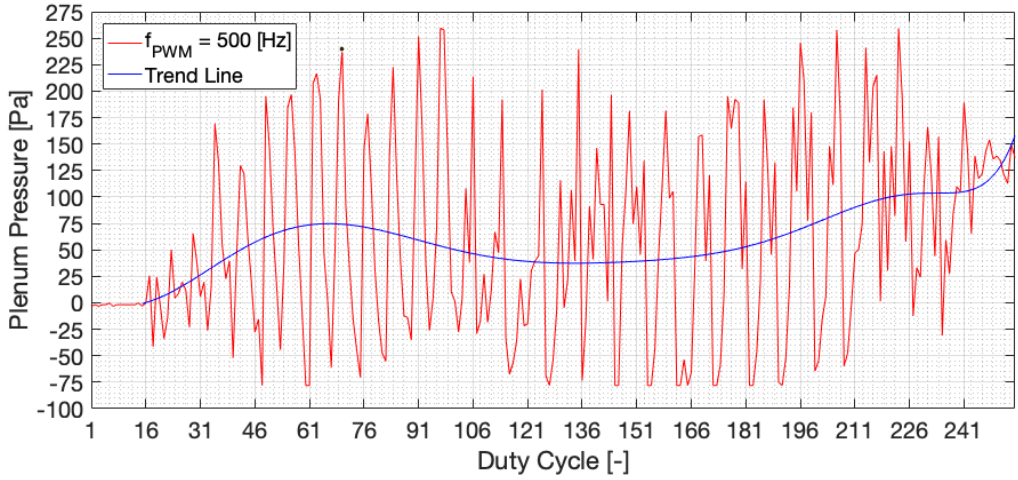

Figure 4.37: Plenum pressure and duty cycle sweep at 500 [Hz]

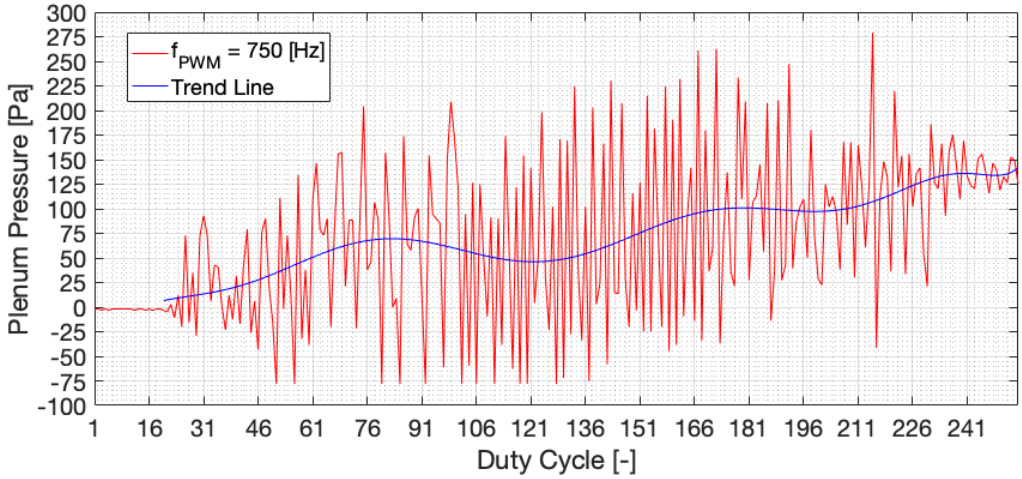

Figure 4.38: Plenum pressure and duty cycle sweep at 750 [Hz]

At 25 [Hz] frequency, the default minimum pulse duration of 35 [ms] is achieved at 2.23 [-] duty cycle, and since duty cycle only have whole numbers, the 2.23 is rounded to 2 [-]. It can be seen from Figure 4.33 only around a duty cycle of 15 [-] the first pressure measurements are obtained. The stability of the pressure increases with the duty cycle. At around 226 [-] DC and onwards there are no significant pressure drops. It means that the plenum and the tube between the thruster and the valve is saturated with nitrogen gas. Thus, the minimum pulse duration at this value would be 35 [ms]. The opposite effect is seen at low duty cycle values from 1 to around 60 [-] DC. The pressure spikes are very narrow with longer gaps between the the next one. It means that for a number of duty cycle values the tube and the plenum needs to be saturated with the gas. Throughout the whole duty cycle sweep the maximum achieved pressure in the plenum is consistent,which is around 175 [Pa]. However, the maximum 300 [Pa] is not reached. It means that the 25 [Hz] PWM frequency is not optimal.

At 50 [Hz] frequency, the default minimum pulse duration of 35[ms] is achieved at 4.46 [-] DC, which would be around 4-5 [-]. It can be clearly seen that the from around 60 and up to around 180 [-] DC, there is a lot of noise and the valve is struggling to saturate the plenum. From around 180 DC and onwards the plenum pressure becomes more stable for a longer period of time with the increasing duty cycle. However, the valve is still struggling to reach higher pressure values than 175 [Pa]. At around 200 [-] DC the plenum pressure seems to be the first longer stable pressure region. If 200 [-] DC is considered, then its minimum pulse duration would correspond to 150 [ms].

At 125 [Hz] frequency, the default minimum pulse duration is achieved at 11.15 [-] DC, which would be 11 [-]. Only from around 120 [-] DC the pressure values become more consistent and reaches a maximum of 225-250 [Pa]. Although, the valve is struggling to fill the plenum with the gas and reach a stable value for any given duty cycle. However, if by looking at the trend line (blue line in Figure 4.35) the duty cycle of 120 is considered sufficient, it would correspond to the minimum pulse duration of 38.4 [ms].

At 250 [Hz] frequency, the default minimum pulse duration is at 22.31 [-] DC, which corresponds to 22 [-]. It can be seen that the valve is almost reaching the maximum required plenum pressure of 300 [Pa] at the very end of the duty cycle range and only at a couple of peaks. However, the full saturation is not reached for a sustained period of time. From around 90 [-] DC and onwards there are 3 bigger peaks of pressure lasting around 50 [-] duty cycle values

(ref. Figure 4.36 blue trend line). If the first peak at 120 [-] DC is considered, then minimum pulse duration is 19.2 [ms].

At 500 [Hz] frequency, the default minimum pulse duration is achieved at 44.6 [-] DC, which would be around 45 [-] value. It can be seen that the valve reaches a maximum of 250 [Pa] pressure at around 100 and 200-220 [-] DC for a brief moment. Only from around 230 DC seem that the plenum reaches saturation at 125 [Pa]. if 230 [-] DC is considered as a stable point, then the minimum pulse duration would be 18.4 [ms].

At 750 [Hz] frequency, the default minimum pulse duration is achieved at 66.9 [-] DC, which would be 67 [-]. Looking at the trend line, the plenum pressure increases with the higher values of duty cycle. It seems that from around 230 [-] DC value, the plenum is more or less saturated, but reaches only around 125 [Pa]. Although, in general, the valve is still struggling to saturate the plenum. There are a lot of narrow spikes throughout the range especially at around 100 - 180 [-] DC. It means that the pressure sensor in the plenum was able to register more pulses of the incoming gas at this frequency. If 230 [-] DC is considered as a stable value, then the minimum pulse duration would be 12.27 [ms].

From the test results can be seen that the highest linearity is achieved at 50 [Hz] and would be chosen as the favorable operating frequency. However, the frequent instability of the desired plenum pressure at 50 [Hz] shows that this set-up can be undesirable from the thruster's operational perspective. The best stability of the plenum pressure is achieved at 250 [Hz] frequency. The optimal duty cycle for the valve's operation would be from around 120 [-] and onwards. Furthermore, the performance of the valve at 250 [Hz] is in line with the test results from *Silvestrini* [29]. The snapshots during the minimum pulse duration sweep at various frequencies is shown in Figure 4.39:

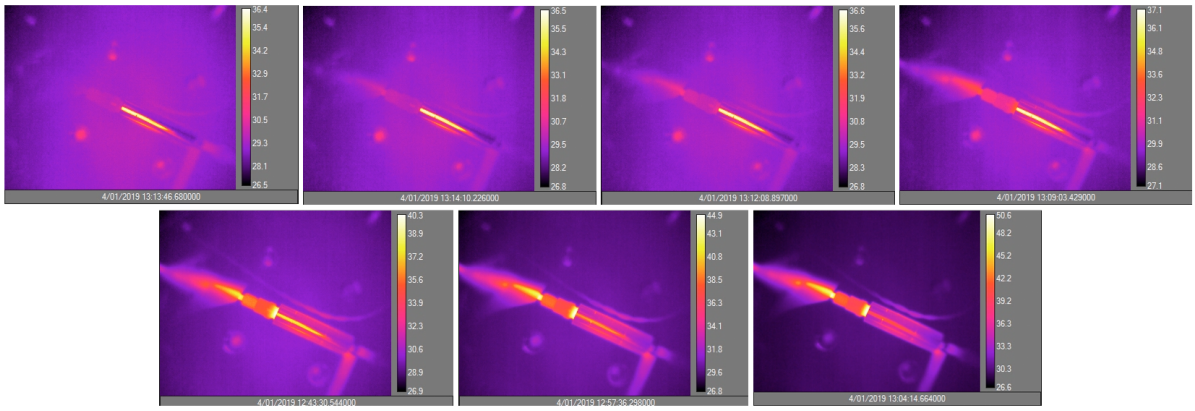

Figure 4.39: Snapshots of the valve during the maximum pulse duration at various frequencies. Top left to right: at nominal valve situation, at 25 [Hz], at 50 [Hz], at 25 [Hz], at 250 [Hz], Bottom left to right: at 250 [Hz], 500 [Hz], 750 [Hz]

It can be seen that the tube at the outlet of the valve warms up compared to the ambient surrounding. Using the same ROI markers as from the PWM frequency sweep, the temperature change during the pulse duration sweep is shown in the following figures:

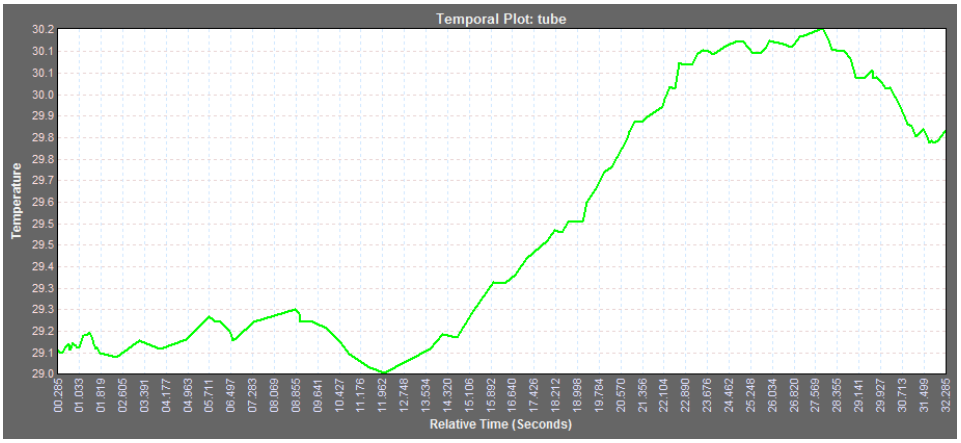

Figure 4.40: Temporal plot of the temperature change at the *inlet* ROI at 25 [Hz] during pulse duration sweep

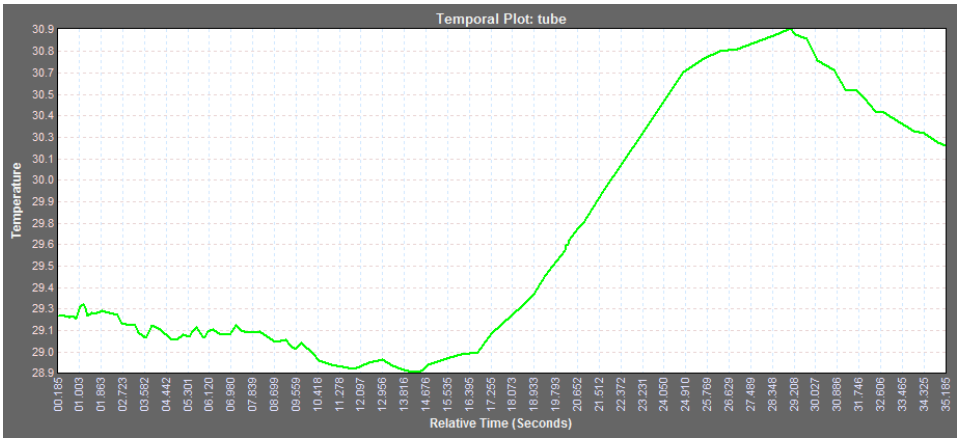

Figure 4.41: Temporal plot of the temperature change at the *inlet* ROI at 50 [Hz] during pulse duration sweep

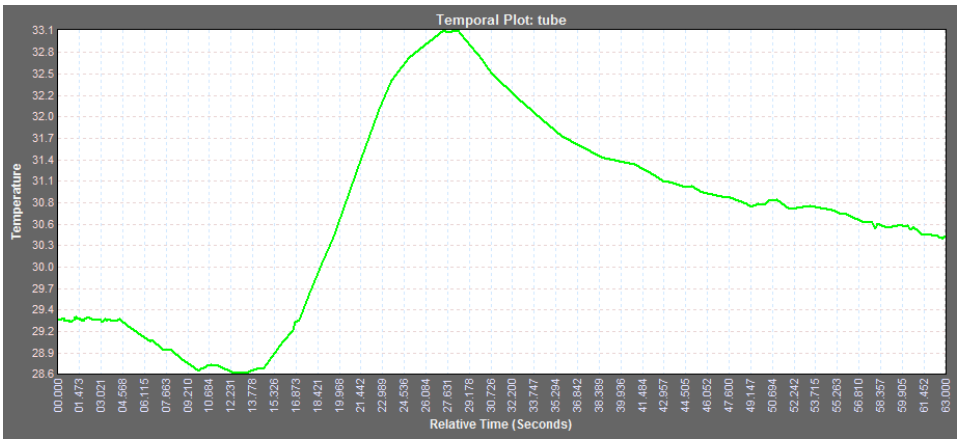

Figure 4.42: Temporal plot of the temperature change at the *inlet* ROI at 125 [Hz] during pulse duration sweep

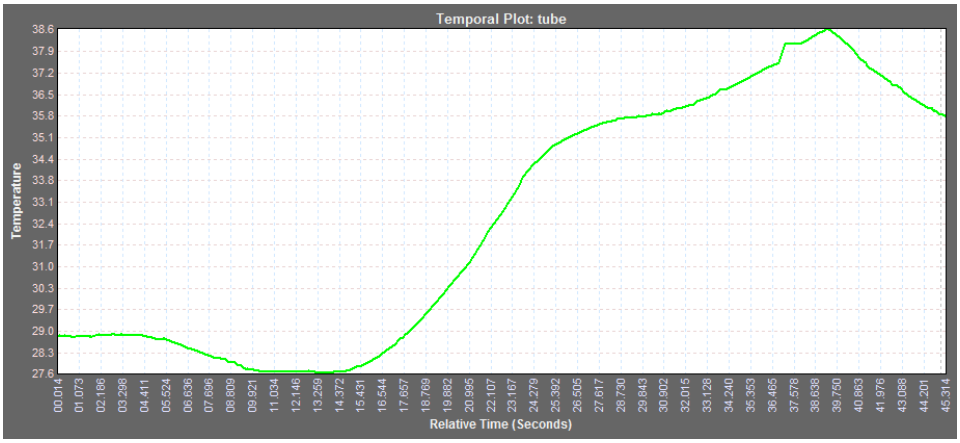

Figure 4.43: Temporal plot of the temperature change at the *inlet* ROI at 250 [Hz] during pulse duration sweep

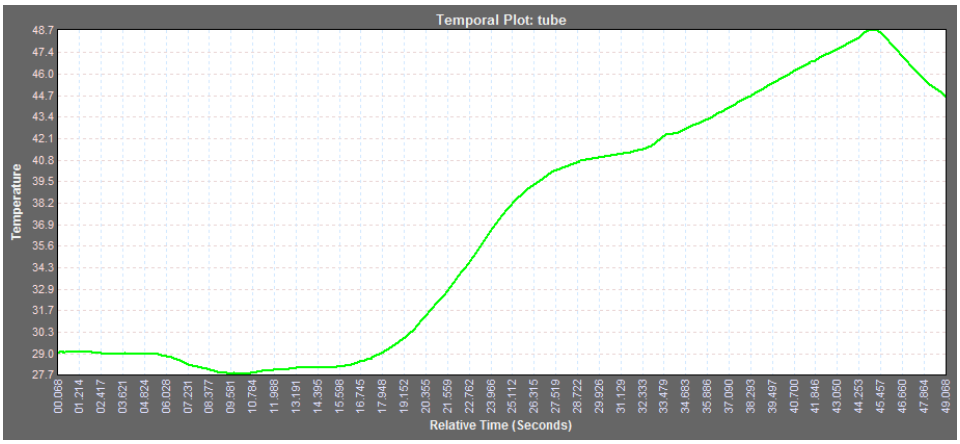

Figure 4.44: Temporal plot of the temperature change at the *inlet* ROI at 500 [Hz] during pulse duration sweep

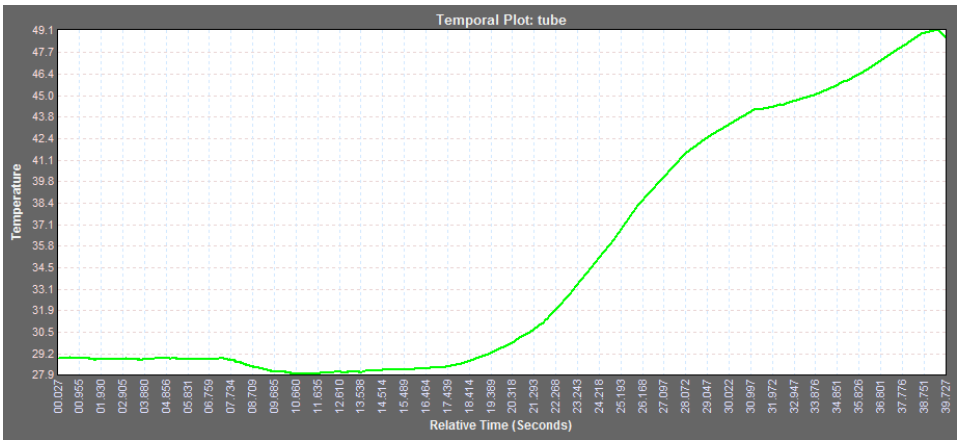

Figure 4.45: Temporal plot of the temperature change at the *inlet* ROI at 750 [Hz] during pulse duration sweep

All the temporal plots show a similar behavior. The rise of the temperatures is observed from

half of the duty cycle range. As it is expected, the higher the frequency the higher the maximum temperature is reached. This can be related the same to the frequency sweep at fixed duty cycle. The other similarity between the plots is the drop in the temperature at low duty cycle values. This behavior could be due to the flow of the gas coming from the tank, which cools down the tube before the valve starts warming up at the higher duty cycles. The only different temperature behavior of the temperature at the tube is observed at 125 [Hz] duty cycle sweep. It can been that he valve warms at the lower duty cycles than the rest. This effect should be investigated further if necessary, because at this stage it is hard to conclude what could be the reason for early jump in the temperature readings.

4.4.4. Plenum Pressure Stability at Various PWM Frequencies

From the previous 2 tests it can be seen that to achieve a stable pressure in the plenum is a challenge. The goal of this test is to find the most optimal PWM frequency and duty cycle values to achieve a stable plenum pressure. From [1] it is known that the minimum plenum pressure should be 50 [Pa] and the maximum pressure should not exceed 300 [Pa]. Thus, the 3 chosen plenum pressures, which are tested, are 50, 150, and 300 [Pa]. The initial tank pressure of 0.2 [bar] (20 000 [Pa]) and the thrusting time of 200 [s] is used according to [3].

However, from the previous tests it is noticed that to measure a full PWM frequency or duty cycle range, the design length of the propellant tank which is in total 0.3 [m], is not enough. It is decided to use an extra length of the tube coming from the GPFS flow divider (middle yellow butterfly valve). It means that the propulsion tank is extended and filled with nitrogen from GPFS until and included the PPD tank. It adds up to around 2 [m].

From Section 4.4.3, it is known that the only PWM frequency, which is the most stable and consistent, is 250 [Hz]. A fixed duty cycle of 71 [-], which corresponds to the minimum achievable value by the valve, is chosen first. The following Figure 4.46 shows the attempt reaching 300 [Pa] plenum pressure with 0.2 [bar] tank pressure and PWM frequency of 250 [Hz]:

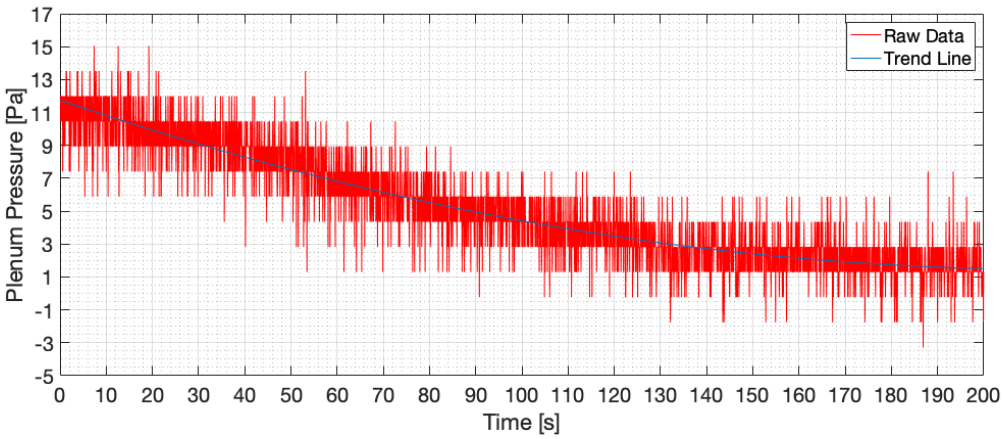

Figure 4.46: Plenum pressure stability at the minimum duty cycle using 250 [Hz] frequency

As it can be seen from the plot, the pressure stability in the plenum is not achieved for a sustained time over 200 second pulsing. The achieved plenum pressure is in the range of 1 - 12 [Pa], which is 25 times less than the target pressure of 300 [Pa]. It means a fixed duty cycle value does not work for a finite supply of the gas. A variable duty cycle should be used, which

is adjusted to every consecutive plenum pressure value. This is achieved by introducing a linear pressure controller equation:

$$y = bx \tag{4.39}$$

x is the tank pressure, y is the plenum pressure, and b is the linear duty cycle multiplier. Equation 4.39 can be re-phrased and re-written in the following form:

$$b = \frac{P_{target}}{P_{outlet}} \tag{4.40}$$

P_{target} would be the required plenum pressure and P_{outlet} is the incoming pressure from the valve/tank. 3 duty cycle multipliers have been used to perform the test with the varying duty cycle at a 250 [Hz]:

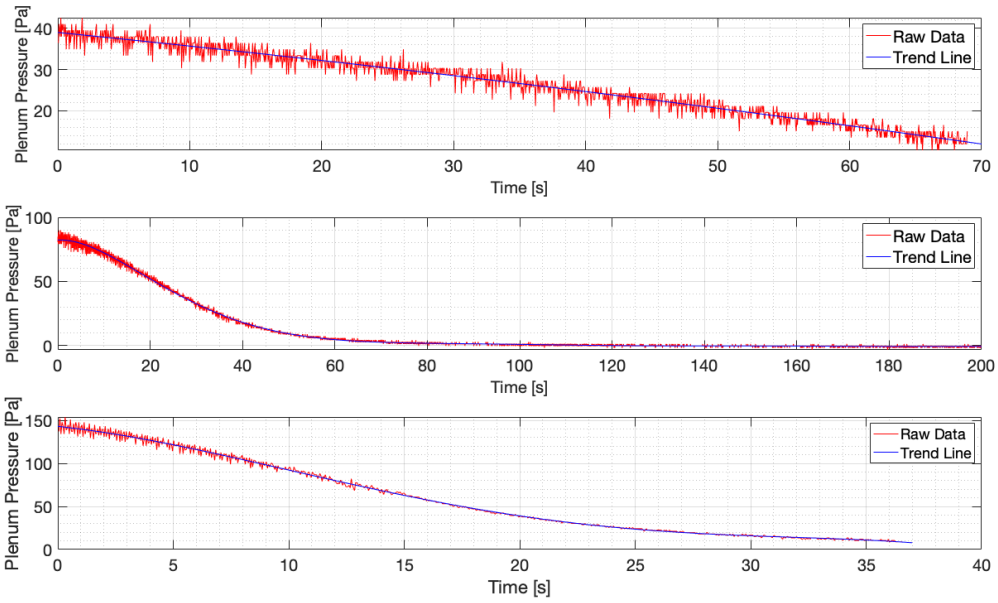

Figure 4.47: Plenum pressure stability using a linear duty cycle multiplier at 250 [Hz] frequency. Top to bottom: with multiplier 10, 20, and 30

The multiplier values are arbitrary and chosen to check the behavior of the plenum stability. It can be seen that using higher multipliers yields to a higher plenum pressure. However, the stability of the pressure is insufficient. The gas loss seems to be too quick by looking at the time it takes to empty the tank, which in this case is all the way from GPFS to PPD. Since the gas runs out fast, it is decided to increase the propellant pressure inside the tank up to 400 [mbar]. Furthermore, to check if the higher values of plenum pressure can be achieved for a substantial time, the duty cycle multiplier is increased as well, but kept at one value of 60. Moreover, to save time these new parameters are tested using extra 4 PWM frequencies (125 [Hz], 500 [Hz], 750 [hz], and 1000 [Hz]). The lower bound is chosen to be 125 [Hz] and not 25 [Hz] or 50 [Hz], because it expected to reach the saturated plenum at lower duty cycle values. The upper bound of 1000 [Hz] is chosen due to the limit of the maximum operating frequency according to the manufacturer.

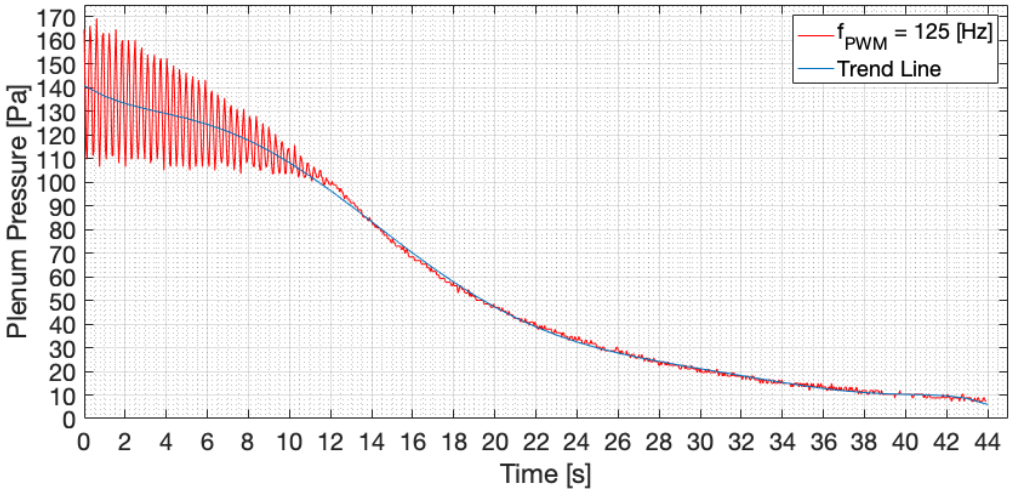

Figure 4.48: Plenum pressure stability using a multiplier of 60 at 125 [Hz]

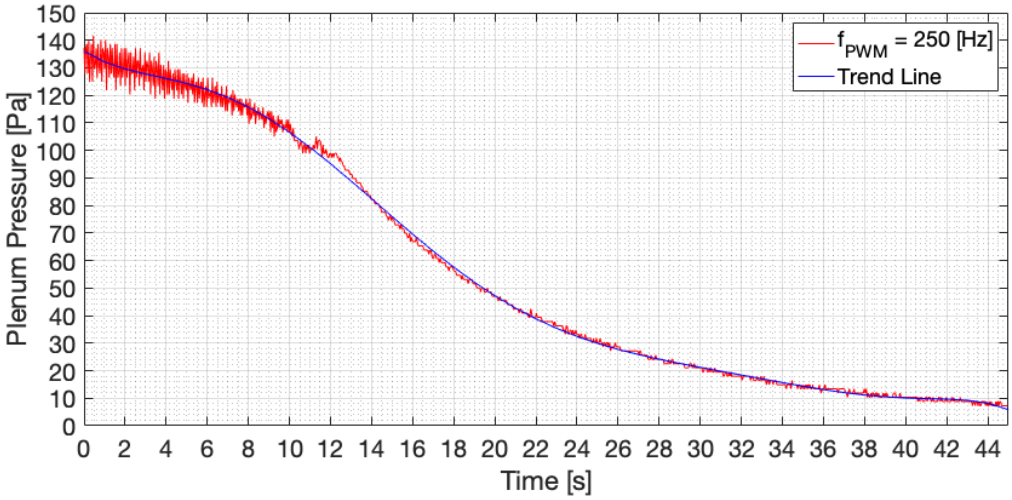

Figure 4.49: Plenum pressure stability using a multiplier of 60 at 250 [Hz]

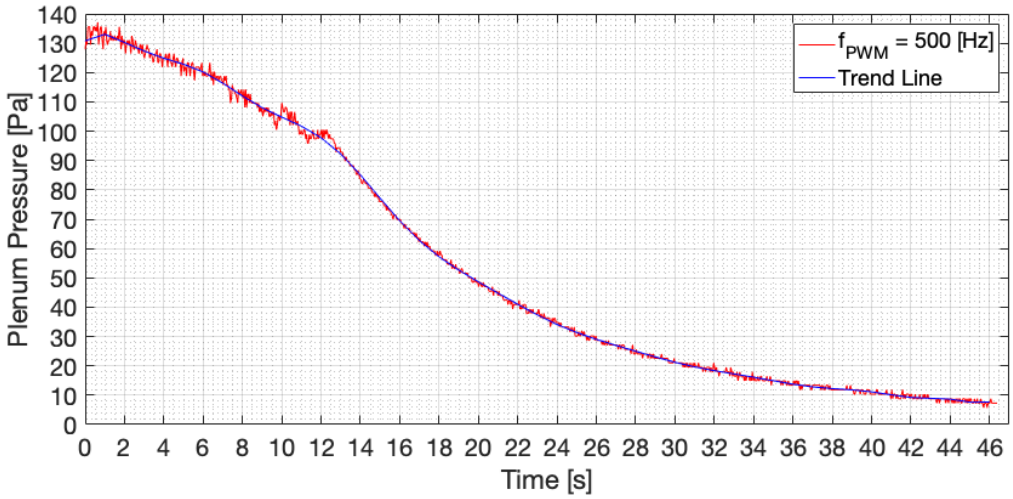

Figure 4.50: Plenum pressure stability using a multiplier of 60 at 500 [Hz]

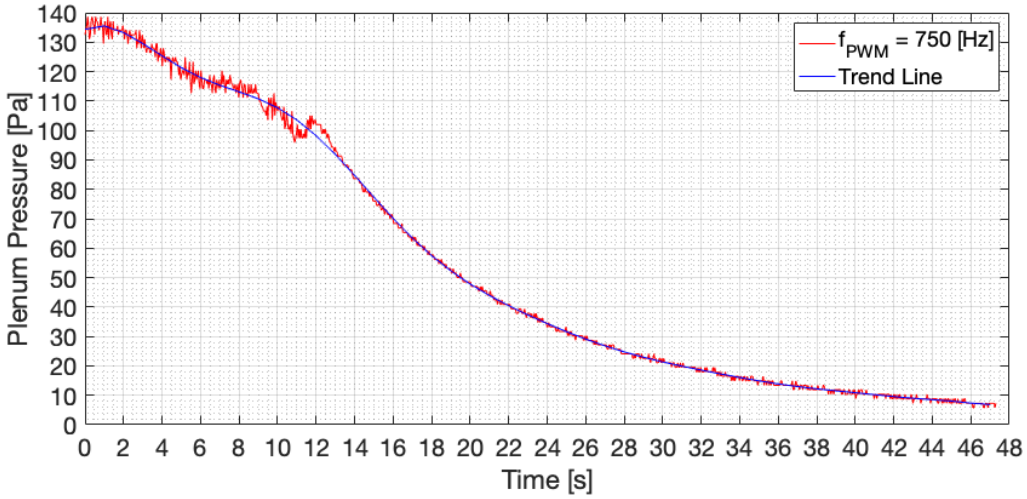

Figure 4.51: Plenum pressure stability using a multiplier of 60 at 750 [Hz]

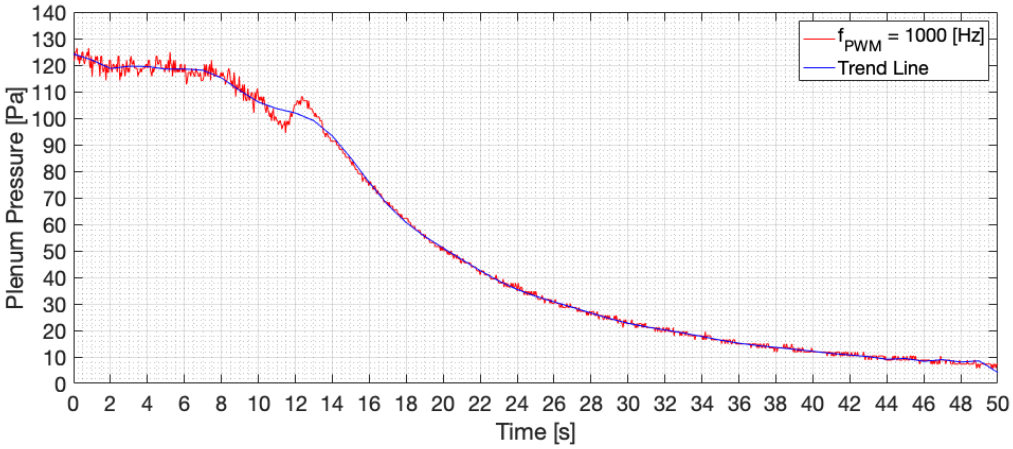

Figure 4.52: Plenum pressure stability using a multiplier of 60 at 1000 [Hz]

From Figures 4.48 to 4.52 can be seen that the increase of the linear multiplier and tank pressure at various PWM frequencies does not suffice to reach a target plenum pressure of 300 [Pa]. At all frequencies can be seen that the tank is emptied within 50 [s]. Although, the frequencies of 125 [Hz] and 1000 [Hz] produce the most unstable pressures in the plenum compared to the rest of the frequencies. The influence of the various PWM frequencies on the tank pressure stability and performance is checked:

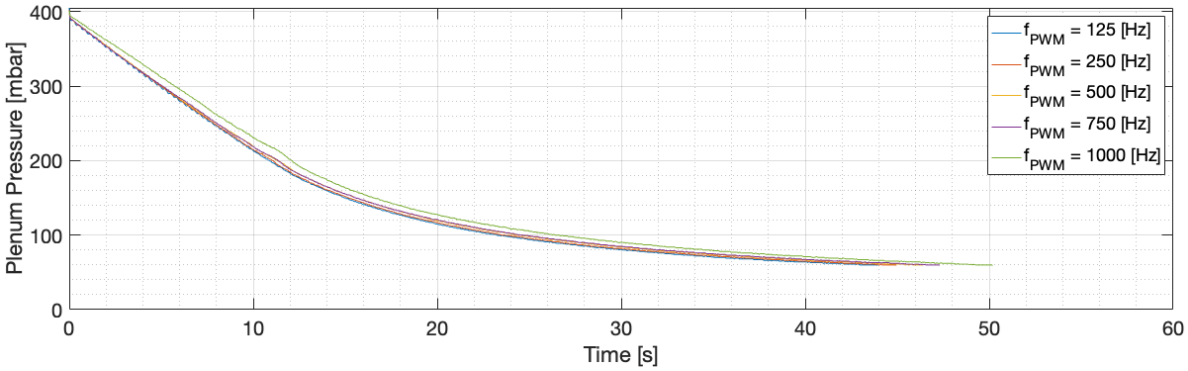

Figure 4.53: Tank pressure stability at various frequencies. The initial tank storage pressure is 400 [mbar]

From Figure 4.53 can be seen that there is no influence of PWM frequency on the tank pressure. Thus, it is assumed that it is true throughout the remaining test parts of TEST-COM-01 test. Although, it seems that the stability of the plenum pressure and the target pressure can be improved. Therefore, there is a quadratic relation which can improve the stability of the pressure at the beginning. At this point, It is decided to increase the tank pressure to 600 [mbar] and 800 [mbar], introduce a quadratic multiplier and test using 250 [Hz] frequency. This way a check can be done whether the improved feedback loop is sufficient to achieve the required 300 [Pa]. The quadratic multiplier corresponds to following expression:

$$y = ax^2 + bx \tag{4.41}$$

Coefficient *a* is determined from the previous experimental data with a value of $1.43469 \cdot 10^{-8}$.

Figure 4.54 presents the outcome of using the quadratic multiplier with 600 and 800 [mbar] tank pressure at 250 [Hz]:

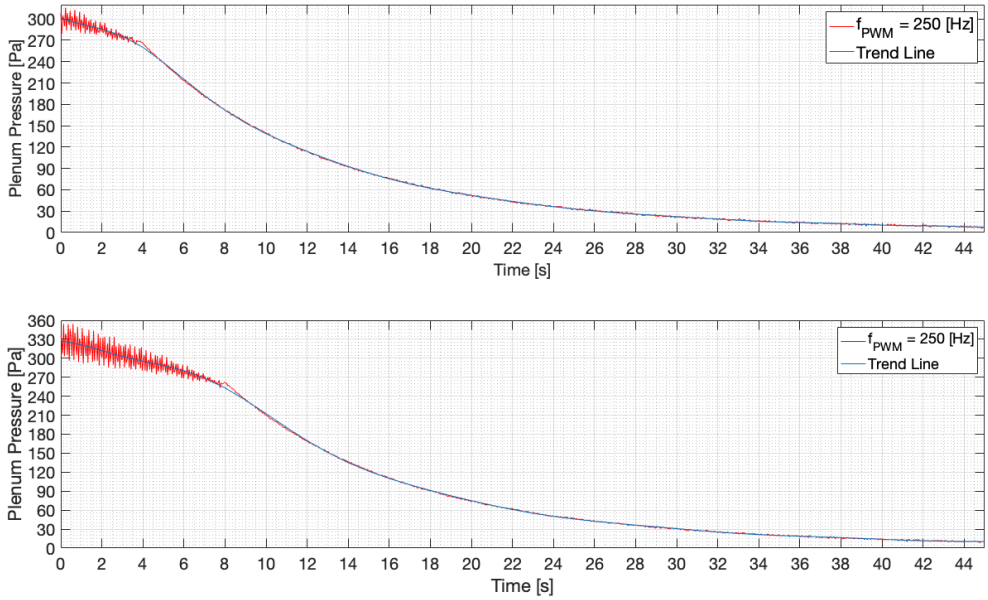

Figure 4.54: Plenum pressure stability using a quadratic multiplier at 250 [Hz]. Top to bottom: 600 [mbar] and 800 [mbar] tank pressure

It can be immediately seen that the plenum pressure is saturated around 300 [Pa]. Compared to the same PWM frequency graph from Figure 4.49, the lower more stable plenum pressure is achieved with a linear multiplier of the duty cycle and 400 [mbar] tank pressure, but higher plenum pressure is achieved with a quadratic multiplier of the duty cycle, and 600 and 800 [mbar] tank pressure. However, the 300 [Pa] pressure is achieved for a brief moment between 2 - 4 seconds. Nonetheless, the quadratic feedback multiplier improves the system's performance.

It is noticed that increasing the tank pressure at a fixed PWM frequency and using the same quadratic multiplier, the stability of the pressure and its magnitude increases. There are still too many combinations of the quadratic multiplier, tank pressure, and PWM frequencies, which would let reach the required plenum pressure. At the end, it is decided to characterize the plenum pressure stability for 3 different target plenum pressures at a fixed quadratic multiplier and tank pressure, and various PWM frequencies. The new tank pressure is set to 1000 [mbar]. The quadratic multiplier is the same. The chosen PWM frequencies are: 50, 250, 500 [Hz]. 50 [Hz] is chosen to check even lower bound of PWM frequency than the tested 125 [Hz]. 250 [Hz] is chosen as it could be the most optimal frequency as noticed from all the previous tests. 500 [Hz] is chosen, because it is shows a trend of upper limit of the stability from higher frequency range. Figures 4.55 to 4.57 show the test results of these settings.

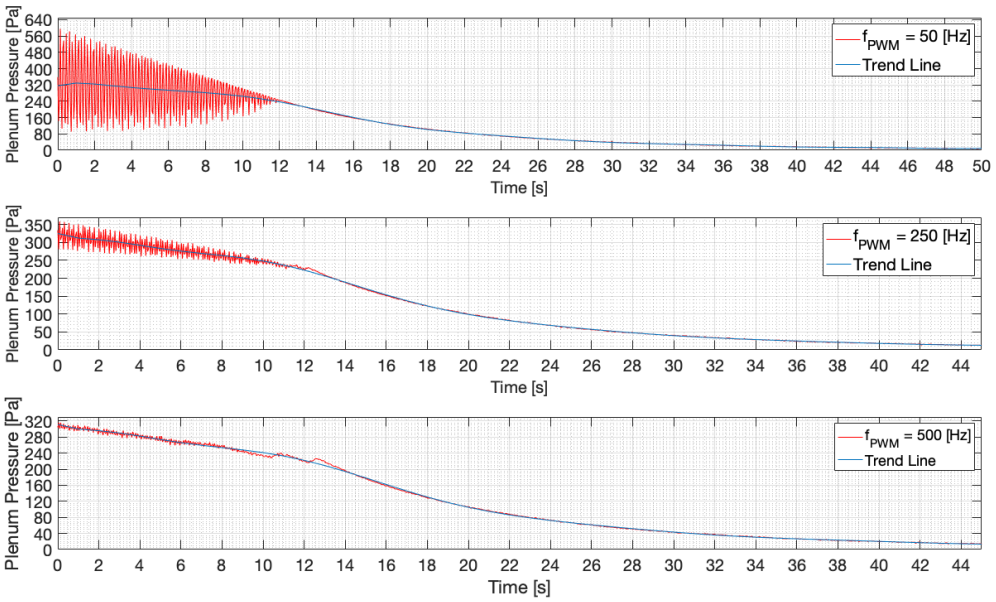

Figure 4.55: Plenum pressure stability using a quadratic multiplier and 1000 [mbar] tank pressure at 50, 250, 500 [Hz] frequencies for 300 [Pa] target plenum pressure

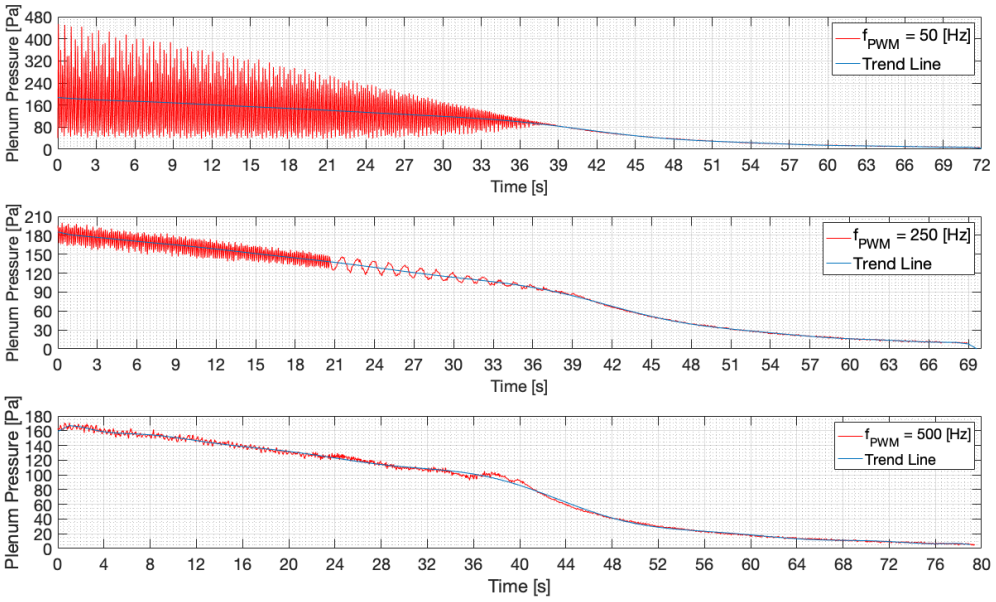

Figure 4.56: Plenum pressure stability using a quadratic multiplier and 1000 [mbar] tank pressure at 50, 250, 500 [Hz] frequencies for 150 [Pa] target plenum pressure

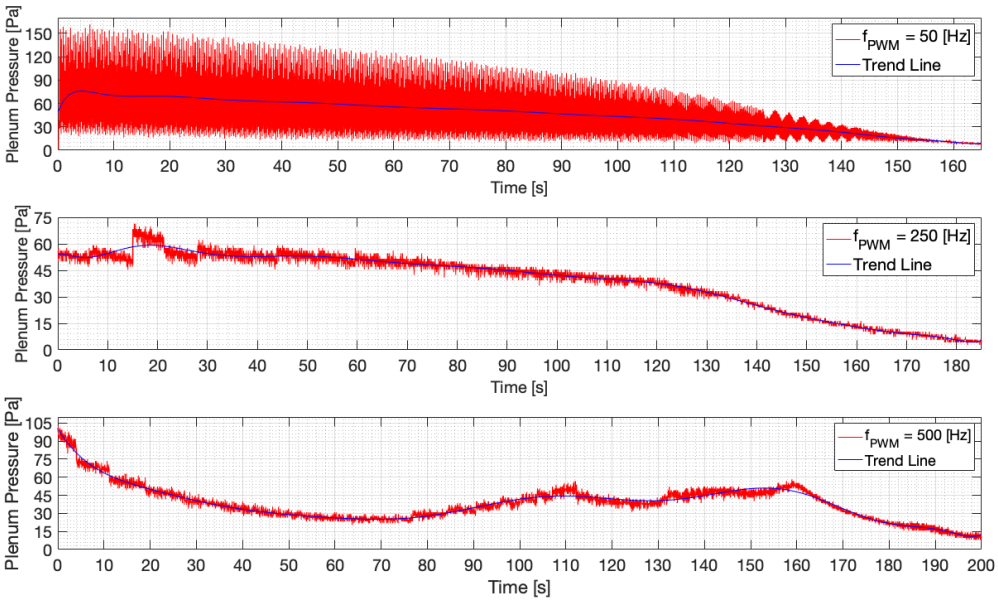

Figure 4.57: Plenum pressure stability using a quadratic multiplier and 1000 [mbar] tank pressure at 50, 250, 500 [Hz] frequencies for 50 [Pa] target plenum pressure

From Figure 4.55 can be seen that the valve performs the best between 50 and 250 [Hz] PWM frequencies. There is a slight overshoot of the target pressure of 300 [Pa] at both frequencies. It seems that at 50 [Hz] a stable pressure around 320 [Pa] is achieved for around 10 [s]. Although, the noise is quite significant. Very similar plenum pressure stability and overshoot is between 250 and 500 [Hz]. The target pressure of 300 [Pa] is achieved only for 2 [sec] with an overshoot of around 20 [Pa]. Although the tank for all three frequencies is emptied out within 50 [s].

From Figure 4.56 can be seen that a stable pressure of around 150 [Pa] in the plenum is achieved for a longer time for all 3 frequencies, and the total thrusting time is increased to almost 70-80 [s]. The highest noise in the plenum pressure values is observed at 50 [Hz] test. The pressure jumps are ranging from 80 [Pa] to almost 480 [Pa]. Thus at 50 [Hz] value the system is not stable. For 250 [Hz] the stability of the plenum pressure improves. The overshoot is about 30 [Pa] from 150 [Pa] at the beginning. It seems that from around 140 - 130 [Pa] at 250 [Hz] the plenum is saturated for longer periods of time. The best performance is obtained at 500 [Hz] value. It has the smallest overshoot of the plenum pressure (160 [Pa]).

From Figure 4.57 can be seen that there is a significant difference between the 3 frequencies on how the 50 [Pa] pressure is achieved. At 50 [Hz] the quadratic part seems to have a lot of noise throughout the whole test duration with the dissipation at the the very end. There is almost a 100 [Pa] overshoot at the very beginning . At 250 [Hz] the 50 [Pa] pressure is achieved for a significant time of around 60 [s]. The quadratic part stops working at around 120 [s], where from that time and onwards the linear part kicks in. There is a strange increase of 20 [Pa] in pressure between 15-20 [s]. It is possible that there was a reading error in the low pressure sensor, because the rest of the values do not show any random behavior. At 500 [Hz] the 50 [Pa] pressure barely achieved. There is an overshoot of around 50 [Pa] at the very beginning of the test. The quadratic part of the controller is struggling to stabilize the plenum pressure at 50 [Pa]. Only for a brief moment around 110 - 160 [s] 50 [Pa] is achieved, which

means only at a lower remaining tank pressure this value can be achieved at this setting. In general, this test shows that the thrusting can be achieved for almost the whole span of 200 [s] compared to the other two tests for 300 and 150 [Pa] plenum target pressure.

In conclusion, the the optimal performance of the solenoid valve depends on the plenum target pressure. To reach 50 [Pa] plenum pressure, solenoid valve should work at 250 [Hz]. To reach 150 [Pa] plenum pressure, the solenoid valve works best at 500 [Hz]. To reach 300 [Pa] plenum pressure, the best choice would be 50 [Hz]. Therefore, it seems there is no trend between the target pressure and the PWM frequency. Although, 250 [Hz] PWM frequency shows a lot of promising performance at various operating regimes compared to the rest of the tested frequencies.

4.4.5. Plenum Pressure Stability at FOE Values in a Closed System

After the characterization of the plenum stability and valve performance under various conditions, the most optimal parameters setting is taken and tested with FOE values using a closed (no feed of nitrogen from GPFS) PPD system. The valve uses the same quadratic and linear controller, and it is set to work at 250 [Hz] PWM frequency. The nitrogen pressure in the tank is set to 0.2 [bar]. The plenum target pressure is set to 300 [Pa]. The following results are shown in Figure 4.58:

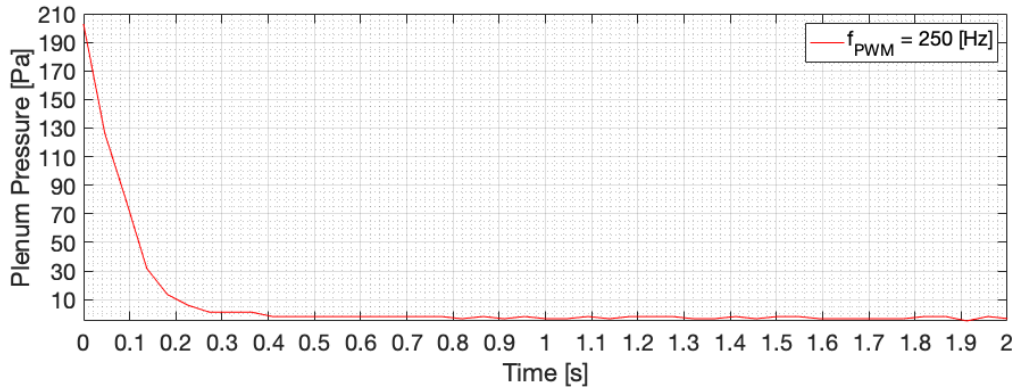

Figure 4.58: Plenum pressure stability using final operational envelope values for a target pressure of 300 [Pa] at 250 [Hz]

It can be clearly seen that 0.2 [bar] tank pressure is not enough. The tank has been emptied out within 0.5 [s]. The target pressure of 300 [Pa] is not reached. The maximum value of 200 [Pa] is reached. This presents a challenge to the design parameters defined by *Turmaine* [3]. It seems seems that 0.2 [bar] tank pressure is not enough. By looking at the results from Section 4.4.4, a tank pressure of 1 [bar] is necessary to reach at least 50 - 300 [Pa] plenum pressure. Such a deviation from the original design parameters might require redesign not only of the pressurization and propellant amount values, but also hardware design such as the tank tubes.

Since it is noticed that the performance at FOE values with the closed system, the other plenum target pressure such as 50 and 150 [Pa] are not tested, because the same system's behavior is expected.

4.4.6. Coil Resistance of the Valve due to the Temperature Increase

As it can be seen from the minimum voltage pulse duration and maximum operating frequency tests, the solenoid valve warms up. According to the manufacturer, the coil resistance of the valve is 40 [Ω] at 24 [VDC] spike voltage. Its ambient operating temperature is 4 - 49 [°C] (277.15 - 322.14 [K]), and a maximum coil temperature should not exceed 66 [°C] (339.15 [K]) [44].

Using the above mentioned information, the solenoid valve's coil resistance is measured at 6 different temperatures. The change in the coil resistance would provide data on the increase of the power usage on the total propulsion system power requirements, especially when the valve requires spike voltage. Figure 4.59 shows the relation between the temperature increase of the solenoid valve and the coil resistance behavior:

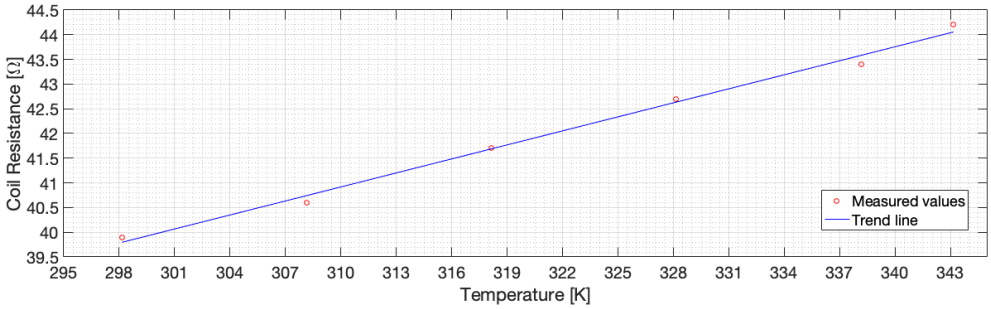

Figure 4.59: Graph of the temperature effect on the solenoid valve coil resistance

It can be seen that the resistance has a linear trend w.r.t. increasing temperature. The first measurement is performed when the valve is at the room temperature, and the last measurement is performed above the maximum coil temperature. The required power for spiking and hold the valve is found using the following Equations 4.42 and 4.43:

$$P_{sp} = \frac{V_{sp}^2}{R_{coil}} \tag{4.42}$$

$$P_{hl} = \frac{V_{hl}^2}{R_{coil}} \tag{4.43}$$

V_{sp} is the spike voltage and is equal to 24 [VDC], and V_{hl} is the hold votlage, which requires 3.2 [VDC] as the input (recommended by the manufacturer). The 6 temperature inputs and their corresponding coil resistance and power values are given in Table 4.16:

Table 4.16: 6 measured temperature values and their corresponding coil resistance values and estimated power

T_{sv} [K]	R_{coil} [Ω]	P_{sp} [W]	P_{hl} [W]
298.15	39.9	14.44	0.26
308.15	40.6	14.19	0.25
318. 15	41.7	13.81	0.25

328.15	42.7	13.49	0.24
338.15	43.4	13.27	0.24
343.15	44.2	13.03	0.23

With the increasing resistance, the input power requirement decreases. However, the power drop for hold and spike is small compared to the steps of the temperature increase (every 10 [K]). Thus, the weight on the propulsion system power requirement is not that significant. Furthermore, by looking at Figure 4.28 during the frequency sweep the maximum temperature of 39.1 [^{o}C] (312 [K]) is achieved. This value is within the operational temperature range. Thus, in general, there is no significant increase of the required power to the total power budget.

In this section, a small discussion about the freezing of the propellant inside the feed and tank tubes is discussed. From all of the obtained data, there is no trend of any significant temperature drop inside the tank tube or the feed tube between the thruster interface and valve. Actually, a slight increase of the temperature in the propellant tank is observed in terms of 0.1 - 0.15 [^{o}C]. It could be due to the friction of the nitrogen molecules against the tube walls and heat dissipation of the valve during the PWM operation.

All *MatLab* codes used for this test can be found in Appendix F.

4.4.7. Design and Requirements Verification

It can be concluded that by using solenoid valve's PWM mode it is possible to achieve 50 - 300 [Pa] plenum's target pressure. However, it is advisable to select a frequency which can match the required plenum and tank pressure ratio such that duty cycle would be as close as possible to 50%. In such a way, the most optimal spike and hold power values of the valve can be reached. Although, from the obtained test data it can be seen that the lower bound of frequencies ranging from 500 [Hz] and lower are more suitable for PWM operation. One has to take into account that from 125 [Hz] and lower, a possibility of overshooting the target pressure increases with the decreasing frequencies as seen in the test data. The most promising PWM frequency is 250 [Hz]. It has the best performance characteristics from all the tested frequencies. This frequency can be used specifically to achieve 50 [Pa] plenum pressure (ref. Figure 4.57). The temperature of the valve at this frequency is around 36 [^{o}C] (if operated continuously) and remains within the max. operating temperature of 49 [^{o}C] and note exceeding max. coil temperature of 66 [^{o}C] (ref. Figure 4.43).

However, in order to use the stated frequencies and achieve the target pressures, the propellant tank length and pressure might be affected. It is shown that FOE values are insufficient (ref. Figure 4.58) and that by increasing the propellant tank from 0.2 [bar] to 1 [bar], increases the chance to achieve the plenum's target pressure, but also to sustain a stable plenum's pressure for a certain amount of time. Furthermore, the increase of the length of the propellant tank has an influence on the success of the PWM operation. Thus, it is most likely necessary to find an a new optimal combination between the required tank pressure and tank tube length.

Furthermore, in this section the requirements related to TEST-COM-01 test (ref. Table 2.6) are verified and discussed. Furthermore, the design of the PPD verification is also discussed.

PROP-SYST-300 requirement can be partially verified by looking at the coil resistance test results. It was shown that the hold power values are within 4 [W] budget and it decreases with the increasing valve temperature. Furthermore, by looking at the results from Figure 4.57 it

can be seen that the valve can operate between 160 - 200 [s], which the valve operates the longest from all the tests to achieve the target pressure. These values fall within the required FOE design parameters. For now the 160 - 200 [s] can be used as the initial values for PROP-SYST-300 requirement. The TBD can be replaced as such:

***PROP-SYST-300**: The peak power consumption of the propulsion system during ignition or heating shall be not higher than 4 [W] and duration shall not be longer than 200 [s] per day*

200 [s] is used as the upper limit in the requirement. However, it can be considered as a TBC value, which will be adjusted from the optimized design of PPD.

PROP-FUN-100 requirement can be partially verified from the test results. The same conclusion can be made as it is explained above for PROP-SYST-300 requirement.

PROP-FUN-300 requires that the system works in a closed configuration. By looking at the results of Section 4.4.5 and 4.4.4, this requirement cannot be verified. It requires an optimized design of the propellant tank and amount of the propellant. Although, the system is able to work in a closed configuration as it is shown in Section 4.4.5, but would not deliver the required performance.

PROP-FUN-500 requirement was verified by a demonstration of the capabilities of the valve, μController, and software code. It was shown during the initial tests, that the system can be pressurized to the required propellant pressure, but also emptied out completely. To not damage the tube after emptying the gas inside them due to the pressure difference at ambient and tank, it was shown that the system can be emptied to a certain internal pressure and switched off.

PROP-INT-200 requirement was verified during the maximum operating frequency sweep, minimum pulse duration, and coil resistance tests. It is shown during the maximum operating frequency test that the maximum temperature of 83.3 [^{o}C] is achieved at 3000 [Hz] 4.27. However, it is just a test value during a check of the operational frequency range. At least, it is known what value of temperature can be expected. Furthermore, from the technical data sheet of the valve manufacturer, it is known that the maximum operating temperature of the valve should not exceed 66 [^{o}C], which is well below the upper limit of the PROP-INT-200.

The maximum pressure of 1000 [mbar] has been used for this test, which might become a new design parameters to operate LPM. Therefore, PROP-RAMS-200 requirement is verified by looking at TEST-COM-01 results.

4.5. TEST-COM-04: Heater Efficiency Test

The results of TEST-COM-04 are presented in this section. First, a summary of VLM thruster chips which have been tested is presented. Second, the preliminary power-pressure test and thrust bench test results for each chip are analyzed. Finally, the verification of the requirements is discussed.

4.5.1. Summary of Tested VLM Chips

Originally, 4 operational VLM thruster chips were available for this test (ref. Table 3.24). However, due to the fact that the selected chips have already been used previously and some were damaged, it is decided to test all the available first generation thruster chips in the cleanroom. In this way if the selected thrusters broke during the testing, extra ones can be used

a back up. The following Table 4.17 is a summary of all 7 tested VLM thruster chips during TEST-COM-04:

Table 4.17: The summary of all VLM thruster chips which have been tested in TEST-COM-04

-	Chip code	R_{ini} [Ω]	Comments
1.	01-Ls2-01	6.6	Semi-damaged heater bridges. Heater and nozzle compartment contamination
2.	01-LS1-01	10	Blocked nozzle
3.	01-BS2-01	7.65	Semi-damaged heater bridges
4.	01-Ld1-01	9.44	Big heater compartment contamination
5.	01-Ws1-01	12.3	Semi-damaged heater bridges. Slight heater compartment contamination
6.	01-WS1-01	12.3	Damaged heater electric pads and some bridges
7.	01-WS2-01	6.84	Virtually no damage on the heaters

The additional 3 chips are *01-Ls2-01*, *01-Ws1-01*, and *01-WS-01*. The comments in Table 4.17 describe the initial conditions of all the chips before testing them.

4.5.2. Numerical Analysis Equations

Due to the test set-up conditions, some of the thruster parameters cannot be determined directly, such as chamber pressure and temperature. Thus, it requires *Ideal Rocket Theory* to relate some of the performance parameters of the thruster with the experimentally obtained values. Before applying any equations, the following assumptions are defined to simplify the application of this theory in real case:

- Perfect and calorically ideal fluid
- No mixing between the propellant and pressurant
- Flow is steady, mono-dimensional and with purely axial velocity
- No friction or external forces

In order to know what power is required to achieve the vaporization in the thruster, the chamber temperature needs to be defined. To determine it, the power required to be received by the water is calculated by using Equation 4.44 [3]:

$$\dot{Q} = \dot{m} \cdot \left[h_{vap} + c_{pl} \cdot \left(T_{vap} - T_0\right) + c_{pg} \cdot \left(T_c - T_{vap}\right)\right] \tag{4.44}$$

$\dot{Q}$ is the power [W], $\dot{m}$ is the propellant mass flow [kg/s], h_{vap} is the latent heat of the propellant vaporization [kJ/kg], c_{pl} is the specific heat of the liquid propellant phase at constant pressure [J/K/kg], T_{vap} is the propellant vaporization temperature [K], T_0 is the propellant temperature in the plenum [K], c_{pg} is the specific heat of the gaseous propellant phase at constant pressure [J/K/kg], and T_c is the chamber temperature [K].

The propellant mass flow from Equation 4.44 can be expressed using *Ideal Rocket Theory* [60]:

$$\dot{m} = \frac{P_c \cdot A^*}{\sqrt{\frac{R_A}{M_W} \cdot T_c}} \cdot \sqrt{\gamma \cdot \left(\frac{1+\gamma}{2}\right)^{\frac{\gamma-1}{1-\gamma}}} \tag{4.45}$$

P_c is the pressure in the chamber [Pa], which can be translated to the pressure in the plenum, in this case. γ is the specific heat ratio [-], and A^* is the nozzle throat area [-]. According to [3], the minimum vaporization temperature method is the most feasible to find the required power. In this method, T_{vap} is the same as T_c, which is related to the pressure in the chamber, boiling temperature and its pressure. This approach is selected, because it is known that the propulsion system has a *Blow Down* configuration. It means that the system is closed and the pressure inside the tank is going to drop during the thrusting over the time. Thus, the pressure change is influencing the required vaporization temperature. The vaporization temperature can be found using *Clausius-Clapeyron* relation [65] in Equation 4.46:

$$T_{vap} = \frac{T_1 \cdot h_{vap} \cdot M_W}{T_1 \cdot R_A \cdot ln\left(\frac{P_1}{P_c}\right) + h_{vap} \cdot M_W} \tag{4.46}$$

T_1 is the water boiling temperature [K] at 1 [atm], and P_1 is the water pressure at which it begins to boil [Pa]. After substituting the liquid mass flow and the vaporization temperature expressions into Equation 4.44, the expression for the power required to vaporize the water in the chip. It depends only depends on the required chamber pressure, and is found by applying the following expression:

$$\dot{Q} = \frac{P_c \cdot A^*}{\sqrt{\frac{R_A}{M_W}}} \cdot \sqrt{\gamma \cdot \left(\frac{1+\gamma}{2}\right)^{\frac{\gamma-1}{1-\gamma}} \cdot \frac{T_1 \cdot R_A \cdot ln\left(\frac{P_1}{P_c}\right) + h_{vap} \cdot M_W}{T_1 \cdot h_{vap} \cdot M_W}} \cdot \left[c_{pl} \cdot \left(\frac{T_1 \cdot h_{vap} \cdot M_W}{T_1 \cdot R_A \cdot ln\left(\frac{P_1}{P_C}\right) + h_{vap} \cdot M_W}\right) + h_{vap}\right] \tag{4.47}$$

Although, to find the required theoretical chamber pressure values for the T_c = T_{vap} method, it requires a numerical method to solve mass flow equation when the vaporization equation is substituted. This is done by using *Matlab* function *vpasolve*. In this way, the theoretical chamber pressure values can be directly related to the chosen mass flow range which in turn can be related to the measured real power. Finally, the thrust can be determined from *Ideal Rocket Theory* [60]:

$$F_T = \dot{m} \cdot I_{sp} \cdot g_0 \tag{4.48}$$

I_{sp} is the specific impulse [s] and g_0 is the gravitational acceleration [m/s^2]. The fixed value constants, which are used in the above equations , are presented in Table 4.18:

Table 4.18: Constants used to determine power

Constant	Value	Units	Description

A^*	$4.5 \cdot 10^{-9}$	[m^2]	Nozzle throat area [3]
R_A	8.314	[J/K/mol]	Universal gas constant
M_W	18.02	[g/mol]	Molecular mass of water vapour
γ	1.32	[-]	Specific heat ratio of water vapour
T_1	373	[K]	Water boiling temperature
P_1	1	[atm]	Water pressure at the boiling point
h_{vap}	2256	KJ/kg	Latent heat of water vaporization
c_{pg}.	1996	J/K/kg	Specific heat of water vapour at constant pressure
c_{pl}	4187	J/K/kg	Specific heat of liquid water at constant pressure

It is decided to keep the throat area constant throughout all the tested chips. In this way it is easier to compare the results with the theoretical values. Furthermore, there is no exact information of the throat area given by *Silva* [2].

Numerical Analysis Corrections

The Equations 4.44 to 4.48 are used for the calculations when the system is working at vacuum conditions. This test is performed only at ambient conditions. Therefore, finding a required power at a given chamber pressure in this case, it is necessary to vary the voltage provided to the heaters. As it would be a time consuming task to maintain every pressure value, the increments of voltage inputs are used and the required chamber pressure is determined according to that value. During the data processing these increments (data points) are used to derive a possible power-pressure trend line.

The other issue is presented when it comes to controlling the chamber pressure during the whole operation of the thruster. Since the system is not closed and not tested at vacuum, and there is no direct method, at the moment, to control the chamber pressure, using the mass flow equation, the chamber pressure can be represented by a fixed mass flow provided by the syringe pump. However, such a method does not provide that of the different values of the chamber pressure and would not effect the actual required power values. From the ideal case (at vacuum conditions) the expected chamber pressure values for mass flow from 0.5 to 3 [mL/h] are expected to be in the range of $1.8 \cdot 10^4$ [Pa] - $1.2 \cdot 10^5$ [Pa]. It is noticed from the obtained pressure data of all the chips, the pressure in the plenum is in the magnitude of 10^5 [Pa]. Nonetheless, for testing at ambient conditions and this test set-up, such an approach is currently the only means to relate the chamber pressure to the required power.

Another issue is that there is no means to measure directly the chamber temperature. Therefore, it is decided to assume that the chamber temperature is equal to the vaporization temperature. Using this approach the chamber temperature can be measured indirectly by applying the vaporization temperature equation.

These numerical analysis corrections are applied during the processing of the test data. In such a way the ideal power-pressure values can be compared to the assumed chamber pressure and real power values all together. As it is a preliminary power-pressure test, it provides the initial information of the thruster performance for the further studies of such VLM thruster chips.

4.5.3. Preliminary Power-Pressure Tests

In this section the results of the preliminary power-pressure tests are presented, which were performed according to the test procedure and set-up described in Table 3.29 and 3.25 accordingly. It is important to point out that for each chip the order of the test results at specific mass flow is chronological. As there was no information how the thrusters would perform at their current condition, the choice of the specific mass value from the defined range is arbitrary. Thus, it doe not follow the order of from minimum to maximum value or vice verse.

The test results are presented in a form of a table and graph. The table shows the incremental steps of reducing power at each time-stamp. The test is begun at the highest input power level and being reduced every moment when the user assumes that the system is stable. The stability of the system is deduced by looking at the microscope camera and observing the behavior of the water and steam flow. Although, the plenum pressure and temperature are measured continuously during the test, but only the values at the chosen time-steps are presented in the tables. The whole data of the pressure and temperature for each chip with the photos of the no-flow and over-flow is presented in Appendix E. Furthermore, the minimum input power at which the over-flow might occur is presented in a graph. The graph uses ideal pressure chamber values to relate the minimum measured input power and the ideal input power.

The full comments of each mass flow measurement for each chip can be found in the excel sheet on the web drive. Web drive is File Transfer Protocol (FTP) server from TU Delft where all the research work is stored from the micro-propulsion research group. The location path for the excel sheet is: *staff-umbrella > Micropropulsion > Technical Descriptions & Interface Document > Antanas > test_data > vlm_power_pressure_test_data > massflow_timestamp_data_all_chips.xlsx*. The video footage of the microscope and thermal imaging camera is also found on the web drive: *staff-umbrella > Micropropulsion > Technical Descriptions & Interface Documents > Antanas > test_data > vlm_power_pressure_test_data* (the footage is accessed per chip).

All *MatLab* codes used for this test can be found in Appendix F.

01-Ls2-01 Thruster Chip

The test data is achieved at 2 mass flow values (3 and 2,5 [mL/h]) only. This test is considered incomplete, because there was no data obtained at which the overflow was observed. At 3 [mL/h] mass flow the test was stopped prematurely, because there was observed instability in the voltage and current values from the Power Supply Unit (PSU). The thruster was barely working at 2.5 [mL/h] test, where the heater bridges have been damaged completely and its resistance became 108 [Ω]. The following Figure 4.60 shows the front and back condition of the thruster after the testing:

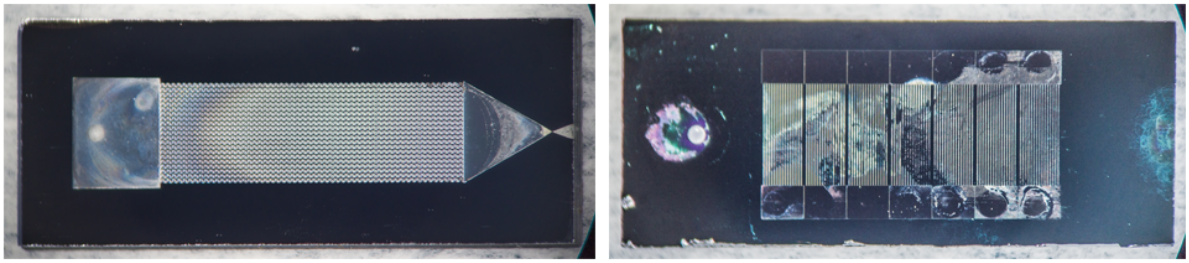

Figure 4.60: Front and back view of *01-Ls2-01* chip after the tests

The up-close view of the damage of the heaters and their bridges, and the oxidation around the inlet is shown in Figure 4.69:

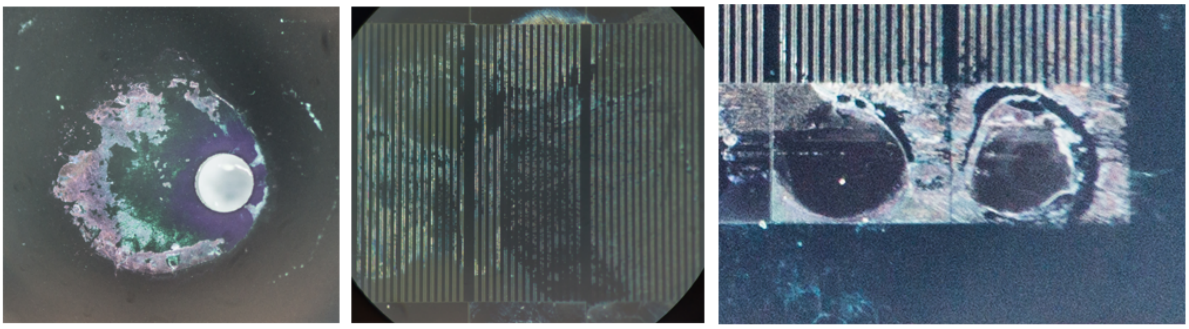

Figure 4.61: Back view of *01-Ls2-01* chip after the tests

The heaters are based on molybdenum. It reacts very easily when a combination of the heat and water is present on it. From Figure 4.61 can be seen where water was under the chip. The biggest impact of the heat and water damage is present on the heater bridges. Since they are almost as thick as a single human hair, they tend to break very easily. That is why the internal resistance has risen to 108 [Ω] for this particular chip.

There are two explanations on how the water gets under the chip (these reasons are applicable to all chips). One is during the overflow of the chip, when the water is coming out of the nozzle to the ambient. Most of the times the water forms a bubble at the exit of the nozzle and creeps under the chip. Due to the hot/warm chip the surface tension of the water decreases with the increased water temperature. Thus, the water can easier penetrate a very tight gap between the chip and the interface. Figure 4.62 shows the formation of the water bubble at the exit of the nozzle:

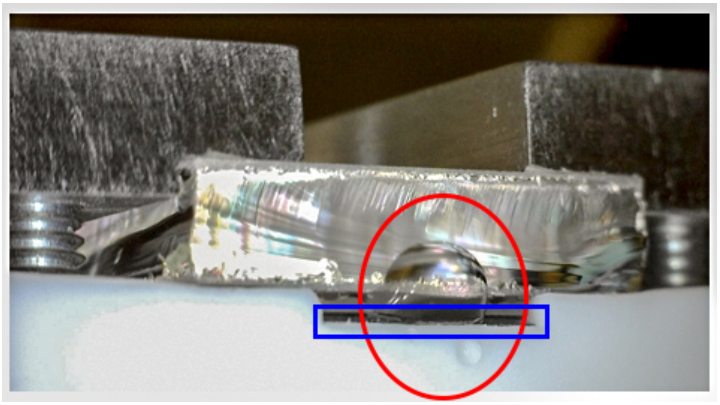

Figure 4.62: Up-close view of one of chips and the interface. A formation of hot/warm water bubble is encircled in red. The gap between the chip and interface is shown in blue rectangle. NOTE: this is a vertically flipped photo of the thrust bench test (the only clear footage of the water formation at the nozzle). That is why the bubble is pointing upwards in this photo

The second explanation of water creeping under the chip can be related to the surface imperfections of the chip at the plenum side and the interface. The thruster interface is made from a teflon material. The area on which the chip is placed (plenum side of the chip and interface) is polished such that it would create vacuum between the chip's surface and the interface. Thus

the inlet hole of both the chip and the interface has a really good connection. Nonetheless, as it can be seen on some of the chips, the chip area around the inlet can be eroded or has some contamination. Thus, it might create a faulty seal between the chip and the interface. Consequently, letting some of the water to creep under the heaters. The view of the plenum area and its outlet to the chip on the interface is shown in Figure 4.63:

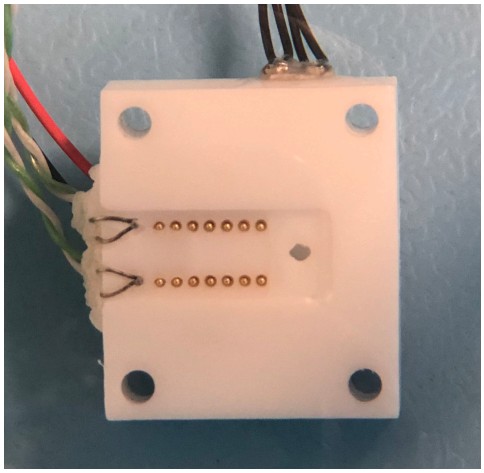

Figure 4.63: Up-close view of the interface without the chip. Two rows of gold plated pins for the heaters can be seen. A hole between the pin rows is the outlet of the plenum to the chip

It was noticed before the test that the chip is dirty and there is a contamination inside the heaters and the nozzle. The up-close view of that is shown in Figure 4.64

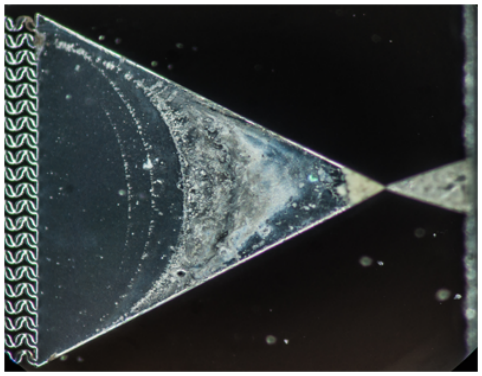

Figure 4.64: Up-close view of *01-Ls2-01* the heaters and the nozzle

In order to avoid any clogging inside the heater channels and nozzle, a de-mineralized water is used for such tests. However, from the figure it can be seen that the water still has some particles which from boiling the water off collect in the nozzle. This would definitely have an impact on the nozzle efficiency and the overall performance of the chip. It is very plausible that that is the reason why only 2 mass flow values could be tested and instabilities during the thrusting are observed. The following Table 4.19 presents the test results at 3 [mL/h] mass flow:

Table 4.19: *01-Ls2-01* chip test input and output parameters at 3 [mL/h]

Time Stamp	V_i [V]	I_i [A]	P_i [W]	T_0 [°C]	P_{pl} [Pa]
00:00:00	6	0.91	5.46	23.95	$1.795 \cdot 10^5$
00:02:30	8.4	1.15	9.66	25.33	$1.93 \cdot 10^5$
00:03:25	7.5	1	7.5	31.84	$1.142 \cdot 10^6$
00:05:30	6.5	0.87	5.65	52.76	$1.203 \cdot 10^6$
00:06:35	6	0.81	4.86	60.2	$1.182 \cdot 10^6$
00:09:45	5.5	0.78	4.29	60.71	$6.1 \cdot 10^5$

The following Table 4.20 presents the test results at 2.5 [mL/h] mass flow:

Table 4.20: *01-Ls2-01* chip test input and output parameters at 2.5 [mL/h]

Time Stamp	V_i [V]	I_i [A]	P_i [W]	T_0 [°C]	P_{pl} [Pa]
00:00:00	6	0.91	5.4	27.95	$3.877 \cdot 10^5$
00:01:18	6	0.88	5.28	27.76	$3.627 \cdot 10^5$
00:04:38	5.5	0.79	4.35	30.83	$5.313 \cdot 10^5$
00:06:24	5	0.73	3.65	N/A	N/A
00:07:29	4.5	0.75	3.38	N/A	N/A

During the last two time-stamps in Table 4.20, the *LabView* software did not record any temperature/pressure data. As the whole test is inconclusive, the last input power values at both mass flow settings are taken as the possible overflow conditions, which are 4.29 [W] at 3 [mL/h] and 4.35 [W] at 2.5 [mL/h]. A summary of *01-Ls2-01* performance results together with theoretical values is shown in Table 4.21:

Table 4.21: Summary of *01-Ls2-01* chip results

$\dot{m}$ [mL/h]	P_c (ideal) [Pa]	T_{vap} (ideal) [K]	$\dot{Q}$ (ideal) [W]	P_i [W]	T_0 [K]	P_{pl} [Pa]
2.5	$9.52 \cdot 10^4$	371	1.7	(3.38)	N/A	N/A
3	$1.15 \cdot 10^5$	376	2.1	(4.29)	333	$6.1 \cdot 10^5$

From the above results it can be seen that the the actual required power is almost twice than the ideal. The following Figure 4.65 shows the power and chamber pressure relation at the measured mass flows:

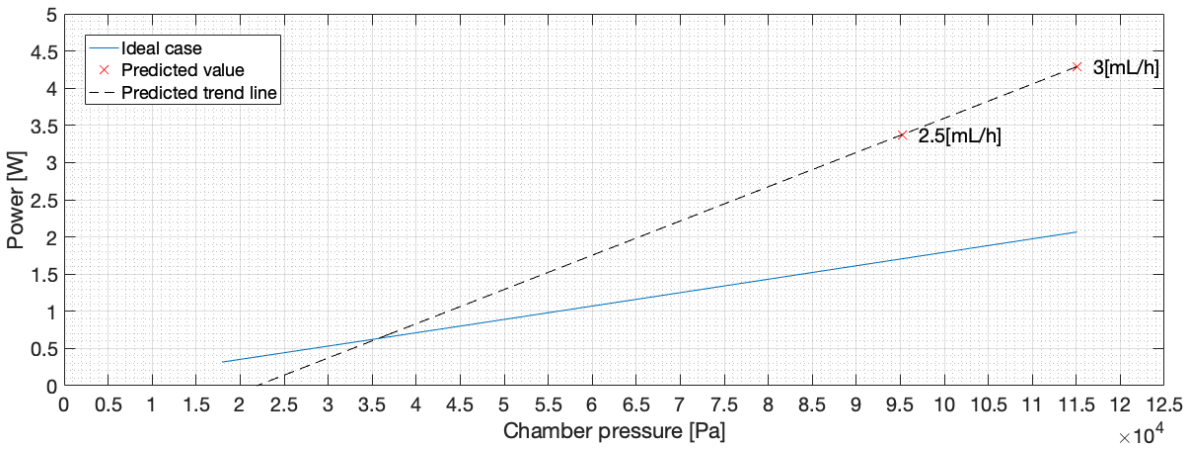

Figure 4.65: *01-Ls2-01* power-pressure graph at 2.5, and 3 [mL/h]

The predicted trend line is only based on two predicted values. Therefore, the validity of these results should be checked experimentally with the new chip. It is very unlikely that the actual trend line would cross the ideal case values (shown in blue line) compared to the rest of the tested thrusters. Nonetheless, the results of *01-Ls2-01* are presented, because these are the only high mass flow values have been checked for all of the chips in Table 4.17.

01-LS1-01 Thruster Chip

As there was no information about this chip, it was decided to test it at a mass flow value of 1.5 [mL/h]. Once the chip has heated up to around 90 [^{c}C] and the water start flowing, the pressure started to increase rapidly (1 [bar] every second), which led to the crack of the chip. After investigating the chip under the microscope, it is deduced that the nozzle has been blocked from the previous tests. Figure 4.66 shows the destroyed chip:

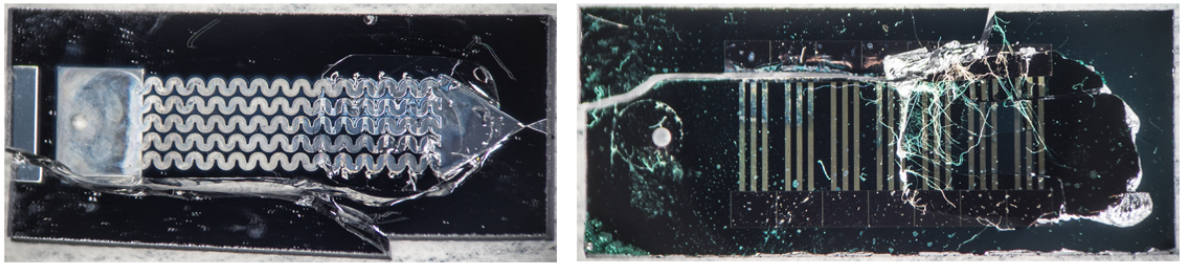

Figure 4.66: Front and back view of *01-LS1-01* chip after the test

The close-up look of the extent of the damage inside the chip:

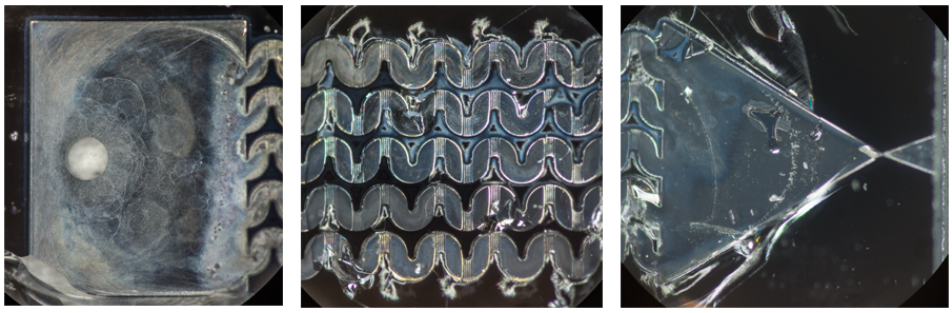

Figure 4.67: Front view of *01-LS1-01* chip after the test

01-BS2-01 Thruster Chip

This chip has been tested at 4 mass flow values (0.5, 1, 1.5, and 2 [mL/h]). The front and back condition of the chip can be seen in Figure 4.68:

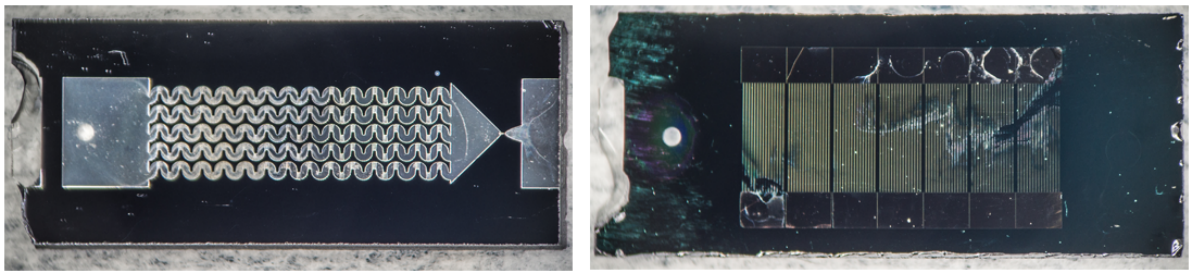

Figure 4.68: Front and back view of *01-BS2-01* chip after the tests

It can be seen that the chip is chipped off on the plenum side. During the testing it is noticed that sometimes small pieced of the chip layers would come off. These small pieces can easily go under the chip and would hinder a proper seal when it the thruster is being tightened inside teh interface. The up-close view of the damage of the heaters and their bridges are shown in Figure 4.69:

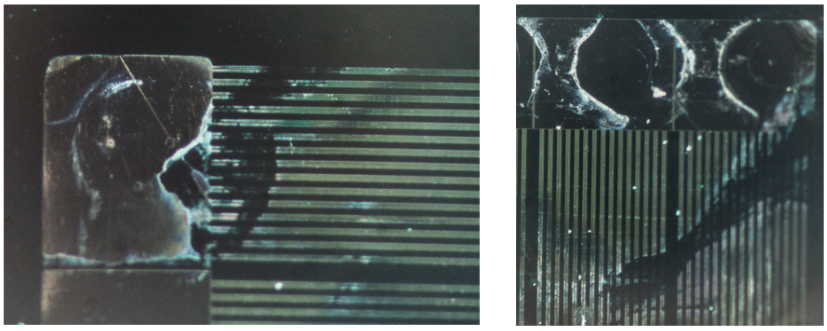

Figure 4.69: Up-close *01-BS2-01* view of the damaged heaters and their bridges

The heat and water damage is very similar to the previous chip. In this case it can be really well seen how the electrical contact of the heater degrades. The up-close view of the contamination of the heaters and nozzle is shown in Figure 4.70:

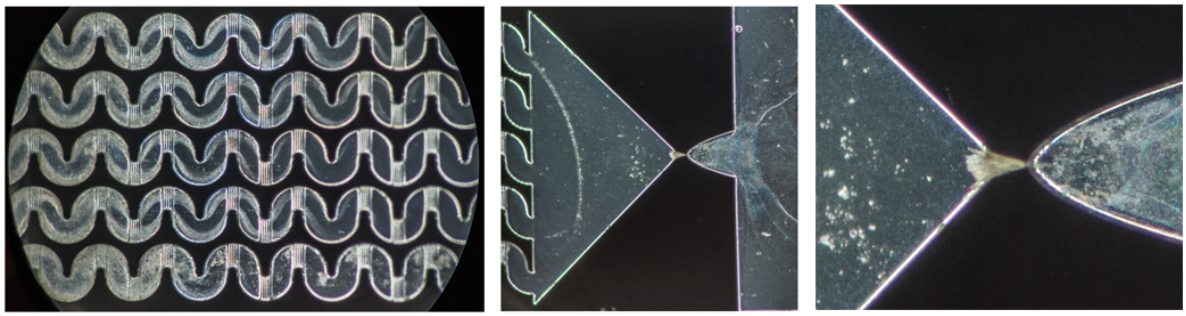

Figure 4.70: Up-close *01-BS2-01* view of the heaters and the nozzle

The contamination is very uneven inside the heater channels. On the left part of Figure 4.70 can be seen that the heater channels are more contaminated on the left side, which is closer to the plenum. This could be due to the vaporization of the water happening closer to the plenum. The most noticeable dirt feature is seen in the throat (ref. Figure 4.70 right part). It almost looks like the nozzle is clogged up with the residue of the particles from the water vapor. This is very well plausible that the performance of the test is affected due to the conditions of the thrusters.

The chip got damaged beyond the workable conditions at 2 [mL/h]. Table 4.22 presents the attempted measurements at 1.5 [mL/h]:

Table 4.22: *01-BS2-01* chip test input and output parameters at 1.5 [mL/h]

Time Stamp	V_i **[V]**	I_i **[A]**	P_i **[W]**	T_0 **[°C]**	P_{pl} **[Pa]**
00:00:00	6.5	0.85	5.53	31.25	$2.86 \cdot 10^5$
00:02:16	6	0.76	4.56	N/A	N/A

Table 4.23 presents data at 1 [mL/h]:

Table 4.23: *01-BS2-01* chip test input and output parameters at 1 [mL/h]

Time Stamp	V_i **[V]**	I_i **[A]**	P_i **[W]**	T_0 **[°C]**	P_{pl} **[Pa]**
00:00:00	6.5	0.55	3.58	27.5	$1.104 \cdot 10^5$
00:04:46	6.7	0.55	3.69	41.34	$1.942 \cdot 10^5$
00:05:37	6.6	0.54	3.56	42.89	$2.454 \cdot 10^5$
00:08:04	6.4	0.51	3.26	46.31	$2.644 \cdot 10^5$
00:11:08	6	0.51	3.06	48.4	$2.537 \cdot 10^5$
00:13:32	5.7	0.46	2.62	48.46	$3.234 \cdot 10^5$

Table 4.24 presents data at 0.5 [mL/h]:

Table 4.24: *01-BS2-01* chip test input and output parameters at 0.5 [mL/h]

Time Stamp	V_i [V]	I_i [A]	P_i [W]	T_0 [°C]	P_{pl} [Pa]
00:00:00	6.5	0.53	3.45	24.5	$1.045 \cdot 10^5$
00:02:34	6.5	0.53	3.45	27.09	$1.193 \cdot 10^5$
00:07:39	6	0.48	2.88	42.54	$2.113 \cdot 10^5$
00:10:29	5.8	0.47	2.73	46.74	$2.381 \cdot 10^5$
00:12:36	5.6	0.45	2.52	47.92	$2.555 \cdot 10^5$
00:14:49	5.4	0.43	2.32	48.32	$2.977 \cdot 10^5$
00:16:46	5.1	0.41	2.09	48.62	$3.791 \cdot 10^5$

Table 4.25 presents data at 2 [mL/h]:

Table 4.25: *01-BS2-01* chip test input and output parameters at 2 [mL/h]

Time Stamp	V_i [V]	I_i [A]	P_i [W]	T_0 [°C]	P_{pl} [Pa]
00:00:00	8	0.62	4.96	35.21	$1.052 \cdot 10^5$
00:01:23	8	0.61	4.88	37.23	$1.108 \cdot 10^5$
00:04:10	7.5	0.58	4.35	47.35	$3.714 \cdot 10^5$
00:07:30	7.4	0.57	4.22	54.7	$4.371 \cdot 10^5$
00:11:28	8	0.6	4.8	55.49	$4.182 \cdot 10^5$
N/A	7.3	0.56	4.09	N/A	N/A

Initially the chip has been tested at 1.5 [mL/h] value, but has failed after already one input power increment. Therefore, no valuable data has been obtained for 1.5 [mL/h]. However, due to the performance similarities between *01-BS2-01* and *01-Ws1-01* chips, a predicted power input value is considered for *01-BS2-01* power-pressure relation. It can be used only as an indicator of what to expect performance wise.

By looking at Table 4.23, the last power increment is when the overflow happened. Thus, the minimum required power can be considered between the last two power inputs: 3.06 and 2.62 [W]. The middle value of the two is taken: 2.8 ± 0.2 [W]. From Table 4.24, the overflow at 0.5 [mL/h] happens at 2.09 [W]. Similarly, the last two power increments are considered, where the minimum power is required just before the overflow. These are 2.32 and 2.09 [W]. The middle value would be 2.2 ± 0.1 [W]. During the 2 [mL/h] run, the heaters were already degraded significantly (see Figure 4.69), thus the last power increment in Table 4.25 is a possible overflow value (assumed by the user from the flow behavior in the chip at 7.4[W] increment). To prevent the total damage of the chip, the voltage has been increased to 8 [V] to prevent the overflow and in order to save the chip for the other mass flow runs. However, the damage on the heaters was already beyond usable condition. Thus, for the 2 [mL/h] mass flow, the minimum power is considered between 4.22 and 4.09 [W]. Taking the average of it, it becomes 4.1 ± 0.1 [W]. A summary of *01-BS2-01* performance results together with theoretical values is shown in Table 4.26:

Table 4.26: Summary of *01-BS2-01* chip results

$\dot{m}$ [mL/h]	P_c (ideal) [Pa]	T_{vap} (ideal) [K]	$\dot{Q}$ (ideal) [W]	P_i [W]	T_0 [K]	P_{pl} [Pa]
0.5	$1.79 \cdot 10^4$	329	0.3	2.2	321	$3.791 \cdot 10^5$
1	$3.67 \cdot 10^4$	346	0.7	2.8	321	$3.234 \cdot 10^5$
1.5	$5.58 \cdot 10^4$	357	1	4.6 (3.4)	N/A	N/A
2	$7.53 \cdot 10^4$	365	1.3	4.1	N/A	N/A

The following Figure 4.71 shows the power and chamber pressure relation at the measured mass flows:

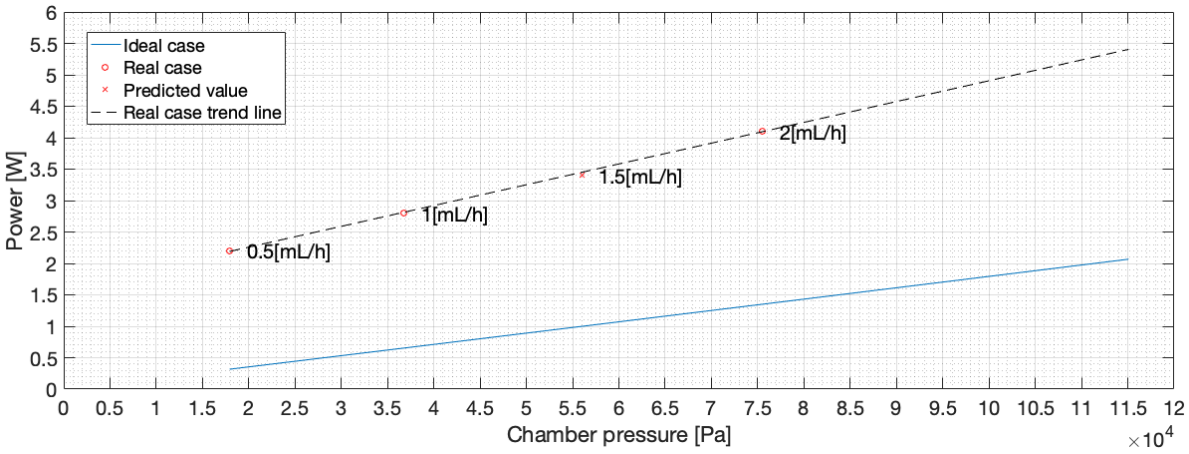

Figure 4.71: *01-BS2-01* power-pressure graph at 0.5, 1, 1.5, and 2 [mL/h]

It can be seen that from the obtained mass flow values the trend line is linear and almost parallel with the ideal case values. Thus, the results can be assumed valid and positive. One has to remember that the obtained power values are obtained at ambient conditions. However, even at such conditions for the mass flows from 0.5 t o 2 [mL/h] the power required is within 4 [W] budget. The lowest required power is between 2-2.5 [W] at 0.5 [mL/h].

01-Ld1-01 Thruster Chip

This chip has been tested at 4 mass flow values (0.5, 1, 1.5, and 2 [mL/h]). The chip got damaged beyond the workable conditions at 2 [mL/h]. Figure 4.72 shows the the chip condition after the testing:

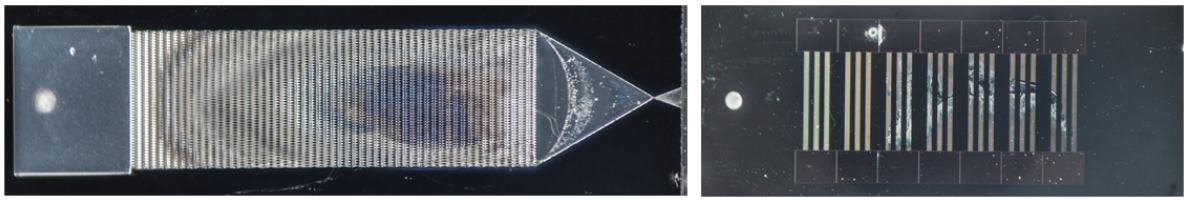

Figure 4.72: Front and back view of the *01-Ld1-01* chip

Figure 4.73 shows the extent of the heaters damage on the back of the chip:

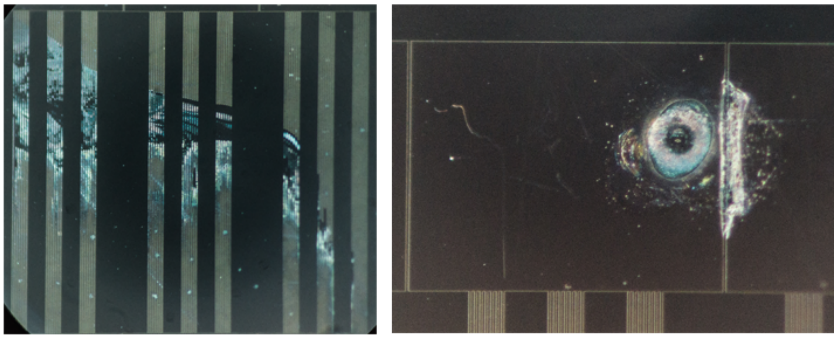

Figure 4.73: Front and back view of the *01-Ld1-01* chip

A very similar damage to the heater bridges as compared to the other chips is observed. On the left of the figure can be seen how the water propagated under the chip. Figure 4.74 shows the up-close view of the condition of the inside of the chip:

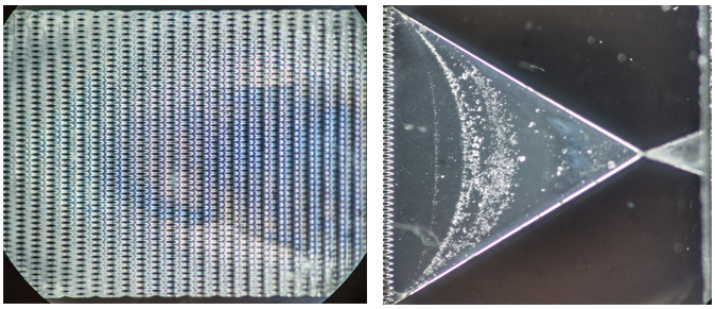

Figure 4.74: Front and back view of the *01-Ld1-01* chip

There is a visible contamination inside the heater channels and the nozzle of the chip. The blue stains between the diamond heaters do not look like residue particles from the water. It is possible that it is some kind of oxidation. The nozzle has a very similar contamination pattern like the rest of the chips. The up-close of the nozzle throat is not shown, because it was difficult to get the photo in focus.

During the 1.5 [mL/h] test, the test was stopped prematurely. It has to do with the fact that the water flow was pumped a bit too early before reaching the right heater temperature. It was also noticed from the images of the microscope camera that there might be some water under the chip. Furthermore, *LabView* code has stopped prematurely as well. Table 4.27 presents data at 1.5 [mL/h]:

Table 4.27: *01-Ld1-01* chip test input and output parameters at 1.5 [mL/h]

Time Stamp	V_i **[V]**	I_i **[A]**	P_i **[W]**	T_0 **[°C]**	P_{pl} **[Pa]**
00:00:00	6.7	0.71	4.76	25.92	$1.039 \cdot 10^5$
00:01:29	6.7	0.71	4.76	26.21	$1.124 \cdot 10^5$
00:03:17	6.4	0.68	4.35	32.77	$1.965 \cdot 10^5$

The last power value was measured at 4.35 [W]. However, by looking at 1 [mL/h] and 2 [mL/h] power values, it is more safe to assume that the minimum required power level at 1.5 [mL/h] could be around 3.8 [W]. It is determined from the linear trend line in Figure 4.75. Therefore, it is considered as a predicted value. Table 4.28 presents data at 1 [mL/h]:

Table 4.28: *01-Ld1-01* chip test input and output parameters at 1 [mL/h]

Time Stamp	V_i [V]	I_i [A]	P_i [W]	T_0 [°C]	P_{pl} [Pa]
00:00:00	6.7	0.71	4.76	26.97	$1.066 \cdot 10^5$
00:01:35	6.7	0.71	4.76	27.38	$1.081 \cdot 10^5$
00:05:04	6.5	0.67	4.36	40.34	$2.268 \cdot 10^5$
00:06:58	6.3	0.65	4.1	45.63	$2.675 \cdot 10^5$
00:09:44	6	0.62	3.72	49.28	$2.99 \cdot 10^5$
00:11:50	5.8	0.6	3.48	50.25	$2.93 \cdot 10^5$
00:14:11	5.8	0.59	3.3	49.94	$2.849 \cdot 10^5$
00:16:44	5.4	0.52	3.08	49.72	$2.61 \cdot 10^5$

The overflow took place at 3.08 [W]. Thus, the minimum required power would be between the last two measured points: 3.3 and 3.08 [W]. The average of the two is 3.2 ± 0.1 [W], which is considered the minimum power input at 1 [mL/h]. Table 4.29 presents data at 0.5 [mL/h]:

Table 4.29: *01-Ld1-01* chip test input and output parameters at 0.5 [mL/h]

Time Stamp	V_i [V]	I_i [A]	P_i [W]	T_0 [°C]	P_{pl} [Pa]
00:00:00	6.7	0.72	4.82	26.61	$1.048 \cdot 10^5$
00:02:06	6.7	0.7	4.69	28.87	$1.338 \cdot 10^5$
00:04:02	6.2	0.64	3.97	37.07	$1.857 \cdot 10^5$
00:05:50	5.7	0.6	3.42	43.34	$1.883 \cdot 10^5$
00:07:27	5.2	0.55	2.86	46.87	$2.049 \cdot 10^5$
00:09:15	5	0.63	2.65	48.84	$2.114 \cdot 10^5$
00:11:43	4.9	0.52	2.55	48.81	$1.921 \cdot 10^5$

For 0.5 [mL/h] the overflow happened at 2.55 [W]. Thus, the minimum required power is taken between 2.65 and 2.55 [W], which would be 2.6 ± 0.1 [W]. Table 4.30 presents data at 2 [mL/h]:

Table 4.30: *01-Ld1-01* chip test input and output parameters at 2 [mL/h]

Time Stamp	V_i [V]	I_i [A]	P_i [W]	T_0 [°C]	P_{pl} [Pa]
00:00:00	8	0.82	5.65	26.89	$1.048 \cdot 10^5$
00:01:23	8	0.8	6.4	27.34	$1.049 \cdot 10^5$

00:04:06	7.6	0.76	5.78	41.95	$6.854 \cdot 10^5$
00:06:00	7.3	0.73	5.33	49.24	$6.513 \cdot 10^5$
00:08:05	7	0.7	4.9	52.97	$6.096 \cdot 10^5$
00:10:01	6.8	0.68	4.62	54.63	$5.295 \cdot 10^5$
00:12:04	6.6	0.67	4.42	55.4	$4.904 \cdot 10^5$
00:14:24	6.5	0.65	4.22	55.37	$4.403 \cdot 10^5$

For 2[mL/h] the minimum required power before the overflow would be between 4.62 and 4.22 [W]. Thus, the average of the two is 4.3±0.1 [W]. After this run, the chip has been significantly damaged. Its internal resistance rose from 9 [Ω] to more than 40 [Ω]. Therefore, no further mass flow values have been tested. A summary of *01-Ld1-01* performance results together with theoretical values is shown in Table 4.31:

Table 4.31: Summary of *01-Ld1-01* chip results

$\dot{m}$ [mL/h]	P_c (ideal) [Pa]	T_{vap} (ideal) [K]	$\dot{Q}$ (ideal) [W]	P_i [W]	T_0 [K]	P_{pl} [Pa]
0.5	$1.79 \cdot 10^4$	329	0.3	2.6±0.1	321	$1.921 \cdot 10^5$
1	$3.67 \cdot 10^4$	346	0.7	3.2±0.1	322	$2.61 \cdot 10^5$
1.5	$5.58 \cdot 10^4$	357	1	4.35 (3.8)	305	$1.965 \cdot 10^5$
2	$7.53 \cdot 10^4$	365	1.3	4.3±1	328	$4.403 \cdot 10^5$

The following Figure 4.75 shows the power and chamber pressure relation at the measured mass flows:

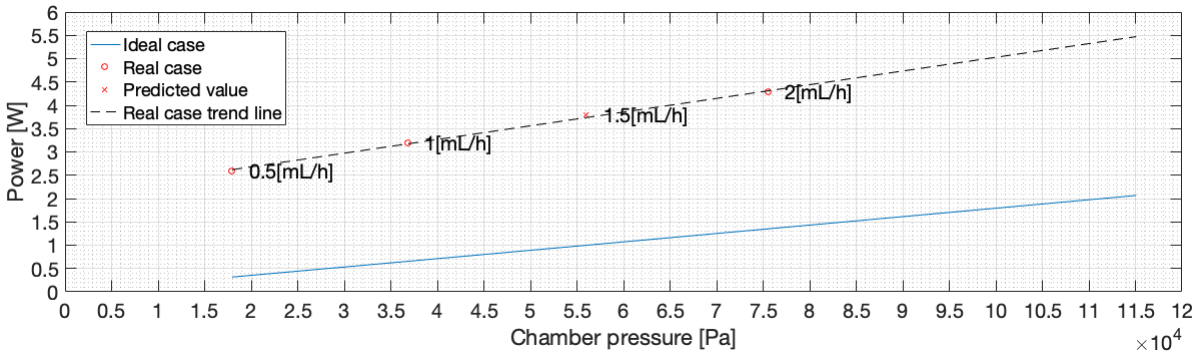

Figure 4.75: *01-Ld1-01* power-pressure graph at 0.5, 1, 1.5, and 2 [mL/h]

From the trend line obtained in Figure 4.75 can be seen that the power pressure relation is linear. For the tested 4 mass flow values, the required power is almost within the budget of 4 [W] even at the ambient conditions. Th real case trend line is almost parallel to the ideal case. Therefore, the test results can be considered valid. These results can be easily compared to *01-BS2-01* chip results, because they show a very similar behavior and trend.

01-Ws1-01 Thruster Chip

This chip has been tested at 3 mass flow values (0.5, 1, and 1.5 [mL/h]). The front and back view of the chip after the tests is shown in Figure 4.76:

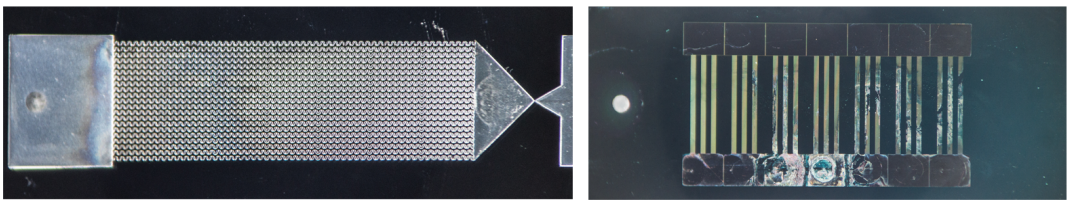

Figure 4.76: Front and back view of the *01-Ws1-01* chip

The damaged heaters on the back of the chip are shown in Figure 4.77

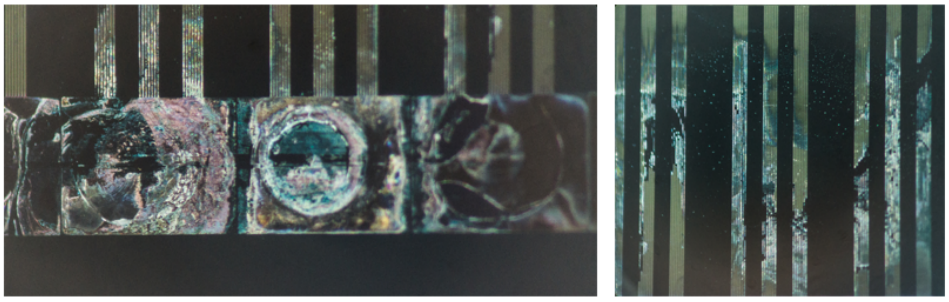

Figure 4.77: Back view of the *01-Ws1-01* chip heaters

The damage on the heater electrical pads is very similar to the one on *01-Ls2-01* chip. However, it is noticed from comparing such a damaged between all of the chips, there is no consistent damage pattern. It seems that some of the chips are more robust than the other ones. This could be due to the manufacturing inaccuracies. The only visible contamination is seen in the nozzle part of the chip as shown in Figure 4.78:

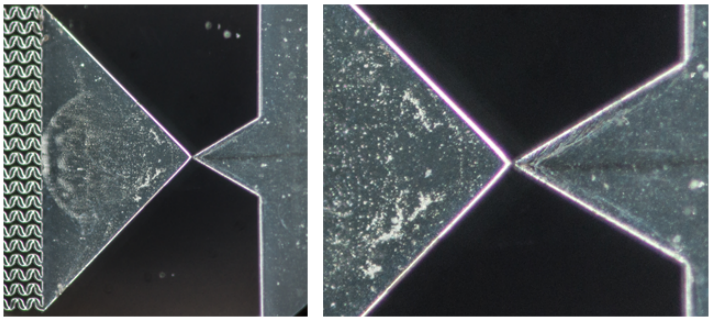

Figure 4.78: Close-up view of the *01-Ws1-01* chip nozzle

The contamination is visible, but very minimal. It can be seen that for this nozzle there is no obvious clogging up in the throat, since it can be clearly seen how the convergent part os is transitioning to the divergent part of the nozzle. Table 4.32 presents data at 1.5 [mL/h]:

Table 4.32: *01-Ws1-01* chip test input and output parameters at 1.5 [mL/h]

Time Stamp	V_i [V]	I_i [A]	P_i [W]	T_0 [°C]	P_{pl} [Pa]
00:00:00	7.5	0.61	4.58	28.35	$1.048 \cdot 10^5$
00:00:52	7.5	0.6	4.5	31.13	$1.048 \cdot 10^5$
00:04:12	7.2	0.57	4.1	40.39	$1.801 \cdot 10^5$
00:05:47	6.9	0.55	3.8	43.4	$1.851 \cdot 10^5$
00:07:24	6.7	0.54	3.62	44.89	$1.827 \cdot 10^5$
00:09:28	6.5	0.53	3.45	45.86	$1.728 \cdot 10^5$
00:11:29	6.4	0.52	3.33	45.95	$1.739 \cdot 10^5$

From Table 4.32 the minimum cut-off power is consider between the last two measured values: 3.45 and 3.33 [W]. The average of the would be 3.4 ± 0.1 [W]. Table 4.33 presents data at 1 [mL/h]:

Table 4.33: *01-Ws1-01* chip test input and output parameters at 1 [mL/h]

Time Stamp	V_i [V]	I_i [A]	P_i [W]	T_0 [°C]	P_{pl} [Pa]
00:00:00	7	0.57	3.99	27.27	$1.066 \cdot 10^5$
00:02:01	7	0.55	3.85	28.71	$1.047 \cdot 10^5$
00:05:43	6.7	0.52	3.48	39.27	$1.507 \cdot 10^5$
00:06:56	6.4	0.5	3.2	41.43	$1.49 \cdot 10^5$
00:10:23	6.2	0.48	2.98	44.13	$1.347 \cdot 10^5$
00:12:03	6	0.47	2.82	N/A	N/A
00:14:27	5.9	0.46	2.71	N/A	N/A
00:15:54	5.8	0.45	2.61	N/A	N/A

For 1 [mL/h] mass flow the overflow happened at 2.61 [W]. Again taking the last two input power values (2.71 and 2.61 [W]), the minimum required power would be 2.6 ± 0.1 [W]). Table 4.34 presents data at 0.5 [mL/h]:

Table 4.34: *01-Ws1-01* chip test input and output parameters at 0.5 [mL/h]

Time Stamp	V_i [V]	I_i [A]	P_i [W]	T_0 [°C]	P_{pl} [Pa]
00:00:00	6.7	0.52	3.48	25.29	$1.047 \cdot 10^5$
00:02:26	6.7	0.52	3.48	28.05	$1.046 \cdot 10^5$
00:08:23	6.2	0.47	2.91	43.8	$1.179 \cdot 10^5$
00:09:56	5.9	0.46	2.71	45.53	$1.174 \cdot 10^5$
00:10:57	5.6	0.43	2.41	46.47	$1.198 \cdot 10^5$

00:14:10	5.3	0.41	2.17	46.81	$1.12 \cdot 10^5$

For 0.5 [mL/h] mass flow the minimum required power is 2.3±0.1 [W]. A summary of *01-Ws1-01* performance results together with theoretical values is shown in Table 4.35:

Table 4.35: Summary of *01-Ws1-01* chip results

$\dot{m}$ [mL/h]	P_c (ideal) [Pa]	T_{vap} (ideal) [K]	$\dot{Q}$ (ideal) [W]	P_i [W]	T_0 [K]	P_{pl} [Pa]
0.5	$1.79 \cdot 10^4$	329	0.3	2.3±0.1	319	$1.12 \cdot 10^5$
1	$3.67 \cdot 10^4$	346	0.7	2.6±0.1	N/A	N/A
1.5	$5.58 \cdot 10^4$	357	1	3.4±0.1	319	$1.739 \cdot 10^5$

The following Figure 4.79 shows the power and chamber pressure relation at the measured mass flows:

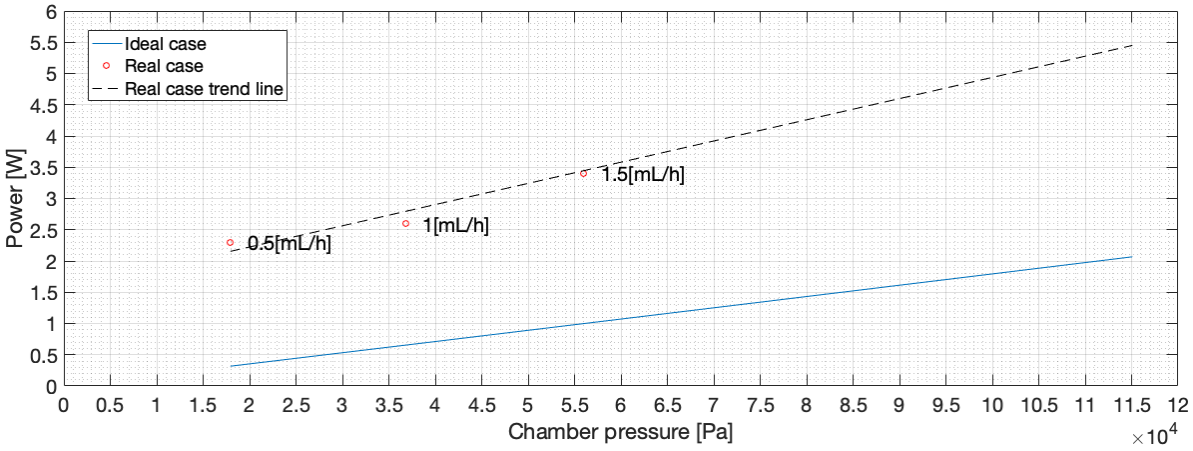

Figure 4.79: *01-Ws1-01* power-pressure graph at 0.5, 1, and 1.5 [mL/h]

This chip has performed very well at the given mass flow values for its condition. The real case trend line is very similar to the ideal case values. The power values obtained from the test fall within the maximum 4 [W] budget. The minimum required power is obtained at 0.5 [mL/h], which is between 2 - 2.5 [W].

01-WS1-01 Thruster Chip

This chip has a blocked nozzle. The front and back view of the chip can be seen in Figure 4.80. The blocked nozzle and partial contamination of the heaters is shown in Figure 4.81.

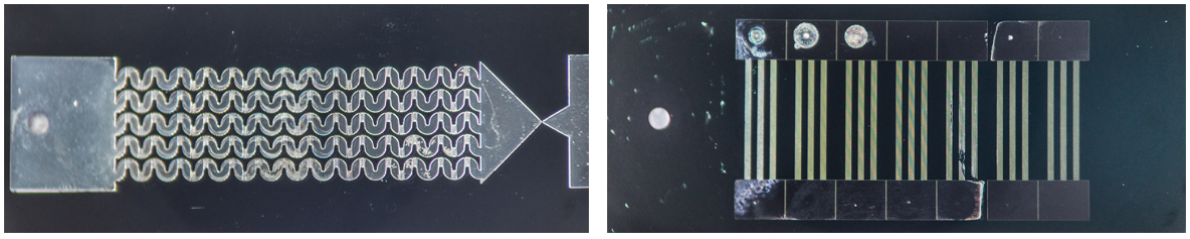

Figure 4.80: Front and back view of the *01-WS1-01* chip

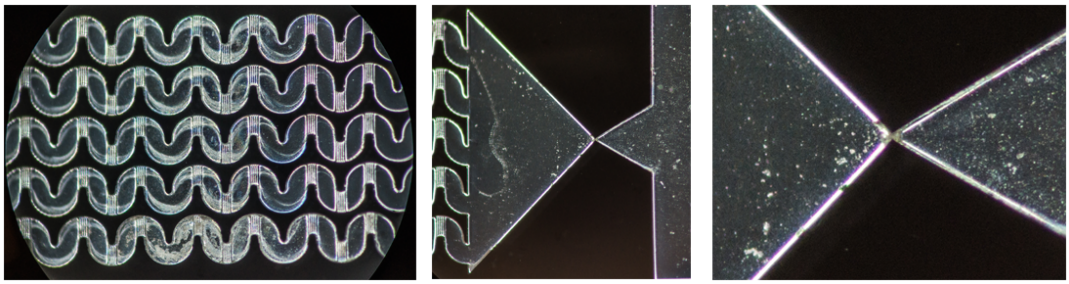

Figure 4.81: Close-up view of the *01-WS1-01* chip contaminated heaters (l), nozzle (m), and blocked throat (r)

The blockage can be seen on the right part of Figure 4.81. Most likely the blockage is due to the water vapour residue, because it can be clearly seen from the figure that there is some brown distinct mass accumulated in the throat. The cause of such a blockage could be due to the manufacturing errors during the depositing of the layers as described by *Silva* [2].

01-WS2-01 Thruster Chip

This chip has been tested for 3 mass flow values (0.5, 1, and 1.5 [mL/h]). The front and back of the chip is shown in Figure 4.82:

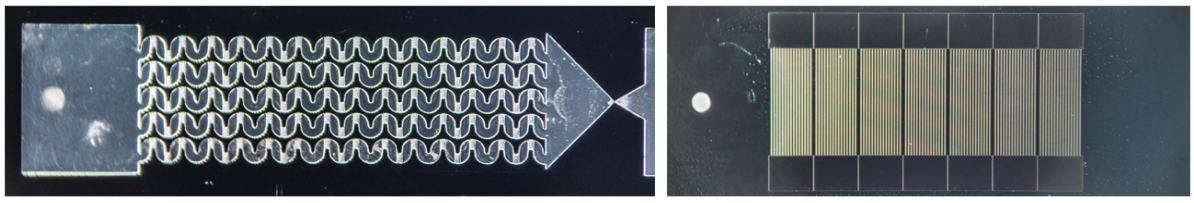

Figure 4.82: Front and back view of the *01-WS2-01* chip

Figure 4.83 is a good example of the intact heaters and heater bridges. However, this chip was very unpredictable and unstable during the testing. A plausible reason for that could be a partially blocked nozzle or due to the contamination of the heater channels.

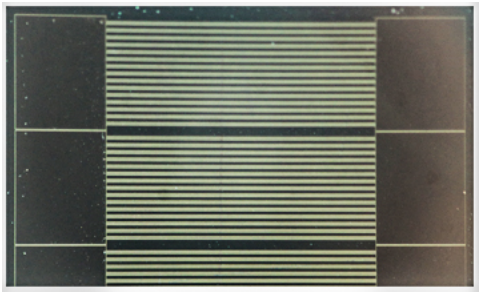

Figure 4.83: Close-up view of the *01-WS2-01* chip heaters

The contaminated nozzle and heaters are shown in the up-close photo in Figure 4.84:

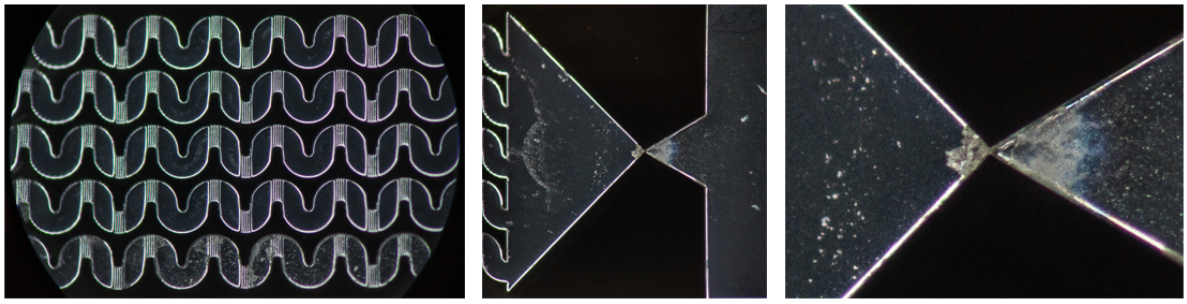

Figure 4.84: Close-up front view of the *01-WS2-01* chip. The contaminated heaters (bottom heater) and the nozzle throat

There is very minimal dirt inside the heater channels. However, the nozzle shows a distinct accumulation of some sort of dirt. Table 4.36 presents data at 1.5 [mL/h]:

Table 4.36: *01-WS2-01* chip test input and output parameters at 1.5 [mL/h]

Time Stamp	V_i **[V]**	I_i **[A]**	P_i **[W]**	T_0 **[°C]**	P_{pl} **[Pa]**
00:00:00	6.5	0.95	6.18	25	$1.054 \cdot 10^5$
00:01:08	6.5	0.93	6.05	25.39	$1.054 \cdot 10^5$
00:03:59	6	0.84	5.04	39.51	$1.566 \cdot 10^5$
00:05:45	5.5	0.77	4.24	47.28	$2.904 \cdot 10^5$

The minimum required power is between 5.04 and 4.24 [W] for 1.5 [mL/h]. The average of the two is taken as the cut-off power, which is 4.64 ± 0.4 [W]. Table 4.37 presents data at 1 [mL/h]:

Table 4.37: *01-WS2-01* chip test input and output parameters at 1 [mL/h]

Time Stamp	V_i **[V]**	I_i **[A]**	P_i **[W]**	T_0 **[°C]**	P_{pl} **[Pa]**
00:00:00	6	0.87	5.22	31.11	$1.058 \cdot 10^5$
00:00:55	6	0.85	5.1	31.17	$1.068 \cdot 10^5$

00:03:43	5.7	0.8	4.56	40.56	$1.901 \cdot 10^5$
00:06:13	5.5	0.78	4.29	50.58	$4.569 \cdot 10^5$

The minimum required power for 1 [mL/h] is between 4.29 and 4.56 [W], which gives 4.43 ± 0.2 [W]. Table 4.38 presents data at 0.5 [mL/h]:

Table 4.38: *01-WS2-01* chip test input and output parameters at 0.5 [mL/h]

Time Stamp	V_i **[V]**	I_i **[A]**	P_i **[W]**	T_0 **[°C]**	P_{pl} **[Pa]**
00:00:00	5.8	0.85	4.93	28.76	$1.152 \cdot 10^5$
00:00:43	5.8	0.84	4.87	31.95	$1.099 \cdot 10^5$
00:02:42	5.6	0.79	4.42	38.8	$1.245 \cdot 10^5$
00:08:16	5.6	0.78	4.37	56.28	$3.633 \cdot 10^5$
00:13:02	5.5	0.77	4.24	63.3	$6.53 \cdot 10^5$
00:14:36	5.4	0.76	4.1	63.76	$6.516 \cdot 10^5$
00:15:53	5.2	0.73	3.8	64.38	$6.111 \cdot 10^5$
00:17:51	5.1	0.72	3.62	63.65	$5.185 \cdot 10^5$
00:19:23	5	0.71	3.55	63.1	$4.779 \cdot 10^5$
00:21:06	4.9	0.69	3.38	62.09	$4.288 \cdot 10^5$
00:23:07	4.8	0.68	3.26	61.26	$4.05 \cdot 10^5$
00:25:10	4.7	0.66	3.1	59.18	$4.928 \cdot 10^5$
00:27:10	4.5	0.64	2.88	58.28	$7.7 \cdot 10^5$

For 0.5 [mL/h] mass flow there was no actual overflow observed. The test was stopped after it was noticed that the plenum pressure is unstable and big. The lowest power achieved is 2.88 [W], which can be taken as a predicted overflow value. An attempt was made to measure at 2 [mL/h], but the test was stopped immediately after one power increment, because the chip was overflown and it was decided to save it for the thrust bench test. A summary of *01-WS2-01* performance results together with theoretical values is shown in Table 4.39:

Table 4.39: Summary of *01-WS2-01* chip results

$\dot{m}$ **[mL/h]**	P_c **(ideal) [Pa]**	T_{vap} **(ideal) [K]**	$\dot{Q}$ **(ideal) [W]**	P_i **[W]**	T_0 **[K]**	P_{pl} **[Pa]**
0.5	$1.79 \cdot 10^4$	329	0.3	(2.88)	331	$7.7 \cdot 10^5$
1	$3.67 \cdot 10^4$	346	0.7	4.43 ± 0.2	323	$4.569 \cdot 10^5$
1.5	$5.58 \cdot 10^4$	357	1	4.64 ± 0.4	320	$2.904 \cdot 10^5$

The following Figure 4.85 shows the power and chamber pressure relation at the measured mass flows:

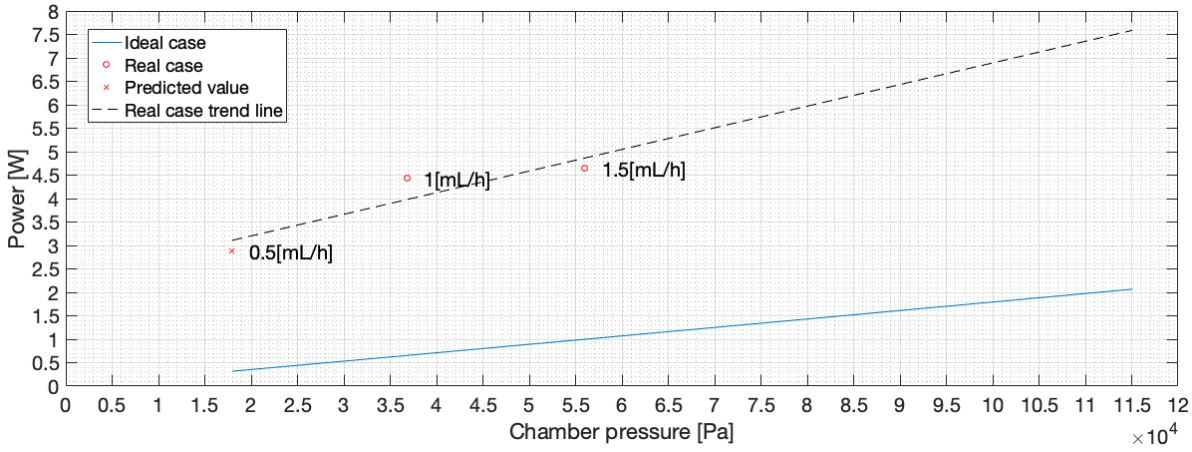

Figure 4.85: *01-WS2-01* power-pressure graph at 0.5, 1, and 1.5 [mL/h]

It can be seen that the required power is above 4 [W] limit. The trend line does not deviate that much from the ideal values and it is linear. Although, the results of this chip can be partially valid, since only two mass flows have valid overflow conditions. Moreover, the instability of the chip most likely affect the obtained results. It would definitely require re-testing of the chip at its brand new condition.

4.5.4. Heater Efficiency

The heater efficiency of the chip is the other important aspect of the this test. Heater efficiency can be found by dividing the ideal power ($\dot{Q}$) over the actual power P. For each of the mass flow value a heater efficiency is determined. The following Table 4.40 shows the heater efficiencies of all tested chips:

Table 4.40: Summary of heater efficiencies of all chips at various mass flows

	Heater Efficiency [-]					
	0.5 [mL/h]	1 [mL/h]	1.5 [mL/h]	2 [mL/h]	2.5 [mL/h]	3 [mL/h]
01-BS2-01	0.14	0.23	(0.29)	0.33	(0.36)	(0.38)
01-Ld1-01	0.12	0.2	(0.26)	0.31	(0.35)	(0.37)
01-Ws1-01	0.14	0.23	0.3	(0.34)	(0.38)	(0.41)
01-WS2-01	(0.1)	0.16	0.2	(0.23)	(0.25)	(0.27)

The values in the brackets are either the missing test data (2.5 and 3 [mL/h] values which have not been tested) or a predicted overflow power value at the tested mass flow (these correspond to the power/pressure graph values for each chip). The heater efficiency varies between 0.12 to 0.33 [-] for the tested mass flow values. It can be clearly seen that none of the chips reach 0.6 [-] efficiency as suggested by *Turmaine* [3]. There could be two explanations. One could be due to the damaged heaters as explained in Section 4.5.3. The other explanation is that the mass flow is not high enough. It means that the heating power is wasted at evaporating the water too close to the plenum and not at the optimal area around the nozzle as it was explained previously. However, the brand new batch of the same chips should be tested first.

Due to the conditions at which this batch of chips was, the heater efficiency is insufficient for an optimal thruster performance, at this moment.

Consequently this affects the maximum power used by the heaters. From the data can be seen that up to around 5.5 [W] of power is required. Thus, 4 [W] budget is overshot. Furthermore, for FOE values in Table 3.26, the required power is twice of what was expected in theory.

4.5.5. Thruster Comparison

After analyzing all the chips and their test data, a preliminary comparison of the thrusters can be done. Thrusters which managed to be tested for at least 2 mass flows, according to *SC-TC04-09* success criteria, and have achieved an actual overflow are considered. The chips, which are considered, are *01-BS2-10*, *01-Ld1-01*, *01-Ws1-01*, and *01-WS2-01*. Figure 4.86 presents the trend lines obtained for all the chips at real power input values:

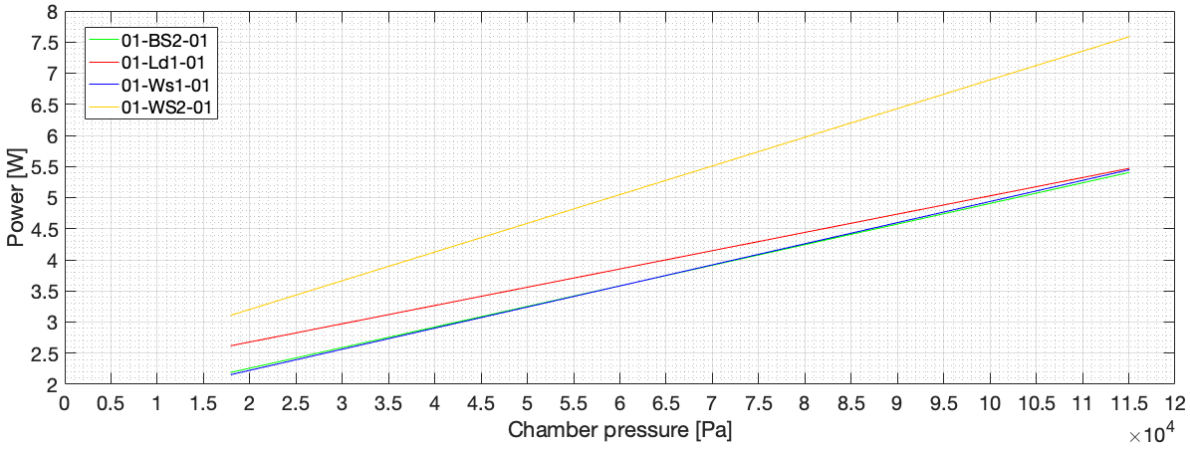

Figure 4.86: Comparison of the thruster chip power-pressure trend lines

It can be seen that *01-BS2-01* and *01-Ws1-01* chips have a very similar trend line, which means they correspond close to the same power-pressure values. Looking at the maximum allowable 4 [W] power, both of the chips reach around $7.5 \cdot 10^4$ [Pa] chamber pressure. These similarities can be related to the fact that both of the thrusters have the same large serpentine heater configuration with 30 lines of heaters. Although, *01-BS2-01* chip has a bell shape nozzle and *01-Ws1-01* has a wide nozzle, it seems that there is not much of a difference if compared to the power-pressure values. Nonetheless, the attention should be paid to the condition of the heaters and the inside of the chip itself. As it can be seen from Figure 4.78 and 4.70, the nozzles and the heater channels are not in the ideal conditions. Therefore, it would be good to test the same chips in their brand new conditions and compare the values with the preliminary tests.

By looking at *01-Ld1-01* chip trend line, there is a small difference in the maximum allowable power and chamber pressure compared to the two latter chips. 4 [W] limit is achieved at around $6.5 \cdot 10^4$ [Pa] chamber pressure. It means that a small diamond heater configuration requires a small chamber pressure, which in terms requires a small mass flow value. However, the same contamination and condition aspects should be taken into account for this chip. Figure 4.74 shows that there is some degradation/contamination of the heater channels in the middle of the chip, where there is some sediment at the nozzle area. Thus, it is a good idea to retest the brand new *01-Ld1-01* at the same values to see how much the difference is between the

new and old chip.

It seems that *01-WS2-01* chip requires the smallest chamber pressure of around $3.5 \cdot 10^4$ [Pa] to achieve the maximum allowable power of 4 [W]. it can be seen that this chip can not be related to the rest of the 3 chips in any way. Although, there are 4 design aspects which can be compared with *01-BS2-01* and *01-Ws1-01* chips. Those are the shape of the nozzle shape, number of heaters, size of the heaters, and the shape of the heaters. All 3 chips share the same serpentine shape of the heaters. However, *01-BS2-01* and *01-WS2-01* share the same size and number of the serpentine heaters. Moreover, *01-WS2-01* and *01-Ws1-01* share the same wide nozzle shape. Nevertheless, *01-WS2-01* performs completely differently than *01-BS2-01* and *01-Ws1-01*, which have almost the same performance. Therefore, it would be interesting to see how much the power-pressure values would differ if a brand new *01-WS2-01* is tested and compared to its old values and the other two chips. By looking at Figure 4.84, the inside of the chip is also contaminated in the channels and the nozzle area.

4.5.6. Thrust Bench Test

After the preliminary power-pressure tests, the secondary goal was to test the chips on the thrust bench. After inspecting all the chips after the preliminary power-pressure tests, chip *01-Ws1-01* was still in a good condition and performed reasonably well. To follow the same test chronological order, the thrust bench test was performed at 1.5 [mL/h] mass flow first. However, for a second attempt at 1 [mL/h] it was not possible, because the heaters have been damaged beyond the operational conditions.

The only way to observe the water overflow in the chip is to use the microscope camera pointing towards the exit of the chip interface. However, it is already known from Table 4.32 at what power level to expect the overflow. Therefore, the camera is good indicator whether the expected power values are reached. Table 4.41 presents thrust bench test data at 1.5 [mL/h]:

Table 4.41: *01-Ws1-01* chip test input and output parameters at 1.5 [mL/h] during the thrust bench test

Time Stamp	V_i [V]	I_i [A]	P_i [W]	T_0 [°C]	P_{pl} [Pa]	Δ_{displ} [μm]
00:00:00	9.5	0.45	4.28	29.8	$1.059 \cdot 10^5$	1984.7
00:03:37	9.5	0.45	4.28	38.11	$1.065 \cdot 10^5$	1982
00:06:00	9.2	0.44	4.05	47.13	$1.301 \cdot 10^5$	1977
00:07:30	8.8	0.42	3.7	51.1	$1.658 \cdot 10^5$	1974
00:09:30	8.5	0.4	3.4	53.15	$1.674 \cdot 10^5$	1967

Figure 4.87 shows the relation between each power increment and the pendulum displacement:

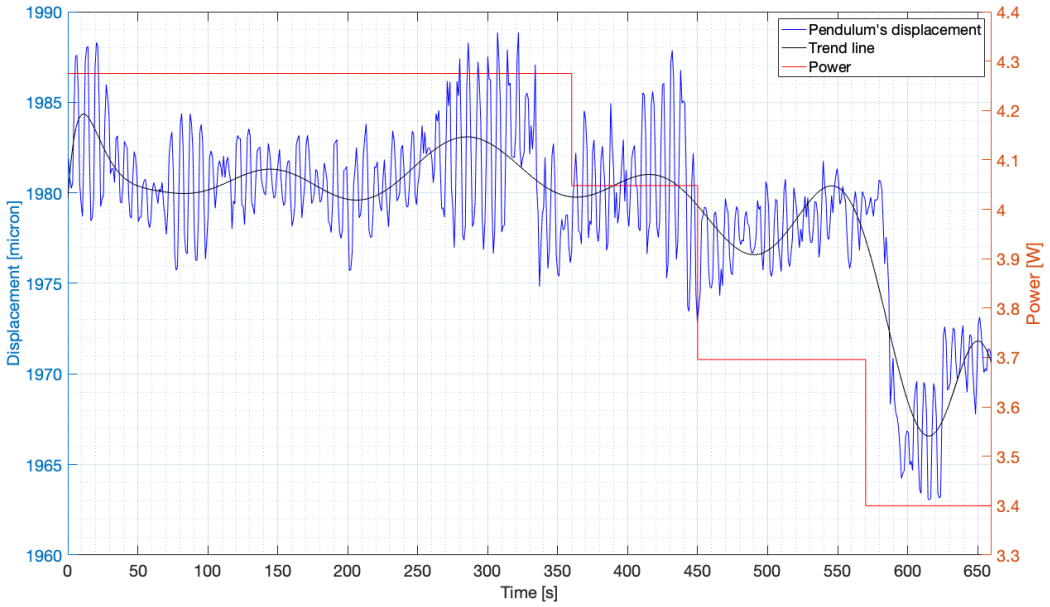

Figure 4.87: Power versus the displacement of the pendulum using *01-Ws1-01 chip* at 1.5[mL/h]

The thrust bench test is considered to be successful, because the pendulum displacement and the thruster overflow has been reached at the expected power values. To validate the results, the snapshots from the microscope video footage are shown in Figure 4.88:

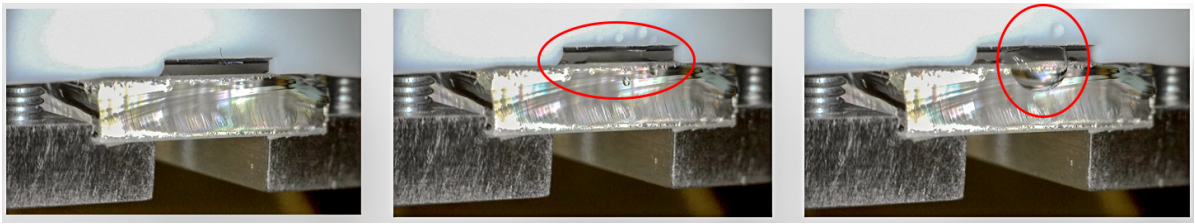

Figure 4.88: Snapshots of *01-Ws1-01 chip* video footage. Initial state of the thruster (l) at 0 [s], water spitting/struggling thruster at around 550 - 580 [s] (m), and and the overflow reached at around 600 - 600 [s] (r)

4.5.7. Design and Requirements Verification

From all the 7 chosen VLM thruster chips, 4 have provided useful performance information. The chips are *01-BS2-01*, *01-Ld1-01*, *01-Ws1-01*, and *01-WS2-01*. The power-pressure tests are considered as the preliminary tests and were performed at ambient conditions. The chips performed the best at lower end of mass flow range (0.5 - 1.5 [mL/h]) as it can be seen from the power-pressure graphs.

By comparing the heater efficiency value of 0.6 assumed by *Turmaine* [3], the current efficiency values range from 0.12 at the lowest pressure to 0.33 at higher chamber pressures for the measured mass flows. That is around 2 to 5 times less, than what is expected. It is expected from the data trend-lines that the efficiency can go up to max. 0.41 [-]. There can be

two explanations for such a low efficiency. One is the condition in which the chips were before the testing. There was some contamination inside the heater channels and the nozzles. Furthermore, some of the heater bridges and pads were damaged from a previous testing. The true nominal performance could not be achieved during this test. The second explanation could be that a lot of power is wasted at vaporizing the water at the plenum instead of area close to the nozzle. Thus, higher mass flow values could move the vaporization location and, consequently, increase the heater efficiency. Although, the maximum power used to vaporize the water should be taken into account. It was shown that overshot of max. allowable 4 [W] is possible.

The biggest issue observed during the test is the corrosion of the heaters during the operations. The corrosion happens due to the heat and water interaction on the molybdenum heaters. This happens due to the quick overflow of the chip and the creeping water under the chip which is hot at the moment. It is noticed that the overflow happens within 1-2 seconds and there is not enough time to cool down the chip to avoid the damage of the heaters. One temporary solution was to attach a piece of napkin with a tape. In such a way the outgoing water could be absorbed by the napkin and theoretically no water would go under the chip. However, it is not a robust solution. Therefore, it requires an optimized design of the thruster interface. Either a leak seal should be added at the location of the nozzle exit between the chip and the interface or channels should be made that the excess of the water can be directed away from the heaters.

It can be seen that *01-BS2-01* and *01-Ws1-01* chips have the closest trend line to the ideal power-pressure line. It could possibly be due to the serpentine shape of the heaters. This suggests that serpentine shape heaters perform the better than the diamond shape ones.

01-BS2-01, *01-Ld1-01*, and *01-Ws1-01* show a similar performance behavior at low mass flow values. For values between 0.5 and 1.5 [mL/h], the maximum power requirement of 4 [W] is met. it is possible that at higher mass flow ranges if the thruster is tested at vacuum conditions the power requirement can also be met. However, it is important to remember that obtained power levels during the test represent the minimum required power to not overflow th chips. Therefore, in the future similar tests it is recommended to increase the input power to around 0.1 - 0.2 [W], which in turn means to increase T_c above T_{vap}.

For this test the ideal case of the mass flow and chamber pressure relation has been used. Thus, in the future this assumption needs to be checked at the actual vacuum conditions. Furthermore, in this case a constant mass flow is used for the testing, where in the actual case the system would be closed and have a blow-down condition. Thus, the power-pressure curve would be different, but it would give a good indication on how much the values differ between the preliminary and actual values for each chip.

At this moment, the requirements *PROP-FUN-100* and *PROP-SYST-300* can be verified conditionally with respect to the reasons provided above.

5

Conclusions & Recommendations

In this chapter the conclusions and recommendations based on this thesis are presented. The chapter is split into two sections: conclusions, and recommendations. The conclusions section presents mainly the performed tests and their results. It follows the same chronological order how the experiments have been conducted. Furthermore, the research questions and objectives are described. The recommendations section presents all the observed issues of the PPD design and suggests solutions or give advice on how to improve the design and help to further verify it.

5.1. Conclusions

The following main research objective has been determined for this thesis:

To verify the detailed design and the propulsion subsystem requirements of the LPM and VLM Propulsion Payload Demonstrator for the Delfi-PQ satellite mission using testing and analysis as the verification methods

From which followed the main research question:

What is the outcome of the Propulsion Payload Demonstrator detailed design verification by means of testing and analysis?

A test campaign has been designed and used as a basis in order to reach the research objective and answer the research question. From a total of 11 planned tests, only 4 have been conducted. This suggests how some of the experiments are complex and require a very methodological approach to achieve them. Because of a unique design of PPD and the available testing facilities at Aerospace Engineering faculty, each test set-up required a lot of time and resources to prepare them and execute them by a single person.

The first performed test was *TEST-INT-01: Leak Test*. The main purpose of this test is locate any leaks in the whole propulsion system and determine a leak rate. There were in total 12 leak test performed at various set-ups. The tank pressures range from 5 [bar] to 1.1 [bar]. Each test's duration was either 24 [h] or 48 [h]. From the obtained results it was deduced that there is somewhere in the system a leak. For example, at FOE tank pressure of 1.1 [bar] at ambient conditions the pressure drop is 248.8 [mbar] per 24 [h]. At vacuum conditions with the same set-up, the pressure change is 689.3 [mbar] per 24 [h]. it suggests that the tank would be empty within 48 [h]. By calculating the mass leak rate, the following values are obtained

for these conditions Q_M = 1.53·10^{-12} [mg/s] (at ambient), and Q_M = 4.55·10^{-12} (at vacuum). As these values are not acceptable for the success of *Delfi-PQ* mission, a suggested pressure drop per 24 [h] was determined based on the idling time of the satellite until it is operational in space. Two scenarios were considered: 12 months idling and 1 month idling (these values are based on the industry experience). For the 12 month idle a maximum pressure drop per 24 [h] should be 0.2 [mbar]. For the 1 month idle a maximum pressure drop per 24 [h] should be 3 [mbar]. Additionally, to determining the leakage rates, a leak localization has been also performed. Various leak detection and localization methods have been investigated. From the available resources at TU Delft, some of them have been implemented. However, the leak has not been localized with any means used. Therefore, it was decided to understand the physics behind the leak and try to determine its size. A first order leak simulation has been performed. It suggests that the leak hole/slit size might be of 0.00146 - 0.00255 [mm]. Additionally, by comparing the leak data and the simulation model data, the leakage most likely is of a supersonic nature. It could explain the leak rate velocity observed in the test data. However, since the slit is so small the leak is almost invisible for any detection tools or methods applied beforehand. It is also thought that the leaked out gas is stuck in some crevices of the propulsion components and do not get exposed to the ambient. An additional leak result/observation has been obtained during *TEST-COM-01*. For this test the new tubes with the correct inner diameter (1.57 [mm] instead of 0.81 [mm]) were used. It is possible due to thinner wall of the new tubes, a better seal has been achieved, because no significant leak has been observed at that time. The propulsion requirements related to this test have been verified and discussed in Section 4.2.4.

The second test was *TEST-INT-01: Volume and Mass Test*. First, a preliminary volume test based on the outcome of the detailed design created by *Turmaine* [3] was performed. It showed that with the components suggested by the author, it is not possible to fit the whole propulsion system in 42x42x30 [mm]. An actual volume test has been performed. In this test the missing propulsion system components have been added in CAD model. It suggested that theoretically all the latest version design components do fit in the described volume. Although, the suggested solenoid valve support structure is omitted due to the changed position of the solenoid valves. Furthermore, the initial concept of the propulsion system cage proved to be incomplete and does not meet the safety requirements. The whole purpose of the cage is to create a perfect seal inside the satellite to avoid any propellant contamination on the other spacecraft sub-systems. A systems engineering approach has been applied to create an updated cage. The cage has been actually 3D printed and integrated with the whole propulsion sub-system and mock-up of *Delfi-PQ*. It is observed that a good seal can be achieved and the cage increases marginally the available space for the propulsion components to 46x44.5x30 [mm]. Then a mass test has been performed to check if the mass budget defined by the requirements is not exceeded. All of the used components in the propulsion system have been weighed and compared to the theoretical values. Each component was assigned either to *Structural*, *Electrical*, or *Propulsion* type of mass budgets. The split of the budgets provides useful information on designing *PocketQube* missions for other researchers and designers around the world. At the moment *Delfi-PQ* mass budget is within the required maximum limit. The total mass with 10% contingency is 43.85 [g] out of maximum allowed 75 [g]. It seems it is a positive outcome, but one needs to keep in mind that the propulsion system is still not complete. It means it leaves almost 30 [g] to spare for the rest of the additional components. The requirements related to this test are discussed in Section 4.3.4.

The third test was *TEST-COM-01: Solenoid Valve PWM Test*. It consists of a number of tests which check certain aspects of the solenoid valve. First, the ability to achieve a FOE 0.2

[bar] tank pressure has been performed. It was considered as a check test. It provided useful information about the leakage of the system when the new tubes have been used (see the conclusions of TEST-INT-01). The second test was to check the capabilities of the solenoid valve during the sweep of operational frequencies. The results showed that the solenoid valve and the connected feed tubes can heat up significantly at high pulse frequencies. It was observed that the tube at the outlet of the vale heats up significantly up to 83.3 [^{o}C], which in terms affect the temperature of the outgoing gas to LPM plenum and the plenum pressure itself. A similar effect is observed during the sweep of DC at various fixed PWM frequencies. These heating effects should be taken into the account when a precise plenum target pressure and temperature is required. Furthermore, the warming up of the valve adds up to the thermal control of the satellite, which might be an issue if certain temperature is reached within the propulsion subsystem. Later on the pressure stability at the plenum at various PWM frequencies has been tested. The results showed that in order to achieve 50 -300 [Pa] plenum pressure, a 1 [bar] tank pressure of nitrogen gas is required as well as a longer tube. To reach 50 [Pa] target, the 250 [Hz] is the most optimal frequency. To reach 150 [Pa] target the 500 [Hz] is the most optimal frequency. To reach 300 [Pa] target, the most optimal frequency is 50 [Hz]. Thus, there is obviously no clear trend in this case. However, 250 [Hz] has the most promising performance of them all and is in line with the conclusions from *Silvestrini* [29]. However, during the plenum pressure stability test at FOE values in a closed system, the target pressure was not achieved and the tank was empty within 0.5 [s]. The last check has been performed on the valve coil temperature and the required power. It provides a linear relation in terms of the coil resistance versus coil temperature. Thus, for future tests this trend can be used as an indicator. The discussion of the requirements related to this test is provided in Section 4.4.7.

The final test was *TEST-COM-04: Heater Efficiency Test*. The test was performed to obtain the preliminary required power values to vaporize the water inside VLM chamber. In total 7 chips have been tested, out of which 4 were known to be operational. The obtained power values have been compared to the ideal power values. In order to preserve the chips, the minimum vaporization temperature method has been chosen to obtain the power-pressure relation. This method also helps to compare the test results to the theoretical FOE values obtained by [3]. So far, the best performing chips are: *01-BS2-01*, *01-Ws1-01*, and *01-Ld1-01*. However, only *01-Ws1-01* has been tested on the thrust bench. Although, a good relation between the displacement and the power levels required is found, which was originally expected. Nonetheless, due to the conditions the thruster chips were in, the actual performance should be retested by using brand new versions of the same chips. During this test some of them were unstable, partially blocked, or completely blocked. Thus, the overflow conditions were hard to predict. Moreover, due to the initial damage of the heaters, the chips did not survive the full range of intended mass flow measurements. In Section 4.5.7 the verification of the requirements related to this test is discussed. The heater efficiency of 0.12 - 0.33 [-] has been reached compared to the theoretical value of 0.6 [-] [3].

5.2. Recommendations

1. During the verification and validation of the PPD design only the teflon and aluminium configuration has been considered for the housings of LPM and VLM thrusters. However, for the flight model version of the thruster housings a possibility of using ceramics is recommended by *Guerrieri* [1]. A possible manufacturing company [64] in Germany is found, which can produce the thruster interfaces using ceramic materials and rapid prototyping techniques.

2. If the check valve from *The Lee* is going to be used further in the PS design, a further analysis is required for it. For example, an explicit testing of the check valve leakage is required. It is known that check valve creates only unidirectional flow, but it is possible that there is some back-flow through the inlet. Thus, a *Pressure Change* method can be used to check for a leak at the inlet of the check valve.
3. From the leak test results it is observed that some of the components such as the tubes and the adapters wear off from cycling mounting and dismounting. It means there is a limited testing cylce of the components, which should be replaced after some time. Furthermore, the tubes have the metal spherules which are made to create leak tight seals when are connected to other components. However it is possible that if not enough torque is applied during the tube fitting, the leak tight seal is not achieved. Moreover, due to the significant change of pressure inside the tube during the tests, the tube stretches out and can become lose at the connection points. Although, the manufacturer provides the maximum operational conditions at which the components can operate and fail. It means not much can be done about it. However, a further investigation of the tubes can be performed.
4. The safety screens used in both thrusters should be further investigated, because due to their bulkiness they reduce a significant amount of volume inside required 42x42x30 [mm] space. Even though the manufacturer suggests to use them together with its other components, it is not known if there is any actual added value to the performance of the system.
5. To fully understand the behavior of VLM chips and the required power levels, TEST-COM-04 should be redone with a brand new set of the same chips. In order to avoid total damage and obtain useful data, the mass flow values of 2, 2.5, and 3 [mL/h] should be used first. Although, a protective design detail at the exit of the nozzle and interface should be added, to avoid water creeping under the chip and damaging the cheaters.

A

Test Campaign Gantt Chart

Gantt Chart - *Delfi-PQ* Propulsion Sub-System Testing Campaign			Legend					S - Start					Prepartion (orange)					Analysis (blue)					Contingency (red)				
								E - End					Testing (green)					Reporting (yellow)					N/A				
Testing Phase	**Test Name**	**Duration**	Sep: Week 3					Sep: Week 4					Oct: Week 1					Oct: Week 2					Oct: Week 3				
			17	18	19	20	21	24	25	26	27	28	01	02	03	04	05	08	09	10	11	12	15	16	17	18	19
Components	TEST-COM-01: Solenoid Valve PWM Test	15 days	S						E	S	E	S		E	S	E											
	TEST-COM-02: Fill/Drain Valve Test	14 days																S						E	S	E	S
	TEST-COM-03: VLM & LPM Test																										
	TEST-COM-04: Heater Efficiency Test																										
Assembly and Integration	TEST-INT-01: Leak Test																										
	TEST-INT-02: Volume and Mass Test																										
	TEST-INT-03: Electrical & Software Test																										
Prototype	TEST-PRO-01: Vaporization Test																										
	TEST-PRO-02: Pressure Profile Test																										
	TEST-PRO-03: Mass Flow Profile Test																										
	TEST-PRO-03: Thrust Profile Test																										

Testing Phase	**Test Name**	**Duration**	Oct: Week 4					Nov: Week 1					Nov: Week 2					Nov: Week 3					Nov: Week 4				
			22	23	24	25	26	5	6	7	8	9	12	13	14	15	16	19	20	21	22	23	26	27	28	29	30
Components	TEST-COM-01: Solenoid Valve PWM Test																										
	TEST-COM-02: Fill/Drain Valve Test	14 days	E	S	E																						
	TEST-COM-03: VLM & LPM Test	16 days				S							E	S		E	S		E	S	E						
	TEST-COM-04: Heater Efficiency Test	15 days																					S				
Assembly and Integration	TEST-INT-01: Leak Test																										
	TEST-INT-02: Volume and Mass Test																										
	TEST-INT-03: Electrical & Software Test																										
Prototype	TEST-PRO-01: Vaporization Test																										
	TEST-PRO-02: Pressure Profile Test																										
	TEST-PRO-03: Mass Flow Profile Test																										
	TEST-PRO-03: Thrust Profile Test																										

Testing Phase	**Test Name**	**Duration**	Dec: Week 1					Dec: Week 2					Dec: Week 3					Dec: Week 4					Jan: Week 1				
			3	4	5	6	7	10	11	12	13	14	17	18	19	20	21	24	25	26	27	28	7	8	9	10	11
Components	TEST-COM-01: Solenoid Valve PWM Test																										
	TEST-COM-02: Fill/Drain Valve Test																										
	TEST-COM-03: VLM & LPM Test																										
	TEST-COM-04: Heater Efficiency Test	15 days		E		S	E	S		E	S	E															
Assembly and Integration	TEST-INT-01: Leak Test	17 days			N									S					N	N		E	S				E
	TEST-INT-02: Volume and Mass Test				/														/	/							
	TEST-INT-03: Electrical & Software Test				A														A	A							
Prototype	TEST-PRO-01: Vaporization Test																										
	TEST-PRO-02: Pressure Profile Test																										
	TEST-PRO-03: Mass Flow Profile Test																										
	TEST-PRO-03: Thrust Profile Test																										

Figure A.1: Preliminary test campaign schedule and plan in a form of a Gantt chart (PART 1)

Testing Phase	Test Name	Duration	Jan: Week 2					Jan: Week 3					Jan: Week 4					Feb: Week 1					Feb: Week 2				
			14	15	16	17	18	21	22	23	24	25	28	29	30	31	1	4	5	6	7	8	11	12	13	14	15
Components	TEST-COM-01: Solenoid Valve PWM Test																										
	TEST-COM-02: Fill/Drain Valve Test																										
	TEST-COM-03: VLM & LPM Test																										
	TEST-COM-04: Heater Efficiency Test																										
Assembly and Integration	TEST-INT-01: Leak Test	17 days	S	E	S	E																					
	TEST-INT-02: Volume and Mass Test	14 days						S						E	S	E	S	E	S	E							
	TEST-INT-03: Electrical & Software Test	14 days																				S					
Prototype	TEST-PRO-01: Vaporization Test																										
	TEST-PRO-02: Pressure Profile Test																										
	TEST-PRO-03: Mass Flow Profile Test																										
	TEST-PRO-03: Thrust Profile Test																										

Testing Phase	Test Name	Duration	Feb: Week 3					Feb: Week 4					Mar: Week 1					Mar: Week 2					Mar: Week 3				
			18	19	20	21	22	25	26	27	28	1	4	5	6	7	8	11	12	13	14	15	18	19	29	21	22
Components	TEST-COM-01: Solenoid Valve PWM Test																										
	TEST-COM-02: Fill/Drain Valve Test																										
	TEST-COM-03: VLM & LPM Test																										
	TEST-COM-04: Heater Efficiency Test																										
Assembly and Integration	TEST-INT-01: Leak Test																										
	TEST-INT-02: Volume and Mass Test																										
	TEST-INT-03: Electrical & Software Test	14 days	E	S	E	S	E	S	E																		
Prototype	TEST-PRO-01: Vaporization Test	14 days									S						E	S	E	S	E	S	E				
	TEST-PRO-02: Pressure Profile Test																								S		
	TEST-PRO-03: Mass Flow Profile Test																										
	TEST-PRO-03: Thrust Profile Test																										

Testing Phase	Test Name	Duration	Mar: Week 4					Apr: Week 1					Apr: Week 2					Apr: Week 3					Apr: Week 4				
			25	26	27	28	29	1	2	3	4	5	8	9	10	11	12	15	16	17	18	19	22	23	24	25	26
Components	TEST-COM-01: Solenoid Valve PWM Test																										
	TEST-COM-02: Fill/Drain Valve Test																										
	TEST-COM-03: VLM & LPM Test																										
	TEST-COM-04: Heater Efficiency Test																										
Assembly and Integration	TEST-INT-01: Leak Test																					N/A	N/A				
	TEST-INT-02: Volume and Mass Test																										
	TEST-INT-03: Electrical & Software Test																										
Prototype	TEST-PRO-01: Vaporization Test																										
	TEST-PRO-02: Pressure Profile Test	14 days				E	S	E	S	E	S	E															
	TEST-PRO-03: Mass Flow Profile Test	14 days												S						E	S			E	S	E	S
	TEST-PRO-03: Thrust Profile Test																										

Testing Phase	Test Name	Duration	May: Week 1					May: Week 2					May: Week 3					May: Week 4					N/A				
			29	30	1	2	3	6	7	8	9	1-	13	14	15	16	17	20	21	22	23	24					
Components	TEST-COM-01: Solenoid Valve PWM Test																						N/A				
	TEST-COM-02: Fill/Drain Valve Test																										
	TEST-COM-03: VLM & LPM Test																										
	TEST-COM-04: Heater Efficiency Test																										
Assembly and Integration	TEST-INT-01: Leak Test																										
	TEST-INT-02: Volume and Mass Test																										
	TEST-INT-03: Electrical & Software Test																										
Prototype	TEST-PRO-01: Vaporization Test																										
	TEST-PRO-02: Pressure Profile Test																										
	TEST-PRO-03: Mass Flow Profile Test	14 days	E																								
	TEST-PRO-03: Thrust Profile Test	14 days			S						E	S	E	S	E	S	E										

Figure A.2: Preliminary test campaign schedule and plan in a form of a Gantt chart (PART 2)

Gantt Chart - *Delfi-PQ* Propulsion Sub-System Testing Campaign

Legend

S - Start	Prepartion (orange)	Analysis (blue)	Contingency (red)
E - End	Testing (green)	Reporting (yellow)	N/A

Testing Phase	Test Name	Duration	Sep: Week 3					Sep: Week 4					Oct: Week 1					Oct: Week 2					Oct: Week 3				
			17	18	19	20	21	24	25	26	27	28	01	02	03	04	05	08	09	10	11	12	15	16	17	18	19
Components	TEST-COM-01: Solenoid Valve PWM Test																										
	TEST-COM-02: Fill/Drain Valve Test																										
	TEST-COM-03: VLM & LPM Test																										
	TEST-COM-04: Heater Efficiency Test																										
Assembly and Integration	TEST-INT-01: Leak Test	93 days	S																								
	TEST-INT-02: Volume and Mass Test																										
	TEST-INT-03: Electrical & Software Test																										

Testing Phase	Test Name	Duration	Oct: Week 4					Nov: Week 1					Nov: Week 2					Nov: Week 3					Nov: Week 4				
			22	23	24	25	26	5	6	7	8	9	12	13	14	15	16	19	20	21	22	23	26	27	28	29	30
Components	TEST-COM-01: Solenoid Valve PWM Test																										
	TEST-COM-02: Fill/Drain Valve Test																										
	TEST-COM-03: VLM & LPM Test																										
	TEST-COM-04: Heater Efficiency Test																										
Assembly and Integration	TEST-INT-01: Leak Test	93 days																									E
	TEST-INT-02: Volume and Mass Test																										
	TEST-INT-03: Electrical & Software Test																										

Testing Phase	Test Name	Duration	Dec: Week 1					Dec: Week 2					Dec: Week 3					Dec: Week 4					Jan: Week 1				
			3	4	5	6	7	10	11	12	13	14	17	18	19	20	21	24	25	26	27	28	7	8	9	10	11
Components	TEST-COM-01: Solenoid Valve PWM Test																										
	TEST-COM-02: Fill/Drain Valve Test																										
	TEST-COM-03: VLM & LPM Test				N														N	N							
	TEST-COM-04: Heater Efficiency Test				/														/	/							
Assembly and Integration	TEST-INT-01: Leak Test	93 days	S		A														A	A							
	TEST-INT-02: Volume and Mass Test																										
	TEST-INT-03: Electrical & Software Test																										

Testing Phase	Test Name	Duration	Jan: Week 2					Jan: Week 3					Jan: Week 4					Feb: Week 1					Feb: Week 2				
			14	15	16	17	18	21	22	23	24	25	28	29	30	31	1	4	5	6	7	8	11	12	13	14	15
Components	TEST-COM-01: Solenoid Valve PWM Test																										
	TEST-COM-02: Fill/Drain Valve Test																										
	TEST-COM-03: VLM & LPM Test																										
	TEST-COM-04: Heater Efficiency Test																										
Assembly and Integration	TEST-INT-01: Leak Test	93 days															E	S									E
	TEST-INT-02: Volume and Mass Test																										
	TEST-INT-03: Electrical & Software Test																										

Testing Phase	Test Name	Duration	Feb: Week 3					Feb: Week 4					Mar: Week 1					Mar: Week 2					Mar: Week 3				
			18	19	20	21	22	25	26	27	28	1	4	5	6	7	8	11	12	13	14	15	18	19	29	21	22
Components	TEST-COM-01: Solenoid Valve PWM Test	30 days																								S	
	TEST-COM-02: Fill/Drain Valve Test																										
	TEST-COM-03: VLM & LPM Test																										
	TEST-COM-04: Heater Efficiency Test																										
Assembly and Integration	TEST-INT-01: Leak Test	93 days	S									E															
	TEST-INT-02: Volume and Mass Test	13 days											S		E	S		E	S			E	S		E		
	TEST-INT-03: Electrical & Software Test																										

Testing Phase	Test Name	Duration	Mar: Week 4					Apr: Week 1					Apr: Week 2					Apr: Week 3					Apr: Week 4				
			25	26	27	28	29	1	2	3	4	5	8	9	10	11	12	15	16	17	18	19	22	23	24	25	26
Components	TEST-COM-01: Solenoid Valve PWM Test	30 days			E	S						E	S								E			S			
	TEST-COM-02: Fill/Drain Valve Test																										
	TEST-COM-03: VLM & LPM Test																					N	N				
	TEST-COM-04: Heater Efficiency Test	27 days							S			E	S			E	S					/	/		E	S	
Assembly and Integration	TEST-INT-01: Leak Test																					A	A				
	TEST-INT-02: Volume and Mass Test																										
	TEST-INT-03: Electrical & Software Test																										

Testing Phase	Test Name	Duration	May: Week 1					May: Week 2					May: Week 3					May: Week 4					N/A				
			29	30	1	2	3	6	7	8	9	10	13	14	15	16	17	20	21	22	23	24					
Components	TEST-COM-01: Solenoid Valve PWM Test	30 days					E																				
	TEST-COM-02: Fill/Drain Valve Test																										
	TEST-COM-03: VLM & LPM Test																										
	TEST-COM-04: Heater Efficiency Test	27 days										E															
Assembly and Integration	TEST-INT-01: Leak Test																										
	TEST-INT-02: Volume and Mass Test																										
	TEST-INT-03: Electrical & Software Test																										

Figure A.3: Actual test campaign schedule and plan in a form of a Gantt chart

B

Gluing Tools and Materials

The list of tools and materials used in the gluing process of the pressure interface and *MS5837-30BA* pressure/temperature sensor:

1. PROSAT presaturated wipes PS-911 (70% IPA 30% DI water) by Contec.

2. Kombi Metaal Colle Epoxy Lijm by Bizon.

3. Loctite EA 3421 Epoxy by Henkel.

4. MR PE/PP Primer.

5. MR PE/PP Primer manual.

Gebruiksaanwijzing MR PE/PP Primer:

De te lijmen delen eerst ontvetten met ***MR*** ontvetter of alcohol of aceton, *geen* spiritus, wasbenzine, terpentine of nagellakremover gebruiken !!
Op beide delen met het kwastje de PE/PP Primer 3 of 4 x *dik* opbrengen, *minmaal* 3 minuten uit laten dampen, dan eenzijdig en DIK de ***MR*** Industriekrachtlijm erop doen, de delen samenvoegen (het liefst klemmen) en 8 tot 24 uur laten uitharden , en uw verbinding is optimaal.

Let op, dat het flesje stevig staat en niet omvalt als het is geopend!
Zet het bijv. in een stukje piepschuim.

MR Industrielijm
Turfkade 2
8701 JK Bolsward
Tel. 065 3511552
www.123lijm.comi
E-mail: info@123lijm.com

MR Promotions kan nimmer aansprakelijk worden gesteld voor enige schade, gevolgschade of letsel, in welke vorm of grootte dan ook, ontstaan door het gebruik van de door MR Promotions geleverde lijm en/of daaraan gerelateerde producten, het gebruik van de producten is ten allen tijde voor eigen risico!

6. MR Industriekrachtlijm glue.

7. MR Industriekrachtlijm glue.

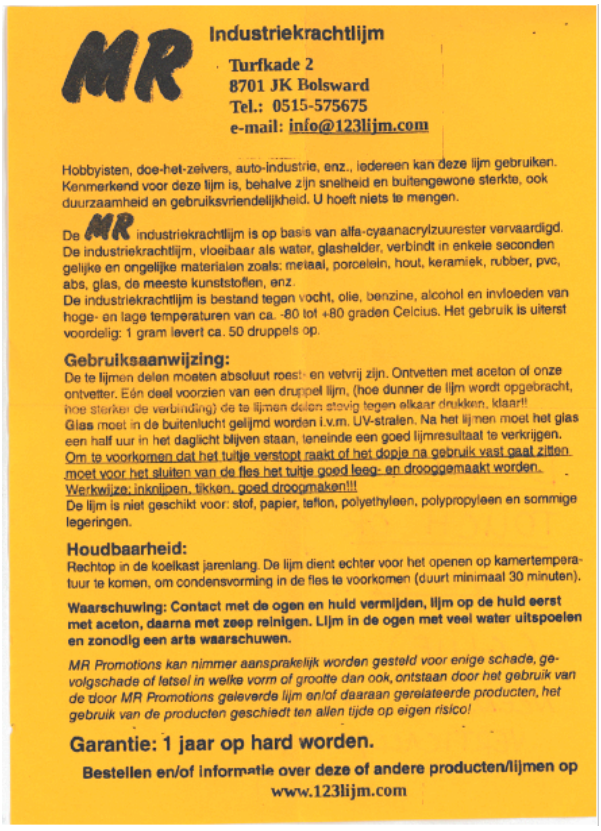

MR **Industriekrachtlijm**

Turfkade 2
8701 JK Bolsward
Tel.: 0515-575675
e-mail: info@123lijm.com

Hobbyisten, doe-het-zelvers, auto-industrie, enz., iedereen kan deze lijm gebruiken. Kenmerkend voor deze lijm is, behalve zijn snelheid en buitengewone sterkte, ook duurzaamheid en gebruiksvriendelijkheid. U hoeft niets te mengen.

De MR industriekrachtlijm is op basis van alfa-cyaanacrylzuurester vervaardigd. De industriekrachtlijm, vloeibaar als water, glashelder, verbindt in enkele seconden gelijke en ongelijke materialen zoals: metaal, porcelein, hout, keramiek, rubber, pvc, abs, glas, de meeste kunststoffen, enz.
De industriekrachtlijm is bestand tegen vocht, olie, benzine, alcohol en invloeden van hoge- en lage temperaturen van ca. -80 tot +80 graden Celcius. Het gebruik is uiterst voordelig: 1 gram levert ca. 50 druppels op.

Gebruiksaanwijzing:
De te lijmen delen moeten absoluut roest- en vetvrij zijn. Ontvetten met aceton of onze ontvetter. Eén deel voorzien van een druppel lijm, (hoe dunner de lijm wordt opgebracht, hoe sterker de verbinding) de te lijmen delen stevig tegen elkaar drukken, klaar!!
Glas moet in de buitenlucht gelijmd worden i.v.m. UV-stralen. Na het lijmen moet het glas een half uur in het daglicht blijven staan, teneinde een goed lijmresultaat te verkrijgen.
Om te voorkomen dat het tuitje verstopt raakt of het dopje na gebruik vast gaat zitten moet voor het sluiten van de fles het tuitje goed leeg- en drooggemaakt worden.
Werkwijze: inknijpen, tikken, goed droogmaken!!!
De lijm is niet geschikt voor: stof, papier, teflon, polyethyleen, polypropyleen en sommige legeringen.

Houdbaarheid:
Rechtop in de koelkast jarenlang. De lijm dient echter voor het openen op kamertemperatuur te komen, om condensvorming in de fles te voorkomen (duurt minimaal 30 minuten).

Waarschuwing: Contact met de ogen en huid vermijden, lijm op de huid eerst met aceton, daarna met zeep reinigen. Lijm in de ogen met veel water uitspoelen en zonodig een arts waarschuwen.

MR Promotions kan nimmer aansprakelijk worden gesteld voor enige schade, gevolgschade of letsel in welke vorm of grootte dan ook, ontstaan door het gebruik van de door MR Promotions geleverde lijm en/of daaraan gerelateerde producten, het gebruik van de producten geschiedt ten allen tijde op eigen risico!

Garantie: 1 jaar op hard worden.

Bestellen en/of informatie over deze of andere producten/lijmen op www.123lijm.com

C

Miscellaneous

Figure C.1: Electrolube The Solutions People soap liquid spray

D

The Lee Company Components

The list of *The Lee Company* components used in the testing phase and building PPD:

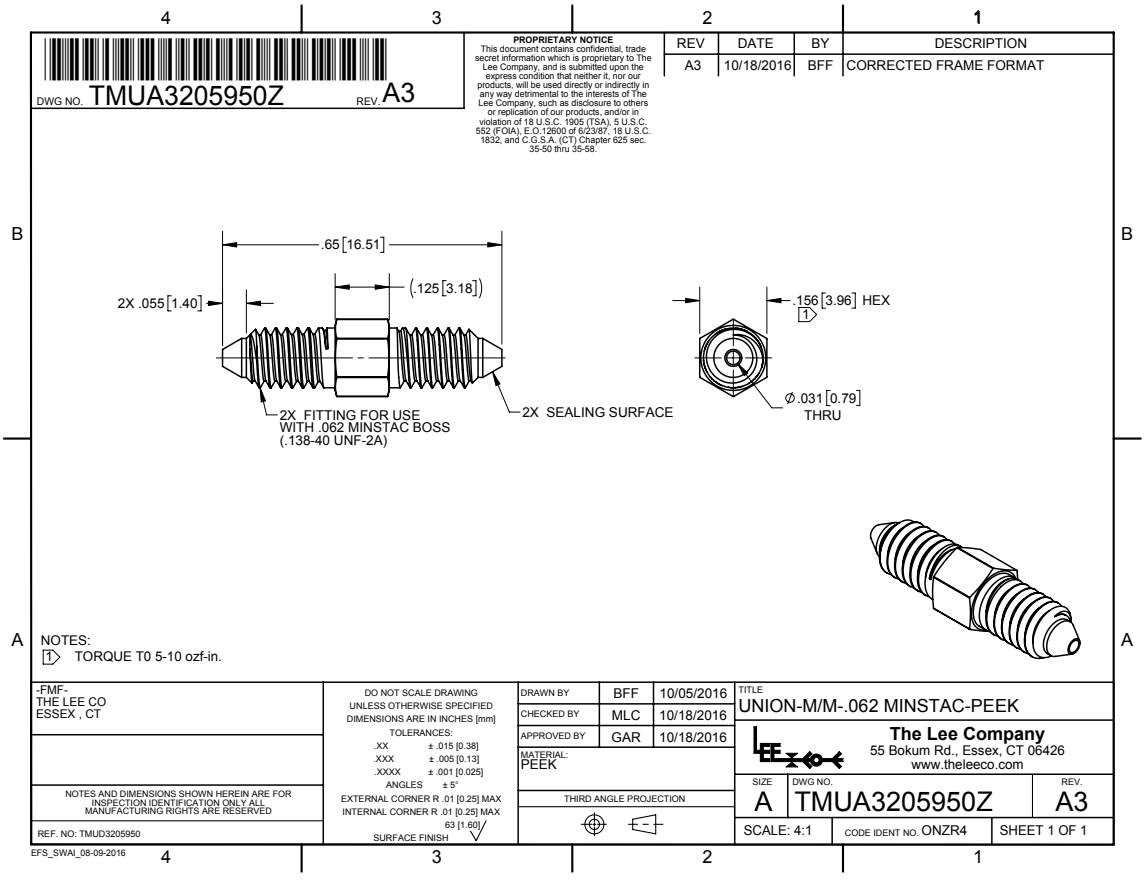

Figure D.1: TMUA3205950Z .062 MINSTAC PEEK male to male adapter

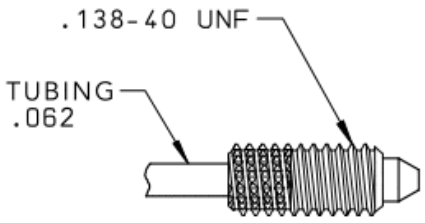

Figure D.2: .062 MINSTAC tube and 0.138-40 UNF connector

E

Overflow of VLM chips

Overflows of *01-BS2-01* chips at various mass flow settings:

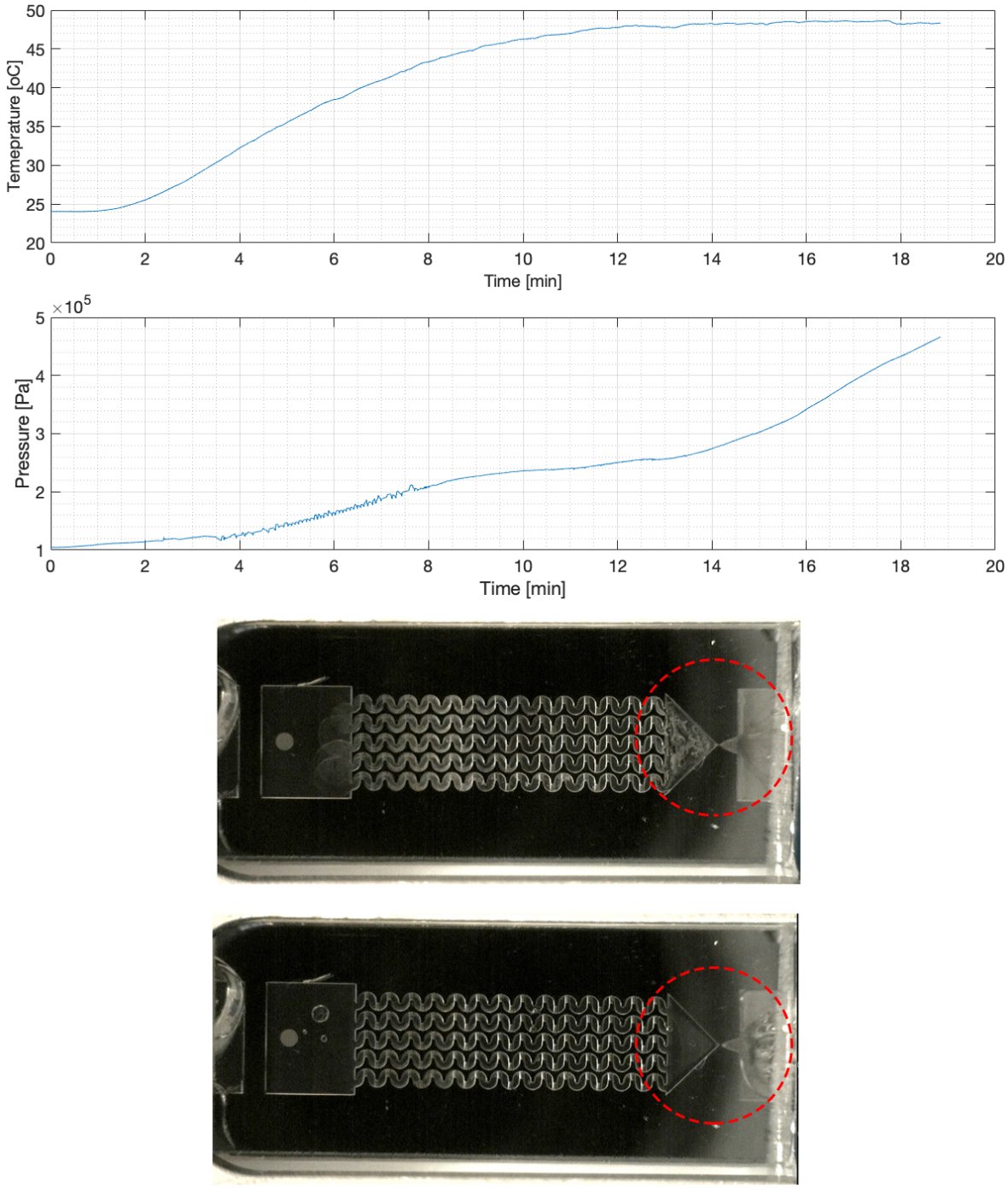

Figure E.1: Plenum temperature and pressure graph. Snapshots of just before the overflow and at the overflow of *01-BS2-01* chip at 0.5 [mL/h] at around 19 [min]

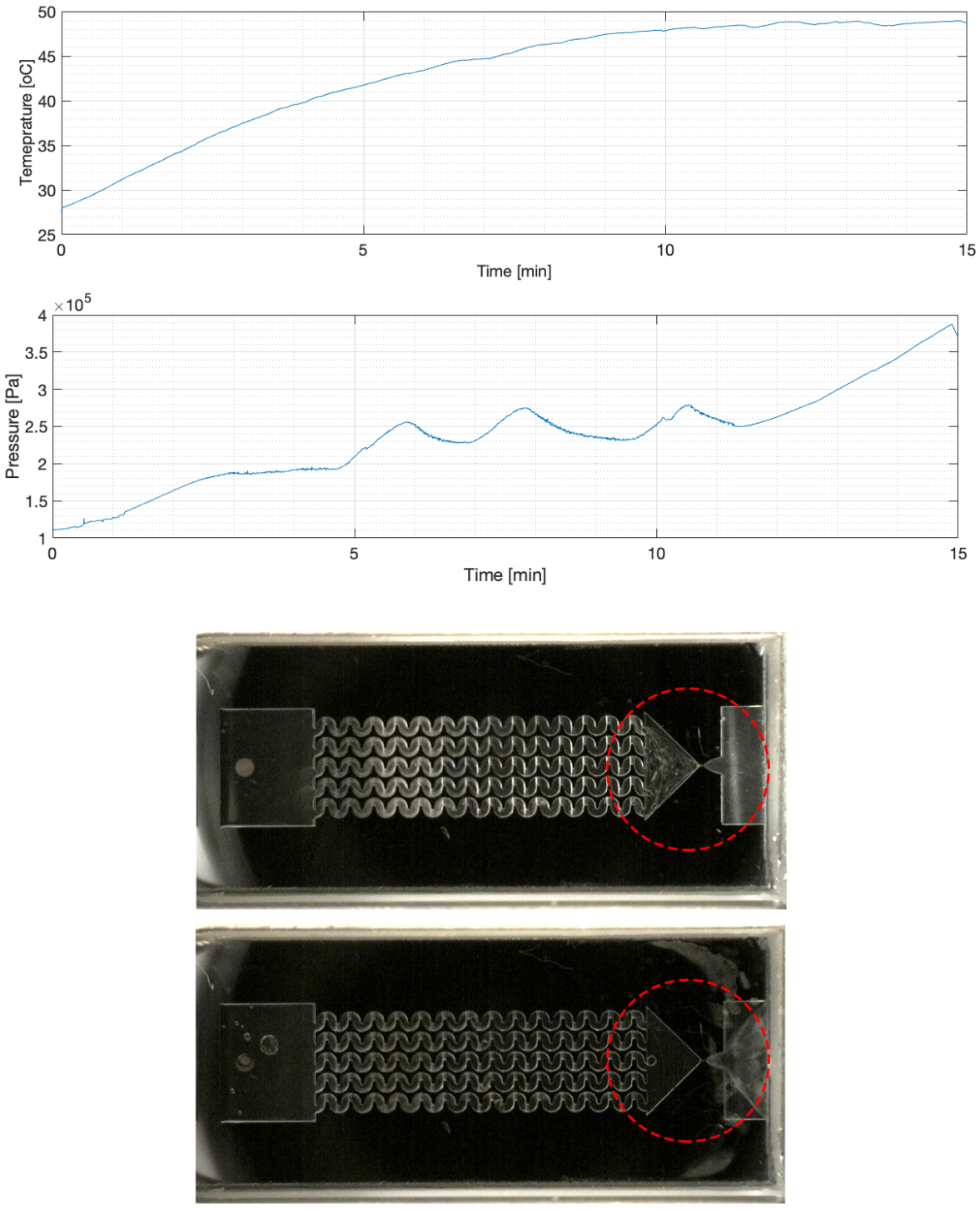

Figure E.2: Plenum temperature and pressure graph. Snapshots of just before the overflow and at the overflow of *01-BS2-01* chip at 1 [mL/h] at around 15 [min]

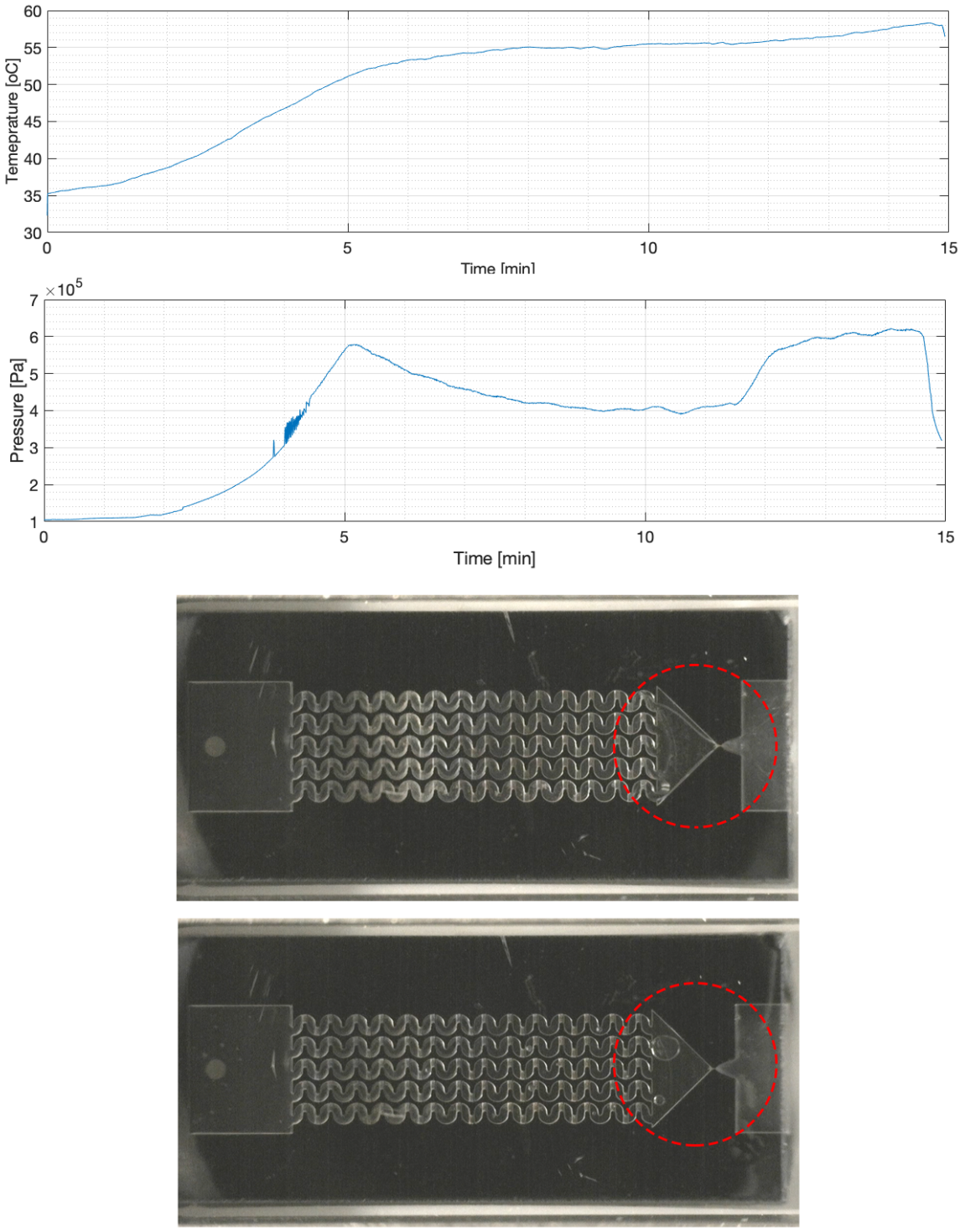

Figure E.3: Plenum temperature and pressure graph. Snapshots of just before the overflow and at the overflow of *01-BS2-01* chip at 2 [mL/h] at around 15 [min]

Overflows of *01-Ld1-01* chips at various mass flow settings:

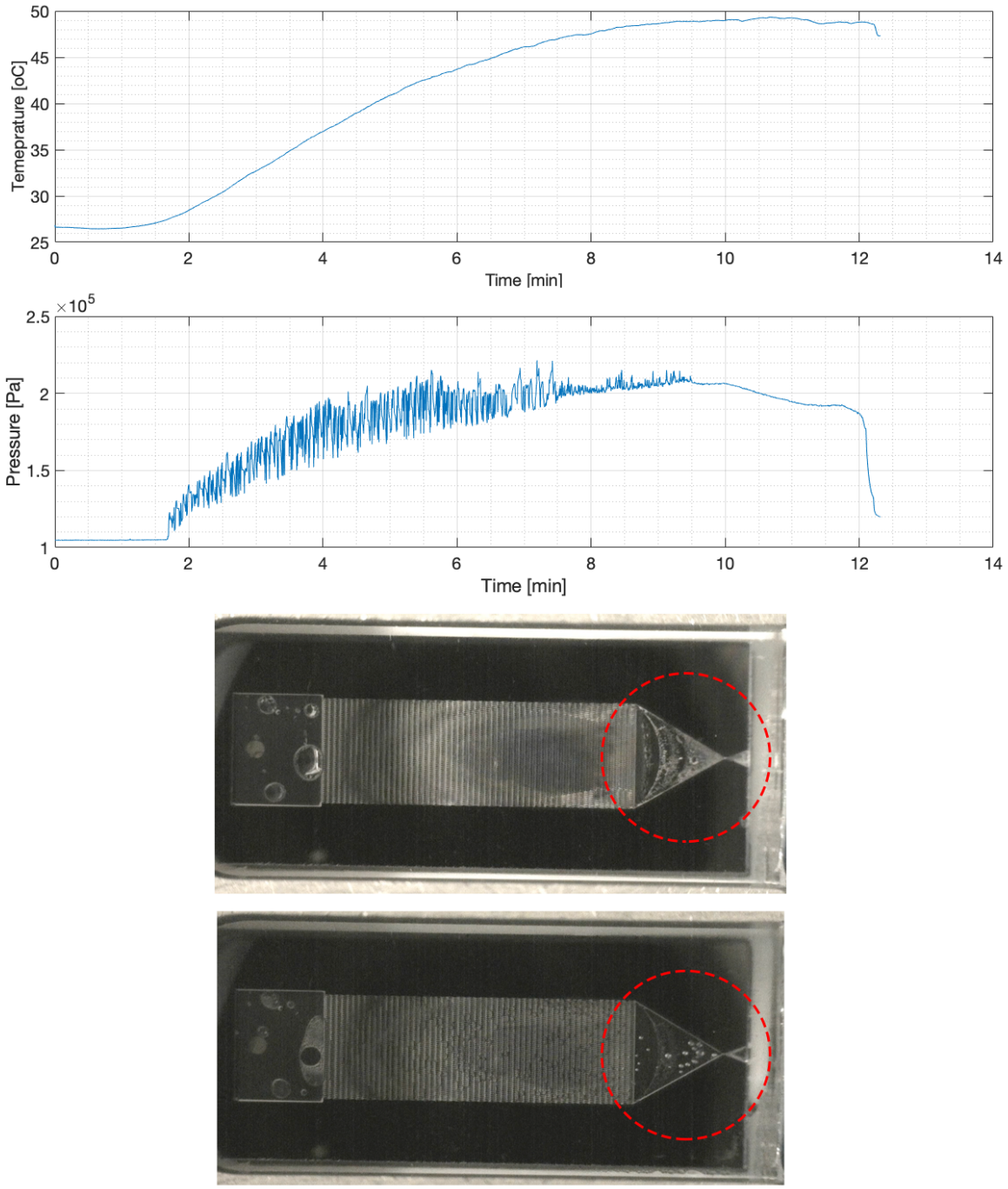

Figure E.4: Plenum temperature and pressure graph. Snapshots of just before the overflow and at the overflow of *01-Ld1-01* chip at 0.5 [mL/h] at around 12 [min]

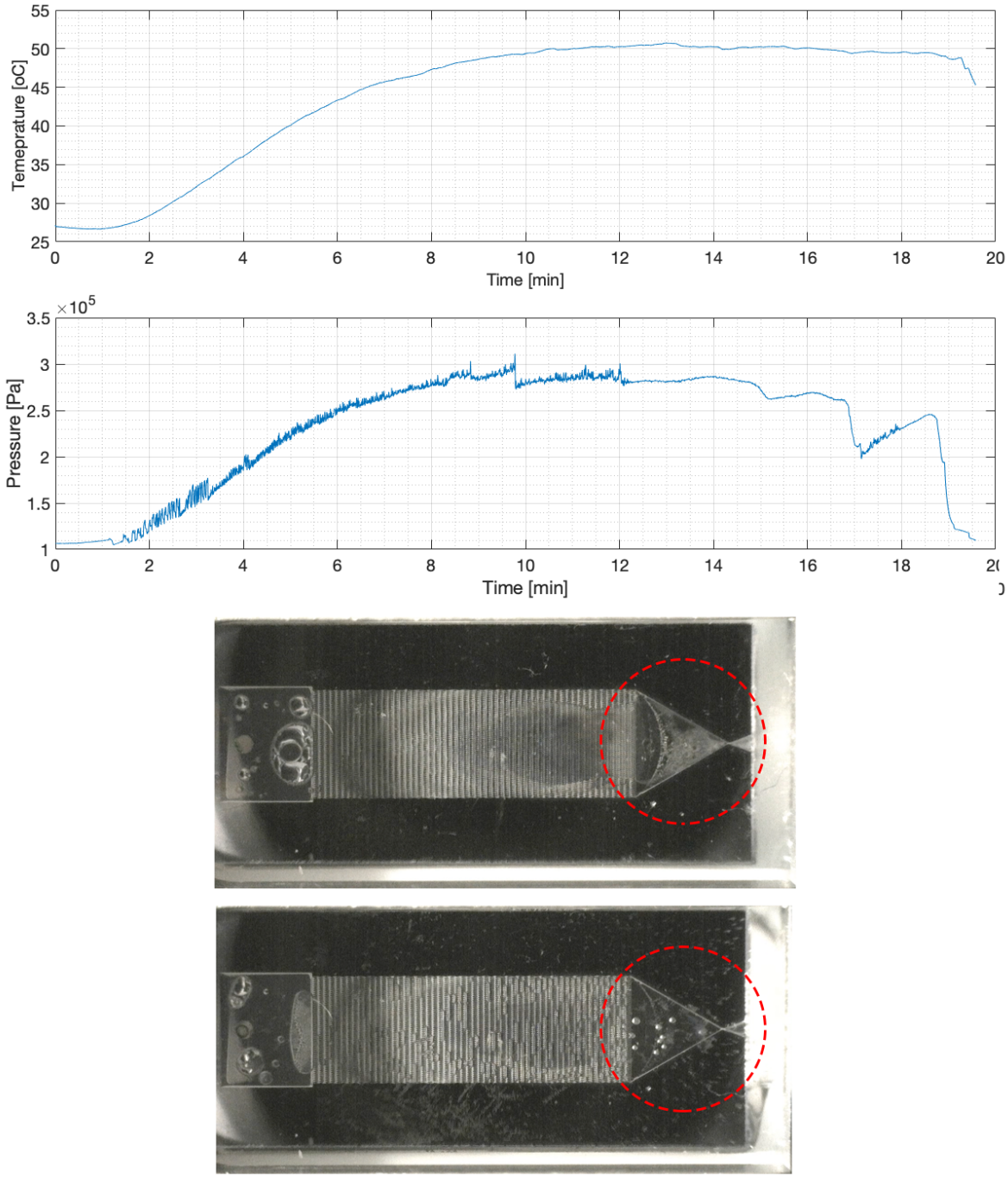

Figure E.5: Plenum temperature and pressure graph. Snapshots of just before the overflow and at the overflow of *01-Ld1-01* chip at 1 [mL/h] at around 19 [min]

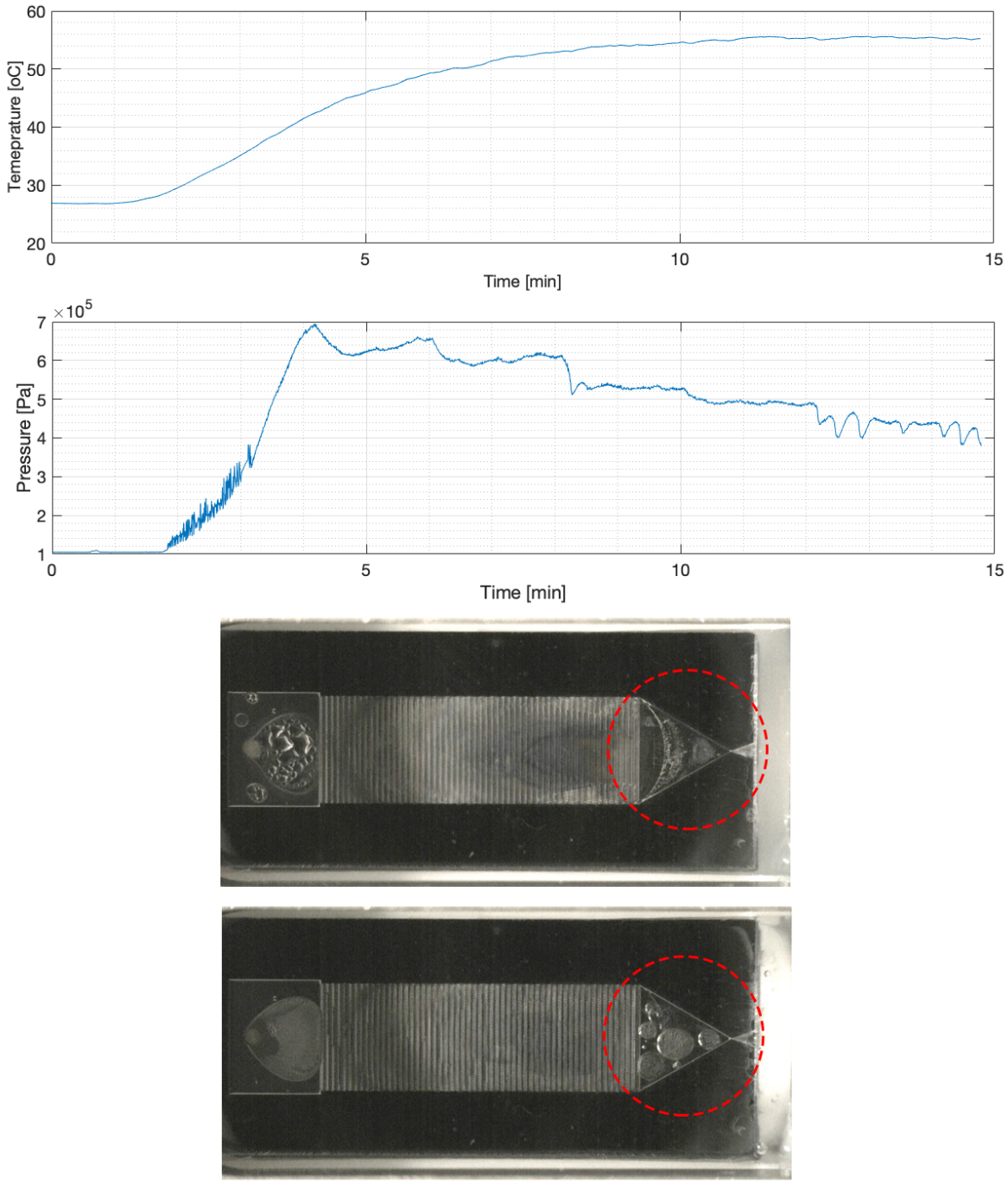

Figure E.6: Plenum temperature and pressure graph. Snapshots of just before the overflow and at the overflow of *01-Ld1-01* chip at 2 [mL/h] at around 14-15 [min]

Overflows of *01-Ws1-01* chips at various mass flow settings:

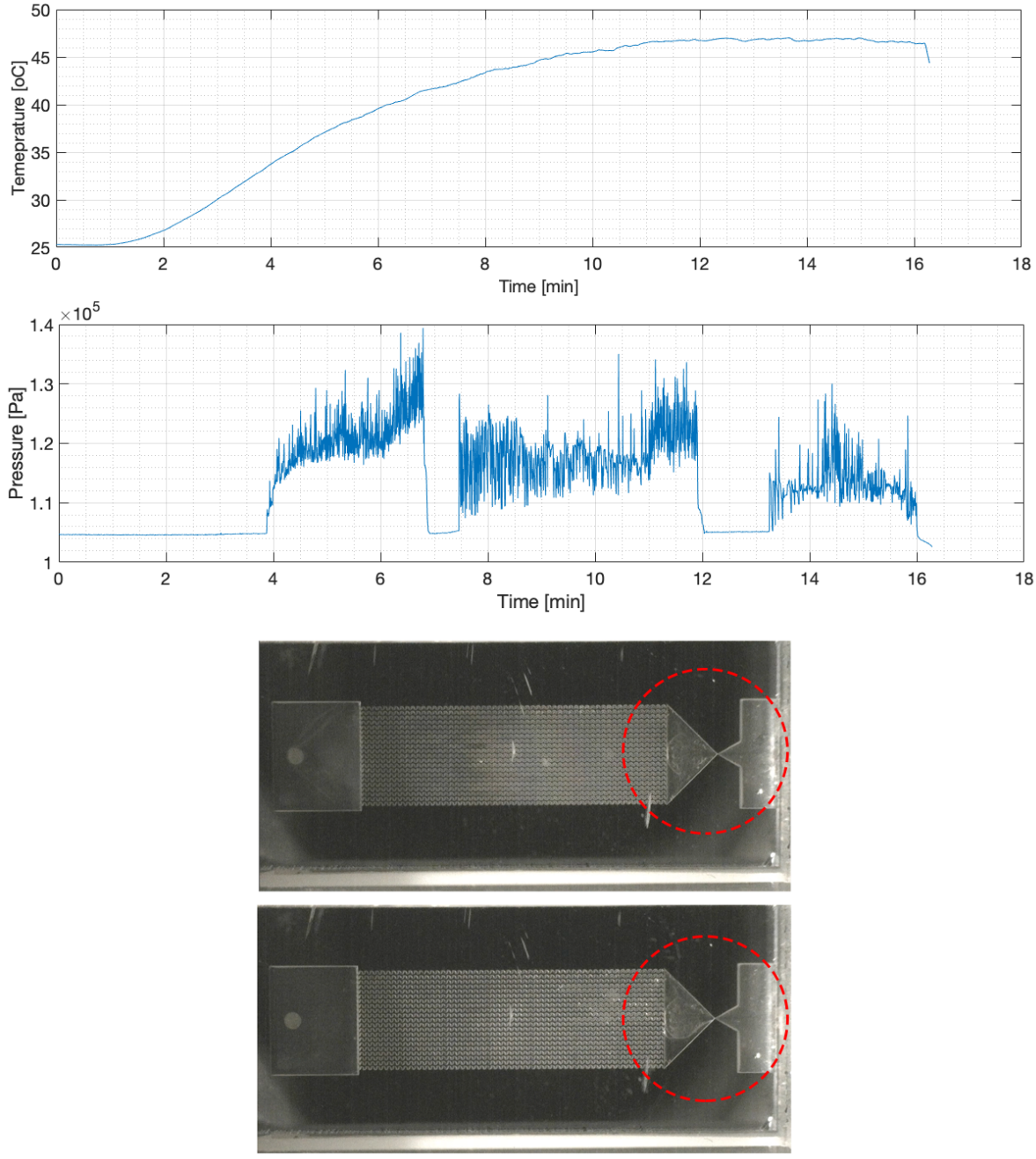

Figure E.7: Plenum temperature and pressure graph. Snapshots of just before the overflow and at the overflow of *01-Ws1-01* chip at 0.5 [mL/h] at around 16 [min]

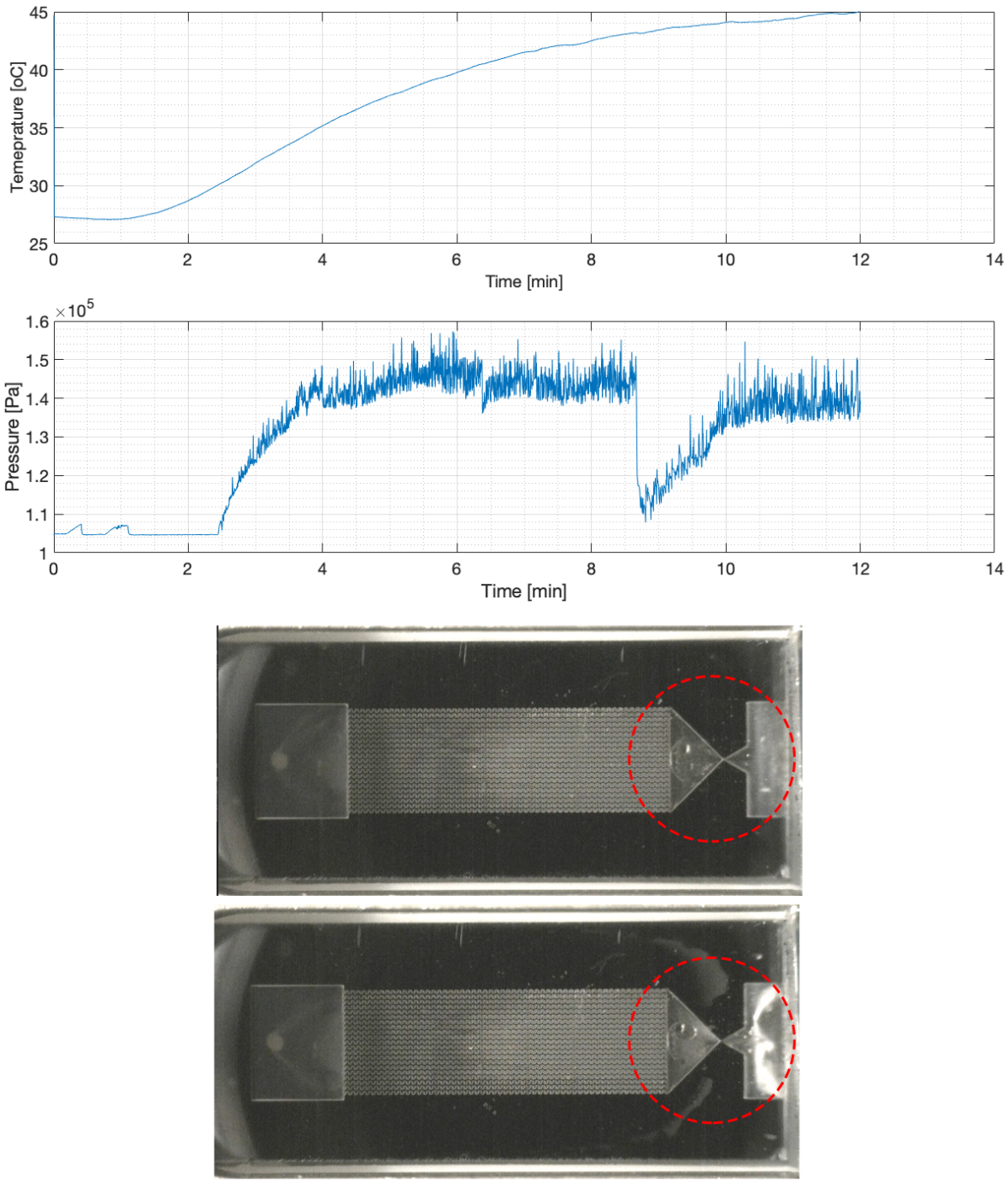

Figure E.8: Plenum temperature and pressure graph. Snapshots of just before the overflow and at the overflow of *01-Ws1-01* chip at 1 [mL/h] at around 12 [min]

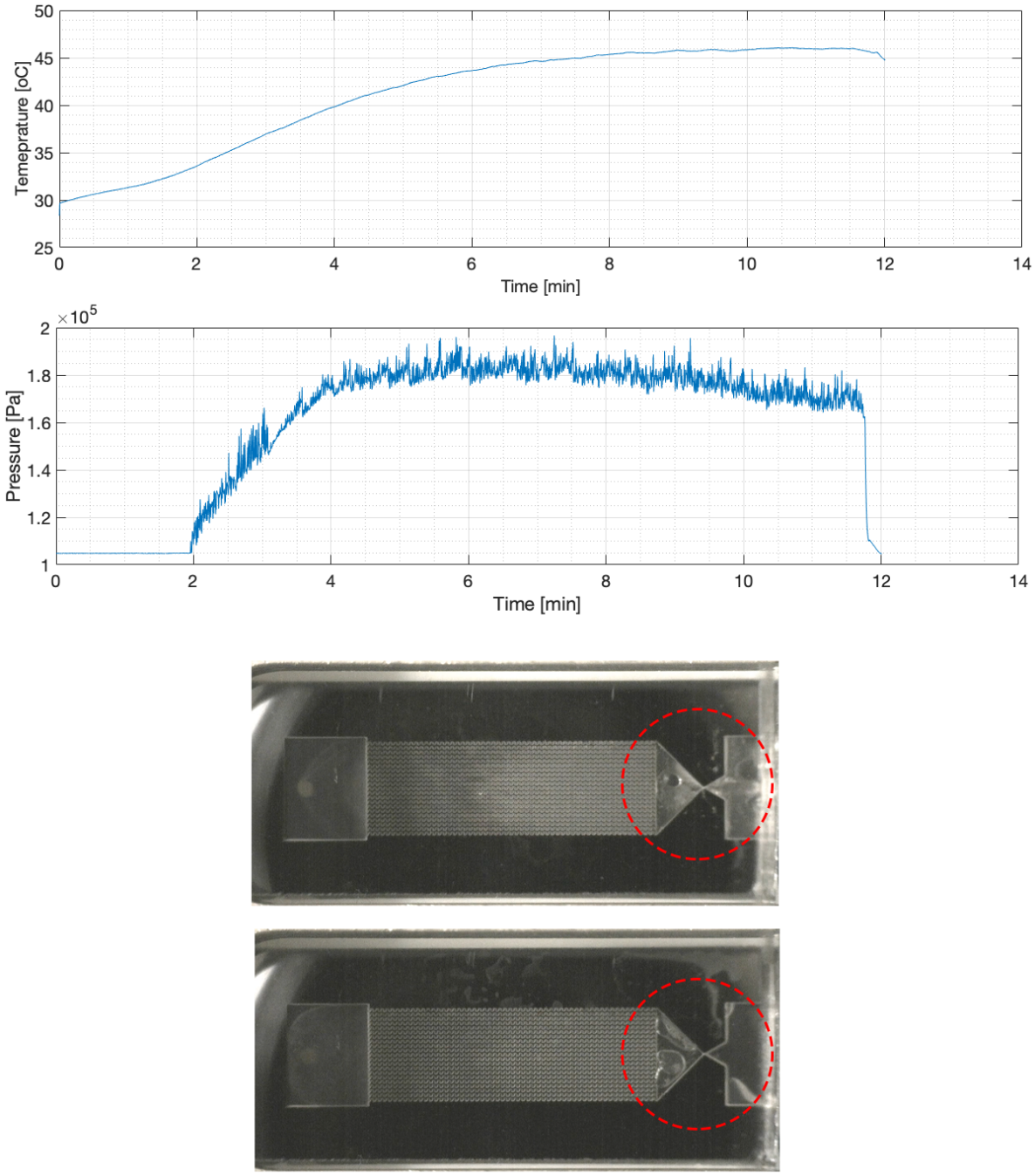

Figure E.9: Plenum temperature and pressure graph. Snapshots of just before the overflow and at the overflow of *01-Ws1-01* chip at 1.5 [mL/h] at and around 12 [min]

Overflows of *01-WS2-01* chips at various mass flow settings:

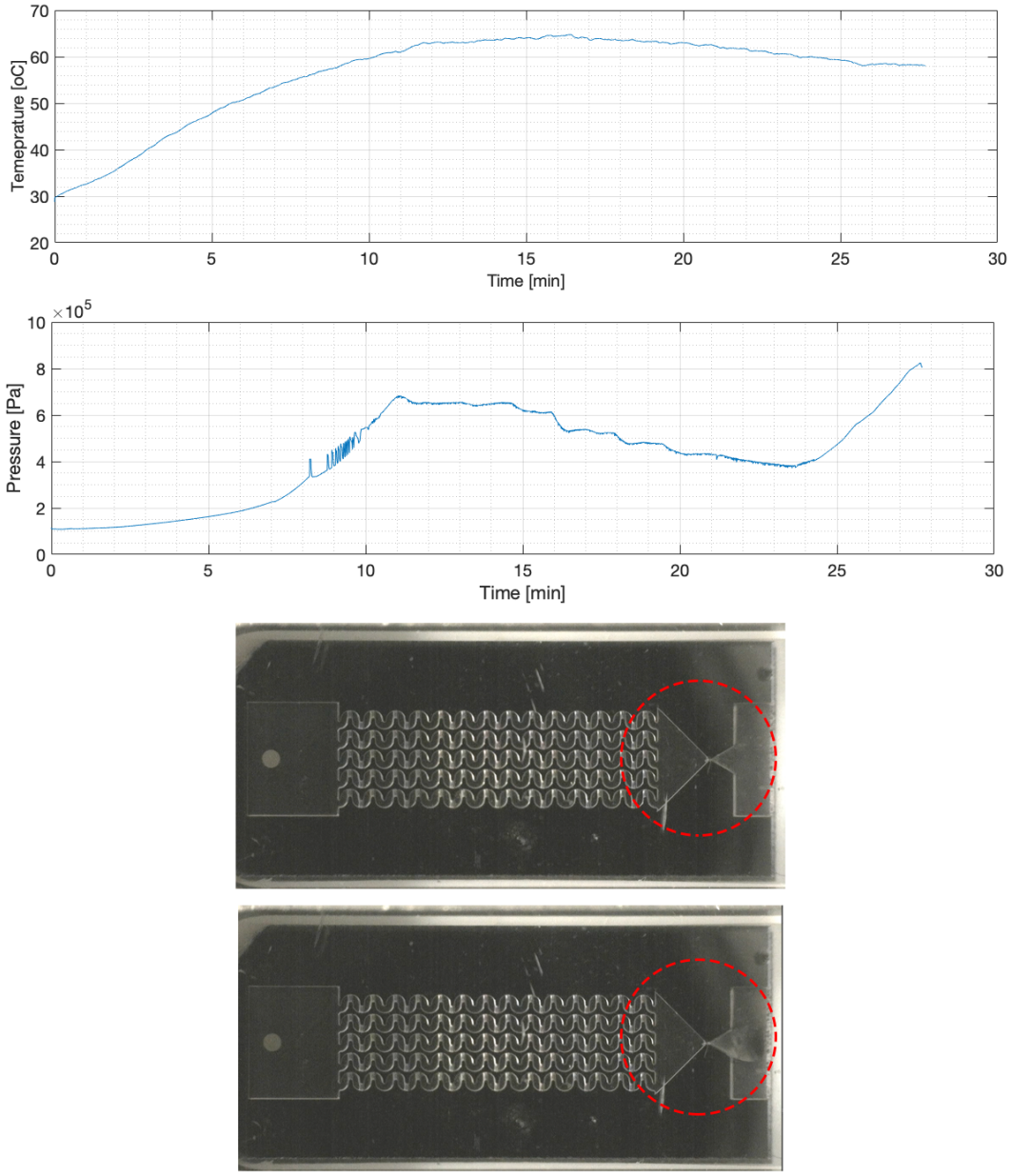

Figure E.10: Plenum temperature and pressure graph. Snapshots of just before the overflow and at the overflow of *01-WS2-01* chip at 0.5 [mL/h] at around 27 [min]

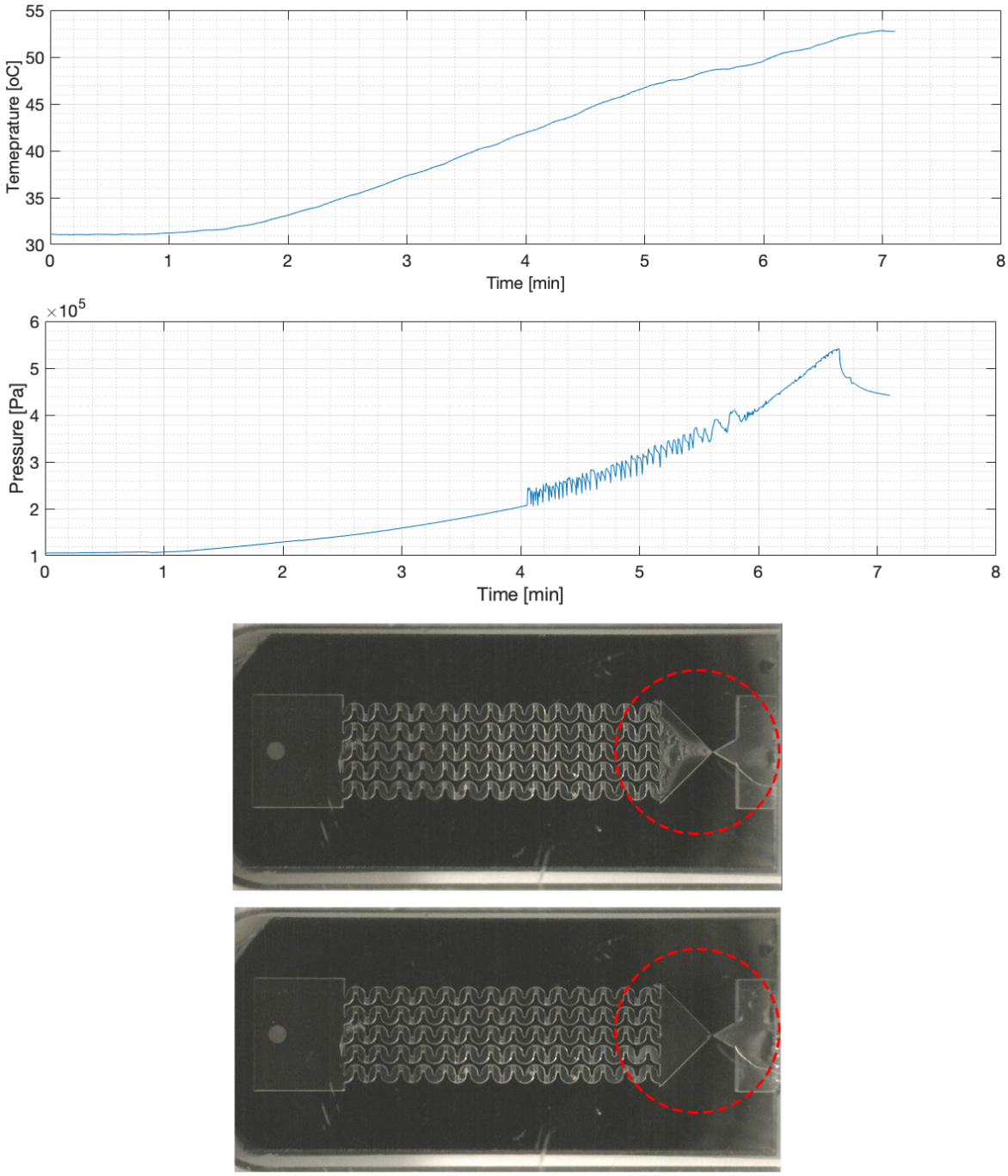

Figure E.11: Plenum temperature and pressure graph. Snapshots of just before the overflow and at the overflow of *01-WS2-01* chip at 1 [mL/h] at around 6-7 [min]

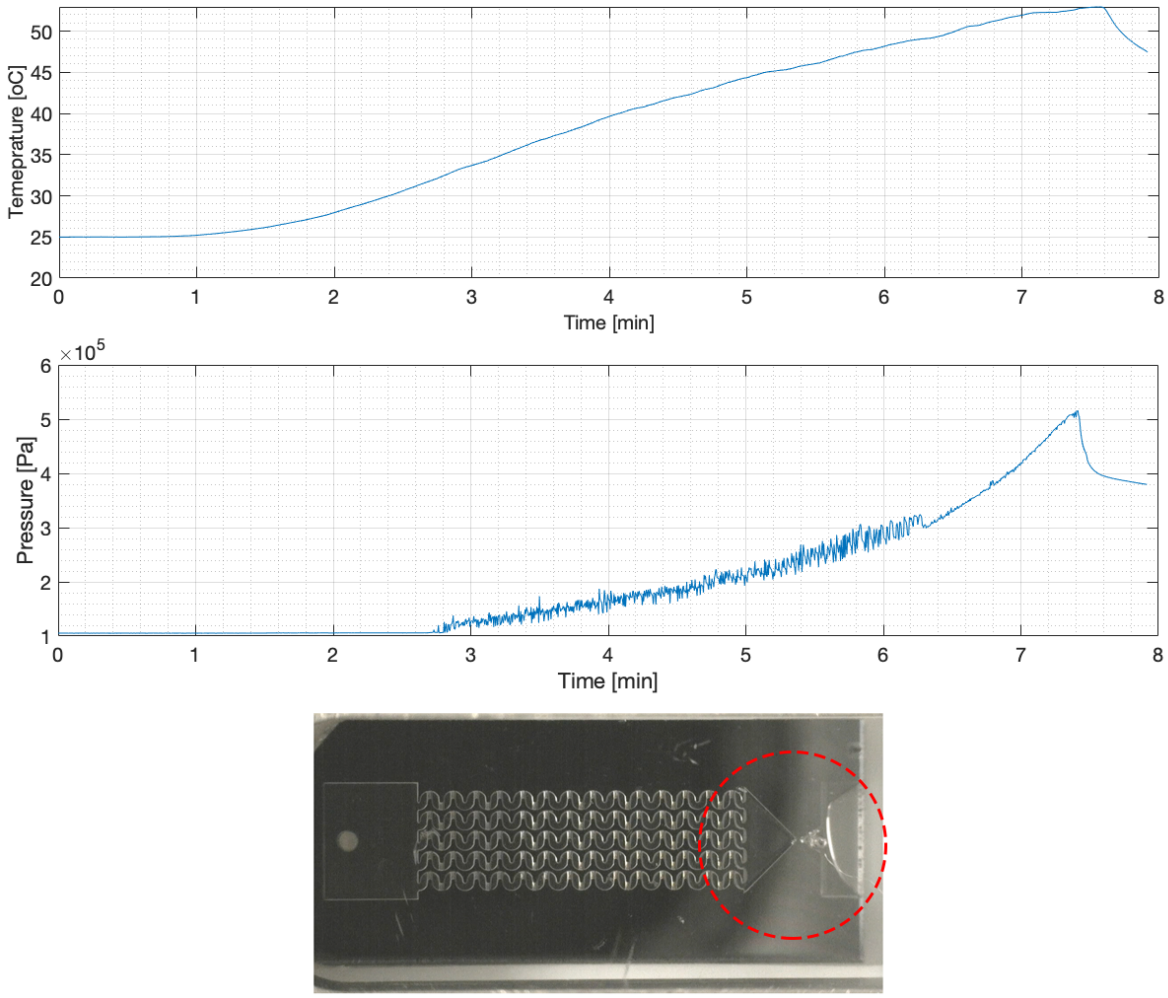

Figure E.12: Plenum temperature and pressure graph. Snapshot of the overflow of *01-WS2-01* chip at 1.5 [mL/h] at around 7 [min]. NOTE: The before overflow state is missing, because the interface was moved during the recording

F

MatLab Code

Matlab code of combined 1.5, 2.5, and 3.5 [bar] leak test:

```
clear all;
close all;
clc

%% === READ TEST DATA FILES ===

A = dlmread('TEST_INT_01_LeakTest_2_5bar_03012019.lvm');
B = dlmread('TEST_INT_01_LeakTest_1_5bar_07012019.lvm');
C = dlmread('TEST_INT_01_LeakTest_3_5bar_09012019.lvm');

%% === PROCESS THE TEST DATA ===

AAt = smooth(A(:,1));    % smooth the noisy data with function smooth
AAP = smooth(A(:,3));

BBt = smooth(B(:,1));
BBP = smooth(B(:,3));

CCt = smooth(C(:,1));
CCP = smooth(C(:,3));

tsecA = A(:,1);          % convert time in first data column to min
    and hrs
tminA = tsecA/60;
thA = tsecA/3600;

tsecB = B(:,1);
tminB = tsecB/60;
thB = tsecB/3600;

tsecC = C(:,1);
tminC = tsecC/60;
```

```
32 thC = tsecC/3600;
33
34 Pamb = repmat(1.030,size(CCP)); % equalize the ambient pressure to a
       single value
35
36 P2500mbar = A(:,3);       % convert pressure from mbar to bar
37 P25bar = P2500mbar/1000;
38
39 P1500mbar = B(:,3);
40 P15bar = P1500mbar/1000;
41
42 P3500mbar = C(:,3);
43 P35bar = P3500mbar/1000;
44
45 P2500mbarsmooth = AAP;      % convert smooth pressure from mbar to
      bar
46 P25barsmooth = P2500mbarsmooth/1000;
47
48 P1500mbarsmooth = BBP;
49 P15barsmooth = P1500mbarsmooth/1000;
50
51 P3500mbarsmooth = CCP;
52 P35barsmooth = P3500mbarsmooth/1000;
53
54 grad_matrix_25bar = [tsecA(4:end), P2500mbarsmooth(4:end)];  %
      calculate gradient and average pressure change
55 gradient_25bar = diff(grad_matrix_25bar);
56 mean_grad_25bar = mean(gradient_25bar)
57
58 grad_matrix_15bar = [tsecB(4:end), P1500mbarsmooth(4:end)];
59 gradient_15bar = diff(grad_matrix_15bar);
60 mean_grad_15bar = mean(gradient_15bar)
61
62 grad_matrix_35bar = [tsecC(4:end), P3500mbarsmooth(4:end)];
63 gradient_35bar = diff(grad_matrix_35bar);
64 mean_grad_35bar = mean(gradient_35bar)
65
66 %% === PLOT DATA ===
67
68 plot(thC,P35barsmooth,'b-')
69 hold on
70 plot(thA,P25barsmooth,'r-')
71 hold on
72 plot(thB,P15barsmooth,'m-')
73 hold on
74 plot(thC,Pamb,'g-')
75 grid on
76 grid minor
77 xticks(1:1:24) % define increments of the plot axes values
```

```
yticks(1:0.2:3.7)
set(findall(gcf,'-property','FontSize'),'FontSize',20)
set(gca,'XLim',[0 24]) % define the limits of min and max values on the axes
set(gca,'YLim',[1 3.7])
xlabel('Time [h]')
ylabel('Pressure [bar]')
legend('P_{st,0} = 3.5 [bar]','P_{st,0} = 2.5 [bar]','P_{st,0} = 1.5 [bar]', 'P_{amb}')
```

Matlab code of N_2] gas only leak test:

```
clear all;
close all;
clc

%% === READ TEST DATA FILES ===

F = dlmread('Displacement_Sensor_Data.lvm');

%% === PROCESS TEST DATA ===

FFt = smooth(F(:,1)); % smooth the noisy data with function smooth
FFP = smooth(F(:,3));

tsec = F(:,1);          % convert time in first data column to min and hrs
tmin = tsec/60;
th = tsec/3600;

Pamb = F(:,5)/1000;     % extract ambient pressure column from test data

P = F(:,3);             % extract pressure column and convert from mbar to bar
Pbar = P/1000;

Psmooth = FFP;          % convert smooth pressure from mbar to bar
Pbarsmooth = Psmooth/1000;

grad_matrix = [tsec(4:end), Psmooth(4:end)];    % calculate gradient and average pressure change
gradient = diff(grad_matrix);
mean_grad = mean(gradient)

%% === PLOT TEST DATA ===

plot(th,Pbar,'b-',th,Pamb,'g-')
grid on
grid minor
```

```
xticks(1:1:24)
yticks(1:0.1:3.7)
set(findall(gcf,'-property','FontSize'),'FontSize',14)
set(gca,'XLim',[0 24])
set(gca,'YLim',[1 3.7])
xlabel('Time [h]')
ylabel('Pressure [bar]')
legend('P_{raw}(t)','P_{amb}')
```

Matlab code of combined leak tests using plugs at 2 [bar]:

```
clear all;
close all;
clc

%% === READ TEST DATA FILES ===

A = dlmread('TEST_INT_01_LeakTest_2bar_16012019.lvm');
B = dlmread('TEST_INT_01_LeakTest_2bar_19012019.lvm');
C = dlmread('TEST_INT_01_LeakTest_2bar_21012019.lvm');
D = dlmread('TEST_INT_01_LeakTest_2bar_24012019.lvm');
E = dlmread('TEST_INT_01_LeakTest_2bar_25012019.lvm');

%% === PROCESS TEST DATA ===

Ast = smooth(A(:,1)); % smooth time and pressure data
AsP = smooth(A(:,3));

Bst = smooth(B(:,1));
BsP = smooth(B(:,3));

Cst = smooth(C(:,1));
CsP = smooth(C(:,3));

Dst = smooth(D(:,1));
DsP = smooth(D(:,3));

Est = smooth(E(:,1));
EsP = smooth(E(:,3));

tsecA = A(:,1);  % extract time and convert to min and hrs
tminA = tsecA/60;
thA = tsecA/3600;

tsecB = B(:,1);
tminB = tsecB/60;
thB = tsecB/3600;

tsecC = C(:,1);
tminC = tsecC/60;
```

```
40 thC = tsecC/3600;
41
42 tsecD = D(:,1);
43 tminD = tsecD/60;
44 thD = tsecD/3600;
45
46 tsecE = E(:,1);
47 tminE = tsecE/60;
48 thE = tsecE/3600;
49
50 tsecsmooth = Cst;
51 thsmooth = tsecsmooth/3600;
52
53 Pamb = repmat(1.030,size(CsP)); % convert ambient pressure to single
       value matrix
54
55 P16s = AsP;                    % convert smoothed pressure from mbar
      to bar
56 P16sbar = P16s/1000;
57
58 P19s = BsP;
59 P19sbar = P19s/1000;
60
61 P21s = CsP;
62 P21sbar = P21s/1000;
63
64 P24s = DsP;
65 P24sbar = P24s/1000;
66
67 P25s = EsP;
68 P25sbar = P25s/1000;
69
70 grad_matrix_P16sbar = [tsecA(4:end), P16s(4:end)]; % calculate
      gradient and average pressure change
71 gradient_P16sbar = diff(grad_matrix_P16sbar);
72 mean_grad_P16sbar = mean(gradient_P16sbar)
73
74 grad_matrix_P19sbar = [tsecB(4:end), P19s(4:end)];
75 gradient_P19sbar = diff(grad_matrix_P19sbar);
76 mean_grad_P19sbar = mean(gradient_P19sbar)
77
78 grad_matrix_21sbar = [tsecC(4:end), P21s(4:end)];
79 gradient_21sbar = diff(grad_matrix_21sbar);
80 mean_grad_21sbar = mean(gradient_21sbar)
81
82 grad_matrix_24sbar = [tsecD(4:end), P24s(4:end)];
83 gradient_24sbar = diff(grad_matrix_24sbar);
84 mean_grad_24sbar = mean(gradient_24sbar)
85
```

```
grad_matrix_25sbar = [tsecE(4:end), P25s(4:end)];
gradient_25sbar = diff(grad_matrix_25sbar);
mean_grad_25sbar = mean(gradient_25sbar)

%% === PLOT TEST DATA ===

plot(thE,P25sbar,'b-')
hold on
plot(thD,P24sbar,'r-')
hold on
plot(thC,P21sbar,'m-')
hold on
plot(thB, P19sbar,'Color',[0,0.6,1])
hold on
plot(thA, P16sbar,'k-')
hold on
plot(thC,Pamb,'g-')
grid on
grid minor
xticks(1:2:48)
yticks(1:0.1:2.5)
set(findall(gcf,'-property','FontSize'),'FontSize',20)
set(gca,'XLim',[0 48])
set(gca,'YLim',[1 2.5])
xlabel('Time [h]')
ylabel('Pressure [bar]')
legend('All plugs','Plug on VLM valve','Plug on LPM valve', 'Plug on
    check valve', 'No plugs','P_{amb}')
```

Matlab code of combined leak tests at 1.1 [bar] of FOE at vacuum and ambient conditions:

```
clear all;
close all;
clc

%% === READ TEST DATA FILES ===

A = dlmread('TEST_INT_01_LeakTest_1_1bar_amb_30012019.lvm');
B = dlmread('TEST_INT_01_LeakTest_1_1bar_vac_15022019.lvm');


%% === PROCESS TEST DATA ===

Ast = smooth(A(:,1)); % smooth time, pressure, ambient pressure data
AsP = smooth(A(:,3));
AsaP = smooth(A(:,5));

Bst = smooth(B(:,1));
BsP = smooth(B(:,3));
BsaP = smooth(B(:,5));
```

```
20
21 tsecA = A(:,1); % extract time and convert to min and hrs
22 tminA = tsecA/60;
23 thA = tsecA/3600;
24
25 tsecB = B(:,1);
26 tminB = tsecB/60;
27 thB = tsecB/3600;
28
29 Pamb = repmat(1.030,size(AsP)); % extract ambient pressure from the
       data
30
31 Pambbar = AsaP/1000; % convert pressure from mbar to bar
32 Pvacbar = BsaP/1000;
33
34 P11amb = AsP;                    % convert smoothed pressure from mbar
        to bar
35 P11ambbar = P11amb/1000;
36
37 P11vac = BsP;
38 P11vacbar = P11vac/1000;
39
40 grad_matrix_P11ambbar = [tsecA(4:end), P11amb(4:end)]; % calculate
       gradient and average pressure change
41 gradient_P11ambbar = diff(grad_matrix_P11ambbar);
42 mean_grad_P11ambbar = mean(gradient_P11ambbar)
43
44 grad_matrix_P11vacbar = [tsecB(4:end), P11vac(4:end)];
45 gradient_P11vacbar = diff(grad_matrix_P11vacbar);
46 mean_grad_P11vacbar = mean(gradient_P11vacbar)
47
48 %% === PLOT DATA PLOTTING ===
49
50 plot(thA,P11ambbar,'b-')
51 hold on
52 plot(thB,P11vacbar,'r-')
53 hold on
54 plot(thA,Pambbar,'b--')
55 hold on
56 plot(thB,Pvacbar,'r--')
57 grid on
58 grid minor
59 xticks(1:1:24)
60 yticks(0.75:0.05:1.48)
61 set(findall(gcf,'-property','FontSize'),'FontSize',20)
62 set(gca,'XLim',[0 24])
63 set(gca,'YLim',[0.75 1.48])
64 xlabel('Time [h]')
65 ylabel('Pressure [bar]')
```

```
66 legend('P_{st,0} at ambient conds.','P_{st,0} at vacuum conds.','P_{
       amb} at ambient conds.')
```

Matlab code of FOE leak test part 2 and 3:

```
1  clear all;
2  close all;
3  clc
4
5  %% === READ TEST DATA FILES ===
6
7  A = dlmread('TEST_INT_01_LeakTest_1_1bar_part2_vac_21022019.lvm');
8  B = dlmread('TEST_INT_01_LeakTest_1_1bar_part3_vac_22022019.lvm');
9
10 %% === PROCESS DATA ===
11
12 Ast = smooth(A(:,1));   % smooth time, pressure, ambient pressure
       data
13 AsP = smooth(A(:,3));
14 AsaP = smooth(A(:,5));
15
16 Bst = smooth(B(:,1));
17 BsP = smooth(B(:,3));
18 BsaP = smooth(B(:,5));
19
20 tsecA = A(:,1); % extract time and convert to min and hrs
21 tminA = tsecA/60;
22 thA = tsecA/3600;
23
24 tsecB = B(:,1);
25 tminB = tsecB/60;
26 thB = tsecB/3600;
27
28 Pamb = repmat(1.030,size(AsP)); % extract ambient pressure from the
       data
29 Pvac = B(:,5);  % convert pressure from mbar to bar
30 Pvacbar = Pvac/1000;
31
32 Ppart2 = AsP;                  % convert smoothed pressure from mbar
       to bar
33 Ppart2bar = Ppart2/1000;
34
35 Ppart3 = BsP;                  % convert smoothed pressure from mbar
       to bar
36 Ppart3bar = Ppart3/1000;
37
38 grad_matrix_Ppart2bar = [tsecA(4:end), Ppart2(4:end)];  % calculate
       gradient and average pressure change
39 gradient_Ppart2bar = diff(grad_matrix_Ppart2bar);
40 mean_grad_Ppart2bar = mean(gradient_Ppart2bar)
```

```
41
42 grad_matrix_Ppart3bar = [tsecB(4:end), Ppart3(4:end)];
43 gradient_Ppart3bar = diff(grad_matrix_Ppart3bar);
44 mean_grad_Ppart3bar = mean(gradient_Ppart3bar)
45
46 %% === PLOT TEST DATA ===
47
48 plot(thA,Ppart2bar,'b-')
49 hold on
50 plot(thB,Ppart3bar,'r-')
51 grid on
52 grid minor
53 xticks(1:1:24)
54 yticks(0.45:0.05:1.26)
55 set(findall(gcf,'-property','FontSize'),'FontSize',20)
56 set(gca,'XLim',[0 24])
57 set(gca,'YLim',[0.45 1.26])
58 xlabel('Time [h]')
59 ylabel('Pressure [bar]')
60 legend('P_{st,0} Part 2','P_{st,0} Part 3','P_{amb}')
```

Matlab code of the supersonic and subsonic leak simulations:

```
1 close all
2 clear all
3 clc
4
5 %% === INPUT VARIABLES ===
6
7 prc = 0.0018;                % percentage of inner diameter [-]
8 d_tube_id = 0.00081;     % inner diameter of the tube [m]
9 p0 = 128500;              % initial pressure in the tube [Pa]
10 dt = 1;                  % time increment every measurement
11 t = 0:dt:86400;          % total simulation time [s]
12 pa = 101325;            % ambient pressure outside the tube [Pa]
13 l_tube = 0.05;           % length of the N2 tube [m]
14 M_N2 = 28.02;            % molar mass of N2 [kg/kmol]
15 R = 8314.32;             % universal gas constant [J/kmolK]
16 T = 293.15;              % temperature in the tube (room temperature
     conditions) [K]
17 Gamma = 1.404;           % N2 specific heat ratio [-]
18
19 % A = dlmread('TEST_INT_01_LeakTest_1_1bar_vac_15022019.lvm');    %
     read data values from the .lvm file
20 B = dlmread('TEST_INT_01_LeakTest_1_1bar_amb_30012019.lvm'); % read
      data values from the .lvm file
21
22
23 PB = smooth(B(:,3));                    % pressure from the file and
      smoothed [mbar]
```

```
24 PBbar = PB/1000;                          % pressure in bar [bar]
25 tBsec = B(:,1);                           % read 1st (time) column
     from test data .lvm file [s]
26 tBh = tBsec/3600;                         % convert time from [s] to [
     h]
27
28 Pamb = repmat(1.01325,size(PB));
29 tsecB = B(:,1);
30 tminB = tsecB/60;
31 thB = tsecB/3600;
32
33 %% === FUNCTIONS ===
34
35 d_leak = (prc*d_tube_id)/100;             % diameter (size) of the
     leak gap [m]
36 A_tube_i = pi*((d_tube_id^2)/4);          % tube inner cross-sectional
      area [m2]
37 A_leak = pi*((d_leak^2)/4);               % leak hole cross-sectional
     area [m2]
38 Z_c = 0.5*(1-(A_leak/A_tube_i))^(3/4);    % loss coefficient for
     sudden contraction [-]
39 Z_e = (1-(A_leak/A_tube_i))^2;            % loss coefficient for
     sudden expansion [-]
40 Z = Z_c+Z_e;                              % total loss factor (
     compression followed by expansion) [-]
41 C_d = sqrt(1/Z);                          % discharge coefficient (Cd
     =1 - no loss) [-]
42 V_tube = l_tube*A_tube_i;                 % inner tube volume [m3]
43 c_star = (1/Gamma)*sqrt((R/M_N2)*T);      % characteristic velocity [m
     /s]
44
45
46 %% === SUPERSONIC CASE SIMULATION ===
47
48 rho_supers_ini = (p0/T)*(M_N2/R);            % density at initial
     conditions [kg/m3]
49 m_out_supers_ini = (C_d*p0*A_leak)/c_star;   % mass flow out at
     initial conditions [kg/s]
50 m_N2_supers_ini = rho_supers_ini*V_tube;     % mass of nitrogen in
     the tube at initial conditions [kg]
51
52 p_supers = zeros(1,length(t));
53 p_supers(1) = p0;
54 m_N2_supers = zeros(1,length(t));
55 m_N2_supers(1) = m_N2_supers_ini;
56 m_out_supers = zeros(1,length(t));
57 m_out_supers(1) = m_out_supers_ini;
58 rho_supers = zeros(1,length(t));
59 rho_supers(1) = rho_supers_ini;
```

```
60
61 for i = 2:length(t)
62     m_N2_supers(i) = m_N2_supers(i-1)-m_out_supers(i-1)*dt;
63     rho_supers(i) = m_N2_supers(i)/V_tube;
64     m_out_supers(i) = (C_d*p_supers(i-1)*A_leak)/c_star;
65     p_supers(i) = (p_supers(i-1)/rho_supers(i-1))*rho_supers(i);
66 end
67
68 %% === SUBSONIC CASE SIMULATION ===
69
70 rho_subs_ini = (p0/T)*(M_N2/R);
71 vi_subs_ini = sqrt(1/Z)*sqrt((2*(p0-pa))/rho_subs_ini);
72 m_out_subs_ini = rho_subs_ini*vi_subs_ini*A_leak;
73 m_N2_subs_ini = rho_subs_ini*V_tube;
74
75 p_subs = zeros(1,length(t));
76 p_subs(1) = p0;
77 m_N2_subs = zeros(1,length(t));
78 m_N2_subs = m_N2_subs_ini;
79 m_out_subs = zeros(1,length(t));
80 m_out_subs(1) = m_out_subs_ini;
81 rho_subs = zeros(1,length(t));
82 rho_subs(1) = rho_subs_ini;
83 vi_subs = zeros(1,length(t));
84 vi_subs(1) = vi_subs_ini;
85
86 for j = 2:length(t)
87     m_N2_subs(j) = m_N2_subs(j-1)-m_out_subs(j-1)*dt;
88     rho_subs(j) = m_N2_subs(j)/V_tube;
89     p_subs(j) = (p_subs(j-1)/rho_subs(j-1))*rho_subs(j);
90     vi_subs(j) = sqrt(1/Z)*sqrt((2*(p_subs(j)-pa))/rho_subs(j));
91     m_out_subs(j) = rho_subs(j)*vi_subs(j)*A_leak;
92 end
93
94 p_supers_bar = p_supers/100000;
95 p_subs_bar = p_subs/100000;
96 th_theo = t/3600;
97
98 %% === PLOT SIMULATION RESULTS ===
99
100 plot(tBh,PBbar,'k-')
101 hold on
102 plot(th_theo,p_supers_bar,'b--')
103 hold on
104 plot(th_theo,p_subs_bar,'r--')
105 hold on
106 plot(thB,Pamb,'g-')
107 grid on
108 grid minor
```

```
109 xticks(0:1:24)
110 yticks(1:0.02:1.32)
111 set(findall(gcf,'-property','FontSize'),'FontSize',20)
112 set(gca,'XLim',[0 24])
113 set(gca,'YLim',[1 1.32])
114 xlabel('Time [h]')
115 ylabel('Pressure [bar]')
116 title('Pressure change over time for FOE values at ambient
    conditions')
117 legend ('Leak test data at ambient conditions','Supersonic flow (d_{
    leak} = 0.0018% d_{tube,I.D.})','Subsonic flow (d_{leak} =
    0.0018% d_{tube,I.D.})','P_{amb}')
```

Matlab code of maximum operating frequency sweep:

```
1  clear all;
2  close all;
3  clc
4
5  %% === READ DATA FILES ===
6
7  A = dlmread('ID_F_max_pwm_frequency_test_2bar_01042019.lvm');
8  filename = 'ID_F_max_pwm_frequency_test_2bar_01042019.txt';
9  delimeterIn = ' ';
10 headerlinesIn = 1;
11 B = importdata(filename,delimeterIn,headerlinesIn);
12
13 %% === PROCESS TEST DATA ===
14
15 A_pl_k = A(:,2);          % extract plenum inlet temperature from test
       data
16 A_ch_k = A(:,3);          % extract chip temperature from test data
17
18 B_t_k = B.data(:,3);      % extract tank temperature from test data
19 B_a_k = B.data(:,5);      % extract ambient temperature from test data
20 B_ppl = B.data(:,4);      % extract plenum pressure from test data
21 B_freq = B.data(:,6);     % extract frequency from test data
22
23 B_ppl_pa = B_ppl*100;     % convert pressure to [Pa]
24 coeffs = polyfit(B_freq,B_ppl_pa,18);   % create a trend line
25 xfit = 1:3000;
26 yfit = polyval(coeffs, xfit);
27
28 t_s = (B.data(:,1)-139389)/1000;  % [-139389 is to start measuring
       time from 0[s] (see test data file)]
29
30 %% === PLOT TEST DATA ===
31
32 figure(1)
33 plot(B_freq,B_t_k,'r')
```

```
hold on
plot(B_freq,B_a_k,'b')
grid on
grid minor
set(findall(gcf,'-property','FontSize'),'FontSize',20)
set(gca,'XLim',[0 3000])
xticks(0:300:3000)
yticks(25.5:0.05:26)
xlabel('Frequency [Hz]')
ylabel('Temperature [^{o}C]')
legend('T_{tank}','T_{ambient}')

figure(2)
plot(A(:,1),A_pl_k,'r')
hold on
plot(A(:,1),A_ch_k,'b')
grid on
grid minor
set(findall(gcf,'-property','FontSize'),'FontSize',20)
set(gca,'XLim',[0 170])
xticks(0:10:170)
yticks(24.5:0.5:36)
xlabel('Time [s]')
ylabel('Temperature [^{o}C]')
legend('T_{plenum}','T_{chip}')

figure(3)
plot(B_freq, B_ppl_pa,'r')
hold on
plot(xfit,yfit,'b')
grid on
grid minor
set(findall(gcf,'-property','FontSize'),'FontSize',20)
set(gca,'XLim',[0 3000])
set(gca,'YLim',[-100 500])
xticks(0:300:3000)
yticks(-100:50:500)
xlabel('Frequency [Hz]')
ylabel('Plenum Pressure [Pa]')
legend('Raw Data','Trend Line')
```

Matlab code of minimum voltage pulse duration sweep:

```
clear all;
close all;
clc

%% === READ DATA FILES ===

A = dlmread('ID_G_25Hz.lvm');
```

```
filename1 = 'ID_G_25Hz.txt';
filename2 = 'ID_G_50Hz.txt';
filename3 = 'ID_G_125Hz.txt';
filename4 = 'ID_G_250Hz.txt';
filename5 = 'ID_G_500Hz.txt';
filename6 = 'ID_G_750Hz.txt';

delimeterIn = ' ';
headerlinesIn = 1;

B = importdata(filename1,delimeterIn,headerlinesIn);
C = importdata(filename2,delimeterIn,headerlinesIn);
D = importdata(filename3,delimeterIn,headerlinesIn);
E = importdata(filename4,delimeterIn,headerlinesIn);
F = importdata(filename5,delimeterIn,headerlinesIn);
G = importdata(filename6,delimeterIn,headerlinesIn);

%% === PROCESS TEST DATA ===

B_ppl = B.data(:,4);          % extract plenum pressure from test
    data
B_ppl_pa = B_ppl*100;         % convert to [Pa]
B_dc = B.data(:,7);            % extract duty cycle from test data
coeffs = polyfit(B_dc,B_ppl_pa,12); % create trend line for test
    data
xfit6 = 10:255;
yfit6 = polyval(coeffs, xfit6);

C_ppl = C.data(:,4);
C_ppl_pa = C_ppl*100;
C_dc = C.data(:,7);
coeffs2 = polyfit(C_dc,C_ppl_pa,12);
xfit5 = 10:255;
yfit5 = polyval(coeffs, xfit5);

D_ppl = D.data(:,4);
D_ppl_pa = D_ppl*100;
D_dc = D.data(:,7);
coeffs = polyfit(D_dc,D_ppl_pa,8);
xfit4 = 10:255;
yfit4 = polyval(coeffs, xfit4);

E_ppl = E.data(:,4);
E_ppl_pa = E_ppl*100;
E_dc = E.data(:,7);
coeffs = polyfit(E_dc,E_ppl_pa,12);
xfit = 10:255;
yfit = polyval(coeffs, xfit);

```

```
55 F_ppl = F.data(:,4);
56 F_ppl_pa = F_ppl*100;
57 F_dc = F.data(:,7);
58 coeffs = polyfit(F_dc,F_ppl_pa,10);
59 xfit2 = 15:255;
60 yfit2 = polyval(coeffs, xfit2);
61
62 G_ppl = G.data(:,4);
63 G_ppl_pa = G_ppl*100;
64 G_dc = G.data(:,7);
65 coeffs = polyfit(G_dc,G_ppl_pa,10);
66 xfit3 = 20:255;
67 yfit3 = polyval(coeffs, xfit3);
68
69 %% === PLOT TEST DATA ===
70
71 figure(1)
72 plot(B_dc,B_ppl_pa,'r')
73 hold on
74 plot(xfit6,yfit6)
75 grid on
76 grid minor
77 set(findall(gcf,'-property','FontSize'),'FontSize',20)
78 set(gca,'XLim',[1 255])
79 set(gca,'YLim',[-100 225])
80 xticks(1:15:255)
81 yticks(-100:25:225)
82 xlabel('Duty Cycle [-]')
83 ylabel('Plenum Pressure [Pa]')
84 legend('f_{PWM} = 25 [Hz]','Trend Line')
85
86 figure(2)
87 plot(C_dc,C_ppl_pa,'r')
88 hold on
89 plot(xfit5,yfit5)
90 grid on
91 grid minor
92 set(findall(gcf,'-property','FontSize'),'FontSize',20)
93 set(gca,'XLim',[1 255])
94  set(gca,'YLim',[-100 250])
95 xticks(1:15:255)
96  yticks(-100:25:250)
97 xlabel('Duty Cycle [-]')
98 ylabel('Plenum Pressure [Pa]')
99 legend('f_{PWM} = 50 [Hz]','Trend Line')
100
101 figure(3)
102 plot(D_dc,D_ppl_pa,'r')
103 hold on
```

```
104 plot(xfit4,yfit4,'b')
105 grid on
106 grid minor
107 set(findall(gcf,'-property','FontSize'),'FontSize',20)
108  set(gca,'XLim',[1 255])
109  set(gca,'YLim',[-100 325])
110 xticks(1:15:255)
111 yticks(-100:25:325)
112 xlabel('Duty Cycle [-]')
113 ylabel('Plenum Pressure [Pa]')
114 legend('f_{PWM} = 125 [Hz]','Trend Line')
115
116 figure(4)
117 plot(E_dc,E_ppl_pa,'r')
118 hold on
119 plot(xfit,yfit,'b')
120 grid on
121 grid minor
122 set(findall(gcf,'-property','FontSize'),'FontSize',20)
123 set(gca,'XLim',[1 255])
124 set(gca,'YLim',[-100 350])
125 xticks(1:15:255)
126 yticks(-100:25:350)
127 xlabel('Duty Cycle [-]')
128 ylabel('Plenum Pressure [Pa]')
129 legend('f_{PWM} = 250 [Hz]','Trend Line')
130
131 figure(5)
132 plot(F_dc,F_ppl_pa,'r')
133 hold on
134 plot(xfit2,yfit2,'b')
135 grid on
136 grid minor
137 set(findall(gcf,'-property','FontSize'),'FontSize',20)
138 set(gca,'XLim',[1 255])
139 set(gca,'YLim',[-100 275])
140 xticks(1:15:275)
141 yticks(-100:25:300)
142 xlabel('Duty Cycle [-]')
143 ylabel('Plenum Pressure [Pa]')
144 legend('f_{PWM} = 500 [Hz]','Trend Line')
145
146 figure(6)
147 plot(G_dc,G_ppl_pa,'r')
148 hold on
149 plot(xfit3,yfit3,'b')
150 grid on
151 grid minor
152 set(findall(gcf,'-property','FontSize'),'FontSize',20)
```

```
153 set(gca,'XLim',[1 255])
154 set(gca,'YLim',[-100 300])
155 xticks(1:15:255)
156 yticks(-100:25:300)
157 xlabel('Duty Cycle [-]')
158 ylabel('Plenum Pressure [Pa]')
159 legend('f_{PWM} = 750 [Hz]','Trend Line')
```

Matlab code of pressure stability at 200 [mbar]:

```
1  clear all;
2  close all;
3  clc
4
5  %% === READ DATA FILES ===
6
7  filename = 'ID_H_300Pa_250Hz_706DC.txt';
8  filename2 = 'ID_H_300Pa_250Hz_Linear_x10DC.txt';
9  filename3 = 'ID_H_300Pa_250Hz_Linear_x33DC.txt';
10 filename4 = 'ID_H_300Pa_250Hz_Linear_x33DC.txt';
11 delimeterIn = ' ';
12 headerlinesIn = 1;
13 B = importdata(filename,delimeterIn,headerlinesIn);
14 C = importdata(filename2,delimeterIn,headerlinesIn);
15 D = importdata(filename3,delimeterIn,headerlinesIn);
16 E = importdata(filename4,delimeterIn,headerlinesIn);
17
18 %% === PROCESS TEST DATA ===
19
20 B_ppl = B.data(:,4);              % extract plenum pressure from test
       data
21 B_ppl_pa = B_ppl*100;            % convert to [Pa]
22 t_s = (B.data(:,1)-19146)/1000;     % [-19146 is to start measuring
       time from 0[s] (see test data file)]
23 coeffs = polyfit(t_s,B_ppl_pa,2); % create trend line for test data
24 xfit = 0:200;
25 yfit = polyval(coeffs, xfit);
26
27 C_ppl = C.data(:,4);
28 C_ppl_pa = C_ppl*100;
29 t_s2 = (C.data(:,1)-131114)/1000; % [-131114 is to start measuring
       time from 0[s] (see test data file)]
30 coeffs = polyfit(t_s2,C_ppl_pa,2);
31 xfit2 = 0:70;
32 yfit2 = polyval(coeffs, xfit2);
33
34 D_ppl = D.data(:,4);
35 D_ppl_pa = D_ppl*100;
36 t_s3 = (D.data(:,1)-43)/1000; % [-43 is to start measuring time from
        0[s] (see test data file)]
```

```
37 coeffs = polyfit(t_s3,D_ppl_pa,8);
38 xfit3 = 0:200;
39 yfit3 = polyval(coeffs, xfit3);
40
41 E_ppl = E.data(:,4);
42 E_ppl_pa = E_ppl*100;
43 t_s4 = (E.data(:,1)-88)/1000;   % [-88 is to start measuring time
       from 0[s] (see test data file)]
44 coeffs = polyfit(t_s4,E_ppl_pa,5);
45 xfit4 = 0:37;
46 yfit4 = polyval(coeffs, xfit4);
47
48
49 %% === PLOT TEST DATA ===
50
51 figure(1)
52 plot(t_s,B_ppl_pa,'r')
53 hold on
54 plot(xfit,yfit)
55 grid on
56 grid minor
57 set(findall(gcf,'-property','FontSize'),'FontSize',20)
58 set(gca,'XLim',[0 200])
59 set(gca,'YLim',[-5 17])
60 xticks(0:10:200)
61 yticks(-5:2:17)
62 xlabel('Time [s]')
63 ylabel('Plenum Pressure [Pa]')
64 legend('Raw Data','Trend Line')
65
66 figure(2)
67
68 subplot(3,1,1)
69 plot(t_s2,C_ppl_pa,'r')
70 hold on
71 plot(xfit2,yfit2,'b')
72 grid on
73 grid minor
74 set(findall(gcf,'-property','FontSize'),'FontSize',20)
75 xlabel('Time [s]')
76 ylabel('Plenum Pressure [Pa]')
77 legend('Raw Data','Trend Line')
78
79 subplot(3,1,2)
80 plot(t_s3,D_ppl_pa,'r')
81 hold on
82 plot(xfit3,yfit3,'b')
83 grid on
84 grid minor
```

```
85 set(findall(gcf,'-property','FontSize'),'FontSize',20)
86 xlabel('Time [s]')
87 ylabel('Plenum Pressure [Pa]')
88 legend('Raw Data','Trend Line')
89
90 subplot(3,1,3)
91 plot(t_s4,E_ppl_pa,'r')
92 hold on
93 plot(xfit4,yfit4,'b')
94 grid on
95 grid minor
96 set(findall(gcf,'-property','FontSize'),'FontSize',20)
97 xlabel('Time [s]')
98 ylabel('Plenum Pressure [Pa]')
99 legend('Raw Data','Trend Line')
```

Matlab code of pressure stability at 400 [mbar]:

```
1 clear all;
2 close all;
3 clc
4
5 %% ===== READ DATA FILES =====
6
7 filename = 'ID_H_400mbar_300Pa_125Hz_Linear_x60DC.txt';
8 filename2 = 'ID_H_400mbar_300Pa_250Hz_Linear_x60DC.txt';
9 filename3 = 'ID_H_400mbar_300Pa_500Hz_Linear_x60DC.txt';
10 filename4 = 'ID_H_400mbar_300Pa_750Hz_Linear_x60DC.txt';
11 filename5 = 'ID_H_400mbar_300Pa_1000Hz_Linear_x60DC.txt';
12 delimeterIn = ' ';
13 headerlinesIn = 1;
14 B = importdata(filename,delimeterIn,headerlinesIn);
15 C = importdata(filename2,delimeterIn,headerlinesIn);
16 D = importdata(filename3,delimeterIn,headerlinesIn);
17 E = importdata(filename4,delimeterIn,headerlinesIn);
18 F = importdata(filename5,delimeterIn,headerlinesIn);
19
20 %% === PROCESS TEST DATA ===
21
22 B_ppl = B.data(:,4);              % extract plenum pressure from test
     data
23 B_ppl_pa = B_ppl*100;             % convert to [Pa]
24 t_s = (B.data(:,1)-65578)/1000; % extract test time [-65578 is to
     start measuring time from 0[s] (see test data file)]
25 coeffs = polyfit(t_s,B_ppl_pa,8);   % create trend line for test
     data
26 xfit = 0:44;
27 yfit = polyval(coeffs, xfit);
28
29 C_ppl = C.data(:,4);
```

```
30 C_ppl_pa = C_ppl*100;
31 t_s2 = (C.data(:,1)-43)/1000;   % [-43 is to start measuring time
       from 0[s] (see test data file)]
32 coeffs = polyfit(t_s2,C_ppl_pa,8);
33 xfit2 = 0:45;
34 yfit2 = polyval(coeffs, xfit2);
35
36 D_ppl = D.data(:,4);
37 D_ppl_pa = D_ppl*100;
38 t_s3 = (D.data(:,1)-42)/1000;   % [-42 is to start measuring time
       from 0[s] (see test data file)]
39 coeffs = polyfit(t_s3,D_ppl_pa,20);
40 xfit3 = 0:46;
41 yfit3 = polyval(coeffs, xfit3);
42
43 E_ppl = E.data(:,4);
44 E_ppl_pa = E_ppl*100;
45 t_s4 = (E.data(:,1)-44)/1000;   % [-44 is to start measuring time
       from 0[s] (see test data file)]
46 coeffs = polyfit(t_s4,E_ppl_pa,15);
47 xfit4 = 0:47;
48 yfit4 = polyval(coeffs, xfit4);
49
50 F_ppl = F.data(:,4);
51 F_ppl_pa = F_ppl*100;
52 t_s5 = (F.data(:,1)-43)/1000; % [-44 is to start measuring time from
       0[s] (see test data file)]
53 coeffs = polyfit(t_s5,F_ppl_pa,25);
54 xfit5 = 0:50;
55 yfit5 = polyval(coeffs, xfit5);
56
57
58 %% === PLOT DATA ===
59
60 figure(1)
61 plot(t_s,B_ppl_pa,'r')
62 hold on
63 plot(xfit,yfit)
64 grid on
65 grid minor
66 set(findall(gcf,'-property','FontSize'),'FontSize',20)
67 set(gca,'XLim',[0 45])
68 set(gca,'YLim',[0 175])
69 xticks(0:2:45)
70 yticks(0:10:175)
71 xlabel('Time [s]')
72 ylabel('Plenum Pressure [Pa]')
73 legend('f_{PWM} = 125 [Hz]','Trend Line')
74
```

```
figure(2)
plot(t_s2,C_ppl_pa,'r')
hold on
plot(xfit2,yfit2,'b')
grid on
grid minor
set(findall(gcf,'-property','FontSize'),'FontSize',20)
set(gca,'XLim',[0 45])
set(gca,'YLim',[0 150])
xticks(0:2:45)
yticks(0:10:150)
xlabel('Time [s]')
ylabel('Plenum Pressure [Pa]')
legend('f_{PWM} = 250 [Hz]','Trend Line')

figure(3)
plot(t_s3,D_ppl_pa,'r')
hold on
plot(xfit3,yfit3,'b')
grid on
grid minor
set(findall(gcf,'-property','FontSize'),'FontSize',20)
set(gca,'XLim',[0 47])
set(gca,'YLim',[0 140])
xticks(0:2:47)
yticks(0:10:140)
xlabel('Time [s]')
ylabel('Plenum Pressure [Pa]')
legend('f_{PWM} = 500 [Hz]','Trend Line')

figure(4)
plot(t_s4,E_ppl_pa,'r')
hold on
plot(xfit4,yfit4,'b')
grid on
grid minor
set(findall(gcf,'-property','FontSize'),'FontSize',20)
set(gca,'XLim',[0 48])
set(gca,'YLim',[0 140])
xticks(0:2:48)
yticks(0:10:140)
xlabel('Time [s]')
ylabel('Plenum Pressure [Pa]')
legend('f_{PWM} = 750 [Hz]','Trend Line')

figure(5)
plot(t_s5,F_ppl_pa,'r')
hold on
plot(xfit5,yfit5,'b')
```

```
grid on
grid minor
set(findall(gcf,'-property','FontSize'),'FontSize',20)
set(gca,'XLim',[0 50])
set(gca,'YLim',[0 140])
xticks(0:2:50)
yticks(0:10:140)
xlabel('Time [s]')
ylabel('Plenum Pressure [Pa]')
legend('f_{PWM} = 1000 [Hz]','Trend Line')

figure(6)
plot(t_s,B.data(:,2))
hold on
plot(t_s2,C.data(:,2))
hold on
plot(t_s3,D.data(:,2))
hold on
plot(t_s4,E.data(:,2))
hold on
plot(t_s5,F.data(:,2))
grid on
grid minor
set(findall(gcf,'-property','FontSize'),'FontSize',20)
xlabel('Time [s]')
ylabel('Plenum Pressure [mbar]')
legend('f_{PWM} = 125 [Hz]','f_{PWM} = 250 [Hz]','f_{PWM} = 500 [Hz]
    ','f_{PWM} = 750 [Hz]','f_{PWM} = 1000 [Hz]')
```

Matlab code of pressure stability at 1000 [mbar] for target pressure of 50 [Pa]:

```
clear all;
close all;
clc

%% === READ DATA FILES ===

filename = 'ID_H_1000mbar_50Pa_50Hz_Quadratic_143469E8DC.txt';
filename2 = 'ID_H_1000mbar_50Pa_250Hz_Quadratic_143469E8DC.txt';
filename3 = 'ID_H_1000mbar_50Pa_500Hz_Quadratic_143469E8DC.txt';
delimeterIn = ' ';
headerlinesIn = 1;
A = importdata(filename,delimeterIn,headerlinesIn);
B = importdata(filename2,delimeterIn,headerlinesIn);
C = importdata(filename3,delimeterIn,headerlinesIn);

%% === PROCESS TEST DATA ===

A_ppl = A.data(:,4);            % extract plenum pressure from test
    data
```

```
19 A_ppl_pa = A_ppl*100;            % convert to [Pa]
20 t_s = (A.data(:,1)-43)/1000;     % [-43 is to start measuring time
      from 0[s] (see test data file)]
21 coeffs = polyfit(t_s,A_ppl_pa,15); % create trend line for test data
22 xfit = 0:165;
23 yfit = polyval(coeffs, xfit);
24
25 B_ppl = B.data(:,4);
26 B_ppl_pa = B_ppl*100;
27 t_s2 = (B.data(:,1)-43)/1000; % [-43 is to start measuring time from
      0[s] (see test data file)]
28 coeffs = polyfit(t_s2,B_ppl_pa,15);
29 xfit2 = 0:185;
30 yfit2 = polyval(coeffs, xfit2);
31
32 C_ppl = C.data(:,4);
33 C_ppl_pa = C_ppl*100;
34 t_s3 = (C.data(:,1)-42)/1000; % [-42 is to start measuring time from
      0[s] (see test data file)]
35 coeffs = polyfit(t_s3,C_ppl_pa,15);
36 xfit3 = 0:200;
37 yfit3 = polyval(coeffs, xfit3);
38
39 %% === PLOT TEST DATA ===
40
41 figure(1)
42 subplot(3,1,1)
43 plot(t_s,A_ppl_pa,'r')
44 hold on
45 plot(xfit,yfit,'b')
46 grid on
47 grid minor
48 set(findall(gcf,'-property','FontSize'),'FontSize',20)
49 set(gca,'XLim',[0 165])
50 set(gca,'YLim',[0 170])
51 xticks(0:10:165)
52 yticks(0:30:170)
53 xlabel('Time [s]')
54 ylabel('Plenum Pressure [Pa]')
55 legend('f_{PWM} = 50 [Hz]','Trend Line')
56
57 subplot(3,1,2)
58 plot(t_s2,B_ppl_pa,'r')
59 hold on
60 plot(xfit2,yfit2,'b')
61 grid on
62 grid minor
63 set(findall(gcf,'-property','FontSize'),'FontSize',20)
64 set(gca,'XLim',[0 185])
```

```
set(gca,'YLim',[0 75])
xticks(0:10:185)
yticks(0:15:75)
xlabel('Time [s]')
ylabel('Plenum Pressure [Pa]')
legend('f_{PWM} = 250 [Hz]','Trend Line')

subplot(3,1,3)
plot(t_s3,C_ppl_pa,'r')
hold on
plot(xfit3,yfit3,'b')
grid on
grid minor
set(findall(gcf,'-property','FontSize'),'FontSize',20)
set(gca,'XLim',[0 200])
set(gca,'YLim',[0 110])
xticks(0:10:200)
yticks(0:15:110)
xlabel('Time [s]')
ylabel('Plenum Pressure [Pa]')
legend('f_{PWM} = 500 [Hz]','Trend Line')
```

Matlab code of pressure stability at 1000 [mbar] for target pressure of 150 [Pa]:

```
clear all;
close all;
clc

%% === READ DATA FILES ===

filename = 'ID_H_1000mbar_150Pa_50Hz_Quadratic_143469E8DC.txt';
filename2 = 'ID_H_1000mbar_150Pa_250Hz_Quadratic_143469E8DC.txt';
filename3 = 'ID_H_1000mbar_150Pa_500Hz_Quadratic_143469E8DC.txt';
delimeterIn = ' ';
headerlinesIn = 1;
A = importdata(filename,delimeterIn,headerlinesIn);
B = importdata(filename2,delimeterIn,headerlinesIn);
C = importdata(filename3,delimeterIn,headerlinesIn);

%% === PROCESS TEST DATA ===

A_ppl = A.data(:,4);          % extract plenum pressure from test
    data
A_ppl_pa = A_ppl*100;             % convert to [Pa]
t_s = (A.data(:,1)-43)/1000; % [-43 is to start measuring time from
    0[s] (see test data file)]
coeffs = polyfit(t_s,A_ppl_pa,15); % create trend line for test data
xfit = 0:72;
yfit = polyval(coeffs, xfit);

```

```
25 B_ppl = B.data(:,4);
26 B_ppl_pa = B_ppl*100;
27 t_s2 = (B.data(:,1)-131115)/1000; % [-131115 is to start measuring
      time from 0[s] (see test data file)]
28 coeffs = polyfit(t_s2,B_ppl_pa,15);
29 xfit2 = 0:70;
30 yfit2 = polyval(coeffs, xfit2);
31
32 C_ppl = C.data(:,4);
33 C_ppl_pa = C_ppl*100;
34 t_s3 = (C.data(:,1)-65579)/1000; % [-65579 is to start measuring
      time from 0[s] (see test data file)]
35 coeffs = polyfit(t_s3,C_ppl_pa,15);
36 xfit3 = 0:79;
37 yfit3 = polyval(coeffs, xfit3);
38
39 %% === PLOT TEST DATA ===
40
41 figure(1)
42 subplot(3,1,1)
43 plot(t_s,A_ppl_pa,'r')
44 hold on
45 plot(xfit,yfit)
46 grid on
47 grid minor
48 set(findall(gcf,'-property','FontSize'),'FontSize',20)
49 set(gca,'XLim',[0 72])
50 set(gca,'YLim',[0 480])
51 xticks(0:3:72)
52 yticks(0:80:480)
53 xlabel('Time [s]')
54 ylabel('Plenum Pressure [Pa]')
55 legend('f_{PWM} = 50 [Hz]','Trend Line')
56
57 subplot(3,1,2)
58 plot(t_s2,B_ppl_pa,'r')
59 hold on
60 plot(xfit2,yfit2)
61 grid on
62 grid minor
63 set(findall(gcf,'-property','FontSize'),'FontSize',20)
64 set(gca,'XLim',[0 70])
65 set(gca,'YLim',[0 210])
66 xticks(0:3:70)
67 yticks(0:30:210)
68 xlabel('Time [s]')
69 ylabel('Plenum Pressure [Pa]')
70 legend('f_{PWM} = 250 [Hz]','Trend Line')
71
```

```
subplot(3,1,3)
plot(t_s3,C_ppl_pa,'r')
hold on
plot(xfit3,yfit3)
grid on
grid minor
set(findall(gcf,'-property','FontSize'),'FontSize',20)
set(gca,'XLim',[0 80])
set(gca,'YLim',[0 180])
xticks(0:4:80)
yticks(0:20:180)
xlabel('Time [s]')
ylabel('Plenum Pressure [Pa]')
legend('f_{PWM} = 500 [Hz]','Trend Line')
```

Matlab code of pressure stability at 1000 [mbar] for target pressure of 300 [Pa]:

```
clear all;
close all;
clc

%% ===== READ TEST DATA FILES =====

filename = 'ID_H_1000mbar_300Pa_50Hz_Quadratic_143469E8DC.txt';
filename2 = 'ID_H_1000mbar_300Pa_250Hz_Quadratic_143469E8DC.txt';
filename3 = 'ID_H_1000mbar_300Pa_500Hz_Quadratic_143469E8DC.txt';
delimeterIn = ' ';
headerlinesIn = 1;
A = importdata(filename,delimeterIn,headerlinesIn);
B = importdata(filename2,delimeterIn,headerlinesIn);
C = importdata(filename3,delimeterIn,headerlinesIn);

%% === PROCESS TEST DATA ===

A_ppl = A.data(:,4);          % extract plenum pressure from test
    data
A_ppl_pa = A_ppl*100;           % convert to [Pa]
t_s = (A.data(:,1)-43)/1000;  % [-43 is to start measuring time from
    0[s] (see test data file)]
coeffs = polyfit(t_s,A_ppl_pa,15);  % create trend line for test
    data
xfit = 0:50;
yfit = polyval(coeffs, xfit);

B_ppl = B.data(:,4);
B_ppl_pa = B_ppl*100;
t_s2 = (B.data(:,1)-43)/1000; % [-43 is to start measuring time from
    0[s] (see test data file)]
coeffs = polyfit(t_s2,B_ppl_pa,15);
xfit2 = 0:45;
```

```
30 yfit2 = polyval(coeffs, xfit2);
31
32 C_ppl = C.data(:,4);
33 C_ppl_pa = C_ppl*100;
34 t_s3 = (C.data(:,1)-65579)/1000; % [-65579 is to start measuring
      time from 0[s] (see test data file)]
35 coeffs = polyfit(t_s3,C_ppl_pa,15);
36 xfit3 = 0:45;
37 yfit3 = polyval(coeffs, xfit3);
38
39 %% === PLOT TEST DATA ===
40
41 figure(1)
42 subplot(3,1,1)
43 plot(t_s,A_ppl_pa,'r')
44 hold on
45 plot(xfit,yfit)
46 grid on
47 grid minor
48 set(findall(gcf,'-property','FontSize'),'FontSize',20)
49 set(gca,'XLim',[0 50])
50 set(gca,'YLim',[0 650])
51 xticks(0:2:50)
52 yticks(0:80:650)
53 xlabel('Time [s]')
54 ylabel('Plenum Pressure [Pa]')
55 legend('f_{PWM} = 50 [Hz]','Trend Line')
56
57 subplot(3,1,2)
58 plot(t_s2,B_ppl_pa,'r')
59 hold on
60 plot(xfit2,yfit2)
61 grid on
62 grid minor
63 set(findall(gcf,'-property','FontSize'),'FontSize',20)
64 set(gca,'XLim',[0 45])
65 set(gca,'YLim',[0 370])
66 xticks(0:2:45)
67 yticks(0:50:370)
68 xlabel('Time [s]')
69 ylabel('Plenum Pressure [Pa]')
70 legend('f_{PWM} = 250 [Hz]','Trend Line')
71
72 subplot(3,1,3)
73 plot(t_s3,C_ppl_pa,'r')
74 hold on
75 plot(xfit3,yfit3)
76 grid on
77 grid minor
```

```
set(findall(gcf,'-property','FontSize'),'FontSize',20)
set(gca,'XLim',[0 45])
set(gca,'YLim',[0 330])
xticks(0:2:45)
yticks(0:40:330)
xlabel('Time [s]')
ylabel('Plenum Pressure [Pa]')
legend('f_{PWM} = 500 [Hz]','Trend Line')
```

Matlab code of pressure stability at FOE values:

```
clear all;
close all;
clc

%% === READ DATA FILES ===

filename = 'ID_I_300Pa_250Hz.txt';
delimeterIn = ' ';
headerlinesIn = 1;
A = importdata(filename,delimeterIn,headerlinesIn);

%% === PROCESS TEST DATA ===

A_ppl = A.data(:,4);    % extract plenum pressure from test data
A_ppl_pa = A_ppl*100;   % convert to [Pa]
t_s = (A.data(:,1)-42)/1000;    % [-42 is to start measuring time
    from 0[s] (see test data file)]
coeffs = polyfit(t_s,A_ppl_pa,20); % create trend line for test data
xfit = 0:50;
yfit = polyval(coeffs, xfit);

%% === PLOT TEST DATA ===

figure(1)
plot(t_s,A_ppl_pa,'r')
grid on
grid minor
set(findall(gcf,'-property','FontSize'),'FontSize',20)
set(gca,'XLim',[0 2])
set(gca,'YLim',[-5 210])
xticks(0:0.1:2)
yticks(-10:20:210)
xlabel('Time [s]')
ylabel('Plenum Pressure [Pa]')
legend('f_{PWM} = 250 [Hz]')
```

Matlab code of coil resistance:

```
close all
clear all
```

```
clc

%% === INPUT TEST DATA ===

T = [25; 35; 45; 55; 65; 70]+273.15;    % input measured
    temperatures and convert from [oC] to [K]
R = [39.9; 40.6; 41.7; 42.7; 43.4; 44.2]; % input measured
    resistance

p1=polyfit(T, R, 1);                    % create trend line
p_fitted=polyval(p1, T);

%% === PLOT TEST DATA ===

plot(T,R,'o','Markeredgecolor','red')
hold on
plot(T,p_fitted,'b')
grid on
grid minor
set(gca,'XLim',[295 345])
set(gca,'YLim',[39.5 44.5])
xticks(295:3:360)
yticks(39.5:0.5:44.5)
set(findall(gcf,'-property','FontSize'),'FontSize',20)
xlabel("Temperature [K]")
ylabel("Coil Resistance [\Omega]")
legend('Measured values', 'Trend line')
```

Matlab code for power-pressure data processing:

```
clear all
close all
clc

%% === INPUT CONSTANTS ===

cpl=4187;       %[J/K/kg] specific heat of liquid water
cpg=1996;       %[J/K/kg] specific heat of gaseous water
lh=2256*1000;   %[J/kg] heat of vaporization of water
Ra=8.314;       %[J/K/mol] constant of gases
Mw=18.02e-3;    %[kg/mol] molecular mass of water vapour
gamma=1.32;     %specific heat ratio of water vapour
p1=1*101325;    %[Pa] standard conditions water boiling pressure
T1=373;         %[K] standard conditions water boiling temperature
    at 1 atm
At=4.5e-9;      %[m^2] nozzle throat area

%user needs to define the mass flow and the chamber temperature

%mdot=2;        %[ml/h] water mass flow in the test
```

```
20 T0=50;           %[C] temeperature in the plenum during the test, I
       keep it at 50 always (at around 45-58 all chips overflow)
21
22 %% === PROCESS TEST DATA ===
23
24 % calculates ideal power, pressure in chamber and Tvap for all the
       mdot used (from 0.5 to 3)
25
26 m_vec=[0.5,1,1.5,2, 2.5, 3];
27 Qdot_ideal_vec=[];
28 pc_ideal_vec=[];
29 Tvap_ideal_vec=[];
30 for i=1:6
31     Qdot_ideal_vec(i)= ideal_power(m_vec(i),T0, At, Ra, Mw, gamma,
           cpl, lh, T1, p1);
32     [pc_ideal_vec(i), Tvap_ideal_vec(i)]=chamber_pressure(m_vec(i),
           At, Ra, Mw, gamma, T1, lh, p1); %[Pa] the chamber pressure in
           vacuum
33 end
34
35 %% === FIT TEST DATA ===
36
37 % TRY TO FIT CURVES WITH POLYNOMIALS OF 1st DEGREE:
38
39 %% CHIP 01-BS2-01
40
41 mdot_1=[0.5, 1, 1.5, 2];          % tested mass flow values
42 Qreal_1=[2.2, 2.8, 3.4, 4.1];     % measured input power values
43
44 mdot_11=[0.5, 1, 2];              % values of mdot with sure results
45 Qreal_11=[2.2, 2.8, 4.1];         % sure input power results
46
47 % this part is for the 01-BS2-01 taking into account the value
       gueesed for 1.5 ml/h
48 p1=polyfit(pc_ideal_vec(1:4), Qreal_1, 1);
49 y_1=polyval(p1, pc_ideal_vec);
50
51 % this part is for the 01-BS2-01 not taking into account the value
       at 1.5 ml/h
52 p11=polyfit([pc_ideal_vec(1:2), pc_ideal_vec(4)], Qreal_11, 1);
53 y_11=polyval(p11, pc_ideal_vec);
54
55 %% CHIP 01-Ld1-01
56
57 mdot_2=[0.5, 1, 2];   %values of mdot
58 Qreal_2=[2.6, 3.2, 4.3];
59
60 p2=polyfit([pc_ideal_vec(1:2), pc_ideal_vec(4)], Qreal_2, 1);
61 pc_2_1=linspace(1.5e4, 11e4, 10);
```

```
62 y_2=polyval(p2, pc_ideal_vec);
63
64 %% CHIP 01-Ws1-01
65
66 mdot_3=[0.5, 1, 1.5];   %values of mdot
67 Qreal_3=[2.3, 2.6, 3.4];
68
69 %here there are only the values for mdot=[0.5, 1, 1.5]
70 p3=polyfit(pc_ideal_vec(1:3), Qreal_3, 1);
71 pc_3_1=linspace(1.5e4, 11e4, 10);
72 y_3=polyval(p3, pc_ideal_vec);
73
74 %this part also guesses a value for mdot=2 ml/h, so the line
       obtained is better
75 p33=polyfit(pc_ideal_vec(1:4), [Qreal_3, 4.2], 1);
76 y_33=polyval(p33, pc_ideal_vec);
77
78 %% CHIP 01-Ls2-01
79
80 mdot_4=[2.5, 3];   %values of mdot
81 Qreal_4=[3.375, 4.29];
82
83 % here there are only the values for mdot=[2.5, 3]
84 p4=polyfit(pc_ideal_vec(5:6), Qreal_4, 1);
85 pc_4_1=linspace(1.5e4, 11e4, 10);
86 y_4=polyval(p4, pc_ideal_vec);
87
88 %% CHIP 01-WS2-01
89
90 mdot_5=[0.5, 1, 1.5];   %values of mdot
91 Qreal_5=[2.88, 4.43, 4.64];
92
93 %here there are only the values for mdot=[0.5, 1, 1.5]
94 p5=polyfit(pc_ideal_vec(1:3), Qreal_5, 1);
95 pc_5_1=linspace(1.5e4, 11e4, 10);
96 y_5=polyval(p5, pc_ideal_vec);
97
98 %% === HEATER EFFICIENCY ===
99
100 BS2_eff = Qdot_ideal_vec ./ y_1;
101 Ld1_eff = Qdot_ideal_vec ./ y_2;
102 Ws1_eff = Qdot_ideal_vec ./ y_3;
103 WS2_eff = Qdot_ideal_vec ./ y_5;
104
105 eff_merge = [BS2_eff; Ld1_eff; Ws1_eff; WS2_eff];
106
107 %% === PLOT FOR 01-BS2-01 ===
108
109 figure
```

```
110 plot(pc_ideal_vec, Qdot_ideal_vec, [pc_ideal_vec(1:2), pc_ideal_vec
      (4)], [Qreal_1(1:2), Qreal_1(4)], 'o', pc_ideal_vec(3), Qreal_1
      (3), 'X', 'Markeredgecolor','red')
111 grid on
112 grid minor
113 set(findall(gcf,'-property','FontSize'),'FontSize',20)
114 text(pc_ideal_vec(1),Qreal_1(1),'    0.5[mL/h]','FontSize',20)
115 hold on
116 text(pc_ideal_vec(2),Qreal_1(2),'    1[mL/h]','FontSize',20)
117 hold on
118 text(pc_ideal_vec(3),Qreal_1(3),'    1.5[mL/h]','FontSize',20)
119 hold on
120 text(pc_ideal_vec(4),Qreal_1(4),'    2[mL/h]','FontSize',20)
121 hold on
122 plot(pc_ideal_vec,y_11,'k--')
123 xticks(0:0.5e4:12e4)
124 yticks(0:0.5:6)
125 xlabel('Chamber pressure [Pa]')
126 ylabel('Power [W]')
127 legend('Ideal case', 'Real case','Predicted value', 'Real case trend
      line')
128
129 %% === PLOT FOR 01-Ld1-01 ===
130
131 figure
132 plot(pc_ideal_vec, Qdot_ideal_vec, [pc_ideal_vec(1:2), pc_ideal_vec
      (4)], Qreal_2, 'o', pc_ideal_vec(3), 3.8, 'X','Markeredgecolor','
      red')
133 grid on
134 grid minor
135 set(findall(gcf,'-property','FontSize'),'FontSize',20)
136 text(pc_ideal_vec(1),Qreal_2(1),'    0.5[mL/h]','FontSize',20)
137 hold on
138 text(pc_ideal_vec(2),Qreal_2(2),'    1[mL/h]','FontSize',20)
139 hold on
140 text(pc_ideal_vec(3),3.8,'    1.5[mL/h]','FontSize',20)
141 hold on
142 text(pc_ideal_vec(4),Qreal_2(3),'    2[mL/h]','FontSize',20)
143 hold on
144 plot(pc_ideal_vec, y_2,'k--')
145 xticks(0:0.5e4:12e4)
146 yticks(0:0.5:6)
147 xlabel('Chamber pressure [Pa]')
148 ylabel('Power [W]')
149 legend('Ideal case', 'Real case', 'Predicted value', 'Real case
      trend line')
150
151 %% === PLOT FOR 01-Ws1-01 ===
152
```

```
153 figure
154 plot(pc_ideal_vec, Qdot_ideal_vec, [pc_ideal_vec(1:2), pc_ideal_vec
    (3)], Qreal_3, 'o', 'Markeredgecolor','red')
155 grid on
156 grid minor
157 set(findall(gcf,'-property','FontSize'),'FontSize',20)
158 text(pc_ideal_vec(1),Qreal_3(1),'    0.5[mL/h]','FontSize',20)
159 hold on
160 text(pc_ideal_vec(2),Qreal_3(2),'    1[mL/h]','FontSize',20)
161 hold on
162 text(pc_ideal_vec(3),Qreal_3(3),'    1.5[mL/h]','FontSize',20)
163 hold on
164 plot(pc_ideal_vec, y_33,'k--')
165 xticks(0:0.5e4:12e4)
166 yticks(0:0.5:6)
167 xlabel('Chamber pressure [Pa]')
168 ylabel('Power [W]')
169 legend('Ideal case', 'Real case', 'Real case trend line')
170
171 %% === PLOT PLOT 01-Ls2-01 ===
172
173 figure
174 plot(pc_ideal_vec, Qdot_ideal_vec, [pc_ideal_vec(5), pc_ideal_vec(6)
    ], Qreal_4, 'X', 'Markeredgecolor','red','MarkerSize',12)
175 grid on
176 grid minor
177 set(findall(gcf,'-property','FontSize'),'FontSize',20)
178 hold on
179 plot(pc_ideal_vec, y_4,'k--')
180 text(pc_ideal_vec(5),Qreal_4(1),'    2.5[mL/h]','FontSize',20)
181 hold on
182 text(pc_ideal_vec(6),Qreal_4(2),'    3[mL/h]','FontSize',20)
183 set(gca,'XLim',[0 12.5e4])
184 set(gca,'YLim',[0 5])
185 xticks(0:0.5e4:12.5e4)
186 yticks(0:0.5:6)
187 xlabel('Chamber pressure [Pa]')
188 ylabel('Power [W]')
189 legend('Ideal case','Predicted value', 'Predicted trend line')
190
191 %% === PLOT FOR 01-WS2-01 ===
192
193 figure
194 plot(pc_ideal_vec, Qdot_ideal_vec, [pc_ideal_vec(2), pc_ideal_vec(3)
    ], Qreal_5(2:3), 'o',pc_ideal_vec(1), Qreal_5(1), 'X' ,'
    Markeredgecolor','red')
195 grid on
196 grid minor
197 set(findall(gcf,'-property','FontSize'),'FontSize',20)
```

```
198 text(pc_ideal_vec(1),Qreal_5(1),'    0.5[mL/h]','FontSize',20)
199 hold on
200 text(pc_ideal_vec(2),Qreal_5(2),'    1[mL/h]','FontSize',20)
201 hold on
202 text(pc_ideal_vec(3),Qreal_5(3),'    1.5[mL/h]','FontSize',20)
203 hold on
204 plot(pc_ideal_vec, y_5,'k--')
205 xticks(0:0.5e4:12e4)
206 yticks(0:0.5:8)
207 xlabel('Chamber pressure [Pa]')
208 ylabel('Power [W]')
209 legend('Ideal case', 'Real case', 'Predicted value', 'Real case
      trend line')
210
211 %% === PLOT ALL TREND LINES TOGETHER ===
212
213 figure
214 plot(pc_ideal_vec,y_11,'g')
215 hold on
216 plot(pc_ideal_vec, y_2,'r')
217 hold on
218 plot(pc_ideal_vec, y_33,'b')
219 hold on
220 plot(pc_ideal_vec, y_5,'Color', [1, 0.8, 0.0])
221 grid on
222 grid minor
223 set(findall(gcf,'-property','FontSize'),'FontSize',20)
224 xticks(0:0.5e4:12e4)
225 yticks(0:0.5:8)
226 xlabel('Chamber pressure [Pa]')
227 ylabel('Power [W]')
228 legend('01-BS2-01', '01-Ld1-01', '01-Ws1-01', '01-WS2-01')
```

Matlab function for chamber pressure:

```
1 function [pc, Tvap]=chamber_pressure(mdot, At, Ra, Mw, gamma, T1, lh
    , p1)
2 %calculates the chamber pressure pc [Pa] in vacuum at which massflow
     is mdot [ml/h]
3 mdot_1=mdot/1000/3600; %converts mdot from ml/h to l/s (equal to kg/
    s) in case of water
4
5 syms x
6 f=0==mdot_1-((x.*At*sqrt(gamma*((1+gamma)/2)^((gamma+1)/(1-gamma))))
    ./sqrt(Ra/Mw*(T1*lh*Mw)/(lh*Mw+T1*Ra*log(p1/x))));
7 pc=vpasolve(f);  %[Pa]
8 pc=double(pc);
9 Tvap_1=(T1*lh*Mw)/(lh*Mw+T1*Ra*log(p1/pc));   %calculates Tvap in [K
    ]
10 Tvap=Tvap_1-273.15;  %converts Tvap_1 in celsius [C]
```

```
11
12 %pc=mdot_1/At*sqrt(Ra/Mw*Tvap_1)/(sqrt(gamma*((1+gamma)/2)^((gamma
       -1)/(1-gamma)))); %[Pa]
13 end
```

Matlab function for ideal power:

```
1  function [Qdot]=ideal_power(mdot,T0, At, Ra, Mw, gamma, cpl, lh, T1,
       p1)
2  %calcualtes the ideal power input Qdot [W] and the vaporization
       temperature Tvap [C] as a function of the mass flow mdot
3  %[ml/h] and the chamber temperature Tc
4  %[K]
5  %needs the other parameters to be defined in the workspace
6
7  T0_1=T0+273.15; %converts T0 from celsius to K
8  mdot_1=mdot/1000/3600; %converts mdot from ml/h to l/s (equal to kg/
       s) in case of water
9  [pc, Tvap]=chamber_pressure(mdot, At, Ra, Mw, gamma, T1, lh, p1); %
       calculates the chamber pressure in vacuum and Tvap
10 Tvap_1=Tvap+273.15; %converts Tvap from celsius to K
11 Qdot=mdot_1*(cpl*(Tvap_1-T0_1)+lh); %calculates Qdot [W]
12 end
```

Matlab code for thrust bench displacement:

```
1  clear all
2  close all
3  clc
4
5  A = dlmread('all_other_data.lvm');
6
7  t = A(:,1);
8  Ampl = A(:,2);
9
10 time=[];
11 Amplitude=[];
12 for i=1:669
13     time(i)=mean(t(((i-1)*104+1):i*104));
14     Amplitude(i)=median(Ampl(((i-1)*104+1): i*104));
15 end
16
17 % create a vector with the power value
18 time_power=[0, 2*60+37, 6*60, 6*60+0.001 , 7*60+30, 7*60+30+0.001,
       9*60+30, 9*60+30+0.001,11*60];
19 power=[9.5*0.45, 9.5*0.45, 9.5*0.45, 9.2 *0.44, 9.2* 0.44, 8.8*0.42,
       8.8*0.42, 8.5*0.4, 8.5*0.4];
20
21 coeffs = polyfit(time,Amplitude,15);
22 xfit = 0:660;
23 yfit = polyval(coeffs, xfit);
```

```
24
25 % create the vector of average displacement
26
27 tt=t(1:end);
28 AA= Ampl(1:end);
29 plot(t,Ampl,'b')
30 figure
31 yyaxis left
32 xlabel('Time [s]')
33 plot(time, Amplitude,'b')
34 ylabel('Displacement [micron]')
35 hold on
36 plot(xfit,yfit,'k-')
37 yyaxis right
38 plot(time_power, power,'r')
39 grid on
40 grid minor
41 set(findall(gcf,'-property','FontSize'),'FontSize',20)
42 ylabel('Power [W]')
43 ylim([3.3 4.4])
44 yticks([3.3 3.4 3.5 3.6 3.7 3.8 3.9 4.0 4.1 4.2 4.3 4.4])
45 set(gca,'Xlim',[0 660])
46 xticks(0:50:660)
47 legend('Pendulum''s displacement','Trend line','Power')
```

Bibliography

[1] D. C. Guerrieri. *The low-pressure micro-resistojet modelling and optimization for future nano- and pico-satellites*. PhD thesis, Delft University of Technology, 2018.

[2] M. A. C. Silva. *Design, Modeling and Control of Vaporizing Liquid Microthrusters*. PhD thesis, Delft University of Technology, 2018.

[3] L. A. Turmaine. A technology demonstrator payload for micro-resistojet thrusters on Delfi-PQ. Master's thesis, Delft University of Technology, 2017.

[4] D.C. Guerrieri and M.A.C. Silva. Micropropulsion system for Delfi-PQ. Poster. Internal document.

[5] J.L. Lens. Verifying and Validating. TU Delft AE4-12 lecture slides, November 2017.

[6] Larson, Kirkpatrick, Sellers, Thomas, and Verma. *Applied Space Systems Engineering*. McGraw-Hill Education, first edition, 2009.

[7] N.H. Crisp, K. Smith, and P. Hollingsworth. Launchf and deployment of distributed small satellite systems. *Acta Astronautica*, 114:65–78, 2015.

[8] R. Sandau. Status and trends of small satellite missions for Earth observation. *Acta Astronautica*, 2010.

[9] J. Bouwmeester and J. Guo. Survey of worldwide pico- and nanosatellite missions, distributions, and subsystem technology. *Acta Astronautica*, 67:854–862, 2010.

[10] T. Villela, C.A. Costa, A.M. Brandao, F.T. Bueno, and R. Leonardi. Towards the Thousandth Cubesat: A Statistical Overview. *International Journal of Aerospace Engineering*, 2019:13, 2019.

[11] J. Crusan and C. Galica. NASA's CubeSat Launch Initiative: Enabling broad access to space. *Acta Astronautica*, 157:51–60, 2019.

[12] A. Poghosyan and A. Golkar. CubeSat evolution: Analyzing CubeSat capabilities for conducting science missions. *Progress in Aerospace Sciences*, 2017.

[13] B. Twiggs. Making it Small. Presentation, https://web.archive.org/web/20160303185449/http://mstl.atl.calpoly.edu/~bklofas/Presentations/DevelopersWorkshop2009/7_CubeSat_Alt/1_Twiggs-PocketQub.pdf, 2009. Accessed on: 2019-05-15.

[14] K. Zack. Development and Operation of the PocketQube T-LogoQube. Presentation, http://mstl.atl.calpoly.edu/~bklofas/Presentations/DevelopersWorkshop2014/Zack_T-LogoQube.pdf. Accesssed on: 2019-09-15.

[15] 50dollarsat. $50SAT-Eagle2. http://www.50dollarsat.info/. Accessed on: 2019-05-15.

[16] GAUSS. UNISAT-5 MISSION. https://www.gaussteam.com/satellites/gauss-latest-satellites/unisat-5/. Accessed on: 15-05-2019.

[17] Gunther'sSacePage. QUbeScout S1. https://space.skyrocket.de/doc_sdat/qubescout-s1.htm. Accessed on: 15-05-2019.

[18] Gunther'sSpacePage. Wren. https://space.skyrocket.de/doc_sdat/wren.htm. Accessed on: 15-05-2019.

[19] Wikipedia. PocketQube. https://en.wikipedia.org/wiki/PocketQube. Accessed on: 2019-05-15.

[20] J. Bouwmeester. Delfi-PQ Mission & Design. Presentation, https://dataverse.nl/dataset.xhtml?persistentId=hdl:10411/3VMD4X. Accessed on: 16-05-2019.

[21] A.D. Ketsdever, R.H. Lee, and T.C. Lilly. Performance testing of a microfabricated propulsion system for nanosatellite applications. *Journal of Micromechanics and Microengineering*, 15:2254–2263, 2005.

[22] K. Palmer, H. Nguyen, and G. Thronell. Fabrication and evaluation of a free molecule micro-resistojet with thick silicon dioxide insulation and suspension. *Journal of Micromechanics and Microengineering*, 23:9pp, 2013.

[23] A. Blanco and S. Roy. Numerical Simulation of a Free Molecular Electro Jet (FMEJ) for In-Space Propulsion. In *51st AIAA Aerospace Sciences Meeting including teh New Horizons Forum and Aerospace Exposition*. American Institute of Aeronautics and Astronautics, Aerospace Research Central, 2013.

[24] D.C. Guerrieri, M.A.C. Silva, B.T.C. Zandbergen, and A. Cervone. Development of a low pressure free molecular micro-resistojet for CubeSat applications. In *66th International Astronautical Congress*, Israel, 2015. International Astronautical Federation.

[25] E.V. Mukerjee, A.P. Wallace, K.Y. Yan, D.W. Howard, R.L. Smith, and S.D. Collins. Vaporizing liquid microthruster. *Sensors and Actuators*, 83:231–236, 2000.

[26] K. Karthikeyan, S.K. Chou, L.E. Khoong, Y.M. Tan, C.W. Lu, and W.M. Yang. Lowe temperature co-fired ceramic vaporizing liquid microthruster for microspacecraft applications. *Applied Energy*, 97:577–583, 2012.

[27] P. Kundu, T.K. Bhattacharyya, and S. Das. Design, fabrication and performance evaluation of a vaporizing liquid microthruster. *Journal of Micromechanics and Microengineering*, 22:15pp, 2012.

[28] M.G. Giorgi and D. Fontanarosa. A novel quasi-one-dimensional model for performance estimation of a Vaporizing Liquid Microthruster. *Aerospace Science and Technology*, 84:1020–1034, 2019.

[29] S. Silvestrini. Closed-loop Thrust Magnitude Control System for Nano- and Pico-Satellite Applicatons. Master's thesis, TU Delft, 2017.

[30] V. Pallichadath. Propulsion Subsystem Requirements for the Delfi-PQ Satellites. techreport 2, Delft University of Technology, 2018.

[31] M. Ryschkewitsch. *NPR 7120.5, NASA Space Flight Program and Project Management Handbook*. National Aeronautics and Space Adminstration, February 2010.

[32] ECSS Secretariat ESA-ESTEC Requirements & Standards Division. Space engineering: Propulsion general requirements. Technical Report ECSS-E-ST-35C Rev.1, European Cooperation for Space Standartization, 2009.

[33] M. Boerci. Launcher loads for small satellites. Internal Document, 2017. (TU Delft).

[34] R.A. Makhan. Performance of the MEMS VaporizingLiquid Microthruster usingcold nitrogen gas as propellan. Master's thesis, TU Delft, 2018.

[35] O. Lvovsky and C. Grayson. Aerospace Payloads Leak Test Methodology. In *SPACECRAFT DESIGN, TESTING AND PERFORMANCE*, number JSC-CN-21358. ARES Corporation, American Society for Nondestructive Testing (ASNT), January 2010.

[36] P.S. Murvay and I. Silea. A survey on gas leak detection and localization techniques. *Journal of Loss Prevention in the Process Industries*, 25(6):966–973, November 2012.

[37] J.S. Almeida, E.C. Garcia, and R.M.P. Demori. Leak Testing The CBERSp-FM2 Satellite Propulsion System. *An Official Journal of the Brazilian Vacuum Society*, 24(2):93–97, 2006.

[38] B.T.C. Zandbergen. Leak analysis fundamentals (draft). Internal Memo, August 2006.

[39] The Lee Company. Manifolds - 3 Boss - The Lee Company. https://www.theleeco.com/products/electro-fluidic-systems/minstac-tubing-components/tube-fittings/manifolds-3-boss/#. Accesssed on: 2018-11-27.

[40] TE Connectivity Sensor Solutions. MS5837-30BA Ultra Small Gel Filled Pressure Sensor. Tech. Data Sheet, https://www.te.com/usa-en/product-CAT-BLPS0017.html#mdp-tabs-content. Accessed on: 2019-06-02.

[41] AE Adam. Highland Portable Precision Balances. Tech. Data Sheet https://www.adamequipment.com/hcb-123. Accessed on: 2019-06-02.

[42] V. Pallichadath. Propulsion Subsystem Mass, Volume & Power Budgets. Technical Report Rev 2.0, Delft University of Technology, 2018.

[43] J. Bouwmeester. PQ9 RS485 Standard. Technical Report Rev. 0.5, Delft University of Technology, 2017.

[44] The Lee Company. VHS Series Solenoid Valves General Specifications. https://www.theleeco.com/products/electro-fluidic-systems/solenoid-valves/dispensing-valves/vhs-series-solenoid-valves/general-specifications/#ec. Accessed on: 2019-03-19.

[45] Y. Bouaanani, P. Baucour, E. Gavignet, and F. Lanzetta. Performance of thermocouple subjected to a variable current. *International Journal of Thermal Sciences*, 134:440–452, 2018.

[46] Dijkstra Vereenigde Laboratorium Aparatuur. Technotes Highlighting Technical Features for Thermo Scientific Vacutherm Vacuum Ovens. Tech. Data Sheet, https://www.laboratorium-apparatuur.nl/media/productfile/thermo-vacuum-ovens-datasheet.pdf. Accessed on: 2019-06-02.

[47] thermocoupleinfo. Type K Thermocouple. Tech. Data Sheet, https://www.thermocoupleinfo.com/type-k-thermocouple.htm. Accessed on: 2019-06-02.

[48] Tenma. Palm Size Digital Multimeters. Tech. Data Sheet, http://www.farnell.com/datasheets/1661853.pdf. Accessed on: 2019-06-02.

[49] FLIR. Datasheets and FOV Calculators. Tech. Data Sheet, https://flir.custhelp.com/app/fl_download_datasheets. Accessed on: 2019-06-02.

[50] The Lee Company. Check Valves. https://www.theleeco.com/products/electro-fluidic-systems/minstac-tubing-components/fluid-control-components/check-valves/. Accessed on: 2019-03-07.

[51] T.C. Dickenson. *Valves, Piping & Pipelines Handbook*. Elsevier Advanced Technology, 3rd Edition edition, 1999.

[52] K. Mivule and C. Turner. Applying Moving Average Filtering for Non-interactive Differential Privacy Settings. *Procedia Computer Science*, 36:409–415, 2014.

[53] N. Marquardt. Introduction to the Principles of Vacuum Physics. https://www.researchgate.net/publication/265934038_INTRODUCTION_TO_THE_PRINCIPLES_OF_VACUUM_PHYSICS. Accessed on: 13-04-2019.

[54] X. Zhang, P. Sun, T. Yan., Y. Huang, Z. Ma, B. Zou, W. Zheng, J. Zhou, Y. Gong, and C.Q. Sun. Water's phase diagram: From the notion of thermodynamics to hydrogen-bond cooperativity. *Progress in Solid State Chemistry*, 43:71–81, 2015.

[55] M.J. Moran, H.N. Shapiro, D.D. Boettner, and M.B. Bailey. *Fundatementals of Engineering Thermodynamics*. Wiley, eighth edition, 2014.

[56] R.H. Perry. *Perry's Chemical Engineers' Handbook*. McGraw-Hill, seventh edition, 1997.

[57] K. Aoki, M. Sawada, and M. Akahori. Freezing due to direct contact heat transfer including sublimation. *International Journal of Refrigeration*, 25:235–242, 2002.

[58] S.W. van Sciver. *Helium Cryogenics*. Springer, second edition, 2012.

[59] Indiana University Northwest. Elementary Gas Laws: Charles Law. http://www.iun.edu/~cpanhd/C101webnotes/gases/charleslaw.html. Accessed on: 2019-03-12.

[60] B.T.C. Zandbergen. *Thermal Rocket Propulsion*. TU Delft, 2.07 edition, August 2018.

[61] Georgia State University. Molar Specific Heats of Gases. http://hyperphysics.phy-astr.gsu.edu/hbase/Kinetic/shegas.html. Accessed on: 2019-03-06.

[62] NIST. Molar Gas Constant. https://physics.nist.gov/cgi-bin/cuu/Value?r. Accessed on: 2019-03-06.

[63] Leakdetection-Technology. Mean free path. http://www.leakdetection-technology.com/science/introduction-to-the-gas-laws/the-mean-free-path-for-some-gases-at-20-c-ar html. Accessed on: 2019-03-13.

[64] Form Ceram. https://www.formceram.de/en.html?gclid=Cj0KEQjwi_W9BRD_3uio_Jz-p8UBEiQANU80vlBBtgWnZrycHLSxoELgfv92nH2Eni6mSv6HztAsb-saAvMW Accessed on: 2019-03-13.

[65] D. Koutsoyiannis. Clausius-Clapeyron equation and saturation vapour pressure:simple theory reconciled with practice. *Earuopean Journal of Physics*, 33(2):295–305, 2012.